INFORMATION TO USERS

This manuscript has been reproduced from the microfilm master. UMI films the text directly from the original or copy submitted. Thus, some thesis and dissertation copies are in typewriter face, while others may be from any type of computer printer.

The quality of this reproduction is dependent upon the quality of the copy submitted. Broken or indistinct print, colored or poor quality illustrations and photographs, print bleedthrough, substandard margins, and improper alignment can adversely affect reproduction.

In the unlikely event that the author did not send UMI a complete manuscript and there are missing pages, these will be noted. Also, if unauthorized copyright material had to be removed, a note will indicate the deletion.

Oversize materials (e.g., maps, drawings, charts) are reproduced by sectioning the original, beginning at the upper left-hand corner and continuing from left to right in equal sections with small overlaps.

Photographs included in the original manuscript have been reproduced xerographically in this copy. Higher quality 6" x 9" black and white photographic prints are available for any photographs or illustrations appearing in this copy for an additional charge. Contact UMI directly to order.

Bell & Howell Information and Learning
300 North Zeeb Road, Ann Arbor, MI 48106-1346 USA

UMI®
800-521-0600

The Second Sphere Coordination of Peroxovanadium Guests with Polyurea, Polyguanidinium and Polyammonium Hosts

Karin J. Yaccato

A thesis submitted to the Faculty of Graduate Studies and Research in partial fufillment of the requirements for the degree of Master of Science

June 1998
Department of Chemistry
McGill University
Montreal, Quebec
Canada

Abstract

New insulin mimetic peroxovanadium compounds were prepared as polyguanidinium, ammonium and polyammonium salts, and their cation-anion interactions were characterized by UV-Vis, ^{51}V NMR and ^{1}H NMR spectroscopy. The X-ray structures of four complexes $[((NH_2)_3CCH_2CH_2)_2][mpV(nta)]$, $[(NH_2NH)_2C(NH_2)][mpV(2,6\text{-}pdc)]$, $[((NH_2)_2C(NH)(CH_2)_3)_2(N_2C_4H_8)][bpV(pic)]\bullet 2H_2O$, and $[(NH_3CH_2CH_2)_2][bpV(bipy]\bullet H_2O$, were determined and are discussed.

$[Et_4N][bpV(phen)]\bullet 2H_2O$ was prepared and it's ability to act as a guest to second sphere coordinating polyurea hosts, in chloroform/DMSO, was studied using NOESY, ^{51}V NMR and ^{1}H NMR; extraction, titration and VT experiments.

The relative stability of 6 complexes in DMEM media, assessed using ^{51}V NMR, is discussed with respect to decomposition products and toxicities in PC-12 cells. Decomposition rates depend upon the number of peroxo groups (1>2) and the ancillary ligands.

Résumé

De nouveaux complexes de peroxovanadium mimiquant l'insuline ont été préparés sous formes de sels de polyguanidinium, d'ammonium et de polyammonium et l'interaction anion-cation de ces sels a été caractérisée par spectroscopie UV-Vis et RMN de ^{1}H et ^{51}V. La structure des rayons X de quatre complexes ($[((NH_2)_3CCH_2CH_2)_2][mpV(nta)]$, $[(NH_2NH)_2C(NH_2)][mpV(2,6\text{-}pdc)]$, $[((NH_2)_2C(NH)(CH_2)_3)_2(N_2C_4H_8)][bpV(pic)]\cdot 2H_2O$, et $[(NH_3CH_2CH_2)_2][bpV(bipy]\cdot H_2O$, a été élucidée et est également analysée.

$[Et_4N][bpV(phen)]\cdot 2H_2O$ a été préparé et son aptitude à se comporter comme un invité pour les hôtes de seconde sphère de coordination de la polyurée, dans le chlorofome/DMSO a été étudiée par NOESY, RMN de ^{1}H et ^{51}V; extraction, titrage et expérience à température variable.

La stabilité relative de six complexes en solution de DMEM, évaluée par RMN du ^{51}V, est étudiée en rapport avec les produits de décomposition et la toxicité dans les cellules PC-12. Les taux de décomposition dépendent du nombre de groupements peroxo (1>2) et des ligands présents.

Acknowledgments

In the course of this degree there have been numerous people who have provided me with help, guidance, encouragement and support.

First of all, I am thankful for the guidance, encouragement and kindness of my supervisor, Dr. A. Shaver. In each and every one of our meetings Dr. Shaver had an amazing capacity to take a lost and frustrated graduate student and find something in the presented research to let them leave his office as a confident, proficient and capable chemist!

I would like to thank Dr. D. Maysinger, Anne Morinville and Lada Rumora for sharing their research and expertise; keeping me busy through the summer of 1997.

Dr. A. M. Lebuis and Dr. F. Sauriol are gratefully acknowledged for their patience and work with all X-ray crystal structures and NOESY spectroscopy, respectively.

I would like to acknowledge the financial support of McGill University and NSERC, through the Max Stern Recruitment and PGSA awards, respectively.

All members of lab 435, past and present, are thanked for their company, patience and ideas. Specifically I would like to thank Dr. K. Rahimian and Virginie Guillemette for always keeping my spirits up! Virginie was also a great help in translating my abstract into french.

I also need to thank the occupants of lab 335, in particular Stephanie Warner, Heather Gas and Claire Edwards for practically adopting me and always making themselves available. Stephanie was also a great help in carefully proofreading this thesis.

Dr. S. Black and the students of lab 101 made TA'ing one of the most rewarding parts of my graduate school experience.

Finally, I must thank my mother for always being my biggest supporter and favorite confidante.
Thanks

Abbreviations

acetpic	3-acetatoxypyridine-2-carboxylato
ada	N-(2-amidomethyl)iminodiacetato
ATP	adenine triphosphate
bG	bisguanidinium
Bicine	N,N-bis(2-hydroxyethyl)glycine
bipy	2,2'-bipyridine
bipy-$(COO)_2$	2,2'-bipyridine-4,4'-dicarboxylato
bipyH	2,2'-bipyridinium
bis-ethyl	N-(3-Aminopropyl)-1,3-propane-diamine
bpg	N,N-bis(2-pyridylmethyl)glycine
bpV	bisperoxovanadium
BSA	bovine serum albumin
bU	bisurea
cit	citrato
cystH	cysteine
DDT	1,1,1-trichloro-2,2-bis[4-chlorophenyl]ethane)
DMEM	Dublecco's Modified Eagle Media
DNA	deoxyribonucleic acid
EDTA	ethylenediaminetetraacetatic acid
ER	extraction ratio
EXAFS	extended X-ray absorption fine structure
GlyGly	glycylglycine
glyH	glycine
HEDTA	ethylenediaminetetraacetic acid
HEPES	4-(2-hydroxyethyl)-1-piperazineethanesulfonic acid
Hheida	N-(2-hydroxyethyl)iminodiacetato
HIV	Human imunodeficiency virus
Hz	Hertz
IDA	iminodiacetato
IRK	insulin receptor kinase
isoquin	isoquinoline-2-carboxylato
LMCT	ligand to metal charge transfer
mG	monoguanidinium
Me_4-phen	3,4,7,8-tetramethyl-1,10-phenanthroline
Me_2-bipy	4,4'-dimethyl-2,2'-bipyridine
Me_2-phen	4,7-dimethyl-1,10-phenanthroline
Me-phen	5-methyl-1,10-phenanthroline
MOPS	4-morpholinepropanesulfonic acid
mpV	monoperoxovanadium
nicH	nicotinic acid
NH_2-phen	5-amino-1,10-phenanthroline
NMR	nuclear magnetic resonance
NO_2-phen	5-nbitro-1,10-phenanthroline
NOE	Nuclear Overhauser Effect
NOESY	Nuclear Overhauser Effect Spectroscopy
nta	nitrilotriacetato
OHpic	3-hydroxypyridine-2-carboxylato
ox	oxalato
pA	polyamine
2,6-pdc	2,6-pyridinedicarboxylato

phen	1,10-phenanthroline
pic	pyridine-2-carboxylato
PIPES	1,4-piperazinebis(ethanesulfonic acid)
pMo	permolybdate
pW	pertungstate
ppm	parts per million
PTP	protein tyrosine phosphatase
pV	peroxovandadate
quin	quinolato
RNA	Ribonucleic Acid
tG	trisguanidinium
tpa	N,N,N-tris(2-pyridylmthyl)amine
tris	tris(hydroxymethyl)aminomethane
tU	trisurea
UV	ultraviolet
UV-Vis	ultraviolet-visible
V(2,6-pdc)	$NH_4[VO_2(2,6\text{-pdc})(H_20)]$
VT	variable temperature

Please see Figures (2.1- Ia, Ib, Ic and 2.1- IIa, IIb) for compound structures and assigned abbreviations

Table of Contents

Appendices

Chapter 1 Peroxovanadium Complexes and Second Sphere Coordination

1.1 Peroxovanadium (pV) Complexes

Peroxovanadium (pV) complexes, (see pg.5, figure 1.5) predominantly studied in the context of their insulin mimetic properties, have developed into powerful biochemical research tools. They act as specific protein tyrosine phosphatase inhibitors.[1] These solid complexes are stable, easily synthesized, inexpensive and highly active. Their activity at the level of the phosphatase allows them to display diverse *in vivo* effects, depending upon the cellular system under investigation. Tyrosine phosphorylation is a highly significant biological signalling mechanism.[2] As well, there is interest regarding the role of pVs in haloperoxidases, natural vanadium containing enzymes.[2,3] Other vanadium(IV and V) complexes, such as bismaltolatooxovanadium(IV)[4] and N-(2-pyridylmethyl)iminodiacetoxooxovanadium(V)[5], have also been investigated with respect to their biological applications. The bio-inorganic chemistry of vanadium complexes represents an area of continued growth and investigation.

1.1.1 pV: Insulin Mimetic Activity

1.1.1.1 Insulin Pathway

Insulin is an important signalling molecule produced by the pancreatic β-cells found in the islets of Langerhans. It is released in response to elevated blood glucose levels. A precursor, once in the bloodstream, is cleaved to give the actual hormone, which then binds to its cell surface receptor.

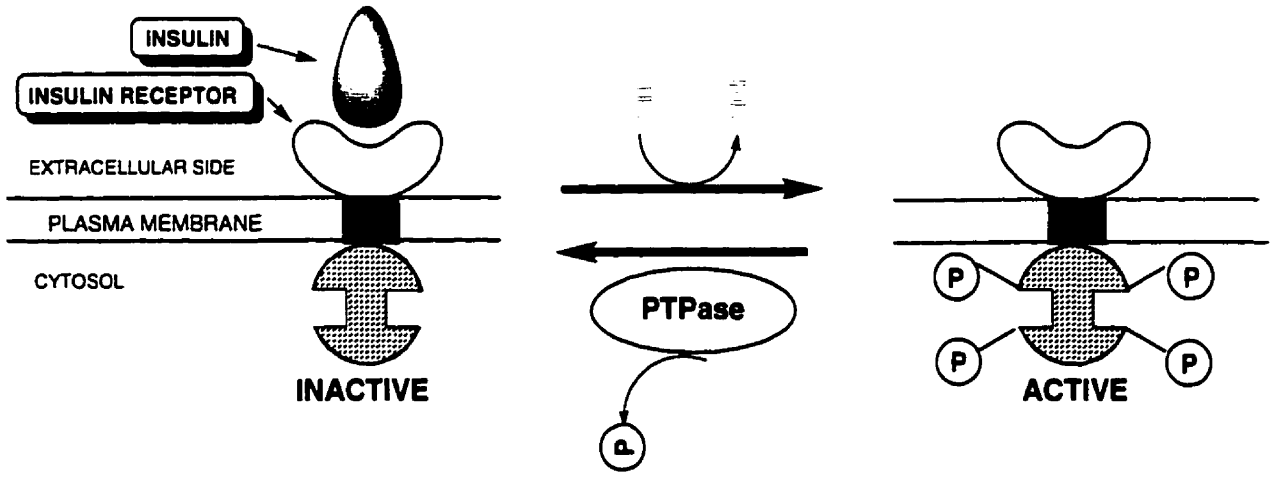

Figure 1.1 Schematic of pVs effects upon the IRK and PTPase

This receptor, the Insulin Receptor Kinase (IRK), is a transmembrane receptor whose intracellular domain has kinase activity. Kinases act to form phosphate esters on target molecules. Upon binding of insulin, the phosphorylation of regulatory tyrosine residues of IRK results in its activation. Once active, IRK phosphorylates various intracellular substrates, initiating the biochemical cascade responsible for insulin's metabolic effects. Intimately associated with the IRK is a protein tyrosine phosphatase (PTPase). This PTPase enzyme regulates IRK activity by cleaving phosphate groups from important regulatory tyrosine residues of the IRK. The dephosphorylated form of the IRK is inactive (Figure 1.1).[6]

1.1.1.2 Protein Tyrosine Phosphatase (PTPase)

Several PTPase enzymes, members of a family which includes more than forty cytosolic and receptorlike transmembrane forms,[7] have been isolated and crystallographically characterized.[8-11] These enzymes can be catagorized into vastly different subfamilies, such as the low and high molecular weight, and dual specificity PTPases. All PTPases share a highly conserved sequence of eleven amino acids that forms the catalytic substrate binding site.[7,12] Within this cavity, the cysteine and arginine residues are essential for catalytic activity (Figure 1.2) and a mechanism for the PTPase enzyme has been postulated (Figure 1.3).[8,13]

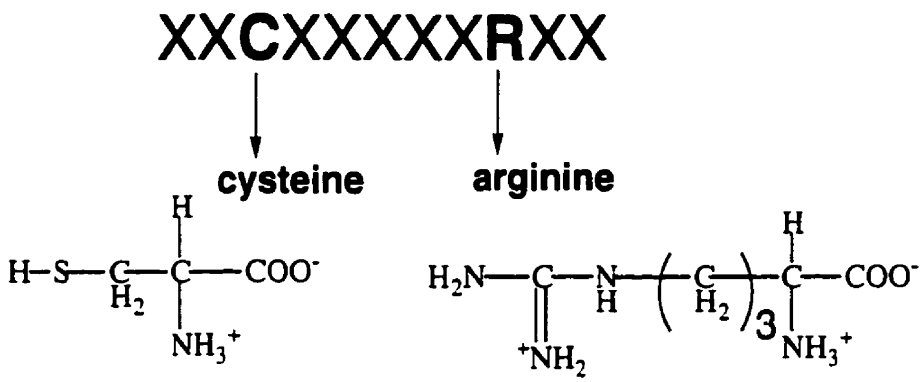

Figure 1.2 Conserved PTPase Active Site Sequence and Catalytically Essential Residues[6]

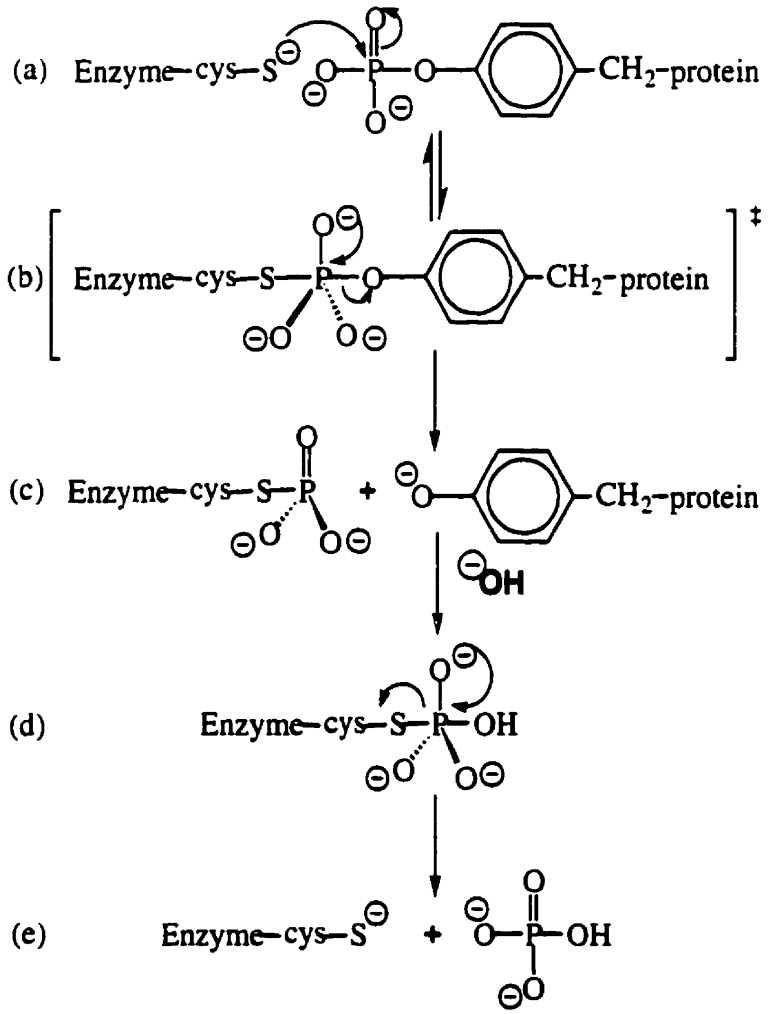

Figure 1.3 Mechanism for the hydrolysis of phosphotyrosine by PTP[8]

The sulfhydryl group of the cysteine residue, with a pKa of 4.9, is deprotonated at physiological pH and acts as the enzyme's nucleophile (Figure 1.3 a). The guanidinium group of the arginine residue coordinates the phosphorylated substrate, through strong hydrogen bonding, thus positioning and stabilizing it as the active site. A dianionic thio-phosphate ester complex is formed at the transition state (Figure 1.3 b). Preferential, hydrogen bond mediated, stabilization of this dianionic transition state, relative to the monoanionic substrate, may effectively lower the energy barrier. This would explain arginine's catalytic necessity. Molecular recognition at the enzyme active site, mediated by phosphate-guanidinium hydrogen bonding, has been noted for many enzymes that require coordination and/or activation of phosphate groups.[14,15,16] For the PTPase enzyme, several other less highly conserved active site residues also form important hydrogen bonds in recognition of the phosphorylated substrate.[12] In the final steps, (Figure 1.3 d,e) the thio-phosphate ester complex dissociates to produce phosphate and regenerate the enzyme's nucleophilic thiol.[7]

1.1.1.3 Mechanism of PTPase Inhibition by pV Complexes

pV complexes are very active oxidizing species, well known for their ability to catalyze the oxidation of diverse organic molecules.[15] Their PTPase inhibitory activity probably results from oxidation of the catalytic cysteine residue to cysteine sulfinic acid.[1,16] The oxidized residue is no longer nucleophilic and the PTPase enzyme is irreversibly inhibited (Figure 1.4). By inhibiting the PTPase, a downregulator of the IRK's kinase activity, pV species indirectly activate the IRK, mimicking the effects of insulin.[17]

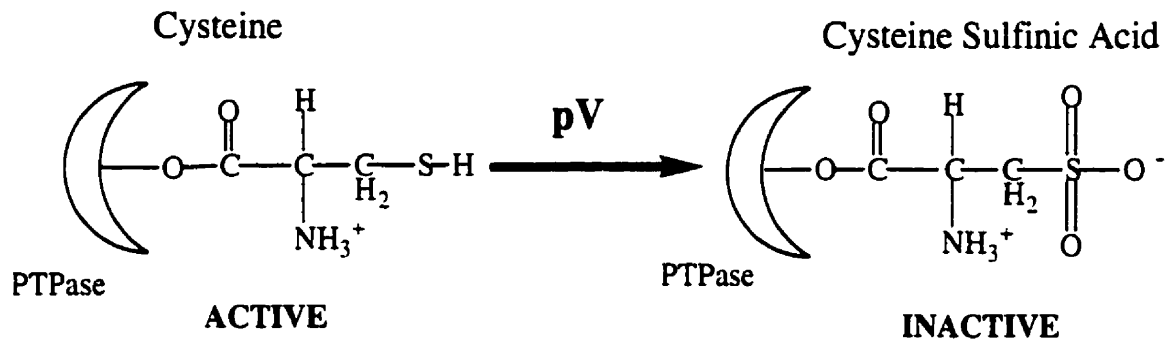

Figure 1.4 pV oxidation of PTPase nucleophile

1.1.1.4 The pV-phosphate Analogy: Structure, Transport and Specificity

The structural analogy between phosphate esters and pV species provides a simplistic analysis of the biological specificity of these inhibitors towards cellular phosphatases. Their three dimensional similarity likely allows vanadate and pV to permeate the cell membrane, via non specific anion channels, and thus enjoy intracellular bioavailability.[17]

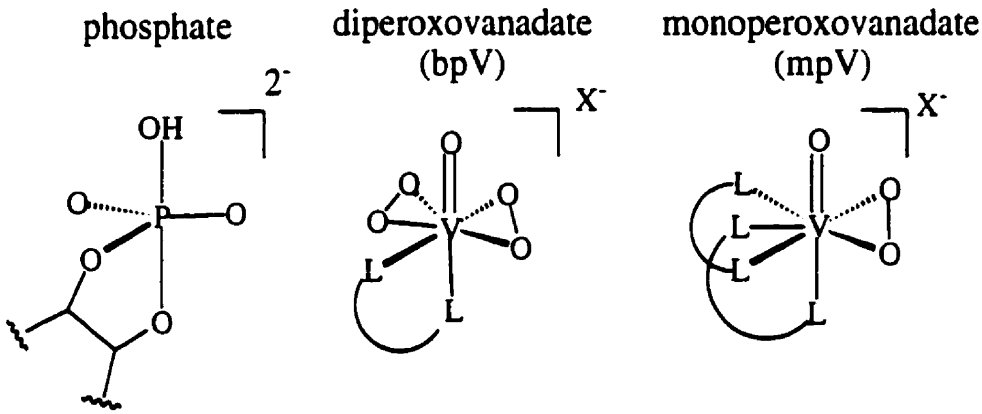

Figure 1.5 pV-Phosphate structural analogy

However, phosphate esters play many important biological roles, and simple structural mimicry does not provide an ample explanation for the PTPase specificity of pV complexes. Phosphoserine and phosphothreonine phosphatase enzymes are also vital cellular components that could conceivably bind pV. These phosphate cleaving enzymes incorporate the alcohol functional group

of a tyrosine residue as the critical active site nucleophile.[2] This mechanistic difference in their phosphate ester cleavage activity renders phosphoserine and phosphothreonine phosphatases much less susceptible to oxidation by pV oxidation. Hence the highly reactive nature of pV towards sulfur containing nucleophiles appears to critically define its biological role and specificity.[16]

Molybdate (MoO_4^{2-}), and tungstate (WO_4^{2-}),[12] as well as their peroxo complexes,[1,18-20] have also been investigated in the context of insulino-mimetic inorganic oxoanions. Structurally, these complexes are replicas of the vanadate (HVO_4^{2-}) and pV species, however they carry an extra positive charge as W and Mo are present in their (VI) oxidation states. Amongst a series of picolinic acid bisperoxo complexes (Figure 1.6) only the vanadium analog proved active in kinase activation assays. Conversely, all three complexes were highly active in PTPase inhibition assays.

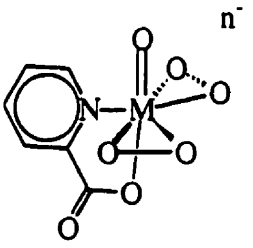

Figure 1.6 M=Mo, W; n=0, M=V; n=1 picolinic acid bisperoxo series[21]

Both the kinase and phosphatase assays equally denote the overall state of the insulin pathway, however, they differ experimentally. The PTPase inhibition assay is carried out with isolated PTPase enzyme, whereas the IRK activation assay involves whole cells. In order to show activity in the IRK activation assay, a PTPase inhibitor must also be capable of permeating the cell membrane to reach its intracellular target.[1] A similar dependence of activity upon experimental protocol, in studies with *in situ* preparations of pMo and pW, has been noted.[19] Transmembranal transport is implicated as an important variable that is capable of determining insulin mimetic potential for very similar oxoanions.[21,22]

1.1.1.5 Diverse Biological Effects

Protein tyrosine phosphorylation is important in regulating diverse fundamental cellular processes, such as growth, proliferation and differentiation.[2,7] The tyrosyl phosphorylation state of a protein in the cell reflects the cellular balance between competing protein tyrosine kinases and the protein tyrosine phosphatases. Specifically, PTPase activity is known to modulate important cellular kinases, including mitogen activated protein kinase (MAP kinase), insulin receptor kinase (IR kinase), and epidermal growth factor receptor kinase (EGFR kinase).[2] pV mediated inhibition prevents dephosphorylation of regulatory tyrosine residues of these kinases, and likely that of other yet unidentified PTPase substrates. This sustained state of tyrosine phosphorylation allows these kinases to remain in their active forms and is responsible for many of the biological effects of pV complexes.

Besides the aforementioned insulin mimetic activity, pV complexes have shown interesting biological effects in several different cell lines. In osteoblast cells, monoperoxo(nitrilotriacetato)oxovanadate, mpV(nta), enhanced cell proliferation, glucose consumption and protein content, while inhibiting differentiation.[23] Pervanadate, a mixture of aqueous pV species prepared *in situ*,[24] elicits proliferation of C3H10T1/2 mouse fibroblasts, and causes translocation of activated MAP kinase to the cell nucleus.[25] In addition, pV activates phospholipase D (PLD) in HL-60 granulocytes,[26] and stimulates inositol phosphate formation in four cell lines, including rat hepatoma (Fao), murine muscle (BC3H-1), Chinese hamster ovary (CHO) and rat basophilic leukemia (RBL).[27] DNA cleavage has been reported for $NH_4[VO(O_2)_2(phen)]$, bpV(phen), in the presence of UV radiation or reducing agents.[28] Potential for use of these complexes as anti bacterial and anti tumor agents has also been discussed.[29,30]

As a result of their broad spectrum of activity, pV complexes are a very active area of chemical and biological research. Continued study of these complexes within different cellular systems will likely uncover new biological pathways that are stimulated by pV treatment.

1.1.1.6 Chemical Structure

The first pV complexes were reported in 1959.[29] Since this time many new and interesting inorganic complexes have been isolated. Structurally, mononuclear pV complexes most commonly display seven coordinate distorted pentagonal bipyramidal geometry. Other geometry's include the crystallographically characterized six coordinate complexes, octahedral mpV(dipic)[31], tetrahedral bpV(NH_3),[32] and the pentagonal pyramidal bpV(imidazole).[33] The pentagonal plane is usually defined by η^2 bound peroxo ligands. A single axial position is occupied by an oxo ligand, while the remaining axial and equatorial positions are occupied by the ancillary ligand. This ancillary ligand plays an important role in determining the overall stability of the complex. Vanadium, in its 5^+ oxidation state, displays a clear preference for nitrogen and oxygen donor ligands.[32]

1.1.1.7 pV Solution State Structure

All reported experimental data suggests that in solution, the complexes retain structures very similar to those determined in the solid state by X-ray crystallography. Recent forays into molecular mechanics and *ab initio* calculations have reinforced the experimental data.[34,35] In the case of certain pV species, bpV(ox) and bpV(NH_3), weak coordination of the ancillary ligand leads to a considerable hydrolysis, immediately upon dissolution of the pure solid complex in water, producing the aquo pV species, $[VO(O_2)_2(H_2O)_x]^-$, x=1,2 and $[VO(O_2)(H_2O)_x]$.[36] This lability renders them unsuitable for development as biological research tools. Other pV species, such as $[VO(O_2)_2X]^{2-}$, X=Cl,[37] F[38] and [VO(O_2)(aminoacid/peptide)], aminoacid= glycine[39], peptide=Phe-Glu, Gly-Tyr[40], are also highly unstable in the solution and solid state. Mononuclear triperoxo[41,42] and dinuclear tri and tetraperoxo[39,43-45] species, have also been reported. To date these complexes have not been studied for their biological activities, likely due to their estimated high toxicity, reactivity and instability.

1.1.1.8 pV Counterions

The majority of anionic pV complexes have been isolated with simple inorganic counterions, such as NH_4^+, Na^+, and K^+. mpV complexes with alkylammonium[46,47] and tetraphenylphosphate counterions have also been synthesized. A number of pV anions have been isolated in several different salt forms. For example, bpV(bipy) has been isolated as its Na^+, NH_4^+, K^+, Cs^+, $(Me)_4N^+$ as well as its 2,2'-bipyridineH^+ salts. The bipyridineH^+ salt clearly shows a π-stacking interaction, between the aromatic anion and cation, in the X-ray crystal structure.[48] Differing biological activity, dependent upon the counterion, has been reported for a series of bpV potassium and ammonium salts.[29] Very recently, a thermally stable dinuclear tetraperoxo complex ($V_2O_8H_{24}^{4+}$) was isolated using diprotonated 5, 5, 7, 12, 14-hexa-methyl-1, 4, 8, 11-tetraazacyclotetradecane as counterion. This publication stressed the role of the cation in determining the overall complex stability.[49]

The association of a counterion with a charged complex may take the form of second sphere coordination (Figure 1.7). New pV complexes incorporating protective or chelating counterions, could tailor the physical properties of these active complexes. Stability and lipophilicity are highly sought after pharmacological properties. The structure of pV complexes allows for hydrogen bonding interactions at the oxo and peroxo sites, as well as hydrophobic π- stacking type interactions with aromatic ancillary ligands. The vast amount of research in the growing field of supramolecular or host-guest chemistry suggests that a strong basis exists for development of molecular hosts for pV guests.

1.2 Second Sphere Coordination Chemistry

Each molecule has two spheres of interaction. The primary sphere consists of covalently bound atoms which define its molecular structure. Its second sphere surrounds the first, and consists of non-covalently associated atoms, molecules or ions (Figure 1.7).

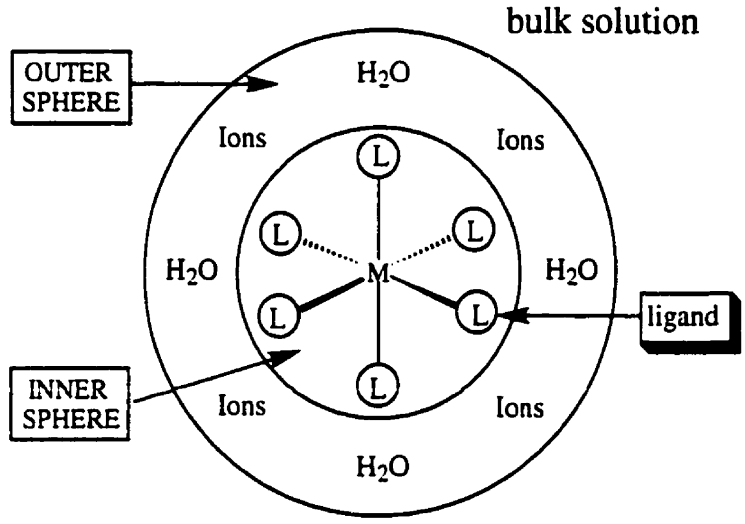

Figure 1.7 Schematic view of inner and outer sphere coordination in solution.

The second sphere is organized by the attractive non covalent forces; hydrogen bonding, electrostatics, Van der Waals and hydrophobic forces. While individually each one of these interactions contributes much less than 1/10th of the strength of a covalent bond, a system of multiple non covalent interactions can provide a very strong intermolecular binding force.[50] This force differs from covalent forces in that it is subject to environmental factors such as temperature, pH, ionic strength, and the dielectric constant of the surrounding media.

Of late, there is heightened interest in the second sphere; the molecular surroundings, the non-covalently bound interacting species, and the role they play in determining physical properties and reactivity. Consequently, several very complete reviews have been published.[51-54] The use of non covalent interactions to alter the chemical nature of simple molecules has diversified rapidly, spreading to research areas including computational,[55,56] organic[57], inorganic,[58-60] polymer,[61,62] analytical,[63,64] and supramolecular[65] chemistry.

The interest surrounding second sphere coordination stems from its potentially widespread and exciting applications. Examples include reaction catalysis,[66] molecular based filters and

machines,[67] as well as electronic,[68] photonic,[60] and ionic devices.[67] Binding, at the molecular level, has also been a main focus of biological research aiming to mimic the activity of enzymes or transport proteins.[69,70] All applications make use of the strong, reversible and very sensitive form of binding provided from intelligent design and synthesis of compatible molecular partners.

1.2.1 Natural Recognition Processes

Molecular recognition is a natural phenomenon. In definition, recognition at the molecular level consists of a selective association between two entities, complementary in their three dimensional shape, resulting in a new complex with a completely novel spatial configuration and set of defining chemical properties. The three dimensional shape of a molecule often determines its biological role. A good example is the interaction between neurotransmitter and bioreceptor at a nerve synapse (Figure 1.8).

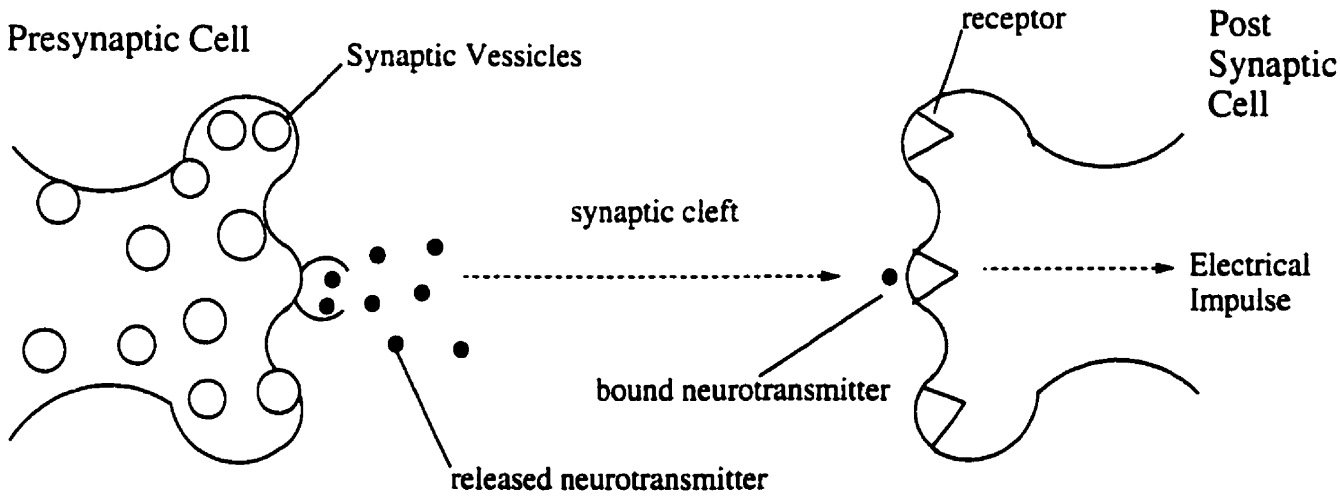

Figure 1.8 Synaptic message transmission[71]

The binding of the guest molecule, a neurotransmitter, leads to a conformational change in the three dimensional structure of the host molecule, a neuroreceptor. These changes transmit a message, in the form of an electrical impulse, from the extra cellular guest (neurotransmitter) to the membrane bound host (receptor) and beyond.[71]

Molecular recognition is endemic in nature. It is essential to living organisms. Hydrogen bonding is the strongest of the intermolecular forces and it defines the helical shape of alpha-keratin and collagen molecules, important structural fibres in skin and hair. Hydrogen bonds also provide the binding strength and recognition pattern, vital to the creation of each DNA double helix which allows for self duplication of molecules, thereby forming the basis of heredity. As well, the previously described interaction between insulin and its receptor (Section 1.1.1.1) constitutes a perfect example of non-covalent mediation of vital biochemical processes.

1.2.2 Chemical Uses

In many of its chemical uses, second sphere coordination is introduced in order to alter the physical properties and reactivity of the guest molecule. As an example, molybdenum(IV) dithiolene complexes, active reducing agents, showed an increase in reduction efficacy for the reaction, Me_3NO----->Me_3N, in the presence of a diamide host molecule that structurally complements the molybdenum guest complex (Figure 1.9).[72]

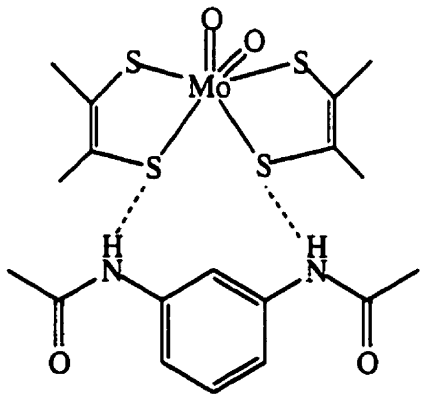

Figure 1.9 Example of modeled interaction between Mo complex(guest) and diamide(host).[72]

This host is thought to exert its catalytic effect through N-H···S hydrogen bonding to the molybdenum guest, accelerating the oxygen transfer reaction by stabilizing the oxo-metal product.[72]

Recently, a water soluble NMR shift reagent was developed based upon strong non covalent π-stacking interactions of an aromatic guest substrate with a bioorganometallic host (Figure 1.10).[73]

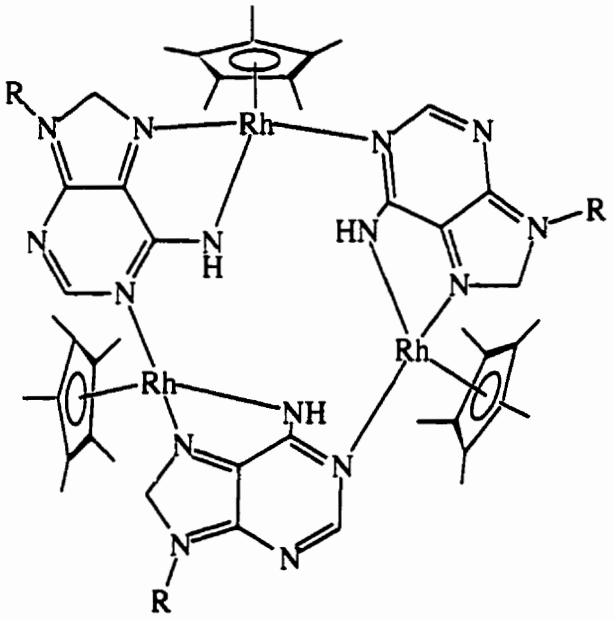

Figure 1.10 Cp*Rh(2'deoxyadenosine)]$_3$(OTf)$_3$[73]

This water soluble reagent alters the physical properties, namely the nuclear resonance frequencies, of aromatic host molecules to such an extent that it becomes useful as a methodological tool in the simplification of complicated NMR spectra.[73] In studying pV second sphere coordination, both proton and ^{51}V NMR may prove to be useful probes of second sphere coordination.

1.2.3 Drug Design

Biophysical properties are very important in the development of novel therapeutic agents. The activity of a drug may be well documented *in vitro*, however *in vivo*, other considerations include the stability, biocompatability and membrane permeability of the molecule. A well designed drug, known to act intracellularly, will prove useless if it cannot permeate the cell membrane or is inactivated prior to reaching its site of activity. The ideal pharmaceutical agent is an active, highly specific, stable and inexpensive solid material. It is non toxic and lipophilic but must retain

sufficient water solubility to enable oral administration. In the past, some active pharmacologic agents have been covalently altered, usually through acetylation of non essential hydroxyl groups, to formulate a more lipid soluble drug that retains its activity.[74] Alternatively, pro drugs have been designed which are enzymatically cleaved to the active molecule upon reaching their active sites.[75] Biocompatable pro drugs have also been formed by attachment of soluble macromolecules, such as proteins and polysaccharides, via degradable linkages.[76] Encapsulation, with different vesicles such as liposomes, polymers or micelles, delves into the expanding research area of sustained drug release.[77]

Another method of altering the physiochemical and phamacokinetic properties of an active drug employs selective drug complexing agents. These 'hosts' form tight host-guest complexes with the active drug. The properties of the complex differ considerably from the lone drug and can be tailored to give desirable characteristics such as increased stability or lipid solubility. Much of the research in this expanding field has centered upon the pharmacokinetic alterations introduced by drug complexation with cyclodextrins.[78,79]

Synthetic adenosine receptors have been synthesized and studied for their ability to selectively enhance transport flux of adenosine derivatives across organic liquid membranes (Figure 1.11).[80]

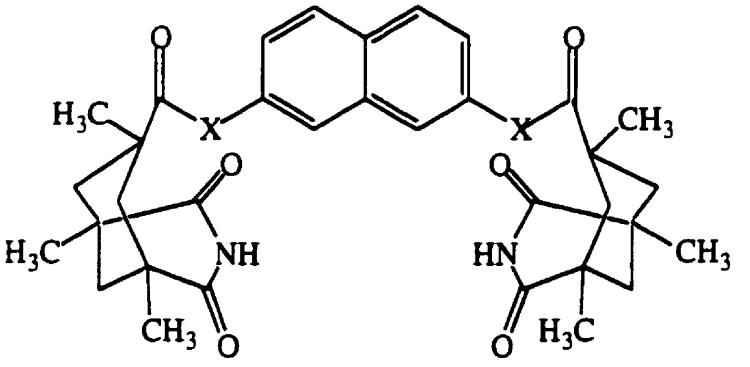

X=NH, Diamide diimide
X=O, Diester diimide

Figure 1.11 Naphthalene diamide diimide, Naphthalene diester diimide[80]

Subsequently, a study of these same receptors and their ability to transport adenosine across human skin and a polydimethylsiloxane membrane (PDMS) was undertaken, the objective being to develop a novel method for the permeation enhancement of drugs. While the inherent metabolic activity of isolated skin interfered with these studies, a ten fold permeation enhancement was noted through PDMS. Similar synthetic membrane transport studies have been utilized to provide models for facilitated transport across biological membranes.[63] These studies are ground breaking and provide insight regarding the intricate biomechanisms of transport. The use of second sphere coordinated therapeutic agents applies a rapidly maturing area in chemistry to important and long-standing pharmacological problems.

1.2.4 Anionic Guest Species

Developments in the recognition of anionic guests have lagged behind that of metal ion and cationic species. This is likely the result of difficulties competing with the more strongly bound anionic solvation shell.[81,82] The main anion hosts studied have been the cationic polyammonium,[66,83-85] and guanidinium salts,[69,86-88] as well as the neutral urea,[89,90] thiourea, amide[91-93] and polyamine[94-96] based receptors. Focus, in terms of guests, has been upon nucleobases such as adenine,[80,97] polycarboxylates,[89,98] important biomolecules such as ATP[99] and phosphate or phosphate ester derivatives.[100,101] Several review articles have been published.[102,103] Of particular interest is the structural design of phosphate complexing agents, due to the structural analogies between phosphate esters and pV complexes. These studies provide a viable starting point in the investigation of pV second sphere coordination.

1.2.4.1 Phosphate and Phosphate Esters

Phosphate, and phosphate ester binding to polyamines and polyguanidinium salts has been the subject of extensive research.[83,104] Much of this work is fueled by the prevalence of arginine residues (Figure 1.2) in peptidic enzymes that require the binding of phosphate, and the stabilization of trigonal bipyramidal phosphate-enzyme intermediates, as part of their biological

function.[14,105] Several naturally occurring polyamines have also been noted to associate with and alter the reactivity of phosphate containing molecules, such as RNA, DNA and ATP.[96] In particular, the naturally ubiquitous polyamines, spermine, spermidine and putrescine, function *in vivo* to regulate cell growth, proliferation, and differentiation. It is thought that these polycationic species act to stabilize biomacromolecules, such as enzymes and polyanionic nucleic acids, via hydrogen bonding and electrostatic interactions.[106]

The greater localized charge density of a protonated polyamine functionality, *versus* guanidinium units, has been shown to lead to stronger anion complexation, when the dominant binding force is provided by ion pairing (Figure 1.12). This is likely the case in very polar, highly competitive solvents. In contrast, the prevalence of arginine residues in enzymatic coordination sites is likely a function of its increased number of proximal hydrogen bonding sites, and its specific pattern of guanidinium mediated hydrogen bonding, *versus* polyamine salts. Therefore, when directed hydrogen bonding provides the maximal stabilizing force for a binding pair in solution, guanidinium salts are the optimal hosts. Also in their favor, alkylguanidinium units (pKa≈13.5)[104] are more strongly basic than alkyl amines (pKa≈7.5)[104] allowing them to remain protonated over a larger range of pH values.

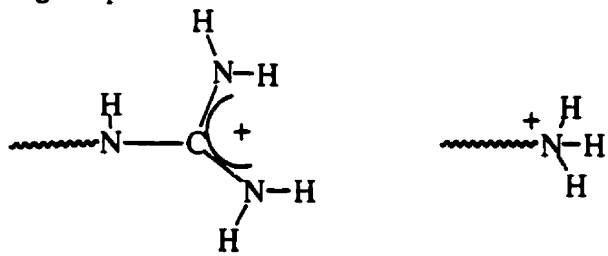

a) b)

Figure 1.12 a) Guanidinium and b) Polyammonium Groups

The aforementioned complementarity between phosphate and guanidinium, as an explanation for the presence of arginine residues at catalytic sites of many enzymes, was first modeled by Cotton et al. in 1973, prior to the development of modern enzyme crystallography (Figure 1.13).[14]

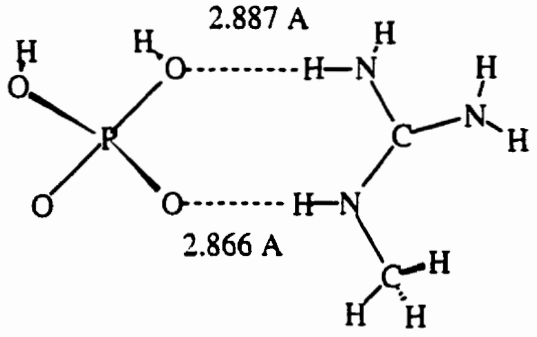

Figure 1.13 Methylguanidinium dihydrogenphosphate crystal structure[14]

The structure of methyl guanidinium dihydrogen phosphate contains two short, linear hydrogen bonds as well as a high degree of preorganization. The general oxo-anion coordinating ability of the guanidinium unit has also been noted in research regarding such diverse topics as the spontaneous self assembly of Metal(II)-arginine-Dianion systems,[107] Cu(II)-dipeptide complexation,[108] as well as synthetic template effects for guanidinium zinc phosphates.[109] As well, decavanadate species ($V_{10}O_{28}H_2^{4-}$), known for their phosphatase inhibitory capacity, have been crystallized as guanidinium decavanadate. This ion pair was postulated to model the interactions between biogenic molecules and large bioactive metal-oxo anions.[110]

1.2.4.2 Model Enzymes

Several mimics of the staphloccocal RNA nuclease have been assembled from multiple guanidinium units. The groups of E.V. Anslyn[69,111] and A.E. Hamilton[101] have developed a series of bisguanidinium receptors (Figure 1.14).

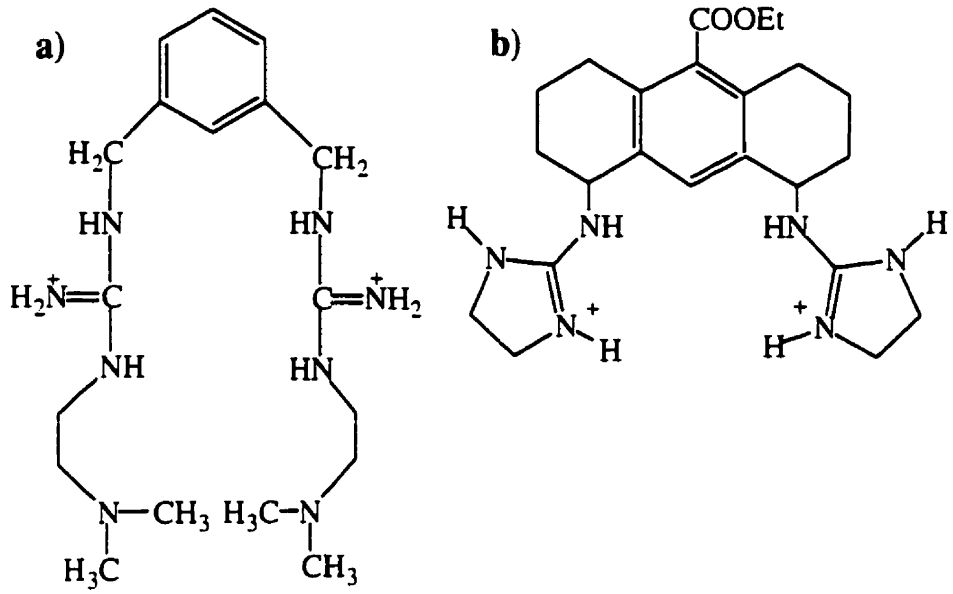

Figure 1.14 Examples of Catalytically Active Bisguanidinium Receptors; a)Phosphate Diesterification Catalyst[101] b) RNA Hyrolytic Catalyst[69]

Similarly, the research from M.S.Muche and Michael W. Gobel has shown the activity of bisguanidinium alcohols in phosphoryl transfer reactions. In general, this work has elucidated the important roles that multiple sites of host-guest interaction, structural complementarity, preorganization, solvent, counterion, ionic strength and pH play in determining the strength and selectivity of any host-guest interaction. It has also shown that specific molecular recognition and subsequent host-guest binding, a vital component of many biological events, can be mimicked by simple synthetic receptors. However, the catalytic activity of natural enzymes still far exceeds synthetic mimics.[70]

The use of these bisguanidinium enzyme mimics has been further developed in the context of possible anti-viral agents. HIV-1 messenger RNA is known to employ a strong complexation reaction, between a tat protein and a specific mRNA segment of 59 nucleotides named TAR, trans activation response element. The principal contact that mediates tat-TAR recognition is formed by a single arginine residue, situated in the middle of tat's basic amino acid affinity sequence. This

tat-TAR complex is responsible for boosting the viral transcription rate and is a requirement for efficient transcription of the viral genome Using the known ability of the bisguanidinium receptors to bind RNA,[69,112] a third guanidinium group was introduced to interact at the arginine binding site of TAR, to give a small molecule tat mimic. Once bound, the guanidinium receptors are known to enhance RNA cleavage, which would inactivate the virus. The new triguanidinium complex (Figure 1.15) was able to bind to and efficiently cleave a truncated TAR sequence. This research clearly displayed the importance of arginine residues in nature, and how their binding power can be synthetically exploited through intelligent design.[100]

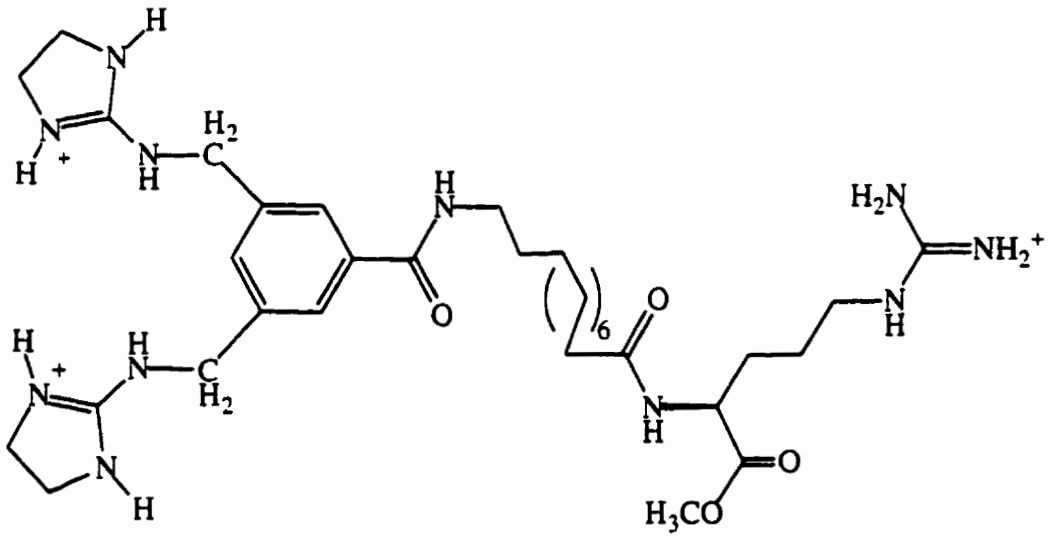

Figure 1.15 Triguanidinium RNA Cleaving Agent[100]

Complementarity, in the hydrogen bond donor-acceptor interaction between carboxylates and guanidinium groups, has also been shown.[113] Carboxypeptidase A, a zinc containing proteolytic enzyme which cleaves single aromatic amino acid residues from oligopeptides, is known to make efficient use of an arginine residue. In order to investigate the importance of this guanidinium-carboxylate interaction, several substrate analogs (competitive inhibitors) were designed, based upon the hydrogen bonding motif at the active site. An electron withdrawing fluorine group, was positioned adjacent to the important carboxylate group of the substrate in order to decrease the pKa

value of the carboyxlate. This fluorinated inhibitor becomes a weaker hydrogen bond acceptor, and, indeed, a weaker inhibitory capacity was noted, the result of weakened binding affinity. These results demonstrate the importance of hydrogen bonding in determining the stability of host-guest interactions at the active site of an enzyme.[114]

Another enzymatic system that employs hydrogen bonding is that of the flavin coenzymes. The flavins function through non covalent bonding with their apoproteins, holding the flavin in an appropriate position, as well as regulating the reactivities of the flavin molecule itself. An artificial flavoenzyme has been created by developing a hydrogen bonding receptor based upon a melamine derivative containing a preorganized guanidinium ion (Figure 1.16). Six hydrogen bonds are formed between the receptor and 6-azaflavin.[115]

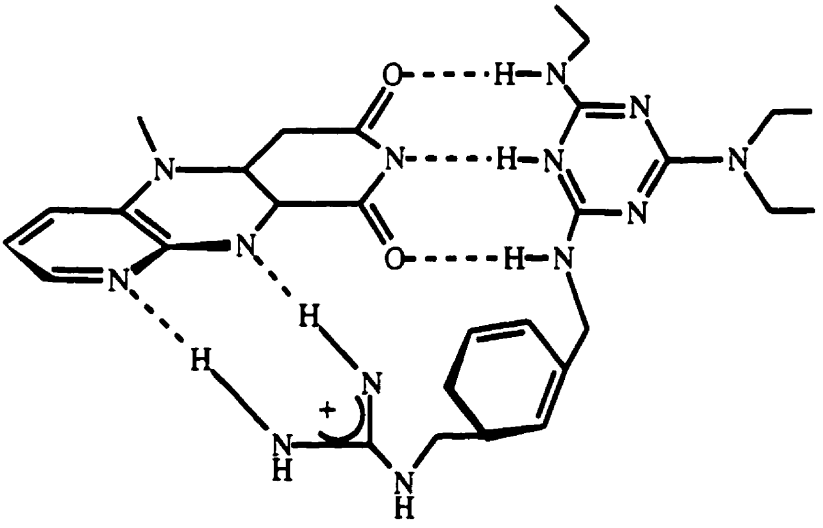

Figure 1.16 H-bonding of Flavin Receptor, N,N'-diacyl-2,6-diaminopyridine derivative[115]

1.2.5 Second Sphere Coordination in the PTPase Active Site

PTPases are also members of this enzymatic 'group' which have an essential arginine residue within their active sites. In the active PTPase, this arginine residue is responsible for binding phosphate and positioning the substrate in the cavity for nucleophilic cysteine attack. Arginine (guanidinium) likely plays a similar role in positioning vanadate, molybdate and tungstate, all weak

PTPase inhibitors, within the PTPase active site. Hydrogen bonding, from several conserved active site residues, has been shown to be highly significant at the active site of PTPases.[7-9] Specifically, the reversible PTPase inhibitor, vanadate, forms nine strong hydrogen bonds between its equatorial oxygens and several donor residues of the protein.[9] Through X-ray crystallography, these bonding interactions have been measured as 0.12-0.18 Å shorter than those arising from phosphate complexation. It appears that the stability arising from this sphere of hydrogen bonds leads to the inhibitory activity of vanadate. The vanadate-cysteine complex is more stable than the transition state phosphate-cysteine complex. Vanadate is therefore a competitive inhibitor of these enzymes.[9]

While these interactions have only been demonstrated for vanadate, they highlight the importance of hydrogen bonding in determining the stability and specificity of the PTPase enzyme-inhibitor complexes. Recently, an abinito calculation illustrated the propensity of pV complexes to coordinate water in their second sphere.[34] Hydrogen bonding at the peroxo group of peroxovanadium species has been discussed, and is thought to have a significant effect upon the stability of the complex.[116,117] As well, pV species appear to *selectively* oxidize only the PTPase sulfhydryl group present within the phosphate binding site. A method of targeting the reactive pV complexes solely to this site must be envisioned, perhaps involving pV-enzyme outer sphere hydrogen bond formation. This concept is reinforced by the recently noted similarity in natural phosphatase and chloroperoxidase enzyme binding sites.[118] These studies, and the repeatedly demonstrated importance of hydrogen bonding in protein enzymatic recognition and catalysis, provide an interesting rationale for studying the peroxo group's hydrogen bond donor-acceptor interactions.

1.2.6 Other Hosts for Anionic Guest Species

Other types of hosts for anionic guest species have been synthesized and studied. The tetracationic cyclobis(paraquat-p-phenylene) has been studied as a receptor for electron rich aromatic guests,

such as the aromatic amino acids, tryptophan, tryosine and phenylalanine. These hosts have been studied as potential redox switchable receptors whose binding strength can be chemically turned on or off by oxidation or reduction of the receptor.[68]

Neutral anion receptors are prized for their potential use in hydrophobic, membranous environments. Applications include potentiometric anionic sensors[119] as well as model systems for *in vivo* ionophore membrane transport.[120] Cyclic or linear aza-ether structures, substituted with triflate groups at each nitrogen (Figure 1.17a) have proved capable of binding chloride anions. These neutral receptors have potential applications as additives in lithium battery electrolytes that act to increase the conductivity and transference numbers of the lithium cation.[121] The linear and macrocyclic polyamines are also neutral (Figure 1.17b), and are capable of interactions with many species, including ruthenium[122,123] and copper complexes[124], as well as phosphate[125,126] and carboxylate[127] species. These receptors are analogous to the widely used crown ether cationic chelators.[54]

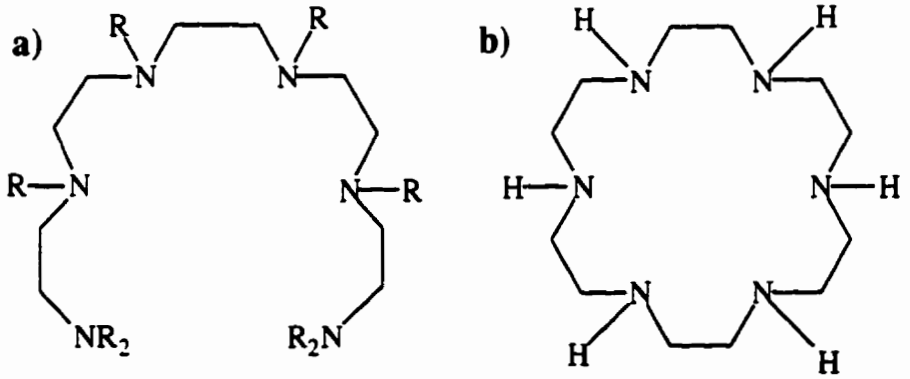

Figure 1.17 a) Aza-triflate Receptor[121] b) Hexacyclen: Macrocyclic Polyamine[81]

Urea[128-131] and thiourea[129,132] based receptors have been extensively studied as neutral analogs of the aforementioned guanidinium receptors. These receptors are weaker anion binders, due to the loss of charge pairing interactions, however they are useful in the study of pure structural recognition, isolated from the effects of ion pairing. As well, hydrogen bonding from the urea NH

is a potential model for the ubiquitous *in vivo* use of peptide amide NH units in creating hydrogen bonding molecular cavities.[133]

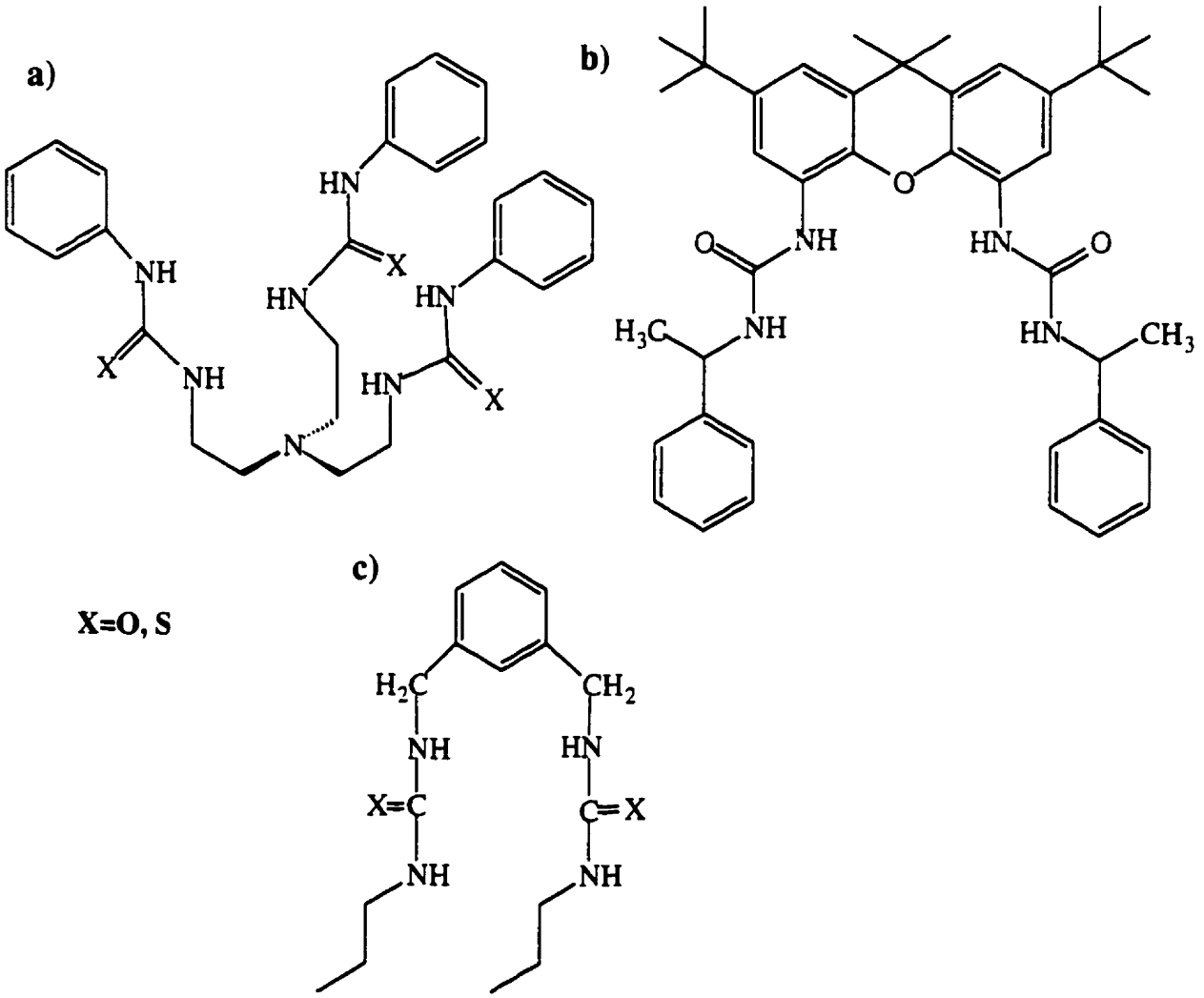

Figure 1.18 Examples of urea and thiourea hosts based upon a) tris(2-aminoethyl)amine[130] b) xanthene[89] and c) 1,3-bis(aminomethyl)benzene[132]

Guests such as phosphate, phosphate esters, sulfate, chlorine, and various carboxylates have been studied. As with charged receptors, binding strength and selectivity is very dependent upon solvent. Several synthetic strategies have been employed to increase binding. Different receptor backbones have been studied, including tris(2-aminoethyl)amine (Figure 1.18a)

tris(aminoethyl)cyclohexane,[130] xanthene[89] (Figure 1.18b), 1,3-bis(aminomethyl)benzene[132] (Figure 1.18c), as well as the large planar porphyrins.[134] The importance of appropriate cavity size and sufficient flexibility is clear. Polarization of the amide NH bond, caused by inductive effects of appropriately positioned electron withdrawing substituents such as NO_2, can significantly increase binding strength.[56,90] When guests incorporate aromatic units, the addition of π-stacking 'arms' to the receptor (Figure 1.18 a,b) can also increase binding strength.[132] Apparent difficulties in growing X-ray quality co-crystals with this type of neutral host has limited structural information, for the bound complexes, to molecular modeling and NOE data.

Research in the area of selective anion coordination is rapidly growing, resulting in a multitude of available hosts. Molecular calculations, regarding host-guest interactions, are also becoming widespread in the literature. As the computational treatment of solvent and electrostatic forces improves, this area will develop rapidly to aid in the rationale design of molecular receptors. Together, these expanding research fields will provide a base of knowledge regarding second sphere coordination that will direct this research field in the near future.

1.3 Statement of Intent

Research has shown, and continues to demonstrate the important role of tyrosine phosphorylation in cellular processes. Regulators of this process are vital tools in research and as potential therapeutic agents. pV complexes are easily synthesized, inexpensive, stable solids. However, pharmacologic usage invokes very rigorous requirements. Acid stability is necessary for orally active drugs to pass intact through the stomach for absorption into the blood stream. Peroxovanadium compounds, while stable in neutral and basic solutions, decompose at low pH. Lipid solubility, required to penetrate hydrophobic membranes, is also a highly valued characteristic for a potential drug. pV complexes have two defined regions, the highly reactive hydrophilic peroxo/oxo portion, and the more inert hydrophobic region of the ancillary ligand (Figure 1.19).

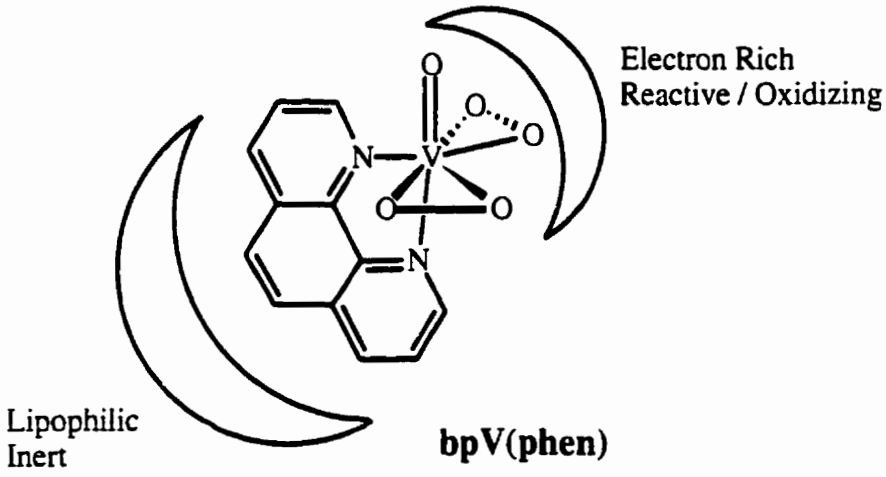

Figure 1.19 Representation of two distinct pV spheres

Second sphere coordination at the 'oxo' sites would shield the hydrophilic and bioactive portion of the molecule. Hydrogen bonding to the oxygen moieties of peroxovanadium species could protect the complex and increase its stability. As well, counterion effects also have potential for altering the solubility of the complex. Lipid solubility is a highly desirable characteristic due to the intracellular target, PTPases, for these hydrophilic molecules.

Other methods for delivery of peroxovanadium species, such as iontophoretic[135] and microencapsulation,[136] have been investigated. Second sphere coordination may provide a novel method for drug delivery, however the aim of the research reported here is to demonstrate second sphere coordination for pV complexes and to determine its effects upon physical properties, such as solubility, stability, and spectral characteristics. As well, the stability of a series of bpV and mpV complexes was assessed under the standard conditions for cell culture studies. This work is initiated with the long term goal of developing the pharmacologically ideal pV complex.

1.4 References

(1) Posner, B. I.; Faure, R.; Burgess, J. W.; Bevan, A. P.; Lachance, D.; Zhang-Sun, G.; Fantus, I. G.; Ng, J. B.; Hall, D. A.; Soo Lum, B.; Shaver, A. *J. Biol. Chem.* **1994**, *269*, 4596-4604.

(2) Hunter, T. *Cell* **1995**, *80*, 225-236.

(3) Colpas, G. J.; Hamstra, B. J.; Kampf, J. W.; Pecoraro, V. L. *J. Am. Chem. Soc.* **1996**, *118*, 3469-3478.

(4) Caravan, P.; Gelmini, L.; Glover, N.; Herring, F. G.; Li, H. L.; McNeill, J. H.; Rettig, S. J.; Setyawati, I. A.; Shuter, E.; Sun, Y.; Tracey, A. S.; Yuen, V. G.; Orvig, C. *J. Am. Chem. Soc.* **1995**, *117*, 12759-12770.

(5) Crans, D.; Keramida, A.; Amin, S.; Anderson, O.; Miller, S. *J. Chem. Soc. Dalton Trans.* **1997**, 2799-2812.

(6) Espinal, J. *Understanding Insulin Action*; Ellis Horwood Ltd.: Great Britain, 1989.

(7) Zongchao, J.; Barford, D.; Flint, A. J.; Tonks, N. K. *Science* **1995**, *268*, 1754-1758.

(8) Barford, D.; Flint, A. J.; Tonks, N. K. *Science* **1994**, *263*, 1397-1404.

(9) Stuckey, J. A.; Schubert, H. L.; Fauman, E. B.; Zhang, Z.-Y.; Dixon, J. E.; Saper, M. A. *Nature* **1994**, *370*, 571-575.

(10) Zhang, Z.; VanEtten, R. L. *J. Biol Chem.* **1991**, *266*, 1516-1525.

(11) Su, X.-D.; Taddei, N.; Stefani, M.; Giampietro, R.; Norlund, P. *Nature* **1994**, *370*, 575-578.

(12) Zhang, M.; Zhou, M.; Van Etten, R.; Stauffacher, C. *Biochemistry* **1997**, *36*, 15-23.

(13) Guan, K.; Dixon, J. E. *J. Biol. Chem.* **1991**, *256*, 17026-17030.

(14) Cotton, F. A.; Hazen, E. J.; Day, W.; Larsen, S.; Norman, J.; Wong, S.; Johnson, K. *J. Am. Chem. Soc.* **1973**, *2*, 2367-2368.

(15) Butler, A.; Clague, M. J.; Meister, G. E. *Chem. Rev.* **1994**, *94*, 625-638.

(16) Huyer, G.; Liu, S.; Kelly, J.; Moffat, J.; Payette, P.; Kennedy, B.; Tsaprailis, G.; Gresser, M.; Ramachandran, C. *J. Biol. Chem.* **1997**, *272*, 843-851.

(17) Willsky, G. R. In *Vanadium in Biological Systems*; N. D. Chasteen, Ed.; Kluwer Academic Publishers: Boston, 1990; pp 1-24.

(18) Goto, Y.; Kida, K.; Ikeuchi, M.; Kaino, Y.; Matsuda, H. *Biochem. Pharm.* **1992**, *44*, 174-177.

(19) Li, J.; Elberg, G.; Gefel, D.; Shechter, Y. *Biochemistry* **1995**, *34*, 6218-6225.

(20) Li, J.; Elberg, G.; Sekar, N.; Bin He, Z.; Shechter, Y. *Endcrinology* **1997**, *138*, 2274-2279.

(21) Shaver, A.; Ng, J. B.; Hall, D. A.; Posner, B. I. *Mol. and Cell. Biochem.* **1995**, *153*, 5-15.

(22) Bevan, P.; Drake, P.; Yale, J. F.; Shaver, A.; Posner, B. *Mol. Cell. Biochem.* **1995**, *153*, 49-58.

(23) Etcheverry, S.; Crans, D.; Keramidas, A.; Cortizo, A. *Arch. Biochem. Biophys.* **1997**, *338*, 7-14.

(24) Fantus, I.; Kadota, S.; Deragon, G.; Foster, B.; Posner, B. I. *Biochemistry* **1989**, *28*, 8864-8871.

(25) Krady, M.; Freyermuth, S.; Rogue, P.; Malviya, A. *FEBS Let.* **1997**, *412*, 420-424.

(26) Bourgoin, S.; Grinstein, S. *J. Biol. Chem.* **1992**, *267*, 11908-11916.

(27) Zick, Y.; Sagi-Eisenberg, R. *Biochemistry* **1990**, *29*, 10240-10245.

(28) Konstantos, J.; Kalatizis, G.; Vrachnou-Astra, E.; Katakis, D. *J. Chem. Soc. Dalton Trans.* **1985**. 2461-2468.

(29) Djordjevic, C.; Wampler, G. *J. Inorg. Biochem.* **1985**, *25*, 51-55.

(30) Djordjevic, C.; Wilkins, P. L.; Sinn, E.; Butcher, R. J. *Inorg. Chim. Acta* **1995**, *230*, 241-244.

(31) Drew, R. E.; Einstein, F. W. B. *Inorg. Chem.* **1973**, *12*, 829-835.

(32) Drew, R. E.; Einstein, F. W. B. *Inorg. Chem.* **1972**, *11*, 1079-1083.

(33) Crans, D.; Keramidas, S.; Hoover-Litty, H.; Anderson, O.; Miller, M.; Lemoine, L.; Pleasic-Williams, S.; Vandenberg, M.; Rossomando, A.; Sweet, L. *J. Am. Chem. Soc.* **1997**, *119*, 5447-5448.

(34) Bagno, A.; Conte, V.; Di Furia, F.; Moro, S. *J. Phys. Chem. A.* **1997**, *101*, 4637-4640.

(35) Cundari, T.; Sisterhen, L.; Stylianopoulos, C. *Inorg. Chem.* **1997**, *69*, 4029-4034.

(36) Campbell, N. J.; Dengel, A. C.; Griffith, W. P. *Polyhedron* **1989**, *8*, 1379-1386.

(37) Chaudhuri, M. K.; Ghosh, S. K. *Inorg. Chem.* **1984**, *23*, 534-537.

(38) Chaudhuri, M. K.; Ghosh, S. K. *Polyhedron* **1982**, *1*, 553-555.

(39) Bhattacharjee, M.; Chaudhuri, M. K.; Islam, N. S.; Paul, P. C. *Inorg. Chim. Acta* **1990**, *169*, 97-100.

(40) Rehder, D. *Angew. Chem. Int. Ed. Engl.* **1991**, *30*, 148-167.

(41) Chaudhuri, M. K.; Ghosh, S. K. *Inorg. Chem.* **1982**, *21*, 4020-4022.

(42) Chaudhuri, M.; Ghosh, S.; Islam, N. *Inorg. Chem.* **1985**, *24*, 2706-2707.

(43) Campbell, N. J.; Flanagan, J.; Griffith, W. P.; Skapski, A. C. *Trans. Met. Chem.* **1985**, *10*, 353-354.

(44) Djordjevic, C.; Puryear, B. C.; Vuletic, N.; Abelt, C. J.; Sheffield, S. J. *Inorg. Chem.* **1988**, *27*, 2926-2932.

(45) Schwendt, P.; Tyrselová, J.; Pavelcik, F. *Inorg. chem.* **1995**, *34*, 1964-1966.

(46) Einstein, F.; Batchelor, R.; Angus-Dunne, S.; Tracey, A. *Inorg. Chem.* **1996**, *35*, 1680-1684.

(47) Lapshin, A.; Smolin, Y.; Shepelev, Y.; Gyepesova, D.; Schwendt, P. *Acta. Cryst.* **1989**, *C45*, 1477-1479.

(48) Stomberg, R.; Szentivanyi, H. *Acta Chem. Scand.* **1984**, *A38*, 121-128.

(49) Sucha, V.; Sivak, M.; Tyrselova, T.; Marek, J. *Polyhedron* **1997**, *16*, 2837-2842.

(50) Morrison, R. T.; Boyd, R. N. *Organic Chemistry* , 3rd Ed. Allyn and Bacon, Inc.: Boston, 1973; pp 27-34.

(51) Raymo, F.; Stoddard, J. F. *Chem. Ber.* **1996**, *129*, 981-990.

(52) Philp, D.; Stoddart, J. F. *Angew. Chem. Int. Ed. Engl.* **1996**, *35*, 1154-1196.

(53) Sutherland, I. *Pure Appl. Chem.* **1989**, *61*, 1547-1554.

(54) Cram, D. J. *Angew. Chem. Int. Ed. Engl.* **1988**, *27*, 1009-1020.

(55) De Mendoza, J.; Gago, F. *Molecular Recognition of Dinucleotides and Amino Acids by Artificial Receptors Containing A Bicyclic Guanidinium Subunit*; Kluwer Academic Publishers: Netherlands, 1994, pp 77-99.

(56) Wilcox, C. S.; Kim, E.; Romano, D.; Kuo, L. H.; Burt, A. L.; Curran, D. P. *Tetrahedron* **1995**, *51*, 621-634.

(57) Bergeron, R. J. *J. Org. Chem.* **1987**, *52*, 1700-1703.

(58) Ando, I. *Polyhedron* **1991**, *10*, 1139-1141.

(59) Harada, A., Ying Hu, Shyoko Yamamoto, and Shigetoshi Takahashi *J. Chem. Soc. Dalton Trans.* **1988**, 729-732.

(60) Beer, P. D. *Chem. Commun.* **1996**, 689-696.

(61) Onda, M.; Yoshihara, K.; Koyano, H.; Ariga, K.; Kunitake, T. *J. Am. Chem. Soc.* **1996**, *118*, 8524-8530.

(62) Guillemette, V. M.Sc. Thesis, McGill University, 1997.

(63) Palet, C.; Muñoz, M.; Valiente, M.; Cynkowski, T.; Daunert, S.; Bachas, L. *Anal. Chim. Acta* **1997**, *343*, 287-294.

(64) Horman, I.; Dreux, B. *Anal. Chem.* **1983**, *55*, 1219-1221.

(65) Kamino, A. *Bull. Chem. Soc. Jpn.* **1996**, *69*, 3619-3631.

(66) Hosseini, M. W.; Lehn, J. M.; Jones, K.; Plute, K.; Mertes, K.; Mertes, M. *J. Am. Chem. Soc* **1989**, *111*, 6330-6335.

(67) Lehn, J. M. *Angew. Chem., Int. Ed. Engl.* **1988**, *27*, 113-158.

(68) Bernardo, A.; Stoddart, J. F.; Kaifer, A. *J. Am. Chem. Soc.* **1992**, *114*, 10624-10631.

(69) Perreault, D.; Cabell, L.; Anslyn, E. V. *Bioorg. Med. Chem.* **1997**, *5*, 1209-1220.

(70) Kirby, A. *Angew. Chem. Int. Ed. Engl.* **1996**, *35*, 707-724.

(71) Zubay, X. In ; pp 1009-1010.

(72) Oku, H.; Ueyama, N.; Nakamura, A. *Inorg. Chem.* **1997**, *36*, 1504-1516.

(73) Ogo, S.; Nakamura, S.; Chen, H.; Isobe, K.; Watanabe, Y.; Fish, R. *J. Inorg. Biochem.* **1997**, 296.

(74) Langer, R. *Science* **1990**, *249*, 1527-1533.

(75) Menger, F. M.; Johnston, D. E. J. *J. Am. Chem. Soc.* **1991**, *113*, 5467-5468.

(76) Menger, F. M. *Chem. Brit.* **1993**, *29*, 300-302.

(77) Maysinger, D.; Morinville, A. *Trends in Biotechnology* **1997**, *15*, 410-418.

(78) Ashnagar, A.; Culnane, P.; Easton, C.; Harper, J.; Lincoln, S. *Aust. J. Chem.* **1996**, *50*, 447-450.

(79) Delgado, R.; Virgili, A.; Garcia-Anton, J.; Parente, A. *J. Incl. Phen. Molec. Recog. Chem.* **1997**, *28*, 205-212.

(80) Benzing, T.; Tjivikua, T.; Wolfe, J.; Jr., R. J. *Science* **1988**, *243*, 267-277.

(81) Scheerder, J.; Engbersen, J.; Reinhoudt, D. *Recueil des Travaux Chimiques des Pays-Bas* **1996**, *115*, 308-321.

(82) Atwood, J.; Holman, K.; Steed, J. *Chem. Commun.* **1996**, 1401-1407.

(83) Dietrich, B.; Hosseini, M.; Lehn, J. M.; Sessions, R. *J. Am. Chem. Soc.* **1981**, *103*, 1282-1283.

(84) Hosseini, M.; Lehn, J. M. *Helvetica Chim. Acta* **1987**, *70*, 1312-1319.

(85) Peter, F.; Gross, M.; Hosseini, M.; Lehn, J. M. *J. Electroanal. Chem.* **1983**, *144*, 279-292.

(86) Dietrich, B.; Fyles, T.; Lehn, J. M.; Pease, L.; Fyles, D. *J. Chem. Soc. Chem. Comm.* **1978**, 934-936.

(87) Muller, G. *Angew. Chem. Int. Ed. Engl.* **1988**, *27*, 1516-1518.

(88) Kato, Y.; Conn, M.; Rebek, J. J. *J. Am. Chem. Soc.* **1994**, *116*, 3279-3284.

(89) Hamann, B.; Branda, N.; Rebek, J. J. *Tet. Lett.* **1993**, *34*, 6837-6840.

(90) Jeong, K. S.; Park, J.; Cho, Y. *Tet. Lett.* **1996**, *37*, 2795-2798.

(91) Fan, E.; Van Arman, S.; Hamilton, A. D. *J. Am. Chem. Soc.* **1993**, *115*, 369-370.

(92) Vicent, C.; Fan, E.; Hamilton, A. *Tet. Lett.* **1992**, *33*, 4269-4272.

(93) Williams, K.; Askew, B.; Ballester, P.; Buhr, C.; Jeong, K. S.; Jones, S.; Rebek, J. J. *J. Am. Chem. Soc.* **1989**, *111*, 1090-1094.

(94) Kimura, E., Yasuhiro Kuramoto, Tohru Koike, Haruto Fujioka, and Mutsuo Kodama *J. Org. Chem.* **1990**, *55*, 42-46.

(95) Fenniri, H., Mir Wais Hosseini and Jean-Marie Lehn *Helvetica Chimica Acta* **1997**, *80*, 786-803.

(96) Nakai, C.; Glinsmann, W. *Biochemistry* **1977**, *25*, 5636-5640.

(97) Rebek, J. J. *Science* **1987**, *235*, 1479-1482.

(98) Metzger, A.; Lynch, V.; Anslyn, E. V. *Angew. Chem.* **1997**, *109*, 911-914.

(99) Bayada, A.; Lawrance, G.; Maeder, M. *Inorg. Chim. Acta* **1997**, *254*, 353-359.

(100) Kurz, K.; Gobel, M. *Helv. Chim. Acta* **1996**, *79*, 1967-1979.

(101) Jubian, V.; Veronese, A.; Dixon, R. P.; Hamilton, R. D. *Angew. Chem., Int. Ed. Engl.* **1995**, *34*, 1237-1239.

(102) Schmidtchen, F. *Pure Appl. Chem.* **1989**, *61*, 1535-1546.

(103) Pierre, J.; Baret, P. *Chim. de France* **1982**,

(104) Dietrich, B.; Fyles, D.; Fyles, T.; Lehn, J. M. *Helv. Chim. Acta* **1979**, *62*, 2763-2785.

(105) Oost, T.; Filippazzi, A.; Kalesse, M. *Tetrahedron* **1997**, *53*, 8421-8438.

(106) Pallan, P. S.; Ganesh, K. N. *Biochem. Biophys. Res. Comm.* **1996**, *262*, 416-420.

(107) Ohata, N.; Masuda, H.; Yamauchi, O. *J. Inorg. Biochem.* **1997**, 452.

(108) Puspita, W.; Funahashi, Y.; Odani, A.; Yamauchi, O. *J. Inorg. Biochem.* **1997**, 294.

(109) Harrison, W.; Phillips, M. *Chem. Comm.* **1996**, 2771-2772.

(110) Wang, X.; Liu, H.; Xu, X.; You, X. *Acta. Cryst. A* **1992**, 77-79.

(111) Kneeland, D. M.; Ariga, K.; Lynch, V. M.; Huang, C.-Y.; Anslyn, E. V. *J. Am. Chem. Soc.* **1993**, *115*, 10042-10055.

(112) Albert, J. S.; Goodman, M. S.; Hamilton, A. D. *J. Am. Chem. Soc.* **1995**, *117*, 1143-1144.

(113) Echavarren, A.; Galan, A.; Lehn, J. M.; De Mendoza, J. *J. Am. Chem. Soc.* **1989**, *111*, 4994-5.

(114) Kim, D.; Park, J. *Bioorg. Med. Chem. Let.* **1996**, *6*, 2967-2970.

(115) Tamura, N.; Kajiki, T.; Nabeshima, T.; Yano, Y. *J. Chem. Soc. Chem. Comm.* **1994**, 2583-2585.

(116) Colpas, G. J.; Hamstra, B. J.; Kampf, J. W.; Pecoraro, V. L. *J. Am. Chem. Soc.* **1994**, *116*, 3627-3628.

(117) Hall, D. Ph.D. Thesis, McGill University, 1996.

(118) Wever, H.; Hemrika, W.; Renirie, R.; Barnett, P.; Messerschmidt, A.; Dekker, H. *J. Inorg. Biochem.* **1997**, 385.

(119) Sessler, J. L.; Andrievsky, A. *Chem. Eur. J.*, **1998** *4* 159-167.

(120) Potentiometric Anion Sensors

(121) Lee, H.; Yang, X.; McBreen, J. *J. Electrochem. Soc.* **1996**, *143*, 3825-3829.

(122) Ando, I.; Daisuke, I.; Kikujiro, U.; Kirondo, K. *Inorg. Chem.* **1994**, *33*, 5010-5014.

(123) Ando, I. e. *Inorganic Chemistry* **1996**, *35*, 3504-3508.

(124) Bianchi, A.; Micheloni, M.; Paoletti, P. *Pure & Appl. Chem.* **1988**, *60*, 525-532.

(125) Aguilar, J.; Garcia-Espana, E.; Guerrero, J.; Santiago, L.; Llinares, J.; Ramirez, J.; Soriano, C. *Inorg. Chim. Acta* **1996**, *246*, 287-294.

(126) Kimura, E.; Kodama, M.; Yatsunami, T. *J. Am. Chem. Soc.* **1982**, *104*, 3182-3187.

(127) Kimura, E.; Sakonaka, A.; Yatsunami, T.; Kodama, M. *J. Am. Chem. Soc.* **1981**, *103*, 3041-3045.

(128) Hughes, M.; Smith, B. *J. Org. Chem.* **1997**, *62*, 4492-4499.

(129) Nishizawa, S.; Bühlmann, P.; Iwao, M.; Umezawa, Y. *Tet. Lett.* **1995**, *36*, 6483-6486.

(130) Raposo, C.; Almaraz, M.; Martin, M.; Weinrich, V.; Mussón, M.; Alcázar, V. *Chem. Lett.* **1995**, 759-760.

(131) Kelly, R.; Kim, M. *J. Am. Chem. Soc.* **1994**, *116*, 7072-7080.

(132) Bühlmann, P.; Nishizawa, S.; Xiao, K.; Umezawa, Y. *Tetrahedron* **1997**, *53*, 1647-1654.

(133) Valiyaveettil, S.; Engbersen, J.; Verboom, W., Reinhoudt, D. *Angew. Chem. Int. Ed. Engl.* **1993**, *32* 900-901.

(134) Jagessar, R.; Burns, D. *Chem. Comm.* **1997**, 1685-1686.

(135) Brand, R.; Duensing, G.; Hamel, F. *Int. J. Pharm.* **1997**, *146*, 115-122.

(136) Unpublished results; Jesse B. Ng, Alan Shaver.

Chapter 2.0 Synthesis and Characterization of Peroxovanadium Host-Guest Complexes

2.1 Introduction

The first pV complexes were reported in by Hartcamp et al. in 1959.[1] Since this time over 60 new and interesting inorganic complexes have been reported (Table 2.1).

Table 2.1 – pV compounds

Abbrev.	Complex	δ (^{51}V)[a]	Reference (X-Ray)
bpV(phen)	$M[VO(O_2)_2(phen)]\cdot 3H_2O$ M=K,Na,Cs,NH_4,	-746	2
bpV(bipy)	$M[VO(O_2)_2(bipy)]\cdot 5H_2O$ M=K,Na,Cs,NH_4	-747	2, (3)b
bpV(ox)	$K_3[VO(O_2)_2(ox)]\cdot 2H_2O$	-739	2, 4, (5)
bpV(NH_3)	$NH_4[VO(O_2)_2(NH_3)]$	-711, -748, -753	6, (7)
mpV(2,6-pdc)	$NH_4[VO(O_2)(2,6\text{-pdc})(H_2O)]\cdot H_2O$	-598	1, (8)
mpV(pic)	$VO(O_2)(pic)(H_2O)_2$	-600	(9)
bpV(pic)	$K_2[VO(O_2)_2(pic)]\cdot 2H_2O$	-744	10, (11)
bpV(Me$_2$phen)	$K[VO(O_2)_2(4,7\text{-}Me_2phen)]\cdot 0.5H_2O$	-748	(12)
mp(but)V(2,6pdc)	$VO(OO\text{-}Bu^t)(H_2O)(2,6\text{-pdc})$	-597	(13)
mpV(ox)	$K_3[VO(O_2)(ox)_2]\cdot 0.5H_2O$	-592	(14)
mpV(picbipy)	$VO(O_2)(pic)(bipy)\cdot H_2O$	-579	(14)
mpV(picphen)	$VO(O_2)(pic)(phen)\cdot H_2O$	-581	15
bpV(OHpic)	$K_2[VO(O_2)_2(3\text{-}OHpic)]\cdot H_2O$	-741	(12)
bpV(Me$_4$phen)	$K[VO(O_2)_2(3,4,7,8\text{-}Me_4phen)]\cdot 5H_2O$	-745	11
bpV[bipy(CO_2^-)]	$K_3[VO(O_2)_2\{bipy\text{-}4,4'\text{-}(COO)_2\}]$	-747	16
bpV(CO_3)	$K_3[VO(O_2)_2(CO_3)]\cdot 3H_2O$	-762	4, 17, (18)
bpV(2,3-pdc)	$K_3[VO(O_2)_2(2,3\text{-pdc})]\cdot 2H_2O$	-743	19
bpV(Mephen)	$K[VO(O_2)_2(5\text{-}Mephen)]\cdot 2H_2O$	-743	20

bpV(NO_2phen)	$K[VO(O_2)_2(5\text{-}NO_2phen)]\cdot 2H_2O$	-739	(21)
	$M[VO(O_2)(IDA)]\cdot 0.5H_2O$; M: K, NH_4		(22)
	$K_2[VO(O_2)(cit)]_2\cdot 2H_2O$	-541, -548	(23)
bpV(2,4-pdc)	$K_3[VO(O_2)_2(2,4\text{-}pdc)]\cdot 3.25H_2O$	-743	(19)
bpV(2,5-pdc)	$K_3[VO(O_2)_2(2,5\text{-}pdc)]\cdot 2H_2O$	-742	19
bpV(NH_2phen)	$K[VO(O_2)_2(5\text{-}NH_2phen)]\cdot 0.5H_2O$	-744	20
mpV(OHpdc)	$NH_4[VO(O_2)(H_2O)(4\text{-}OH\text{-}2,6\text{-}pdc)]\cdot H_2O$	-599	
bpV(acetpic)	$K_3[VO(O_2)_2(3\text{-}acetpic)]\cdot 2H_2O$	-745	(19)
	$NH_4[VO(O_2)_2(isoquin)]\cdot 5H_2O$	-746	9
	$K_2[VO(O_2)_2(pzc)]\cdot xH_2O$	-732	8
	$K_2[VO(O_2)_2(3\text{-}NH_2pzc)]\cdot xH_2O$	-739	
	$M_2[VO(O_2)_2F]$ (M: Na, K, Rb, Cs, NH_4)		(24), 26
	$(NH_4)_3[VO(O_2)_2F_2]$		(25)
	$Cs[VO(O_2)(EDTA)]\cdot H_2O$		27
	$M_3[VO(O_2)(EDTA)]\cdot 2H_2O$; M: Na, NH_4		28
	$H[VO(O_2)(H_2O)(2,6\text{-}pdc)]\cdot H_2O$		28
	$M_2[VO(O_2)(HEDTA)]\cdot 4H_2O$		29
	$M_2[VO(O_2)_2(CH_3COO)]$	-705	28
	$(bipyH)[\{VO(O_2)_2(bipy)\}_2]\cdot xH_2O_2\cdot(6-x)H_2O$ (x:0.5)		(30)
	$(bipyH)[VO(O_2)_2(bipy)]\cdot(3+x)H_2O_2\cdot(2-x)H_2O$ (x:0.4)		(31)
	$PPh_4^+[VO(O_2)(pic)_2]\cdot H_2O$	-596[c]	25
	$VO(O_2)(quin)L$ (L: EtOH, DMF, DMSO, THF)		32
	$M_3[VO(O_2)_2(HPO_4)]\cdot 2H_2O$ (M: K, NH_4)		33
	$K_2[V_2O_2(O_2)_3(cystH)_2]\cdot H_2O$		34
	$M_2[V(O_2)_3F]$ (M: Na, K, NH_4)		35

	$M[V(O_2)_3]$ (M: Na, K)		36
	$NH_4[VO(O_2)(malato)]\cdot H_2O$		27
	$Na_2[VO(O_2)(nta)]\cdot 5H_2O$	-549	(38)
	$K_2[VO(O_2)(nta)]$		37, (39)
	$Ba[VO(O_2)(nta)]\cdot 3H_2O$		(40)
	$M_2[VO(O_2)_2Cl]$ (M: Na, K, NH_4)		37
	$M_2[V(O_2)_3Cl]$ (M: Na, K, NH_4)		37
	$M[VO(O_2)_2(glyH)]\cdot H_2O$ (M: K, NH_4)		41
	$K[VO(O_2)_2(H_2O)_x]$ (x: 1 or 2)	-688 to -695	4, 42
	$(NH_4)_4[\{VO(O_2)_2\}_2O]$		(43)
	$(NH_4)_3[\{VO(O_2)_2\}_2OH]\cdot H_2O$		44
	$K_2[\{VO(O_2)_2\}_2(\mu\text{-nicH})]\cdot H_2O$		45
	$CymH_2[V_2O_2(O_2)_4H_2O]\cdot 2H_2O$		(46)
	$V_2O_2(O_2)_3(glyH)_2(H_2O)_2$	-574	41
mpV(tpa)	$[VO(O_2)tpa]ClO_4$	-543[d]	33
mpV(bpg)	$[VO(O_2)bpg]$	-551	(33)
mpV(ADA)	$K[VO(O_2)ada]$	-744	(33)
bpV(imidazole)	$(C_4H_5N_2)[VO(O_2)_2(imidazole)]$	-565	(47)
mpV(Hheida)	$K[VO(O_2)_2(Hheida)]$	-562	(33)

[a] All ^{51}V NMR spectra were obtained on aqueous solutions on a Varian XL-300 NMR spectrometer operating at 78.891 MHz. Chemical shifts are in parts per million (ppm) with respect to $VOCl_3$ as external reference at 0.00 ppm, with negative shifts being upfield.

[b] NH_4^+ salt.

[c] In CD_3OD.

d In CD_3CN

2.2 Characterization

^{51}V NMR has proven immeasureably useful in the characterization of pV complexes. NMR spectroscopy with this quadrupolar nucleus, I=7/2, is facile due to its relatively low nuclear electric quadrupole moment, 99.76% abundance and rapid rate of relaxation, 7.0492×10^7 rad s^{-1} T^{-1}.[48,49] Reasonable spectra of pV species at concentrations as low as 1mM can be obtained in less than 10 minutes of aquisition time. A pure, mononuclear pV complex displays a single ^{51}V NMR resonance frequency, upfield from the $VOCl_3$ (0.00 ppm) reference. Bisperoxovanadium species, $VO(O_2)_2(L)$, generally lie in the region from -700 to -760 ppm, while monoperoxo species, $VO(O_2)(L)$, are associated with the region from -550 to -620 ppm.[50]

pV complexes have also been characterized through infra red spectroscopy, using the symmetric metal-oxo (υ V=O), symmetric peroxo (υ O-O), as well as the symmetric and antisymmetric metal-peroxo (υ V-O_2) stretching frequencies. Splitting of the peroxo band (υ O-O), does not occur for the mpV species but does for bpV complexes. The metal-peroxo stretching bands vary considerably, depending upon the type and coordination geometry of the ancillary ligand.[51] UV-Vis electronic spectra can also be measured for pV complexes. A broad LMCT band, for the peroxo (π_υ^*) ---> (δs^*) $V(5^+)$ charge transfer, can be noted in the vicinity of 330 nm for bpV, and 450 nm for mpV species. These transitions are only weakly sensitive to the overall complex structure. A second transition, the $(\sigma)\pi_\upsilon^*$ ---> $\delta\sigma^*$, is more difficult to characterize due to its high energy, 190-200 nm, and is rarely reported in the literature.[52] Definitive structural information is obtained solely through X-ray crystallography. The large number of crystallographically characterized pV species is testament to the highly crystalline nature of these complexes (see Table 2.1 for structural references).

The counterion may exhibit second sphere coordination. New pV complexes incorporating protective or chelating counterions, possibly via hydrogen bonding to the oxo and peroxo ligands, could alter the physical properties of these highly active complexes. The vast amount of research in the growing field of supramolecular or host-guest chemistry provides a good basis for the development of molecular hosts for pV guests. Special interest was paid to the large class of host species designed to coordinate phosphate and phosphate ester species.

2.3 Results/Discussion

A series of guanidinium (Figure 2.1-Ia) and polyammonium cationic hosts (Figure 2.1-Ib), as well as neutral bis and tris urea hosts, (Figure 2.1-Ic) were synthesized. Figure 2.1-II is a complete set of pV guest structures and abbreviations, bpV (Figure 2.1-IIa) and mpV (Figure 2.1-IIb). Solid bpV and mpV adducts were obtained and characterized with both guanidinium and polyammonium hosts in an attempt to decipher the role of the host in determining the physical and spectroscopic properties of the pV guest. Representative complexes, bg$(CH_2)_4$•mpV(nta), mG(diamino)•mpV(2,6-pdc), bG(piper)•bpV(pic), and pA(putrescine)•bpV(bipy), were characterized crystallographically in order to determine the nature of these host-guest interactions, in the solid state.

2.3.1 Guanidinium•bpV - Host•Guest Complexes

Eleven bisguanidinium (bG), one triguanidinium (tG), and two monoguanidinium (mG), cationic hosts were synthesized (see experimental) or purchased (Figure 2.1-Ia). Simple ion exchange reactions, from aqueous solutions equimolar in guanidinium host and bpV guest, invariably precipitated a solid guanidinium•bpV adduct. The time taken to precipitate, crystallinity, percentage yield, solubility and color (yellow-orange) of all final products varied with the host. Table 2.2 shows all possible characterization data for the guanidinium adducts prepared from bpV(phen).

Figure 2.1 - I a - Guanidinium Hosts

bG(CH_2)$_n$

n=2,3,4,6,10

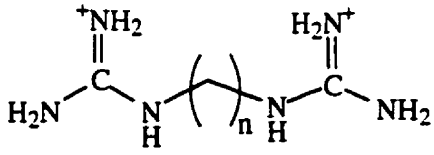

bG(phenyl)

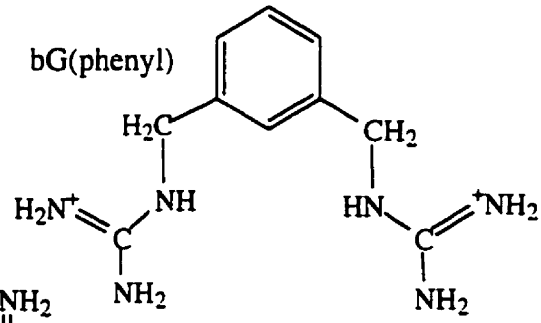

bG(oxo)

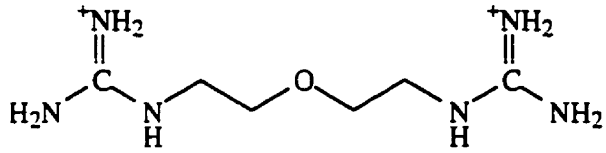

bG(OH)

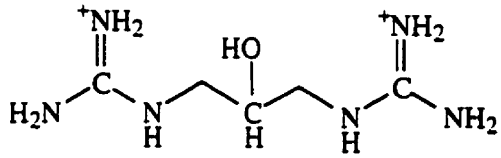

bG(dioxo)

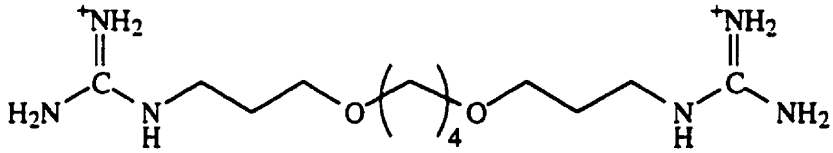

bG(piper)

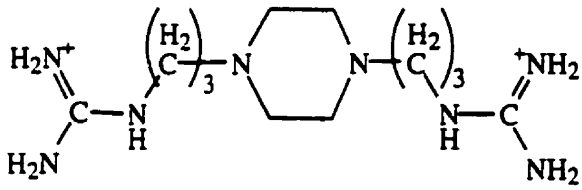

mG(diphenyl)

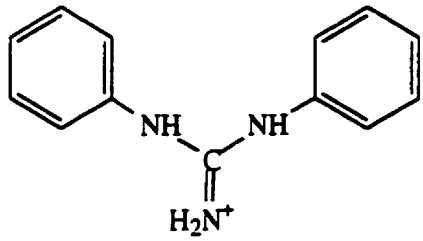

mG(diamino)

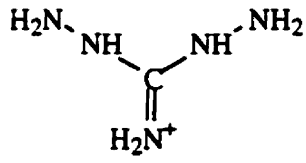

tG(tris)

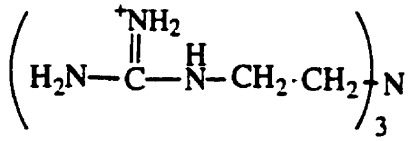

bG(bis)

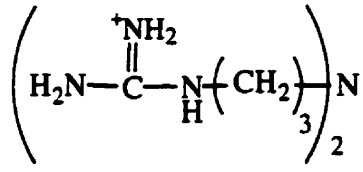

Figure 2.1 - Ib - Protonated Amine Hosts

Putrescine•2H$^+$

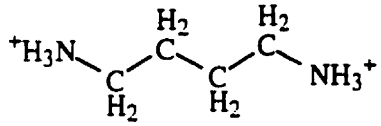

Spermidine•3H$^+$

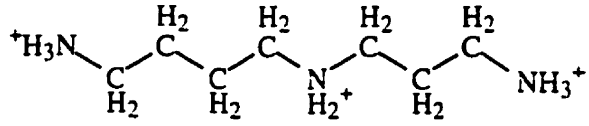

Spermine•4H$^+$

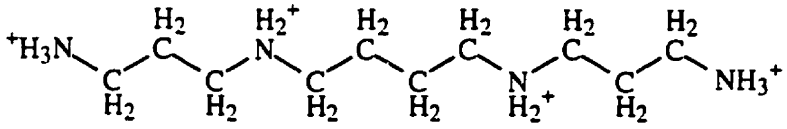

Bispropyl•3H$^+$

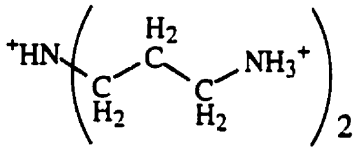

Tris•4H$^+$

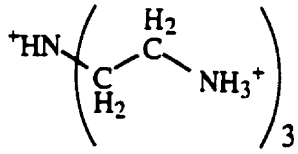

Figure 2.1 - Ic - Polyurea Hosts

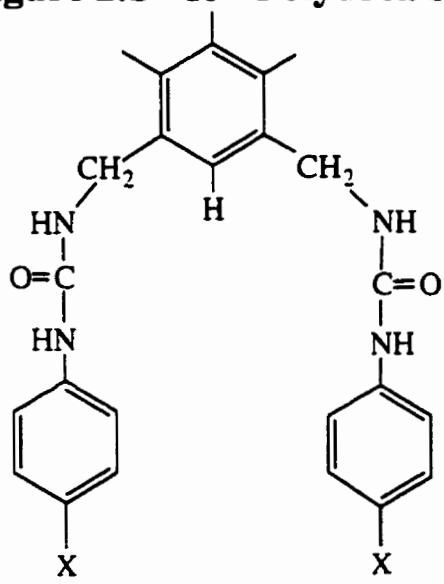

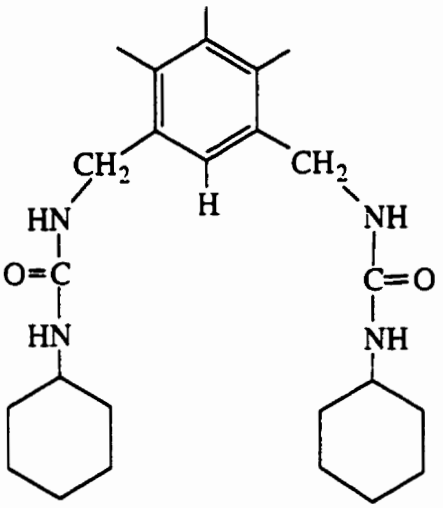

bU(phenyl) X=H
bU(OMe) X=OMe
bU(COOEt) X=COOEt
bU(Cl) X=Cl

bU(cyclohexyl)

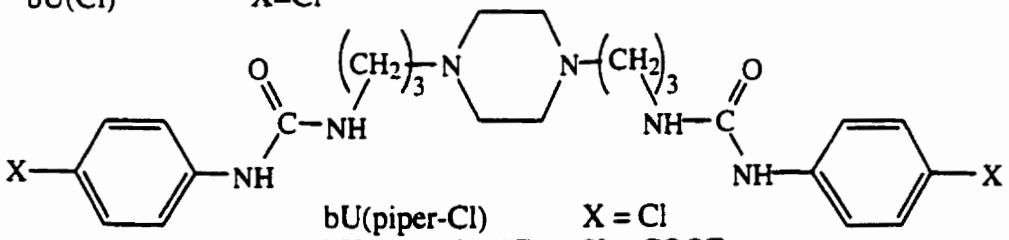

bU(piper-Cl) X = Cl
bU(piper-COOEt) X = COOEt

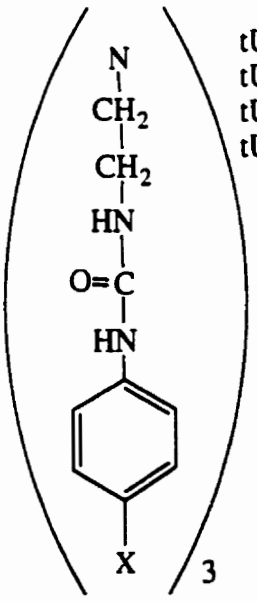

tU(phenyl X= H
tU(OMe) X = OMe
tU(COOEt) X = COOEt
tU(Cl) X = Cl

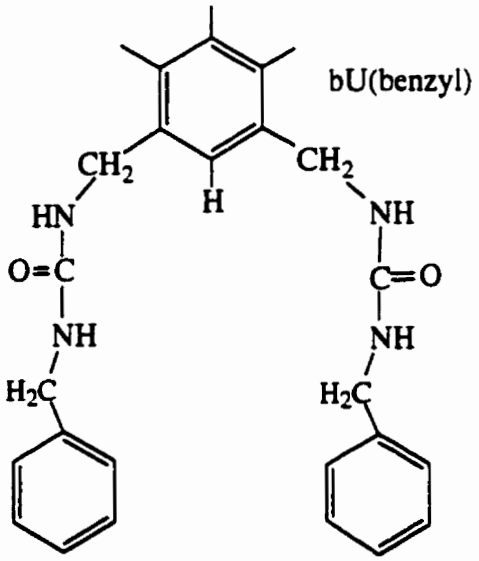

bU(benzyl)

Figure 2.1 - I d Other Hosts

1,3-Bis(3-pyridylmethyl)-2-thiourea

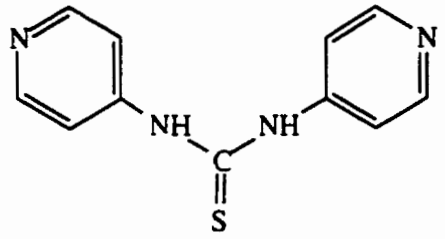

Cyclobis(paraquat-p-phenylene)

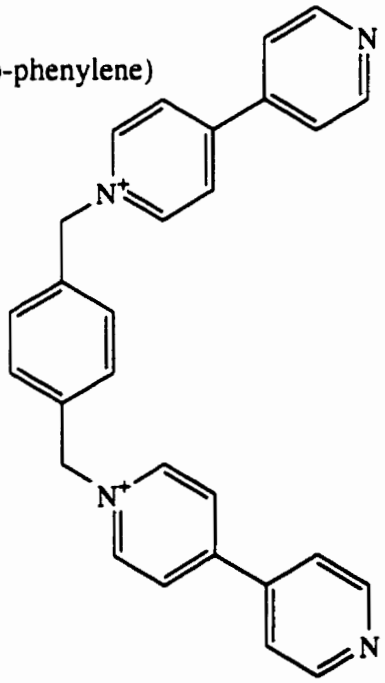

Figure 2.1 - IIa - bpV Guests

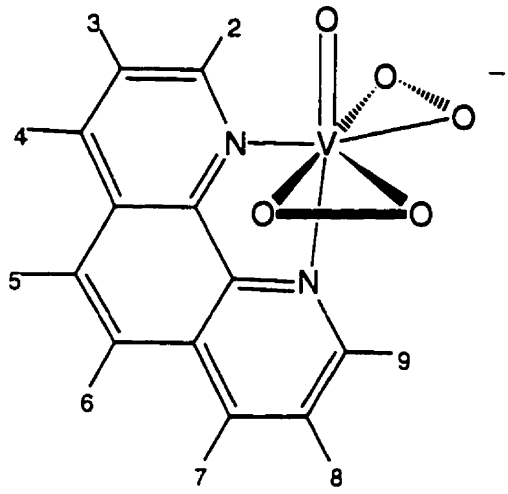

bpV(phen)

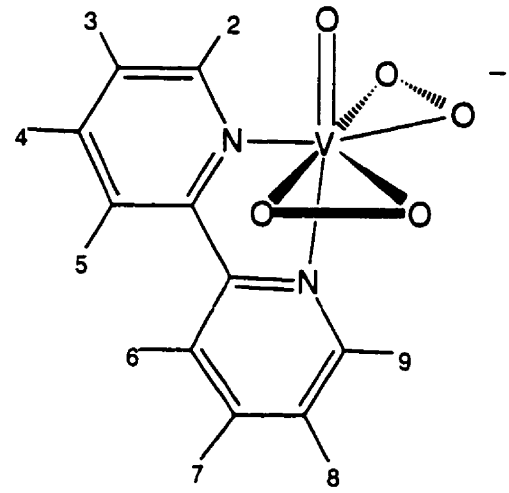

bpV(bipy)

bpV(phen)	2-9 = H
bpV(NO_2-phen)	5 = NO_2; 2-4, 6-9 = H
bpV(NH_2-phen)	5 = NH_2; 2-4, 6-9 = H
bpV(Me-phen)	4 = Me; 2-3, 5-9 = H
bpV(Me_2-phen)	4,7 = Me; 2,3,5,6,8,9 = H
bpV(Me_4-phen)	3,4,7,8 = Me; 2,5,6,9 = H

bpV(bipy)	2-9 = H
bpV((COO^-)$_2$bipy)	4,8 = (COO-); 2,3,5-8,9 = H

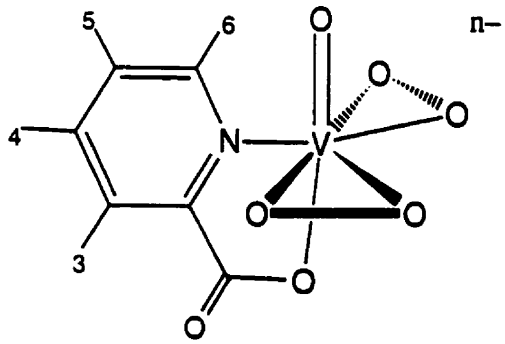

bpV(pic)

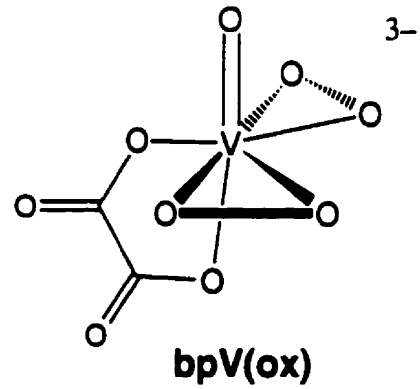

bpV(ox)

bpV(pic)	2-5 = H, n=2
bpV(3-OH-pic)	3 = OH; 4-6 = H, n=2
bpV(2,3-pdc)	3 = (COO^-); 4-6 = H, n=3
bpV(2,4-pdc)	4 = (COO^-); 3,5,6 = H, n=3
bpV(2,5-pdc)	5 = (COO^-); 3,4,6 = H, n=3
bpV(acet-pic)	3 = (CH_2COO^-); 4,5,6 = H, n=3

Figure 2.1 - IIb - mpV Guests

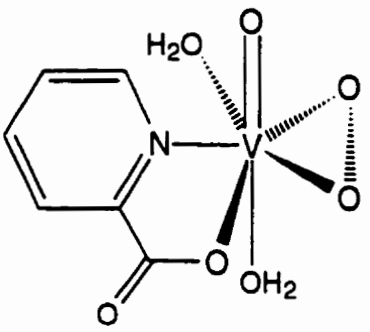

mpV(pic)

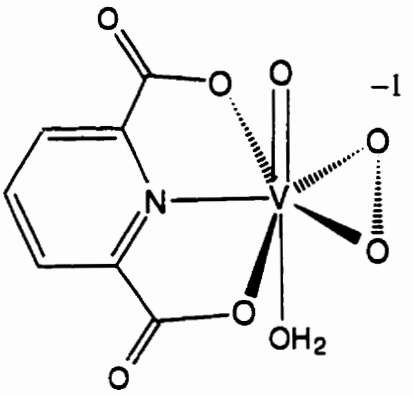

mpV(2,6-pdc)

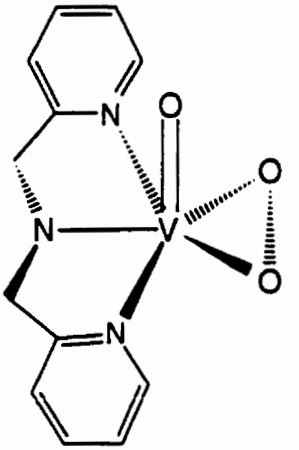

mpV(bpg)

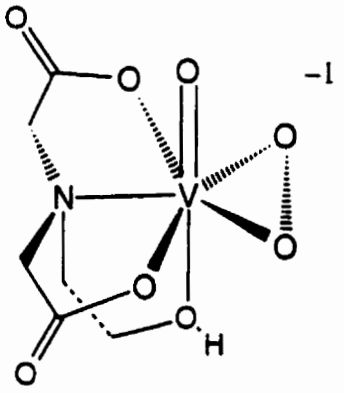

mpV(Hheida)

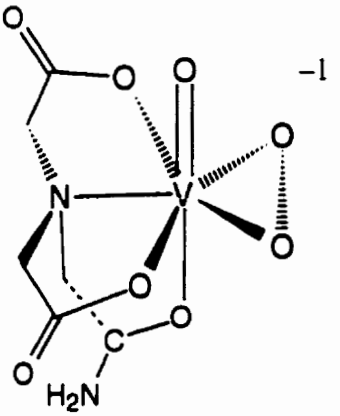

mpV(ada)

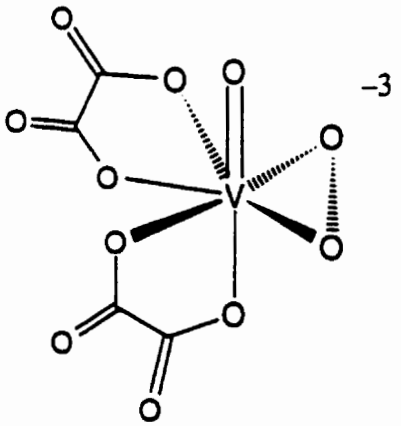

mpV(ox)$_2$

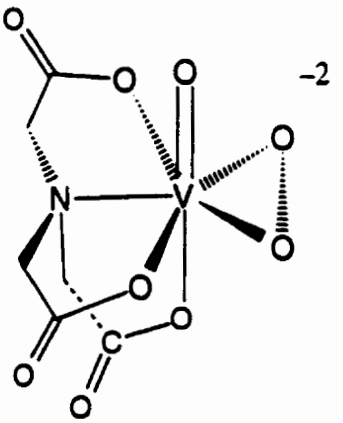

mpV(nta)

Table 2.2 Solid Host•Guest Complexes obtained with bpV(phen)

Host (H)	^{51}V[a] NMR (ppm)	^{1}H NMR[b] (ppm)	Yield[c] (%)	Ratio bpV:H
bG(phenyl)	-742	**d**	57	-
$bG(CH_2)_2$	-747	**d**	59	-
$bG(CH_2)_3$	-744	**d**	48	-
$bG(CH_2)_4$	-746 [a]	**d**	54	-
$bG(CH_2)_6$	-745	**d**	90	-
$bG(CH_2)_{10}$	-746 -557	**d**	74	-
bG(PIPER)	-746	3.17, t, 2H 2.9-2.39, m, 4H 1.73, m, 2H 1.15, t, 2H	32	2 : 1
bG(BIS)	-744	**d**	14	-
tG(TRIS)	-745	3.19, t 2.63, t	34	1 : 0.8
bG(OH)[f]	-743	3.92, sept, 1H 3.27, m, 2H 3.18, m, 2H	<10	2:1
bG(dioxo)[f]	-746	3.51, m, 4H 3.22, t, 2H 1.82, q, 2H 1.58, br.m, 2H	80	2:1
bG(oxo)[f]	-742	**d**	31	-

a All ^{51}V spectra are taken in 20% D_2O/H_2O unless otherwise noted, in the case of multiple resonances, peaks are listed in order of relative integration
b All ^{1}H spectra are taken in D_2O unless otherwise noted; signals for bpV(phen) are excluded for simplicity
c Yield refers to solid product, collected, washed and dried in vacuo
d Data not obtained due to product insolubility
e CD_3OCD_3
f crystalline material

Ion exchange of bpV(phen), $K[VO(O_2)_2(phen)]•2H_2O$, with the short alkane chain bG hosts, such as $bG(CH_2)_n$ n=2,3,4, immediately produced pale yellow powders. These were fairly insoluble in water and organic solvents, and ^{51}V NMR spectra required lengthy aquisition times. These spectra proved that a bpV species was present. The drastly changed solubility is consistent with cation exchange. Extreme insolubility of this nature

has previously been attributed to strong hydrogen bonding within the isoelectronic hydroxylamino-oxovanadium(V) complexes.[53a] Increasing the size of the guanidinium host, as with bG(piper); bG$(CH_2)_n$ n=6, 10; and tG(tris), led to a slower precipitation of solid bpV adducts. This increase in host size did not increase organic solubility. However, bG(piper) and tG(tris) produced water soluble, ^1H NMR characterizable complexes (Table 2.2).

Similar trends, in the physical properties of these products, dependent upon the host of use, were also found with other bpV complexes, such as bpV(bipy) and bpV(pic) (Figure 2.1-IIa). The more highly charged bpV anions, such as bpV(ox) and the bpV(pdc) series, (Figure 2.1-IIa), produced solid guanidinium adducts that showed two or more ^{51}V NMR peaks. These likely result from hydrolysis of the ancillary ligand. For simplicity, as over 120 solid precipitates were obtained, this discussion centered upon the guanidinium adducts of bpV(phen). In the case of bG(piper), large single crystals were isolated from a 1:1 solution with bpV(pic). The single crystal X-Ray structure of the bG(piper)•bpV(pic) complex was obtained.

2.3.1.1 Structural Features: bG(piper)•bpV(pic) Host•Guest Complex

The crystal structure of the bG(piper)•bpV(pic) adduct (Figure 2.2) clearly shows multiple hydrogen bonding interactions between the host and guest (Table 2.3). For reference purposes, hydrogen bonding distances for NH-O systems typically range from 2.80 Å to 3.15 Å.[53b] The anion and cation are present in a one to one ratio, with half of two cations contributing to each individual host-guest unit. The bpV(pic) anion in this complex, previously characterized crystallographically as its potassium salt,[11] shows no significant deviations in bond lengths and angles. For complete tables of bond lengths and angles, structural parameters as well as a packing diagram, see appendix A.1.

Figure 2.2 ORTEP of bG(piper)•bpV(pic)•2H_2O

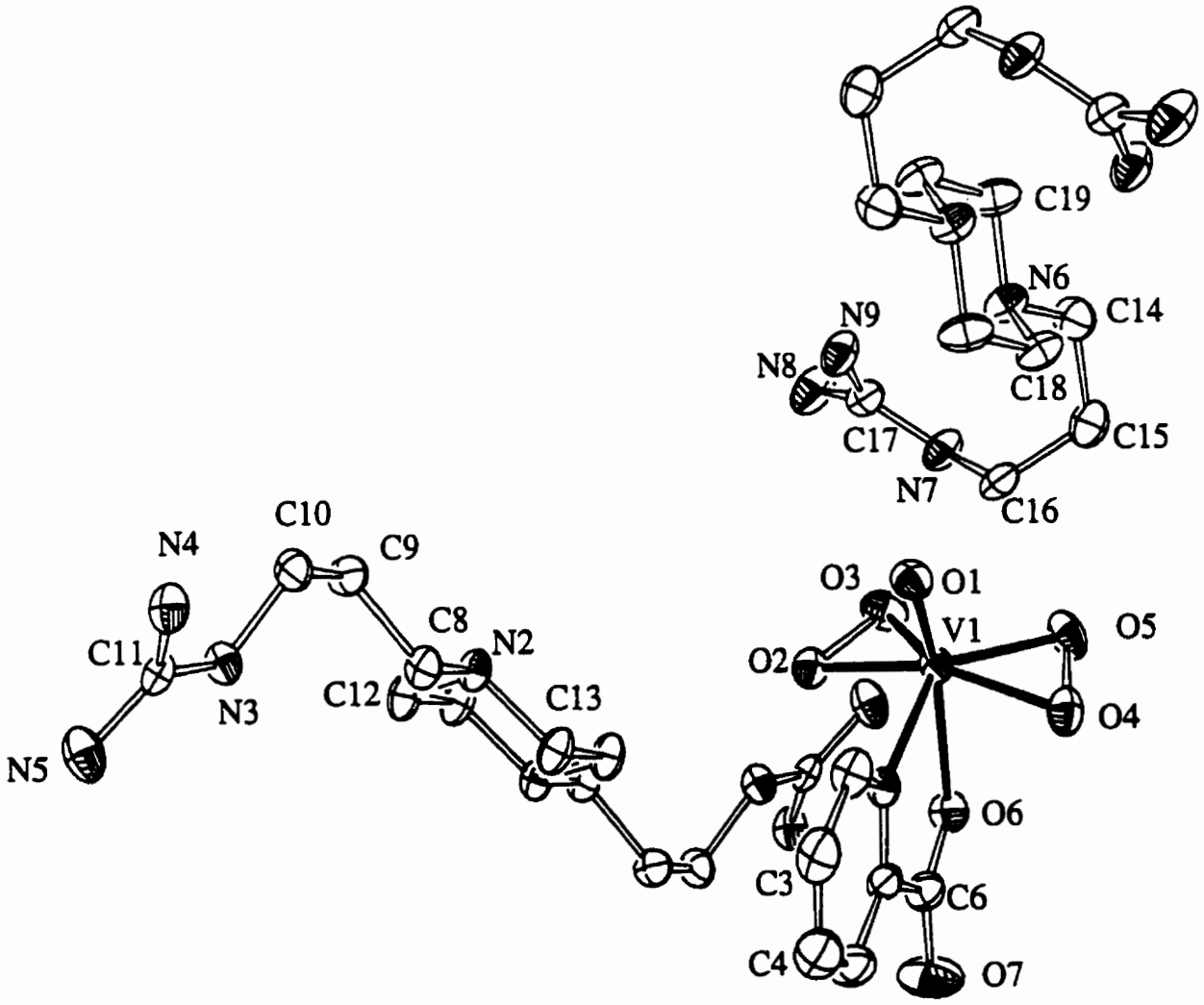

Figure 2.3 Hydrogen bonding in bG(piper)•bpV(pic)•2H_2O

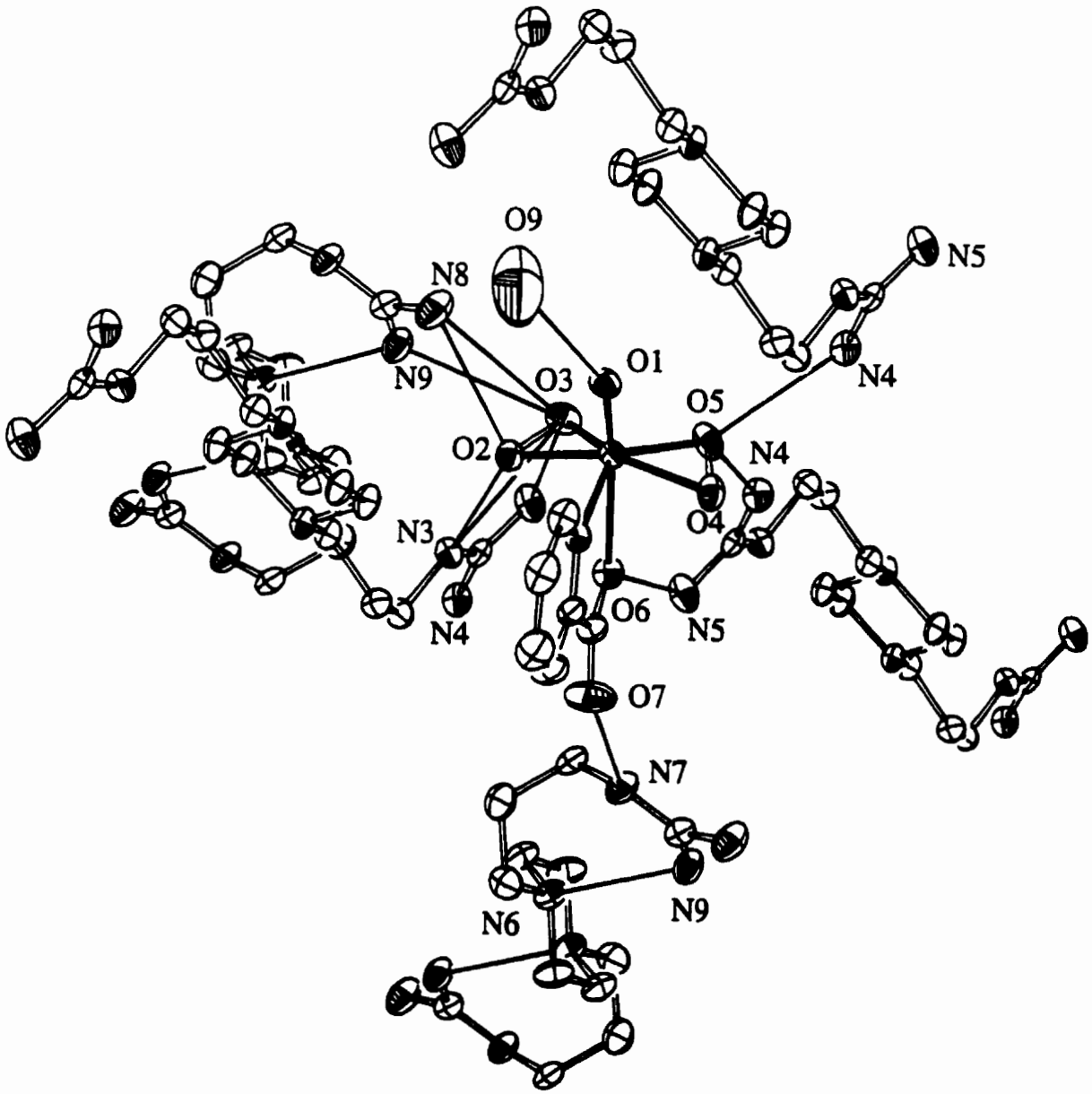

Table 2.3 Bond distances and angles related to hydrogen bonding in bG(piper)•bpV(pic)

D-H...A	D-H	H....A	D...A	< D-H...A	Symmetry Transformation
N3-H33..O2	0.92(4)	1.88(4)	2.789(5)	172(4)	
N3-H33..O3	0.92(4)	2.49(4)	3.306(5)	148(3)	
N4-H44A..O5	0.99(5)	1.97(5)	2.927(5)	162(4)	x+1, y, z
N4-H44B..O5	0.78(4)	2.06(4)	2.767(5)	151(4)	-x+2, -y+2, -z+1
N5-H55A..O3	0.83(4)	2.18(4)	2.985(6)	164(3)	
N5-H55B..O6	0.73(5)	2.32(5)	3.044(5)	169(5)	-x+2, -y+2, -z+1
N7-H77..O7	0.92(4)	1.93(4)	2.827(5)	166(4)	x-1, y-1, z
N8-H88A..O2	0.87(5)	2.03(5)	2.888(5)	169(4)	x-1, y, z
N8-H88A..O3	0.87(5)	2.48(5)	3.251(6)	147(3)	x-1, y, z
N8-H88B..O8	0.77(4)	2.35(4)	3.083(7)	160(4)	-x, -y+1, -z+1
N9-H99A..O3	0.73(4)	2.65(4)	3.346(7)	159.6(7)	x-1, y, z
N9-H99B..N6	0.88(6)	2.09(6)	2.941(7)	164(5)	
O8-HO8A..O9	1.03(4)	1.96(5)	2.715(8)	128(3)	-x+1, -y+1, -z+1
O8-HO8B..N2	1.13(7)	1.74(7)	2.871(6)	172(5)	x-1, y, z-1
O8-HO8C..O7	1.13(6)	1.83(6)	2.911(6)	158(5)	-z+1, -y+2, -z+1

Three of the peroxo (O2, O3, O5) and two ancillary ligand (carboxyl and carbonyl) oxygen atoms (O6, O7) accept hydrogen bonds from four individual counterions in the lattice. A single peroxo oxygen atom (O4) does not accept any hydrogen bonds. There are two distinct conformations of the bG(piper) counterion in the crystal lattice, displayed clearly in Figure 2.2. The more extended cation, (N2, N3, N4, N5) lacking intramolecular hydrogen bonding, forms two hydrogen bonds to the anion, from H44A-N4 to the peroxo oxygen atom O5 (2.927 Å) and H55B-N5 to O6 (3.044 Å), the carboxyl group oxygen atom

coordinated to the vanadium centre. This cation also forms intermolecular hydrogen bonds to the peroxo oxygen atoms O2 and O3. The single hydrogen atom of N3 (N3-H33) is in close contact with both peroxo oxygen atoms O2 (2.789Å) and O3 (3.306 Å). The hydrogen atom of N5, H55A-N5 is in contact with the peroxo oxygen atom O3 (2.985 Å).

The second type of cation (N6, N7, N8 and N9) forms both intermolecular and intramolecular hydrogen bonds. With one guanidinium unit (N7, N8 and N9), hydrogen atom H99B-N9 acts as an intramolecular donor (2.941 Å) to the unprotonated nitrogen atom (N6) of the piperazine ring. The second hydrogen atom of N9, H99A-N9, forms an intermolecular hydrogen bond (3.346 Å) to the peroxo atom O3. Nitrogen atom N8, upon the same guanidinium unit, forms two intermolecular hydrogen bonds (2.888 and 3.251 Å) from its hydrogen atom N8-H88A to the peroxo oxygen atoms O3 and O2, respectively.

Notable within these contacts are the hydrogen bonds between the peroxo group O2-O3 and the two NH_2 groups, N3 and N5, of a single guanidinium unit. This spacial arrangement is similar to that displayed between phosphate and guanidinium (Figue 1.13), with one hydrogen upon each nitrogen forming a bond to one of two adjacent oxygen atoms.

This compound crystallized with two water molecues but the thermal motion of both molecules made it difficult to determine their positions and hydrogen bonding. On one water molecule (O8), the hydrogen atoms are disordered with one site fully occupied with hydrogen bonding to the second water molecule (O9). The second hydrogen atom of O8 is disordered over two sites to form either a H-bond to N2 (2.871 Å) or O7 (2.911 Å). The second water molecule (O9) exhibited much higher thermal motion and no hydrogen atoms were located, although the oxygen atom is within hydrogen bonding distance (2.715 Å) of the oxo ligand (O1) (Figure 2.3).

Thus, the intermolecular contacts in this host-guest system are spread throughout the crystal and not limited to a single host interacting with one guest (Figure 2.3). This type of 1:1 complexation would likely require a more rigid, preorganized host.

2.3.1.2 Guanidinium•bpV - Host•Guest Complexes: Polar Substituents

This structure shows that complexation occurs between the bG host and the oxophilic portion of the bpV molecule (Figure 1.19). The introduction of polar functional groups onto either the bpV ancillary ligand or the host backbone might improve aqueous solubility. bpV complexes, such as bpV($(CO_2^-)_2$-bipy), bpV(acet-pic) or bpV(NO_2-phen) (Figure 2.1-IIa) address this issue, however they hydrolyse easily and the polar groups introduce unwanted ancillary ligand interaction with the guanidinium hosts, which limited their use.

Preferably, polar groups could be placed upon the backbone of the bG host, as with bG(dioxo), bG(oxo) and bG(OH) (Figure 2.1-Ia). This did slow the precipitation of the bG•bpV adducts. Highly crystalline, rather than powdered, bpV(phen) complexes were isolated with all three oxophilic hosts. As well, the polar groups increased water solubility, enabling reasonable ^{1}H NMR spectra to be obtained (Table 2.2.1). All ^{1}H NMR characterized complexes of bpV(phen) were, with the exception of the tG(tris) counterion, identified as the 1:2 bG•bpV electroneutral species. While progress was made in fully characterizing these solids, allowing for potential use in biochemical assays, no UV-Vis, ^{1}H and ^{51}V NMR data, obtained from MeOD/MeOH or D_2O/H_2O solutions, detected association of the bpV anion with its counterion. For this reason, no interaction studies (solution state, ie. full titrations) were undertaken with these host-guest systems.

Ionic association in solution is in direct competition with solvation and water solvates ions, H-bond donors and acceptors very well. The demonstration of second sphere coordination in water requires a host that is strongly preorganized, highly rigid, and capable of

multipoint binding.[54] Aqueous recognition has also been shown in the case where hydrophobic forces play an important role.[55,56]

2.3.2 pA•bpV - Host•Guest Complexes

Five polyammonium salts (Figure 2.1-Ib) were studied as potential counterions for bpV anions. Counterion exchange with bpV complexes was attempted from water solutions. If a solid product precipitated within twenty four hours, pure pA•bpV adducts, characterizable via ^{1}H and ^{51}V NMR, were obtained. Solutions left beyond this time period decomposed to a common, weakly water soluble, red crystalline vanadium complex (^{51}V NMR ~ 596ppm). Polyammonium salts (pkA~7.0) are more acidic than guanidinium salts (pKa~13)[57] and could transfer a proton to a pV complex. This decomposition pathway has been documented for pV complexes in acidic solutions.[58] The putrescine•$2H^{+}$•$(bpV(bipy))_2$ adduct was obtained as large single crystals and its single crystal X-ray structure was measured.

2.3.2.1 Structural Features: putrescine•$2H^{+}$•$(bpV(bipy))_2$•H_2O

The putrescine adduct of bpV(bipy) crystallized with a single molecule of hydration (Figure 2.4). Hydrogen bonds are evident between both the polyamine host, the water molecule and the bpV guest (Table 2.4). The water molecule forms strong hydrogen bonds (2.841 Å) to the protonated amine (N3) as well as to one oxygen atom of the peroxo ligand (O5) (2.914 Å). The protonated amine also acts as a hydrogen bond donor to the O2, O3 and O5 peroxo oxygen atoms, at distances of 2.731 Å, 2.866 Å, 2.735 Å respectively. The crystal structure of the bpV(bipy) anion has also been determined, as its ammonium salt.[59] There are no significant differences in the bond lengths and angles for the anions in these two different salts. For complete tables of bond lengths and angles, structural parameters as well as a packing diagram, please see appendix A.2.

Figure 2.4 ORTEP of putrescine•$2H^+$•$(bpV(bipy))_2$•H_2O

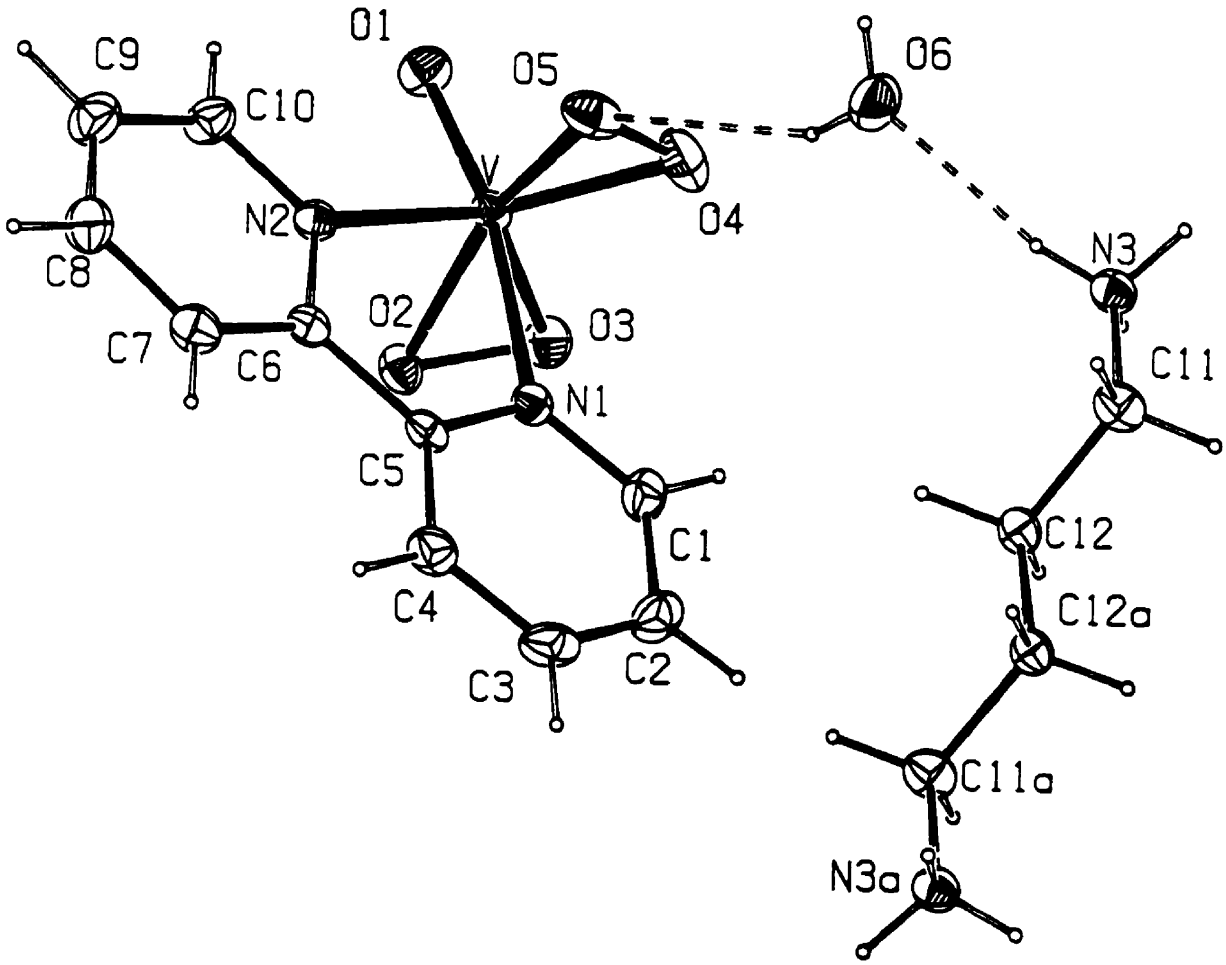

ORTEP view of C12 H17 N3 O6 V

with the numbering scheme adopted. Ellipsoids drawn at

40% probality level. Hydrogens represented by sphere of arbitrary size.

Table 2.4 Bond distances and angles related to the hydrogen bonding for putrescine•$2H^+$•$(bpV(bipy))_2$•H_2O

D-H...A	D-H	H...A	D...A	< D-H...A	Symmetry Transformation
O6-H6A...O5	0.821(43)	2.176(44)	2.914(4)	150(4)	
O6-H6B...O3	0.760(44)	2.113(45)	2.866(4)	171(5)	1+x, y, z
N3-H3A...O6	0.914(43)	1.873(43)	2.735(4)	156(4)	1.5-x,0.5+y,0.5-z
N3-H3C...O2	0.850(40)	1.984(41)	2.821(5)	168(3)	
N3-H3C...O2	0.899(44)	1.871(45)	2.731(4)	160(4)	0.5-x,0.5+y,0.5-z

2.3.3 Guanidinium•mpV - Host•Guest Complexes

mpV complexes are water and DMSO soluble, and the neutral and monoanionic complexes are DMF and often CH_3CN soluble. This increased solubility, versus bpV complexes, allowed for more diversity in studying their complexation with guanidinium and polyammonium salts. Many mpV species (Figure 2.1-IIb) were employed in this work, however solid guanidinium adducts were obtained only with the highly charged, di and tri anioinic mpV species, mpV(nta) and mpV(ox). A single exception, mpV(2,6-pdc), produced extremely large, thermally sensitive, single crystals with the mG(diamino) host. These single crystals were studied by ^1H and ^{51}V NMR, UV-Vis and low temperature X-ray crystallography.

2.3.3.1 Structural Features: mG(diamino)•mpV(2,6-pdc) Adduct

The monoguanidinium adduct of mpV(2,6-pdc) formed large, thermally sensitive, anhydrous crystals (Figure 2.5). The mpV(2,6-pdc) anion has been previously characterized by X-ray crystallography as its ammonium salt.[8] Comparison of the two structures shows that the anion's bond lengths and angles do not deviate significantly. For complete tables of bond lengths and angles, structural parameters as well as a packing diagram, please see appendix A.3.

Figure 2.5 ORTEP of [mG(diamino)][$VO(O_2)$(2,6-pdc)]

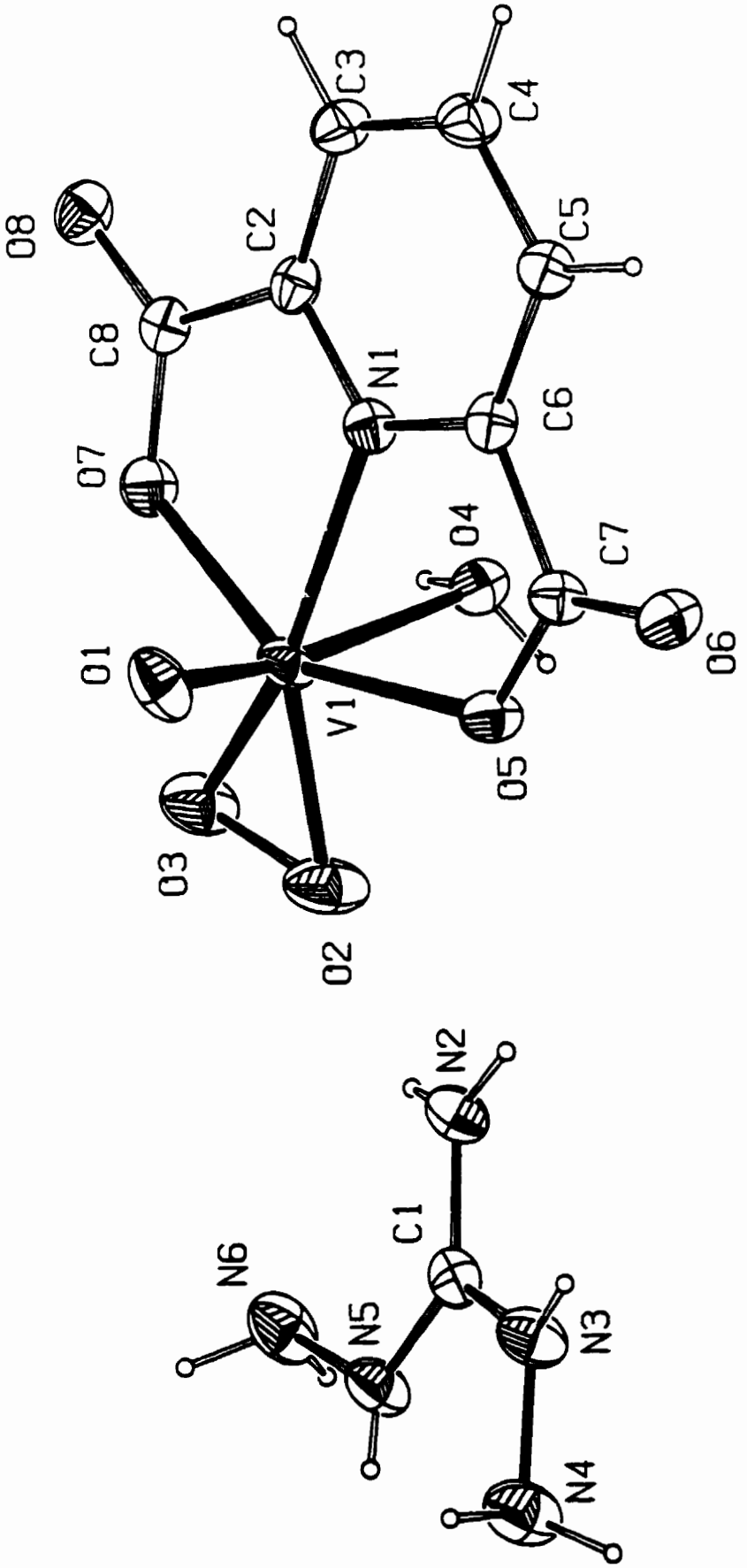

Multiple hydrogen bonds occur between the monoguanidinium host and the mpV guest (Table 2.5). One oxygen atom of the peroxo ligand (O2) is in contact (2.955 Å) with one proton (H22A) of the guanidinium nitrogen atom(N2). The other proton (H22B) acts as a hydrogen bond donor (3.064 Å) to the oxygen atom (O4) of the coordinated water molecule. A second guanidinium nitrogen atom (N3) also has a proton involved in hydrogen bond donation (2.882 Å) to the carboxylate oxygen atom (O8) of the ancillary ligand. The third guanidinium nitrogen atom (N5) has a single hydrogen atom (H55) which forms both an intra (2.609 Å) and an intermolecular (2.806 Å) hydrogen bond, to the adjacent amino nitrogen atom (N4) and to the apical oxo ligand (O1), respectively. This amino group (N4, H44A, H44B) also forms one intramolecular hydrogen bond (3.403 Å) between hydrogen (H44A) and the second amino group nitrogen atom (N6) and one intermolecular bond (3.022 Å) between hydrogen atom (H44B) and the oxygen atom (O7). This oxygen atom (O7) is also accepting a hydrogen bond (3.245 Å) from an amino group hydrogen atom (N6, H66B). The second proton on this amino group (H66A) forms a single hydrogen bond (2.879 Å) to the opposing carboyxlate oxygen atom (O6).

Two of the shortest hydrogen bonds (2.703 and 2.788 Å, respectively) in the structure are intermolecular in nature, extending from both protons of the water ligand. One proton (H4B) acts as a hydrogen bond donor to the carboxylate oxygen atom (O6) of the 2,6-pyridinedicarboxylate ligand. The second water proton (H4A) interacts similarly with the second 2,6-pdc carboxylate oxygen atom (O8). A view of this structure (Figure 2.6), with emphasis upon these hydrogen bonding interactions, shows the intricate network of inter and intramolecular bonding between the cations and the anions.

Figure 2.6 Cation-Anion Interactions within [mG(diamino)][$VO(O_2)$(2,6-pdc)]

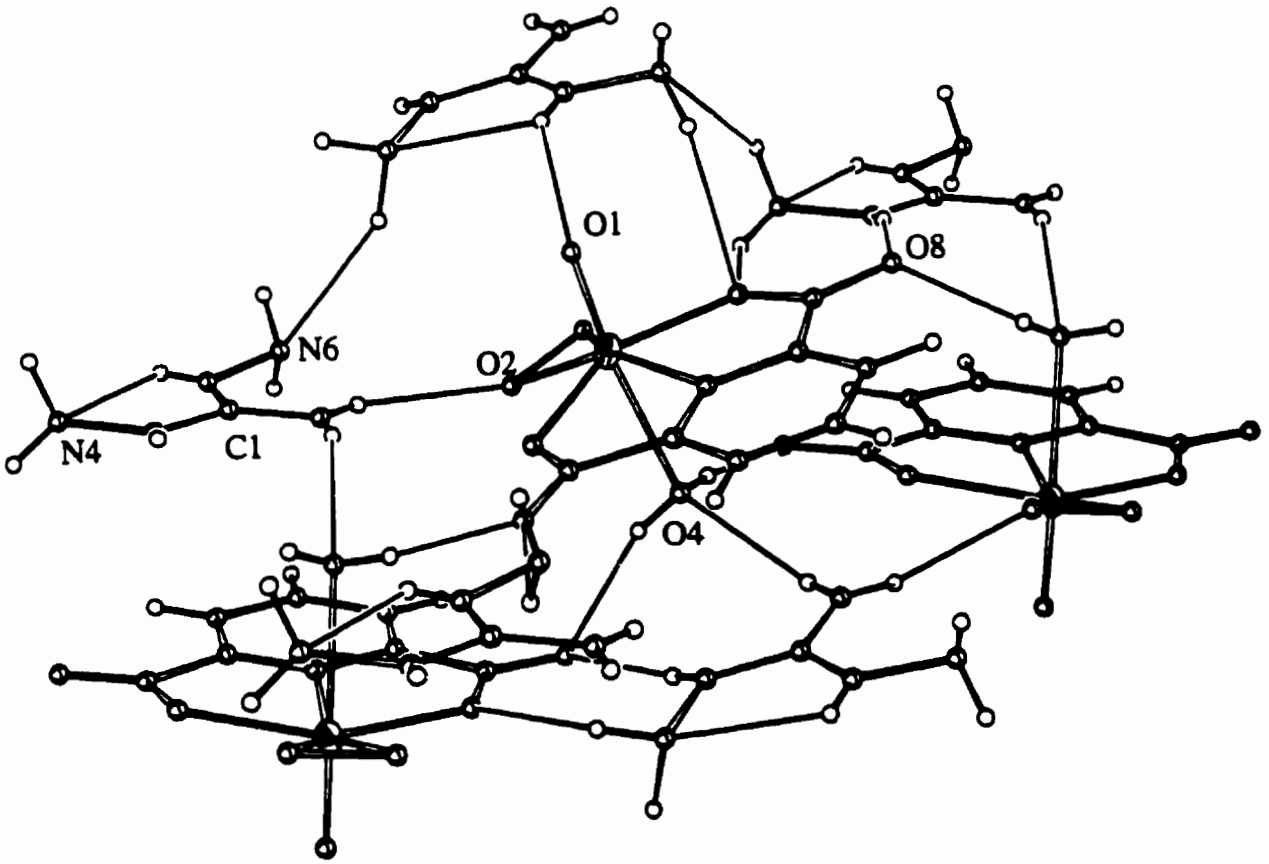

Table 2.5 Bond distances (Å) and angles (°) related to the hydrogen bonding for mG(diamino)•mpV(2,6-pdc)

D-H...A	D-H	H...A	< D-H...A	D...A	Symmetry Transformation
O4-H4A...O8	0.81	2.07	148.1	2.788	-x+1,y-1/2,-z+1
04-H4B...O6	0.82	1.89	171.7	2.703	-x+1,y+1/2,-z+1
N2-H22A...O2	0.77	2.26	150.8	2.955	
N2-H22B...O4	0.80	2.34	150.3	3.064	-x+1,y-1/2,-z+1
N3-H33...O8	0.79	2.11	165.7	2.882	x, y-1, z
N4-H44A...N6	1.06	2.43	151.8	3.403	-x, y-1/2, -z
N4-H44B...O7	0.92	2.32	133.2	3.022	x, y-1, z
N5-H55...O1	0.69	2.24	140.3	2.806	-x, y-1/2, -z
N5-H55...N4	0.69	2.28	111.0	2.609	-
N6-H66A...O6	0.84	2.41	116.2	2.879	x, y, z-1
N6-H66B...O7	0.86	2.40	166.8	3.245	-x, y-1/2, -z

2.3.3.2 mpV(nta)

A series of solid products was obtained from mpV(nta) and the bG(CH_2)n, n=2-4, and bG(phenyl) hosts. These complexes were all isolated from 1:1 solutions, were characterized by elemental analysis, ^{51}V, ^{1}H, ^{13}C NMR, UV-Vis and IR spectroscopy, and identified as pure, hydrated, electroneutral complexes. All of the bG•mpV(nta) salts were soluble in DMSO and DMF. They showed slight shifts in their ^{1}H and ^{51}V NMR spectra, versus the starting Na^+ salt. As well, all of the bG•mpV(nta) adducts were darker in color. The single crystal X-ray structure of bG(CH_2)$_4$•mpV(nta) was obtained as a representative of bG-mpV solid state interactions (Figure 2.7). No pure solid products were obtained with the larger bG hosts, such as bG(piper), and bG(CH_2)$_n$; n=6, 10, however, a pure solid was isolated with tG(tris).

2.3.3.2.1 Structural Features: bG$(CH_2)_4$•mpV(nta)

mpV(nta) has been characterized crystallographically as its K^+ [60,61], Na^+ [38] and Ba^{2+} [40] salts. Slight variations in the bond lengths and bond angles of the anion have been noted for these salts; however, with respect to the structure of bG$(CH_2)_4$•mpV(nta) (Figure 2.7), no significant changes were found. The molecule sits on a mirror plane with V1, O1 and N1 on this plane. In the complex, one of the CH_2-CO_2 groups of nta (C1, C2, O3 and O4) is situated very slightly off the mirror plane. As the space group does not contain this symmetry, disorder occurs between two sites of equal occupation on each side of the plane. The counter-ion is disordered over two sites, with occupancies equal to 0.62 and 0.38. Complete tables of bond lengths and angles, structural parameters and a packing diagram, are included in the appendice A.4.

Figure 2.7 ORTEP of dianion mpV(nta) (host omitted for clarity, see Figure 2.8)

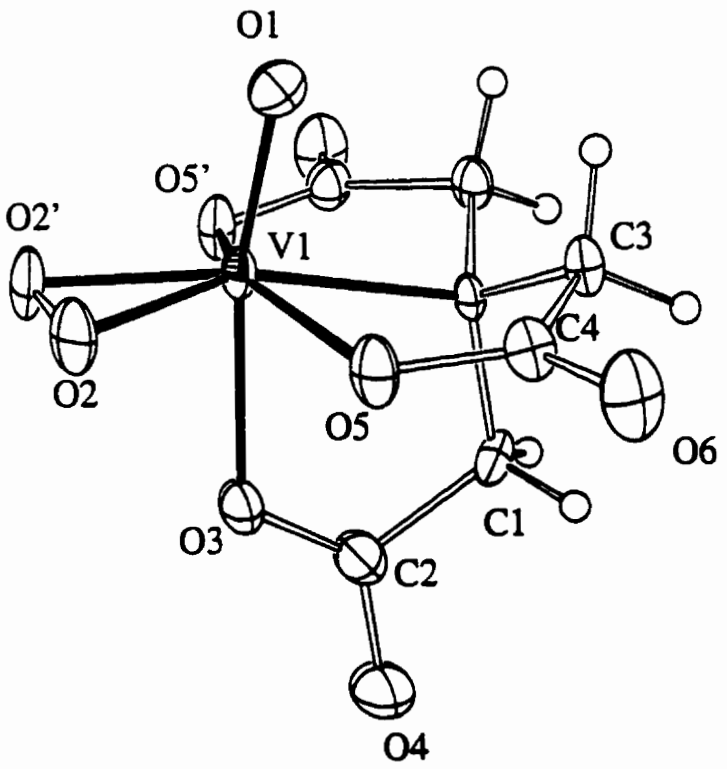

Hydrogen bonding exists at several sites between the bG host and mpV guest (Table 2.6). The strongest intermolecular bonds (2.865 Å, 2.872 Å) result from interactions of the hydrogen atoms of N4 and N3 with the carboxylate oxygen atom O6. The apical oxo ligand (O1) accepts a hydrogen bond (2.895 Å) from the hydrogen atom of N2 upon the bisguanidinium host. As well, two of the carboxyl oxygen atoms, O5 and O3 of nta, also accept hydrogen bonds from protons upon atoms N2 and N3, (2.902 and 3.019 Å respectively) of two separate host molecules. The peroxo ligand is also involved, accepting weaker hydrogen bonds from the bG host (3.025 and 3.147 Å) from the H-N3A and H-N2B hydrogen atoms, respectively. These intermolecular interactions are pictorally represented in Figure 2.8. Hydrogen bonding, while predominant throughout the crystal, is not localized (ie. one guest interacting with a single host), an important feature of the solid state structure of many host-guest complexes.

Table 2.6 Bond Distances and Angles Related to Hydrogen Bonding for $bG(CH_2)_4$•mpV(nta)

D-H..Acceptor	D - H	H...A	D...A	D - H... A	Symmetry Transformation
N2-HN2B..O3	0.860	2.177	3.019(3)	165.95(9)	-x, -y+1, -z
N2-HN2A..O1	0.860	2.163	2.895(4)	142.81(10)	-x, -y+1, -z
N3-HN3B..O6	0.860	2.105	2.872(4)	148.29(10)	x, y, z
N3-HN3A..O5	0.860	2.054	2.902(3)	169.02(10)	-x+1, -y+1, -z
N4-HN4..O6	0.860	2.073	2.865(4)	152.76(9)	x, y, z
N3-HN3A..O2	0.860	2.641	3.025(4)	108.4(1)	1-x, 1-y, -z
N2-HN2B..O2	0.860	2.756	3.147(4)	109.3(1)	1-x, 1-y, -z

Figure 2.8 Hydrogen Bonding in $bG(CH_2)_4$•mpV(nta)

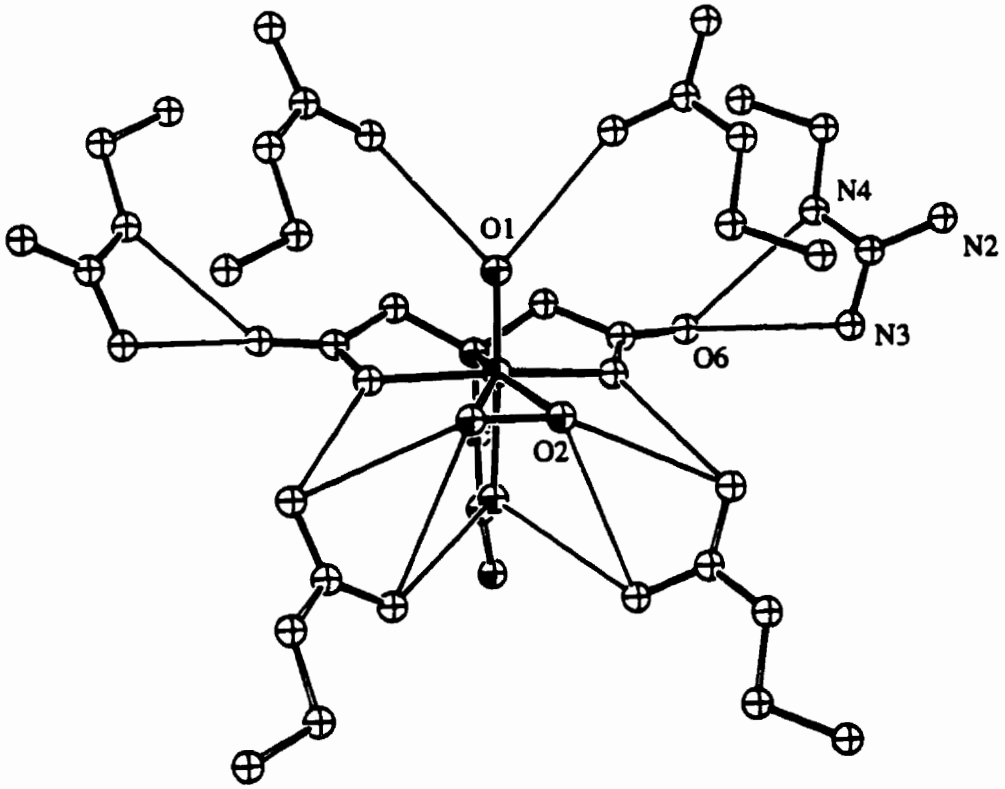

2.3.3.3 mpV(ox)

Solid pA and bG adducts of mpV(ox) were obtained with the spermine, bG$(CH_2)_n$; n= 4, 6, and tG(tris) hosts. The absence of protons on the oxalato ligand led to difficulties in determining the complex stoichiometries. In all cases, the adducts formed were lighter in color and DMSO soluble. The solid products decomposed within hours at room temperature and several days at 5°C.

2.3.4 Other Hosts

Three other types of hosts, B-cyclodextrin hydrate, 1,3-bis(3-pyridylmethyl)-2-thiourea and cyclobis(paraquat-p-phenylene) (Figure 2.1-Id), were prepared or purchased and studied as hosts for various pV guests. No interactions were ever noted betweeen bpV or mpV complexes and the macromolecular cyclodextrins, no precipitation occurred over a period of several days at 5°C. The aqueous bpV guest solutions decomposed to vanadate. Both the neutral thiourea and the cationic paraquot based hosts reacted immediately with all bpV complexes to form several uncharacterized vanadium species.

2.3.5 $N(R)_4^+$•bpV Complexes

Solid tetraalkylammonium salts of bpV complexes were synthesized to increase the organic solubility of bpV complexes. The following complexes, $[Et_4N][VO(O_2)_2(3,4,7,8\text{-}Me_4\text{-}phen)]\bullet 2H_2O$, $[Et_4N][VO(O_2)_2(phen)]\bullet 2H_2O$, $[Me_4N][VO(O_2)_2(phen)]\bullet XH_2O$, and $[Et_4N][VO(O_2)_2(4,7\text{-}Me_2phen)]\bullet 4H_2O$ were isolated and characterized. All of these salts were stable and soluble in water, methanol and ethanol. The Et_4N^+ salts were also soluble, but unstable, in chloroform at room temperature. Decomposition was easily followed (^1H NMR) by observing the increasing concentration of free ancillary ligand. Methyl substitution of the phenanthroline ligand produced a more robust complex; chloroform stability increased in the series $VO(O_2)_2(phen)<VO(O_2)_2(4,7\text{-}Me_2phen)<VO(O_2)_2(3,4,7,8\text{-}Me_4\text{-}phen)$. This points to an electronic effect, by the donor methyl groups, which may

improve stability within non protic environments. The tetramethylphenanthroline bpV complex was stable in $CHCl_3$ for 2 to 3 hours at room temperature. The less substituted phenanthroline bpV complexes decomposed slowly enough at 0°C to permit characterization. In chloroform, these compounds have ^{51}V NMR chemical shifts near δ=-685 ppm, significantly upfield relative to previously reported aqueous bpV species δ=-740 ppm. These Et_4N^+ salts were also soluble but unstable in nitromethane, DMF, DMSO and acetonitrile. There have been no reports of chloroform soluble stable bpV species. Attempts to produce R_4N^+ salts; where R=Me, Et, Butyl, with any other bpV dianions, such as bpV(pic), were unproductive.

2.3.6 Polyurea (bU and tU) Hosts (Figure 2.1-Ic)

A series of seven bU and five tU hosts were prepared in an attempt to isolate hosts capable of hydrogen bonding, that were soluble in non protic solvents. Urea based hosts had been previously noted to bind halide,[62] carboxylate[63] and phosphate[62],[64] anions. While none of the synthesized hosts proved soluble in pure chloroform, they were used in studies of second sphere coordination in non protic solvents, discussed in Chapter 3. All attempts to produce and characterize the pure solid 1:1 host guest complexes of bU•bpV(Me_4-phen) adducts, were unsuccessful. In general, crystal structure data for the reported (solution state) polyurea host•guest complexes, is lacking.[64]

2.4 Conclusions

Representative crystal structures were obtained for the bG•bpV, bG•mpV, pA•bpV, mG•mpV interactions. The guanidinium functionality interacts strongly with bpV species, leading to insolubility. In the solid state, hydrogen bonding of various hosts at the peroxo, oxo and carboxylate sites of the anions. These interactions are assumed to be responsible for the large counterion effect on the solubility of the salts.

A chloroform soluble and stable bpV species, $[Et_4N][VO(O_2)_2(3,4,7,8\text{-}Me_4\text{-}phen)]\cdot 2H_2O$, was isolated and characterized. This complex, and the series of neutral bU and tU hosts, enabled traditional host-guest interaction studies (titrations, NOESY, VT-NMR) to be carried out in media of low polarity (see Chapter 3).

2.5 Experimental: Synthesis

2.5.1 General

2.5.1.1 Chemicals

All compounds, with the exception of 2,2' dipicolylamine, which was purchased from TCI chemicals, were supplied by Aldrich Canada Inc., and used as received. Distilled water was used in all preparations. Anhydrous DMSO was purchased from Laboratoire MAT. All other solvents were ACS reagent grade, from various suppliers. The pV complexes, Na^+, K^+, or NH_4^+ salts, used in these studies were synthesized following previously reported, or slight modifications of, literature procedures, referenced individually in Table 2.1. The following hosts were purchased from Aldrich Canada and used as received: 1,3 diaminopropane•2HCl, putrescine•2HCl, 1,5 diamino pentane•2HCl, spermidine•HCl, spermine•HCl, dibenzylguanidine, B-cyclodextrin hydrate, 1,3-Bis(3-pyridylmethyl)-2-thiourea, and L-arginine•HCl. Two literature guanylating reagents, pyrazole-1-carboxamide[65] and O-methyl isouronium sulphate,[57] were employed for the synthesis of the bisguandinium hosts used in this study. Cyclobis(paraquat-p-phenylene) was prepared, as its chloride as well as its tetrakis(hexafluorophosphate) salt, according to the procedure of Geuder et al.[66]

2.5.1.2 Spectroscopy

^1H NMR spectra were recorded on either a JOEL 270MHz or Varian XL200 spectrometer, referenced using residual protons of the given deuterated solvent. ^{13}C NMR spectra were recorded on either a JOEL 270MHz or Varian XL-300 spectrometer, operating at 67.94 and 75.49 MHz, respectively. Vanadium-51 NMR spectra were recorded, at ambient temperature, on either a JOEL 270 MHz or Varian XL-300 spectrometer, operating at 71.03 and 78.891 MHz, respectively. Vanadium-51 chemical shifts were measured in parts per million (+/-2ppm) using $VOCl_3$ as an external standard at 0.00 ppm, upfield shifts

are considered negative. A typical experiment consisted of 5000 scans, with a relaxation delay of 1s and a pulse angle of 90 degrees. Variable temperature NMR was performed upon both the Varian XL-300 (^{51}V VT-NMR) as well as the JOEL 270MHz (^{1}H-VT-NMR). Infra red spectra were obtained as KBr pellets using either an ANALECT or IFS-48 FT-IR spectrometer. A typical experiment consisted of 64 scans. UV-Vis spectroscopy was obtained with a HP8453 spectrophotometer, operating with a tungsten/deuterium lamp. Elemental analyses were performed by either Guelph Chemical Laboratories, Guelph Canada Ontario, or at the Université de Montréal, Montreal Quebec. Crystal structure determinations were completed by Dr. A. M. Lebuis in the Chemistry Department of McGill University or, where indicated, at the Laboratoire de diffraction des rayons-X, Département de chimie, Université de Montréal.

2.5.2 Synthesis of R_4N^+•bpV Salts

Polyammonium•bpV salts were prepared analagously to the potassium salts, by using 10% R_4NOH solutions instead of aqueous KOH. Addition of ethanol/acetone/ether (2:10:1) mixtures to the solutions maintained at -10°C led to the slow (≈ 1 week) precipitation of crystalline orange-yellow products. In the following assignments, cis and trans refer to proton positions relative to the V=O ligand. 'Distal' methyl groups denote the 4 and 7 positions of the heterocyclic rings of the phenanthroline ligand. For further discussion of these assignments see Section 3.2. The following pure complexes were isolated in this manner:

$[Et_4N][VO(O_2)_2(3,4,7,8\text{-}Me_4\text{-}phen)]\bullet 2H_2O$ 66 % yield; ^{1}H ($CDCl_3$, ppm) 9.87 (s, 1H, **H-trans**), 8.44 (s, 1H, **H-cis**), 7.95 (m, 2H), 3.60 (q, 8H, NCH_2), 2.73 (s, 3H, distal trans-CH_3), 2.58 (s, 3H, trans-CH_3), 2.50 (s, 3H, cis-CH_3) 2.32 (s,3H, distal cis-CH_3) 1.42 (t, 12H, NCH_2CH_3); ^{51}V ($CDCl_3$) -684 ppm, ^{51}V (H_2O) -747 ppm

$[Et_4N][VO(O_2)_2(phen)]\cdot 2H_2O$ 58 % yield; ^1H ($CDCl_3$, 0°C, ppm) 10.12 (d of d, 1H, **H-trans**), 8.75 (d of d, 1H), 8.48 (d of d, 1H), 8.08 (d of d, 1H), 7.80 (m, 3H) 7.44 (q, 1H), 3.55 (q, 8H, NCH_2), 1.42 (t, 12H, NCH_2CH_3); ^{51}V ($CDCl_3$, O°C) -675 ppm, ^{51}V (H_2O, 22°C) -744 ppm

$[Me_4N][VO(O_2)_2(phen)]\cdot XH_2O$ 61 % Yield; ^1H (D_2O, ppm) 9.74 (d, 1H, **H-trans**), 8.49 (m, 1H), 8.42 (d of d, 1H), 8.31 (d, 1H), 7.90 (m, 1H), 7.68 (m, 2H), 7.62 (q, 1H), 3.15 (s, 12H, $N(CH_3)_4$); ^{51}V (D_2O) -743 ppm

$[Et_4N][VO(O_2)_2(4,7\text{-}Me_2phen)]\cdot 4H_2O$ 41% yield; ^1H ($CDCl_3$, ppm) 9.99 (d, 1H, **H-trans**), 8.57 (d, 1H, **H-cis**), 7.96 (m, 2H), 7.65 (d, 1H), 7.25 (s, 1H), 3.57 (q, 8H, NCH_2), 2.87 (s, 3H, trans-CH_3) 2.63 (s, 3H, cis-CH_3), 1.99 (br.s, 8H, H_2O), 1.42 (t, 12H, NCH_2CH_3); ^{51}V ($CDCl_3$, 22°C) -681 ppm, ^{51}V (H_2O, 22°C) -745 ppm

2.5.3 General Procedure for the Exchange of bpV Counterions

A solution of the pV complex, as its potassium salt, was prepared in distilled water. A 10-20 molar equivalent solution of the desired counterion was prepared by dissolving the appropriate chloride salt in distilled water. The clear pV solution was slowly added to the salt solution and the ensuing precipitate collected, washed with water/ethanol (1/1) and dried in vacuo. In the case of several counterions, $EtNH_3^+$, $HC(NH_2)_2^+$, $CH_3C(NH_2)_2^+$, a clear solution resulted, which, after up to 48 hours at 5°C, precipitated the desired product. All compounds were analyzed via ^{51}V and ^1H NMR, the ^1H NMR peak frequencies for the ancillary ligands are omitted for the sake of brevity. Thermogravimetric analysis failed to determine the number of molecules of hydration for each complex. The following compounds were prepared in this manner:

Table 2.6 $A[VO(O_2)_2(phen)]$

A^+	Yield (%)	^{51}V NMR (ppm) (D_2O)	^1H NMR (ppm) (D_2O)
Cs^+	92%	-748	---
$H_3NCH_2CH_3^+$	45%	-747	2.98 (t,2H, $NC\underline{H_2}CH_3$), 1.22 (q,3H, $H_3NCH_2C\underline{H_3}$)
$C(NH_2)_3^+$	85%;	-747	---
$HC(NH_2)_2^+$	13%	-746	7.67 (s, 1H, $\underline{H}$-$C(NH_2)_2$)

Table 2.7 $A[VO(O_2)_2(bipy)]$

A^+	Yield (%)	^{51}V NMR (ppm) (D_2O)	^1H NMR (ppm) (D_2O)
Cs^+	14%	-750	---
$C(NH_2)_3^+$	78%	-750	---
$CH_3C(NH_2)_2^+$	28%	-749	2.17(s,3H,$C\underline{H_3}$-$C(NH_2)_2$)

2.5.4 Preparation of Bisguanidinium Hosts

a) Pyrazole-1-carboxamide[65] One equivalent of diamine free base, two equivalents of diisopropylethyl amine, and 2.2 equivalents of pyrazole-1-carboxamide were dissolved in enough DMF to produce a 2.0 molar solution. This solution was stirred under nitrogen for 3-5 hours at room temperature. Anhydrous ethyl ether, 30ml, was added to complete the precipitation of the solid white product. The salts were collected through vacuum filtration, washed with diethyl ether and then recrystallized, 2-4 times, from boiling CH_3CN/EtOH (80:20) with the slow dropwise addition of hot methanol. The amount of methanol required depended upon the compound, the larger molecules required less MeOH. The collected and dried products were characterized by ^1H (DMSO-d^6)and ^{13}C NMR (D_2O).

The following hosts, bG(phenyl),[67] bG(CH_2)n; n=2,[68] 3, 4,[68] 6, 10, bG(bispropyl) and bG(piper) were prepared in this manner.

bG(CH_2)$_2$ Yield: 64%; ^{1}H NMR (DMSO-d^6, ppm) 7.95 (s, 2H, HNC(NH_2)$_2$), 7.40 (s, v.br, 8H, C(NH_2)$_2$), 3.28 (s, 4H, CH_2), ^{13}C NMR (D_2O) 156.86 (C(NH_2)$_2$), 26.04 (CH_2)

bG(CH_2)$_3$ Yield: 55%; ^{1}H NMR (DMSO-d^6, ppm) 7.55 (s , br, 2H, HNC(NH_2)$_2$), 7.28 (s, v.br, 8H, C(NH_2)$_2$), 3.26 (d, 4H, N-CH_2), 1.52 (m, 2H, $CH_2CH_2CH_2$); ^{13}C NMR (D_2O) 157.09 (C(NH_2)$_2$), 38.70 (N-CH_2), 27.34 ($CH_2CH_2CH_2$)

bG(CH_2)$_4$ Yield: 71%; ^{1}H NMR (DMSO-d^6, ppm) 7.97 (s, 2H, HNC(NH_2)$_2$), 7.16 (br.s, 8H, C(NH_2)$_2$), 3.17 (d, 4H, NCH_2), 1.44 (s, 4H, NCH_2CH_2); ^{13}C NMR (D_2O) 156.97 (C(NH_2)$_2$), 41.00 (NCH_2CH_2), 25.44 (NCH_2CH_2)

bG(CH_2)$_6$ Yield: 92%; ^{1}H NMR (DMSO-d^6, ppm) 7.90 (s, 2H, $NHCH_2$), 7.20 (s, 8H, C(NH_2)$_2$), 3.14 (br.s, 4H, $NHCH_2$), 1.44 (br.s, 4H, $NHCH_2CH_2$), 1.26 (br.s., 4H, $NHCH_2CH_2CH_2$); ^{13}C NMR (D_2O) 156.99, (C(NH_2)$_2$), 41.38, 28.02, 25.68

bG(CH_2)$_{10}$ Yield: 70%; ^{1}H NMR (DMSO-d^6, ppm) 7.84 (br.s, 2H, HNC(NH_2)$_2$), 7.32 (br.s, 8H, C(NH_2)$_2$), 3.08 (t, 4H, NCH_2), 1.44 (br.m, 4H, NCH_2CH_2), 1.26 (s, 12H, (CH_2)$_6$); ^{13}C NMR (D_2O) 156.91(C(NH_2)$_2$), 41.45, 28.75, 28.50, 28.09, 26.04

bG(bispropyl) Yield: 45%; ^{1}H NMR (DMSO-d^6, ppm) 8.00-7.17 (v.br., 10H, HNC(NH_2)$_2$), 3.42 (m, 4H, $HNCH_2$), 3.14 (t, 4H, NCH_2), 1.58 (q, 4H, $NCH_2CH_2CH_2$); ^{13}C NMR (D_2O) 159.45 (C(NH_2)$_2$), 48.21 (NCH_2), 41.79 (NCH_2CH_2), 30.18 ($NCH_2CH_2CH_2$)

bG(piper) Yield: 62%; ^{1}H NMR (DMSO-d^6, ppm) 7.85 (s, 2H, $\underline{H}NC(NH_2)_2$), 7.25 (v.br, 8H, HN-C(N$\underline{H_2}$)$_2$), 3.12 (d, 4H, HN-C$\underline{H_2}$), 2.29 (br. mult., 12H, C$\underline{H_2}$-($N_2C_4\underline{H_8}$)-C$\underline{H_2}$), 1.60 (q, 4H, $CH_2C\underline{H_2}CH_2$); ^{13}C NMR (D_2O) 159.70 ($\underline{C}(NH_2)_2$), 57.05, 54.28, 42.03, 27.60

bG(OH) Yield: 58%; ^{1}H NMR (DMSO-d^6, ppm) 7.77 (s, 2H, $\underline{H}NC(NH_2)_2$), 7.41 (br. s, 8H, HNC(N$\underline{H_2}$)$_2$), 5.69 (s, 1H, O$\underline{H}$), 3.67 (s, 1H, C$\underline{H}$OH), 3.25 (m, br., 4H, C$\underline{H_2}$NH); ^{13}C NMR (D_2O) 157.31 ($\underline{C}(NH_2)_2$), 67.40 ($\underline{C}$HOH), 44.36 ($\underline{C}H_2$)

bG(dioxo) Yield: 61%; ^{1}H NMR (DMSO-d^6, ppm) 7.89 (s, 2H, $\underline{H}NC(NH_2)_2$), 7.30 (br. s, 8H, HNC(N$\underline{H_2}$)$_2$), 3.37, m, 8H, O-C$\underline{H_2}$), 3.15, t, 4H, NC$\underline{H_2}$), 1.68, q, 4H, O-$CH_2C\underline{H_2}$), 1.52 (br.s, 4H, $NCH_2C\underline{H_2}$), ^{13}C NMR (D_2O) 157.17 ($\underline{C}(NH_2)_2$), 69.86, 66.81, 37.88, 28.65, 25.93

bG(oxo) Yield: 52%; ^{1}H NMR (DMSO-d^6, ppm) 7.91 (s, 2H, $\underline{H}NC(NH_2)_2$), 7.42 (br.s, 8H, HNC(N$\underline{H_2}$)$_2$), 3.51 (t, 4H, OC$\underline{H_2}$), 3.34 (t, 4H, NC$\underline{H_2}$); ^{13}C NMR (DMSO-d^6) 158.02 ($\underline{C}(NH_2)_2$), 68.08 (O$\underline{C}H_2$), 45.02 (N$\underline{C}H_2$)

The tetraphenyl borate salt of bG(bispropyl) was synthesized from its chlorine salt.[68]

bG(bispropyl)•2B(Ph)$_4$ Yield: 87%; ^{1}H NMR (CD_3OD, ppm) 7.29 (m, br., 16H, B($\underline{Ph}$)$_4$), 6.96 (m, 16H, B($\underline{Ph}$)$_4$), 6.83 (m, 8H, B($\underline{Ph}$)$_4$), 3.10 (t, 4H, HNC$\underline{H_2}$), 2.49 (t, 4H, NC$\underline{H_2}$), 1.63 (q, 4H, N-$CH_2CH_2\underline{C}H_2$).

b)O-methylisouronium Sulfate

Triethylamine (20 milli-equivalents), 10mL of 6M ammonia solution and 25 milli-equivalents of O-methylisouronium sulfate[69] were placed in a small volume high pressure reactor. The reactor was sealed and heated to 60°C for approximately 8 hours. The thick brown reaction mixture was evaporated to dryness using a rotary evaporator, and the white trisguandinium salt was isolated by multiple recrystallizations from MeOH/EtOH (~4/6) solvent mixtures. The sulfate salt of tG(tris) was prepared in this manner. Yield: 31%; ^{1}H NMR (D_2O, ppm) 3.25 (t, 4H, $(NH_2)_2CN(H)C\underline{\mathbf{H}}_2$), 2.66 (t, 4H, $CH_2C\underline{\mathbf{H}}_2NH$); ^{13}C NMR ($D_2O$) 159.60 ($\underline{\mathbf{C}}(NH_2)_2$), 55.90 ($N\underline{\mathbf{C}}H_2CH_2N(H)C(NH_2)_2$), 44.74 ($NCH_2\underline{\mathbf{C}}H_2N(H)C(NH_2)_2$)

2.5.5 Synthesis of Polyammonium Salts

Polyamines, purchased as free bases, were precipitated as hydrochloride salts from hydrochloric acid (1.0M) in diethyl ether. The solids were filtered, washed with diethyl ether and recrystallized from ethanol/acetonitrile (~7/3). All products were characterized by their ^{1}H NMR spectra. The following hosts were synthesized by this procedure:

dibenzylamine•HCl yield: 71%; ^{1}H NMR (DMSO-d^6, ppm) 9.70 (br.s, 2H, $CN\underline{\mathbf{H}}_2$), 7.54 (m, 4H), 7.42 (m, 6H), 4.13 (s, 4H, $C_6H_4C\underline{\mathbf{H}}_2NH_2$); ^{13}C ($D_2O$) 137.34, 135.59, 134.21, 133.95, 55.02 ($C_6H_4C\underline{\mathbf{H}}_2NH_2$)

tris(2-aminoethyl)amine•4HCl yield: 85%; ^{1}H NMR (D_2O, ppm) 3.09 (t, 4H, $HNCH_2C\underline{\mathbf{H}}_2NH_2$), 2.86 (t, 4H, $HNC\underline{\mathbf{H}}_2CH_2NH_2$)

N(-3-Aminopropyl)-1,3-propanediamine•3HCl yield: 58%; ^{1}H (D_2O, ppm) 3.18 (t, 4H, $HNCH_2CH_2C\underline{\mathbf{H}}_2NH_2$), 3.10 (t, 4H, $HNC\underline{\mathbf{H}}_2CH_2CH_2NH_2$), 2.10 (q, 4H, $HNCH_2C\underline{\mathbf{H}}_2CH_2NH_2$)

2.5.6 Synthesis of Polyurea (bU and tU) Hosts

All polyurea hosts were prepared in a single step from the appropriate polyamine and isocyanate precursors, following the procedure of Taub et al..[70] tU(phenyl)[71] and bU(benzyl)[62] have been previously characterized The following new hosts were characterized:

bU(phenyl) Yield: 32%; ^{1}H (DMSOd^{6}, ppm) 8.55 (s, 2H, N**H**-ph), 7.42 (d, 4H, ph), 7.31 (m, 4H, ph), 7.21 (d, 4H, pH), 6.90 (t, 2H, N**H**CH_2), 4.30 (d, 4H, HNC**H$_2$**); ^{13}C (DMSO-d^{6}, ppm) 155.12 (**C**=O), 140.35, 128.57, 125.86, 125.55, 121.00, 117.63, 42.67 (NH**C**H_2)

bU(COOEt) Yield: 49%; ^{1}H ($CDCl_3$/DMSOd^{6}, 3:1, ppm) 8.27 (s, 2H, N**H**-ph), 7.65 (d, 4H, ph-COOEt), 7.24 (d, 4H, ph-COOEt), 7.02 (m, 4H, ph), 6.23 (t, 2H, N**H**CH_2), 4.18 (d, 4H, HNC**H$_2$**), 4.10 (q, 4H, COOC**H$_2$**CH_3), 1.15 (t, 6H, $COOCH_2$C**H$_3$**); ^{13}C (DMSO-d^{6}, ppm) 155.89 (**C**=O), 141.01, 129.16, 121.58, 118.32, 54.53 (NCH_2**C**H_2), 38.12 (NH**C**H_2)

bU(cyclohexyl) Yield: 72%; ^{1}H (DMSOd^{6}, ppm) 7.24 (m, 1H, ph), 7.09 (m, 3H, ph), 6.12 (m, 2H, **H**NCH_2), 5.79 (d, 2H, N**H**-C_6H_{11}), 4.14 (d, 4H NHC**H$_2$**), 1.65 (br.m, 10H, C_6H_{11}), 1.30 (br. m, 12H, C_6H_{11}); ^{13}C (DMSO-d^{6}, 80°C, ppm) 158.26 (**C**=O), 145.10, 141.53, 126.67, 125.74, 48.67, 43.43, 33.83, 25.99, 24.95

bU(OMe) Yield: 38%; ^{1}H (DMSOd^{6}, ppm) 8.26 (s, 2H, N**H**-ph), 7.28 (d, 4H, **ph**-OMe), 7.19 (m, 4H, ph), 6.80 (d, 4H, **ph**-OMe), 6.46 (t, 2H, N**H**CH_2), 4.28 (d, 4H, HNC**H$_2$**), 3.69 (s, 3H, OC**H$_3$**); ^{13}C (DMSO-d^{6}, ppm) 156.04, 154.72, 141.08, 134.18, 128.82, 126.55, 126.16, 120.25, 114.54, 55.81 (OC**H$_3$**), 43.74 (NH**C**H_2)

tU(phenyl) Yield: 44%; ^{1}H ($CDCl_3$/DMSOd^6, 20:1, ppm) 7.71 (s, 3H, N**H**-ph), 7.10 (m, 6H, ph), 7.00 (m, 6H, ph), 6.77 (t, 3H, N**H**CH_2), 3.15 (q, 6H, $NCH_2C\mathbf{H_2}$), 2.44 (m, 6H, $NC\mathbf{H_2}CH_2$); ^{13}C (DMSO-d^6, ppm) 155.89 (**C**=O), 141.01, 129.16, 121.58, 118.32, 54.53 ($NCH_2\underline{C}H_2$), 38.12 ($NH\underline{C}H_2$)

tU(Cl) Yield: 30%; ^{1}H ($CDCl_3$/DMSOd^6, 3:1, ppm) 7.89 (s, 3H, N**H**-ph), 6.91 (m, 6H, ph), 6.77 (m, 6H, ph), 5.92 (br. m, 3H, N**H**CH_2), 2.97 (q, 6H, $NCH_2C\mathbf{H_2}$), 2.27 (m, 6H, $NC\mathbf{H_2}CH_2$); ^{13}C (DMSO-d^6, ppm) 155.69 (**C**=O), 140.03, 128.96, 125.03, 119.75, 54.38 ($NCH_2\underline{C}H_2$), 38.11 ($NH\underline{C}H_2$)

tU(OMe) Yield: 51%, ^{1}H ($CDCl_3$/DMSOd^6, 10:1, ppm) 7.18 (s, 3H, N**H**-ph), 7.01 (d, 6H, ph), 6.62 (d, 6H, **ph**), 5.89 (t, 3H, N**H**CH_2), 3.60 (s, 9H, $OC\mathbf{H_3}$), 3.22 (q, 6H, $NCH_2C\mathbf{H_2}$), 2.51 (m, 6H, N-$C\mathbf{H_2}CH_2$); ^{13}C (DMSO-d^6, ppm) 156.18 (**C**=O), 154.54, 134.11, 120.22, 114.40, 55.67 ($O\underline{C}H_3$), 54.66 ($NCH_2\underline{C}H_2$), 38.20 ($NH\underline{C}H_2$)

tU(COOEt) Yield: 20%, ^{1}H ($CDCl_3$/DMSOd^6, 10:1, ppm) 8.20 (s, 3H, N**H**-ph), 7.63 (d, 6H, ph), 7.17 (d, 6H, ph), 6.14 (t, 3H, N**H**CH_2), 4.13 (q, 6H, $COOC\mathbf{H_2}CH_3$), 3.11 (br.m, 6H, N-$CH_2C\mathbf{H_2}$), 2.43 (t, 6H, N-$C\mathbf{H_2}CH_2$), 1.18 (t, 9H, $COOC\mathbf{H_2}CH_3$); ^{13}C (DMSO-d^6, ppm) 166.02 ($\underline{C}OOEt$), 155.40 ($NH\underline{C}(O)NH$), 145.62, 130.80, 122.49, 117.29, 60.67 ($COO\underline{C}H_2CH_3$), 55.02 ($NCH_2\underline{C}H_2$), 38.13 ($NH\underline{C}H_2$), 14.7661 ($COOCH_2\underline{C}H_3$)

bU(piper-COOEt) Yield: 28%, ^{1}H (DMSO-d^6, ppm) 8.86 (s, 2H, N**H**-ph), 7.82 (d, 4H, ph), 7.50 (d, 4H, ph), 6.28 (t, 2H, N**H**CH_2), 4.26 (q, 4H, $COOC\mathbf{H_2}$), 3.09 (m, 4H, $CONHC\mathbf{H_2}$), 2.28 (m, 14H), 1.57 (t, 4H, $NHC\mathbf{H_2}$), 1.29 (t, 6H, $COOCH_2C\mathbf{H_3}$); ^{13}C (DMSO-d^6, ppm) 166.00 ($\underline{C}OOCH_2$), 155.27 ($NH\underline{C}(O)NH$), 145.74, 130.83, 122.62, 117.18, 60.68, 55.94, 53.86, 53.42, 38.10, 27.44, 14.81, ($COOCH_2\underline{C}H_3$)

bU(piper-Cl) Yield: 36%, ^{1}H (DMSO-d^6, ppm) 8.49 (s, 2H, N**H**-ph), 7.41 (d, 4H, **ph**), 7.24 (d, 4H, **ph**), 6.11 (t, 2H, N**H**CH_2), 3.11 (q, 4H, C(O)NHC**H$_2$**), 2.28 (m, 12H), 1.57 (q, 4H, $NCH_2C\mathbf{H_2}CH_2$); ^{13}C (DMSO-d^6, ppm) 155.62 (NH**C**(O)NH), 140.17, 128.94, 124.10, 119.72, 55.97, 53.44, 38.13, 27.57 ($NCH_2C\mathbf{H_2}CH_2$)

2.5.7 General Procedures for the preparation of Host•bpV Adducts

2.5.7.1 General Procedure : bpV Guests with Guanidinium Hosts

A concentrated solution of bpV complex, (1-5mL, 0.5-1M) was made in distilled water or water/methanol. A solution (1-5mL) containing 1-2 equivalents of the appropriate host, was prepared in distilled water or water/methanol. The bright yellow, clear bpV solution was added dropwise to the host solution. Reverse addition of the two components produced identical results. A solid pale yellow precipitate was either obtained immediately upon addition, or after various time periods at 5°C. The product was filtered, washed with ethanol, and dried in vacuo. The adducts were generally only very slightly soluble in water, MeOH or aceone and were characterized, where possible, using ^{51}V and ^{1}H NMR. Polar organic solvents, such as DMSO, HMPA or DMF, often dissolved the complexes however ^{51}V NMR spectroscopy showed immediate decomposition to mpV and vanadate species.

bpV anions studied include: bpV(phen), bpV(Me-phen), bpV(Me_2-phen), bpV(Me_4-phen), bpV(NO_2-phen), bpV(NH_2-phen), bpV(bipy), bpV((COO-)$_2$-bipy)), bpV(pic), bpV(3-OH-pic), bpV(2,3-pdc), bpV(2,4-pdc), bpV(2,5-pdc), and bpV(3-acet-pic). Solid products obtained with bpV(phen) are listed and characterized in Table 2.2. The crystalline product of bG(piper) and bpV(pic) was characterized by X-ray crystallography and is listed below.

[bG(piper)][VO(O$_2$)$_2$(pic)]•2H$_2$O Yield: 18%; In aqueous solution bpV(pic)•bG(piper) was ~10% hydrolyzed; ^{51}V(D$_2$O) -741, -712 ppm; ^{1}H (D$_2$O, ppm) 8.85 (br.m, 1H), 8.10 (br.m, 1H), 7.75 (s, 2H), 7.40 (s, 2H), 3.19 (t, 4H, NHC**H$_2$**), 2.64 (v.br.s, 8H, NC**H$_2$**C**H$_2$**), 2.48 (t, 4H, NHCH$_2$CH$_2$C**H$_2$**), 1.77 (q, 4H, NHCH$_2$C**H$_2$**CH$_2$); UV-Vis (H$_2$O) 343 cm^{-1}

2.5.7.2 Structure Deterimation : [bG(piper)][VO(O$_2$)$_2$(pic)]•2H$_2$O

Bright yellow crystals (0.47 x 0.21 x 0.11 mm) of [bG(piper)][VO(O$_2$)$_2$(pic)]•2H$_2$O were obtained upon cooling a 1:1 aqueous host guest solution at 5°C for 1 hour. Cell dimensions were obtained from 24 reflections having 12.5°< θ < 15.0°. A total of 10 356 reflections, having 1.89°<θ< 25.99°, were collected on a Rigaku AFC6S diffractometer using the ω/2θ scan mode with graphite-monochromated Mo Ka radiation (-11≤ h ≤11, -13≤ k ≤13, -16≤ l ≤16); of these 5177 were unique (Rint 0.076) and 3514 having >2\s(I) were employed in the solution and refinement of the structure using the SHELXS-96[72] direct method and refined using SHELXL-96.[73] The space group was confirmed with the PLATON program[74] and the data reduction was performed using DATRD2 in NRCVAX.[75] All non-hydrogen atoms were refined anisotropically, while hydrogen atoms were refined isotropically. Hydrogen atoms on carbon were constrained to the parent site using a riding model; SHELXL96 defaults, C-H 0.93 to 0.98. The isotropic factors, U~iso, were adjusted to be 20% higher than the value for the parent site. The hydrogen atoms on O and N were located by difference map and refined isotropically. The compound crystallizes with two water molecules. On one, the hydrogens are disordered with one site fully occupied and hydrogen bonding to O9, the second hydrogen is disordered over two sites to form either a H-bond to N2 or O7. For these two sites (HO8B and HO8C) the O8-H distances and thermal parameters were restrained to be similar. The second water molecule exhibits much higher thermal motion and no hydrogen atoms could be located although the oxygen is within hydrogen bonding distance of O1(oxo ligand).

The final model is thus missing two hydrogens, but these have been included in the Fw, density and absorption calculations. A final verification of possible voids was performed using the VOID routine of the PLATON program.[74]

2.5.7.3 General Procedure: bpV Guests with polyamine (pA) Hosts

A concentrated solution of pV complex (1-5 mL, 0.5-1M) was prepared in distilled water or water/methanol. A solution (1-5 mL) containing 1-10 equivalents of the polyamine salt was prepared in distilled water or water/methanol. Experiments were attempted with the pH of this salt solution altered to approximately 7.0, using 1.0 M NaOH, as well as with unaltered ambient acidic solutions. The bright yellow, clear pV solution was added dropwise to the host solution. The resulting clear bright yellow solutions were kept at 5°C and monitored by ^{51}V NMR over a period of approximately 48 hours. These spectra generally showed broadening of the bpV peak as well as an increasing proportion of aquo bpV species. If no precipitate ensued less polar solvents, such as ethanol, propanol and acetone were added. With the exception of the two 1,4-diaminobutane•2HCl salts, described below, no pure solid bpV complexes were obtained in this manner. Several solutions that were retained for a prolonged period, produced several dark red solid materials. These solids were insoluble in all solvents and not characterizeable by ^{51}V NMR.

$[NH_3(CH_2)_4NH_3][bpV(phen)]_2 \cdot XH_2O$ Yield: 82%; ^{51}V NMR (H_2O/D_2O) -749 ppm; IR (KBr) 944.5, 873, 845, 727, 621, 586 cm^{-1}

$[NH_3(CH_2)_4NH_3][bpV(bipy)]_2 \cdot 2H_2O$ Yield: 18%; Anal. Calcd (found) for $V_2O_{10}N_6H_{30}C_{28} \cdot 2H_2O$ (M.W 442.3): C 41.15 (40.86); H 4.89 (5.05); N 11.99 (12.06); ^{51}V NMR (H_2O) -751 ppm; ^1H NMR (D_2O, ppm) 9.51 (d, 1H, H-trans), 8.38 (d, 1H), 8.25 (m, 1H), 8.08 (m, 1H), 7.88 (m, 1H), 7.75 (m, 3H), 3.01 (m, 8H,

$^{+}NH_3C\underline{H_2}CH_2$), 1.72 (m, 8H, $^{+}NH_3CH_2C\underline{H_2}$); IR (KBr) 940.1, 848.2, 874.3, 770.2, 584.2 cm^{-1}; X-Ray Structure (see Figure 2.2.3.1).

2.5.7.4 Structure Deterimation : [putrescine•2H][$VO(O_2)_2$(bipy)]$_2$•H_2O

Bright yellow cubic crystals (0.40 x 0.27 x 0.25 mm) of [putrescine•2H][$VO(O_2)_2$(bipy)]$_2$•H_2O were obtained upon cooling a 1:1 aqueous host guest solution at 5°C overnight. Cell dimensions were obtained from 25 reflections having $15° < \theta < 16.5°$. A total of 11 359 reflections, having $2.01° < \theta < 25.96°$, were collected on a Rigaku AFC6S diffractometer using the ω–2θ scan mode with graphite-monochromated Mo Ka radiation ($-8 \leq h \leq 8$, $-16 \leq k \leq 16$, $-19 \leq l \leq 19$); of these 2928 were unique (Rint 0.078) and 2050 having $I > 2\sigma(I)$ were employed in the solution and refinement of the structure using the SHELXS-86[76] direct method and difmap synthesis using SHELXL-93.[77] All non-hydrogen atoms were refined anisotropically, while hydrogen atoms were refined isotropically. Hydrogen atoms on carbon were calculated at idealized positions using a riding model with different C-H distances depending on the carbon atom. The isotropic displacement factors, U~iso~, were adjusted to be 20% higher than the value for the bonded carbon atoms. The hydrogen atoms on O and N were located by difference map and refined isotropically. The data were corrected for absorption (psi scans, transmission range 0.95-1.00).

2.5.8 General Procedure: mpV Guests & bG or pA Hosts

A concentrated solution of mpV complex (1-5mL, 0.5-1M) was prepared in either distilled water, DMSO, DMF, acetonitrile, or mixtures thereof.. A solution containing 1-10 equivalents of the appropriate host was made in distilled water, DMSO and DMF, or mixtures thereof. The clear, dark red monoperoxo vanadium solution was added dropwise to the host solution. The final red solution was filtered, left at 5°C and monitored for

decomposition via ^{51}V NMR. If no precipitation ensued following approximately 48 hours, the volume of the mixture was reduced and small amounts of less polar solvents, such as ethanol, propanol, or acetone, were added. Several solid host•mpV products were obtained in this manner. They were isolated, dried in vacuo and analyzed via ^{51}V, ^{1}H, and solid state IR spectroscopy. Those materials which possessed a stoichiometric ratio between the host and mpV complex, as shown by ^{1}H NMR, were submitted for elemental analysis. Solid products obtained in this manner include:

[bG(phenyl)][mpV(nta)]•H_2O Yield: 32%; Anal. Calcd (found) for $VO_9N_7H_{24}C_{16}•H_2O$ (MW 527.36) C 36.44 (36.25); H 4.96 (3.95); N 18.59 (17.90); ^{51}V NMR (DMSO-d^6) -525, (D_2O): -550 ppm; ^{1}H NMR (DMSO-d^6, ppm): 8.39 (t, 2H, N**H**-CH_2), 7.23 (m, 8H, C(N**H**$_2$)$_2$), 4.40 (d, 4H, Ph-C**H**$_2$)), δ_A=4.04, δ_B=3.59 (d, AB, J=15.82Hz, δ= 119.84 Hz, 4H, C**H**$_2$), 3.38 (s, 2H, C**H**$_2$); ^{13}C NMR (DMSO-d^6, ppm) 177.13, 174.76, 157.45, 138.68, 129.0, 126.89, 68.75, 65.23, 44.01; UV-Vis (DMSO, anhydrous) 431nm; IR (KBr, cm^{-1}) 1661-1556, (υ COO, as. str.), 1336 (υ COO, s.), 946, (υ V=O, s), 922 (υ O-O,s), 565 ,525 (υ V-O_2, s,as)

[($NH_2NH)_2C=NH_2$][mpV(2,6-pdc)]•$6H_2O$ Yield: <10%; ^{51}V(DMSO-d^6): -545.86 ppm ^{1}H (DMSO-d^6, ppm) 8.58 (s, 2H, N**H**-CH_2), 8.35 (t, 1H), 8.04 (s, 1H), 8.01 (s, 1H), 7.16 (s, 2H, C=N**H**$_2$), 4.59 (s, 4H, NHN**H**$_2$); UV-Vis (DMSO, anhydrous) 426nm

[bG(CH_2)$_2$][mpV(nta)]•1/2H_2O Yield: 21%; Anal. Calcd (found) for $VO_9N_7H_{20}C_{10}$•1/2H_2O (M.W 442.3): C 27.16 (27.65); H 4.78 (4.76); N 22.17 (21.79); ^{51}V NMR (DMSO-d^6) -531 ppm; ^{1}H NMR (DMSO-d^6, ppm): 7.87 (s, 2H), 7.32 (br.s, 8H), δ_a=3.99, δ_b=3.50, (AB, J=14.58 Hz, δ=133.77Hz, 4H, equatorial COC**H**$_2$), 3.41 (s, 2H, axial $COCH_2$), 3.26 (s, 4H, C**H**$_2$C**H**$_2$NH); UV-Vis (DMSO, anhydrous) 433nm

[bG(CH_2)$_4$][mpV(nta)]•1/2H_2O Yield: 17%; Anal. Calcd (found) for $VO_9N_7H_{24}C_{12}$•1/2H_2O (MW 470.31): C 30.65 (30.84); H 5.36 (5.32); N 20.85 (21.10); ^{51}V NMR (DMSO-d^6) -526.4 ppm; ^1H NMR (DMSO-d^6, ppm): 7.87 (s, 2H, N**H**CH_2), 7.32 (br.s, 8H, C(N**H$_2$**)$_2$), δ_a=4.02, δ_b=3.55 (AB, J=15.21Hz, δ=129.37Hz, 4H, equatorial COC**H$_2$**), 3.41 (s, 2H, axial COC**H$_2$**), 3.26 (s, 4H, NHC**H$_2$**CH_2), 1.44 (s, 4H, HNCH_2C**H$_2$**); ^{13}C NMR (DMSO-d^6, ppm) 177.24, 174.82, 157.26, 68.0, 66.0, 25.5; UV-Vis (DMSO, anhydrous) 431nm; IR (KBr, cm^{-1}) 1645-1567, (υ COO, as. str.), 1391 (υ COO, s.), 940.5, (υ V=O, s) 912 (υ O-O,s)

2.5.8.1 Structure Determination: [bG(CH_2)$_4$][mpV(nta)]

Dark red crystals (0.5 x 0.48 x 0.15 mm) of [bG(CH_2)$_4$][mpV(nta)] were obtained by cooling a 1:1 aqueous host guest solution to 5°C. Cell dimensions were obtained from 21 reflections having $11° < \theta < 15°$. A total of 7352 reflections having $2\theta < 50.0$ were collected on a Rigaku AFC6S diffractometer using the ω–2θ scan mode with graphite-monochromated Mo Ka radiation ($-9 \le h \le 9$, $-22 \le k \le 22$, $-9 \le l \le 9$); of these 1922 were unique (Rint 0.074) and 1501 having $I > 2\sigma(I)$ were employed in the solution and refinement of the structure using the SHELXS-86[76] direct method and difmap synthesis using SHELXL-93.[77] All non-hydrogen atoms were refined anisotropically, hydrogen atoms were refined isotropically. Hydrogen atoms were calculated at idealized positions using a riding model with different C-H distances depending upon the carbon atom. The isotropic displacement factors, U~iso, were adjusted to be 20% higher than the value for the bonded carbon or nitrogen atoms. For the counterion, one of the two nitrogen atoms (N2 and N3), should be sp^3 hybridized and the other sp^2 hybridized. However, the hydrogens, as located in the difference map, indicated that the two could not be distinguised. The final solution includes hydrogens calculated at idealized positions for an

sp^2 nitrogen. The data were corrected for absorption (psi scans, transmission range 0.95-1.00).

2.5.8.2 Structure Determination: $[(NH_2NH)_2C{=}NH_2][mpV(2,6\text{-}pdc)]$

This structure was solved at the Laboratoire de diffraction des rayons-X, Département de chimie, Université de Montréal. Dark red crystals (0.82 x 0.40 x 0.36 mm) of $[(NH_2NH)_2C{=}NH_2][mpV(2,6\text{-}pdc)]$ were obtained by cooling a 5:1 aqueous host:guest solution to 5°C. Cell dimensions were obtained from 25 reflections having $19° < \theta < 25°$. A total of 4987 reflections having $2\theta < 50.0$ were collected on a Enraf Nonius CAD4 diffractometer using the $\omega/2\theta$ scan mode with CuKalpha radiation. ($-8 \leq h \leq 8$, $-11 \leq k \leq 11$, $-13 \leq l \leq 13$); of these 2534 were independent (Rint 0.085) and 2520 having >2\s(I) were employed in the solution and refinement of the structure using the SHELXS-96[72] extinction correction method and Flack, H.D. absolute structure method.[78] All non-hydrogen atoms were refined anisotropically, hydrogen atoms were refined isotropically. Hydrogen atoms on carbons were constrained to the parent site using a riding model; SHELXL96 defaults, a C-H distance of 0.94 Å. The isotropic factors, Uiso, were adjusted to 20% higher than the value for the bonded carbon or nitrogen atoms. All hydrogens on O and N atoms were located in the difference map and refined isotropically. Hydrogens on O4 (coordinated water) were restrained to an O-H distance of 0.82 Å. A final verification of possible voids was performed using the VOID routine of the PLATON program.[74]

$[bG(CH_2)_6]_3[mpV(ox)_2]_2 \cdot XH_2O$ Yield: 53%; ^{51}V (DMSO-d^6) -554 ppm; ^1H (DMSO-d^6, ppm) 7.93 (s, 2H, $NHCH_2$), 7.17 (s, 8H, $C(N\underline{\mathbf{H}}_2)_2$), 3.09 (br.s, 4H, $NHC\underline{\mathbf{H}}_2$), 1.45 (br.s, 4H, $NHCH_2C\mathbf{H}_2$), 1.27 (br.s., 4H, $NHCH_2CH_2C\underline{\mathbf{H}}_2$)

[bG(CH_2)$_4$]$_3$[mpV(ox)$_2$]$_2$•6H_2O Yield: 17%; ^{51}V (DMSO-d^6) -554 ppm, ^{1}H (DMSO-d^6, ppm) 8.00 (s, 2H, N**H**C(NH_2)$_2$), 7.23 (br.s, 8H, NHC(N**H$_2$**)$_2$), 3.33 (s, 12H, **H$_2$**O), 3.12 (s, 4H, C**H$_2$**), 1.49 (s, 4H, C**H$_2$**)

[spermidine][mpV(ox)$_2$]•XH_2O Yield: 23%; ^{51}V (DMSO-d^6) -534 ppm; ^{1}H (D_2O, ppm) 3.11 (m, 4H, NC**H$_2$**), 2.09 (m, 2H, NCH_2C**H$_2$**), 1.76 (s br., 4H, $NCH_2CH_2CH_2$)

[tG(tris)][mpV(ox)$_2$]•XH_2O Yield: 31%; ^{51}V (D_2O) -599 ppm; ^{1}H (D_2O, ppm) 3.27 (s, 6H, NC**H$_2$**), 2.71 (s, 6H, NCH_2C**H$_2$**)

2.6 References

(1) Hartkamp, H. *Angew. Chem.* **1959**, *71*, 553.

(2) Vuletic, N.; Djordjevic, C. *J. C. S. Dalton*, **1973**, 1137-1141.

(3) Szentivanyi, H.; Stomberg, R. *Acta Chem. Scand.* **1983**, *A37*, 553-559.

(4) Schwendt, P.; Petrovic, P.; Uskert, D.Z. *Anorg. Allf. Chem.* **1980**, *466*, 232-236.

(5) Begin, D.; Einstein, F. W. B.; Field, J. *Inorg. Chem.* **1975**, *14*, 1785-1790.

(6) Schwendt, P.; Pisarcik, M. *Coll, Czech. Chem. Commun.* **1982**, *47*, 1549-1555.

(7) Drew, R. E.; Einstein, F. W. B. *Inorg. Chem.* **1972**, *11*, 1079-1083.

(8) Drew, R. E.; Einstein, F. W. B. *Inorg. Chem.* **1973**, *12*, 829-835.

(9) Mimoun, H.; Saussine, L.; Daire, E.; Postel, M.; Fischer, J.; Weiss, R. *J. Am. Chem. Soc.* **1983**, *105*, 3101-3110.

(10) Quilitzsch, U.; Wieghardt, K. *Inorg. Chem.* **1979**, *18*, 869-871.

(11) Shaver, A.; Ng, J. B.; Hall, D. A.; Soo Lum, B.; Posner, B. I. *Inorg. Chem.* **1993**, *32*, 3109-3113.

(12) Shaver, A.; Soo Lum, B.; Ng, J. B.; Posner, B. I. unpublished results.

(13) Mimoun, H.; Chaumette, P.; Mignard, M.; Saussine, L. *Nouv. J. Chim.* **1983**, *7*, 467-475.

(14) Szentivanyi, H.; Stomberg, R. *Acta Chem. Scand.* **1983**, A37, 709-714.

(15) Shaver, A.; Soo Lum B.; Posner, B. I. unpublished results.

(16) Shaver, A.; Ng, J. B.; Fitzsimons, M. F.; Posner, B. I. unpublished results.

(17) Basumatary, J. K.; Chaudhuri, M. K.; Dutta Purkayastha, R. N.; Hiese, Z. *J. Chem. Soc. Dalton Trans.* **1986**, 709-711.

(18) Stomberg, R. *Acta Chem. Scand.* **1985**, *A39*, 725-731.

(19) Shaver, A.; Hall, D. A.; Ng, J. B.; Posner, B. I. *Inorg. Chim. Acta* **1995**, *229* 253-260.

(20) Shaver, A.; Ng, J. B.; Posner, B. I. unpublished results.

(21) Shaver, A.; Ng, J. B.; Hynes, R. C.; Posner, B. I. *Acta Cryst. Sect. C.* **1994**, *C50*, 1044-1046.

(22) Djordjevic, C.; Craig, S. A.; Sinn. E. *Inorg. Chem.* **1985**, *24*, 1281-1283.

(23) Djordjecic, C.; Leen M.; Sinn, E. *Inorg. Chem.* **1989**, *28*, 719-723.

(24) Stomberg, R.; *Acta Chem. Scand.* **1984**, *A38*, 223-228.

(25) Stomberg, R.; *Acta Chem. Scand.* **1984**, *A38*, 541-545.

(26) Chaudhuri, M. K. ; Ghosh, S. K. *Polyhedron* **1982**, *1*, 553-555.

(27) Djordjevic, C.; Wampler, G. L. J. *Inorg. Biochem.* **1985**, *25*, 51-55.

(28) Vilter, H.; Rehder, D. *Inorg. Chim. Acta* **1987**, *136*, L7-L10.

(29) Schwendt, P.; Sivak, M.; Lapshin, A. E.; Smolin, Y IO.; Shepelev, Y. F.; Gyepesoiva, D. *Trans. Metal Chem.* **1994**, *19*, 34-36.

(30) Szentivanyi, H.; Stomberg, R. *Acta Chem. Scand.* **1984**, *A38*, 101-107.

(31) Stomberg, R.; Szentivanyi, H. *Acta Chem. Scand.* **1984**, *A38*, 121-128.

(32) Bhattarcharjee, M.; Chaudhuri, M. K.; Paul, P. C. *Can. J. Chem.* **1992**, *70*, 2245-2248.

(33) Colpas, G. J.; Hamstra, B. J.; Kampf, J. W.; Pecoraro, V. L. *J. Am. Chem. Soc.* **1994**, *116*, 3627-3628.

(34) Chaudhuri, M. K.; Paul, P. C. *Ind. J. Chem.* **1992**, *31A*, 466.

(35) Chaudhuri, M. K. Ghosh, S. K. *Inorg. Chem.* **1982**, *21*, 4020-4022.

(36) Chaudhuri, M. K. Ghosh. S. K.; Islam, N. S. *Inorg. Chem.* **1985**, *24*, 2706-2707.

(37) Chaudhuri, M. K. Ghosh. S. K. *Inorg. Chem.* **1984**, *23*, 534-537.

(38) Wu, D.; Lei, X.; Cao, R.; Hong, M. *Jiegou Huaxue* **1992**, *11*, 65.

(39) Wei, Y. G.; Zhang, S. W.; Huang, G. Q.; Shao, M. c. *Polyhedron* **1994**, *13*, 1587-1591.

(40) Kuchta, L.; Sivak, M.; Pavelcik, F. *J. Chem. Res.* **1993**, 393.

(41) Bhattarcharjee, M.; Chaudhuri, M. K.; Islam, N. S.; Paul, P. C. *Inorg Chim. Acta*, **1990**, *169*, 97-100.

(42) Bhattarcharjee, M. N.; Chaudhuri, M. K. ; Islam, N. S. *Inorg. Chem.* **1989**, *28*, 2420-2423.

(43) Svensson, I.-B.; Stomberg, R. *Acta Chem. Scand.* **1971**, *25*, 898-910.

(44) Campbell, N. J.; Flanagan, J.; Griffith, W. P.; Skapski, A. C. *Trans. Met. Chem.* 1985, *10*, 353.

(45) Djordjevic, C.; Puryear, B. C. ; Vuletic, N.; Abelt, C. J.; Sheffield, S. *J. Inorg Chem.* **1988**, *27*, 2926-2932.

(46) Sucha, V.; Sivak, M.; Tyrselova, T.; Marek, J. *Polyhedron* **1997**, *16*, 2837-2842.

(47) Crans, D.; Keramidas, S.; Hoover-Litty, H.; Anderson, O.; Miller, M.; Lemoine, L.; Pleasic-Williams, S.; Vandenberg, M.; Rossomando, A.; Sweet, L. *J. Am. Chem. Soc.* **1997**, *119*, 5447-5448.

(48) Howarth, O. *Prog. NMR Spectrosc.* **1990**, *22*, 453-485.

(49) Howarth, O. W.; Hunt, J. R. *J. Chem Soc. Dalton Trans.* **1979**, 1388-1391.

(50) Schwendt, P. *Collection Czechoslovak Chem. Commun.* **1983**, *48*, 248-243.

(51) Lever, A. B.P.; Gray, H. J. B. *Acc. Chem. Res.* **1978**, *11*, 348.

(52) Djordjevic, C.; Puryear, B. C.; Vuletic, N.; Abelt, C. J.; Sheffield, S. J. *Inorg. Chem.* **1988**, *27*, 2926-2932.

(53a) Paul, P.; Angus-Dunne, S.; Batchelor, R.; Einstein, F.; Tracey, A. *Can. J. Chem.* **1997**, *75*, 183-191.

(53b) Nakamoto, K..; Margoshes, M.; Rundle, R. *J. Phys. Chem.* **1955**, *77*, 6480-6482.

(54) Metzger, A.; Lynch, V.; Anslyn, E. V. *Angew. Chem.* **1997**, *109*, 911-914.

(55) Bernardo, A.; Stoddart, J. F.; Kaifer, A. *J. Am. Chem. Soc.* **1992**, *114*, 10624-10631.

(56) Cudic, P. *J.Chem.Soc., Chem. Commun.* **1995**, 1073-1074.

(57) Dietrich, B.; Fyles, D.; Fyles, T.; Lehn, J. M. *Helv. Chim. Acta* **1979**, *62*, 2763-2785.

(58) Colpas, G. J.; Hamstra, B. J.; Kampf, J. W.; Pecoraro, V. L. *J. Am. Chem. Soc.* **1994**, *116*, 3627-3628.

(59) Campbell, N. J.; Capparelli, M. V.; Griffith, W. P.; Skapski, A. C. *Inorg. Chim. Acta* **1983**, *77*, 1215-1216.

(60) Djordjevic, C. Wilkins, P.; Sinn, E.; Butcher, R. *Inorg. Chim. Acta* **1995**, 230, 241-244.

(61) Wei, Y. Zhang, S., Huang, G. Shao, M.; *Polyhedron* **1994**, 13, 1587-1591.

(62) Nishizawa, S.; Bühlmann, P.; Iwao, M.; Umezawa, Y. *Tet. Lett.* **1995**, *36*, 6483-6486.

(63) Jeong, K. S.; Park, J.; Cho, Y. *Tet. Lett.* **1996**, *37*, 2795-2798.

(64) Bühlmann, P.; Nishizawa, S.; Xiao, K.; Umezawa, Y. *Tetrahedron* **1997**, *53*, 1647-1654.

(65) Bernatowic, M. S., Youling Wu, and Gary R. Matsueda *J. Org. Chem.* **1992**, *57*, 2497-2502.

(66) Geuder, W. *Tetrahedron* **1986**, *42*, 1665-1677.

(67) Jubian, V.; Veronese, A.; Dixon, R. P.; Hamilton, R. D. *Angew. Chem., Int. Ed. Engl.* **1995**, *34*, 1237-1239.

(68) Oost, T.; Filippazzi, A.; Kalesse, M. *Tetrahedron* **1997**, *53*, 8421-8438.

(69) Weiss, V. S.; Krommer, H.*Chem. Ztg.* **1974**, *98*, 617-618.

(70) Taub, B.; Hino, J. B. *J. Org. Chem.* **1961**, *26*, 5238-5239.

(71) Raposo, C.; Perez, N.; Almaraz, M.; Mussons, M. L.; Caballero, M. C.; Moran, J. R. *Tet. Lett.* **1995**, *36*, 3525-3528.

(72) Shedrick, G. M. (1996). SHELXS-96. Program for the Solution of Crystal Structures. University of Gottingen, Germany.

(73) Sheldrick, G. M. (1996). SHELXL-96. Program for Structure Analysis. University of Gottingen, Germany.

(74) Spek, A. L. (1990), Acta Cryst. A46, C34, (PLATON-94) version July 1996.

(75) DATRD2 in NRCVAX, Gabe E. J., Le Page Y., Charland J.P., Lee F. L. and White P.S., J. Appl. Cryst. 22, 384-389, 1989.

(76) Sheldrick, G.M. (1985). SHELXS-86. Program for the Solution of Cyrstal Structures. University of Gottingen, Germany.

(77) Sheldrick, G.M. (1995) SHELXL-93. Program for Structure Analysis. University of Gottingen, Germany.

(78) Flack, H.D. (1983). Acta Cryst. A39, 876-881.

Chapter 3 Second Sphere Coordination: Solution State

3.1 Introduction

Second sphere coordination research has relied heavily upon NMR spectroscopy, using techniques ranging from simple proton[1] and heteronuclear[2] NMR titration experiments, to relaxation times,[3] diffusion coefficients[4] and NOE's.[5,6] UV-Vis,[7,8] and fluorescence[9] spectroscopy, conductometry,[10] calorimetry[11] and voltammetry,[12] as well as many less common experimental techniques such as near edge X-ray absorption fine structure, NEXAFS,[13] have also shown potential in the study of the intermolecular bond. Structural features of binding have been assessed through X-ray crystallography, NOE data and most recently, molecular modeling.[5,14] Binding strengths and host selectivity's, estimated quantitatively by evaluation of the rate constant (K) for the equilibrium,

G + H --> GH, where G=guest and H=host, have proven to be highly dependent not only upon chemical structure and host-guest complementarity, but also upon the experimental environment ie. solvent polarity,[15] spectator counterion[16,17] and ionic strength.[17] Intermolecular binding phenomena must be interpreted with a keen eye towards all possible experimental variables; comparisons between different systems must be made cautiously.

3.2 Results/Discussion

3.2.1 pV•bG/pA

The combination of bG or pA host and bpV guest, in equimolar aqueous or methanolic solutions, invariably showed no interaction; using UV-Vis, ^{1}H and ^{51}V NMR spectroscopy. Several combinations resulted in immediate adduct precipitation, characterized in Chapter 2 (Section 2.3.1), circumventing solution state analysis.

Solution studies with the mpV•bG and mpV•pA pairs were more successful due to the use of DMSO. DMSO, although highly coordinating, is a non protic solvent able to dissolve both the mpV guests and bG hosts. A series of bG and pA hosts were employed in UV-Vis titration studies with mpV(nta) as the guest species (Table 3.2.1). In these studies, consecutive UV-Vis spectra were taken from solutions with gradually increasing host concentrations and constant guest concentrations. The mpV(nta) LMCT band (449 nm in anhydrous DMSO), shifted to lower wavelengths upon introduction of each bG host.

Table 3.2.1 Host•mpV(nta) UV-Vis Titration Experiments (DMSO)

Host	**Δ λ Maxima (nm)**	**Host:mpV(nta) Stoichiometry**
spermidine	-11	1:1
bG(phenyl)	-6	1:1
$bG(CH_2)_2$	-16	1:1
$bG(CH_2)_3$	-9	1:1
$bG(CH_2)_4$	-4	2:1
$bG(CH_2)_6$	-2, -7	1:2, 4:1
$bG(CH_2)_{10}$	-2, -4	1:2, 2:1
bG(dioxo)	-2, -7	1:1, 3:1
bG(oxo)	-15	1:1
bG(OH)	-7	1:3

Stoichiometries were determined by plotting the ratio of mpV(nta):host versus the LMCT absorption maxima, as in Figure 3.2.1. Two types of plots were obtained: single plateau plots as observed with $bG(CH_2)_2$ (Fig. 3.2.1-I) and double plateau plots as observed with $bG(CH_2)_{10}$ (Figure 3.2.1-II).

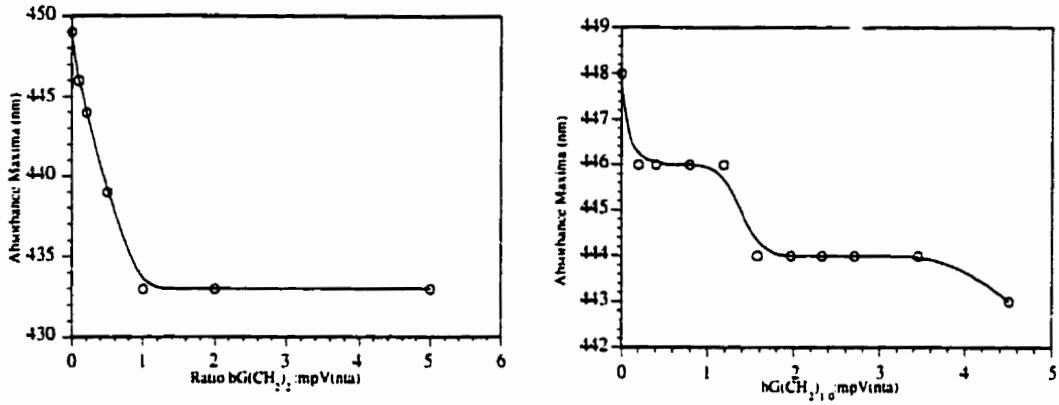

Figure 3.2.1 UV-Vis Titration of mpV(nta) with: I)$bG(CH_2)_2$ and II) $bG(CH_2)_{10}$

Introduction of the host species alters the solution dielectric constant, total ionic concentration and allows for potential complexation. The dielectric and ionic strength effects do not appear to account for the shift magnitudes. Therefore, the magnitude of each shift is a valid measure of complexation strength.[18] The strongest 1:1 complexes appear to result from interaction with the smaller hosts such as $bG(CH_2)_2$ (Figure 3.2.1-I). The charge density of these small hosts is greater due to the closer proximity of its two positively charged guanidinium groups. This effect, of high charge density leading to increased binding strength, has been previously noted.[19]

As the size of the host increases, adducts with variable stoichiometries appear to compete in solution, as demonstrated in the titration plot for $bG(CH_2)_{10}$. (Figure 3.2.1-II) The band widths of the mpV LMCT transitions are very broad and no fine structure or isosbestic points were observed. This data is subject to the large experimental errors associated with UV-Vis spectroscopy,[20] accordingly, no binding constants were estimated from this data. As to the possible structure of the adducts formed, mpV(nta) (Figure 2.2-II), has five electron rich sites, the three carboxylate groups of the ancillary ligand, and each of the

peroxo and oxo ligands. In all titration experiments, the LMCT band shifted to lower wavelengths. As a possible explanation, interaction of the cationic host species with the peroxo ligand would withdraw electron density from this ligand. This might preferentially stabilize the ground state of the LMCT transition, resulting in an increase in the energy ($E_2 > E_1$) of this transition (Figure 3.2.2).

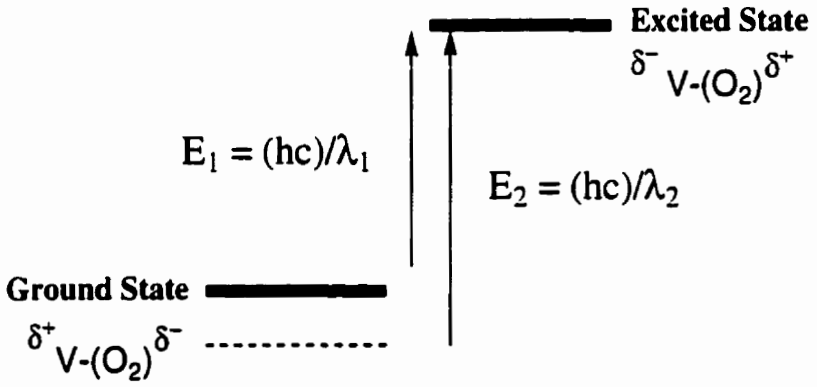

Figure 3.2.2 Postulated Complexation Effect upon LMCT Transition

The crystal structure of the bG$(CH_2)_4$-mpV(nta) adduct (Chapter 2, Figure 2.2.4.2.1) clearly shows strong interaction between the host and the carboxylato, oxo and peroxo groups. Analogously, the solution structure for this adduct likely has the positively charged bG units rapidly exchanging over all five mpV(nta) electron rich sites. An average of these interactions is likely causing the noted blue shift of the LMCT transition.

Identical UV-Vis titration experiments were undertaken with the monoanions; mpV(ADA), mpV(Hheida) and mpV(dipic), as well as with the neutral complexes, mpV(pic) and mpV(bpg) (Figure 2.2-IIb). Despite structural similarities amongst these five mpV's and mpV(nta), (all have carboxylato, peroxo and oxo ligands) none of these monoanionic or neutral mpV species showed notable shifts in their LMCT bands. The strength of the dianionic mpV(nta) interactions are thereby attributed mainly to electrostatic, charge-charge, interactions in solution.

3.2.2 $N(Et)_4$•bpV(Me_4-Phen)•pU Host in $CDCl_3$

The isolation of a chloroform stable bpV complex, $N(Et)_4$•bpV(Me_4Phen), allowed for investigation of the second sphere coordination behavior of bpV species in a non polar, weakly coordinating environment. In a search for chloroform soluble receptors, fourteen different bU and tU receptors (Figure 2.2-Ic) were prepared. None of these receptors were sufficiently soluble in chloroform to enable ^1H NMR titration studies in pure chloroform. All of these pU hosts were soluble in heated DMF or DMSO. While bpV's rapidly decompose in either of these pure solvents, up to a 5:1 $CDCl_3$/DMSO-d^6 solution dissolved most hosts, with minimal bpV decomposition. In general, tU's proved more chloroform solubie allowing studies in 10:1 $CDCl_3$/DMSO-d^6 solutions.

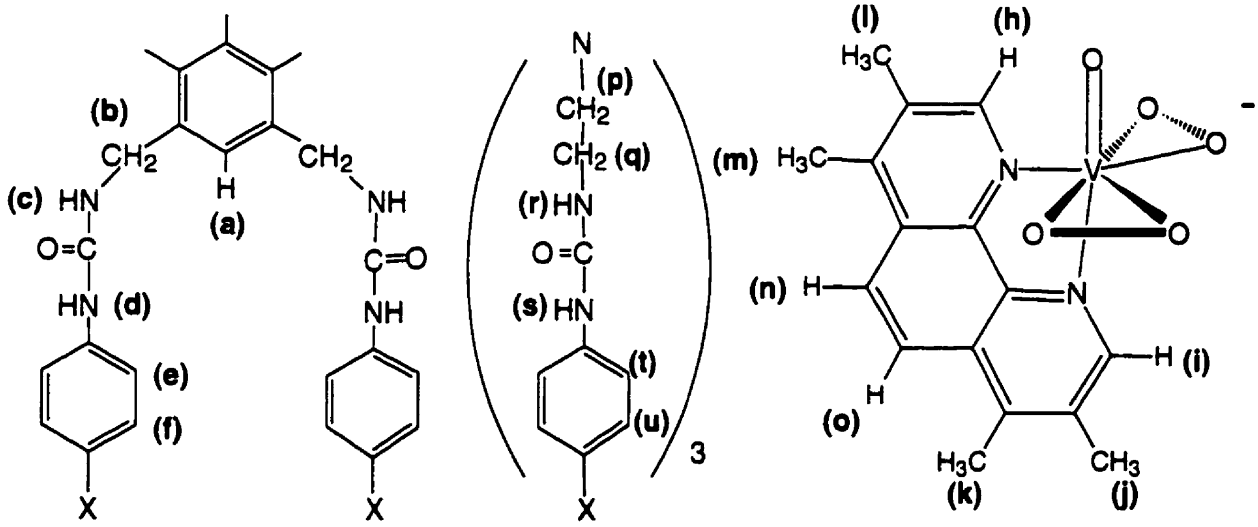

1) bU **2) tU** **3) bpV(Me_4-Phen)**

Figure 3.2.3 Labelled generic bU, tU (X=H, Cl, OMe, COOEt), and bpV(Me_4-Phen)

3.2.2.1 Extraction Ratios

The following hosts: bU(Cl), tU(Cl), and bU(cyclohexyl), were too insoluble to allow for complete ^1H NMR titration experiments in $CDCl_3$/DMSO-d^6. However, all hosts showed improved chloroform solubility in the presence of the anionic bpV species. Dissolution by complexation has been documented for urea based receptors with anionic carboxylate

guests.[21] Extraction ratios (ER) (bU:bpV(Me_4-Phen)) were obtained for all prepared tU and bU hosts by stirring 3 equivalents of solid host into a pure $CDCl_3$ solution containing one equivalent of bpV guest. ^1H NMR spectra were taken and the relative integration of each species was used to determine the host ER values (Table 3.2.2). One representative solution, the complex with bU(phenyl), was studied over a three hour time period. No change in the extraction ratio was observed and all complexation reactions were therefore assumed to have reached equilibrium following the ten minute mixing interval.

Table 3.2.2 Polyurea Host Extraction Experiments in $CDCl_3$

Host	Extraction Ratio (pU:bpV)	*Extraction ^{51}V (ppm) in $CDCl_3$	**Δ (Hz)
bU(phenyl)	0.81	-715	928
bU(benzyl)	0.47	-700	774
bU(OMe)	0.72	-709	1238
bU(Cl)	0.92	-715	990
bU(COOEt)	1.27	-715	1245
bU(cyclohexyl)	0.10	-684	619
bU(PIPER-Cl)	0.85	-696	2166
bU(PIPER-COOEt)	1.27	-707	2794
tU(phenyl)	1.22	-708	959
tU(OMe)	1.27	-708	1086
tU(Cl)	0.85	-706	928
tU(COOEt)	1.30	-712	1145

* ^{51}V NMR refers to signal obtained for bpV(Me_4-phen) after extraction of hosts into pure $CDCl_3$
**Δ (Hz) is the peak width at half height of each ^{51}V NMR signal

Notably, bU(cyclohexyl) extraction was very weak (0.1 eqvt.), showing the importance of intermolecular aromatic ring pie-stacking interactions in complexation of bpV(Me_4-phen). As well, the bU(benzyl) receptor has an ER of well less than one equivalent. Both the additional length and increased flexibility introduced by the methylene group appears to be unfavorable towards pV binding. While moderate host flexibility is required to adapt to the guest structure, excessive flexibility decreases binding constants.[22] All other hosts appear to be extracted to form an approximate 1:1 host-guest complex in pure chloroform solution. This provides additional evidence, taken with the ^1H NMR titration experiments (see Section 3.2.2.3) that 1:1 species predominate in solution.

The chemical shift of bpV(Me_4-phen), (-684 ppm, $CDCl_3$), is another parameter that can, upon extraction of polyurea hosts, reflect the extent of host-bpV interaction in solution. Extraction of each bU into the chloroform solution of bpV, caused peak shifting and broadening, measured in the ^{51}V NMR spectrum for bpV(Me_4-phen). Again, bU(cyclohexyl) shows no interaction ($\Delta\delta$=0 ppm) while bU(benzyl) causes only a $\Delta\delta$= -14 ppm shift, versus a maximal shift of $\Delta\delta$= -31 ppm for bU(phenyl). In studies of the inner sphere coordination dependencies of the ^{51}V NMR frequency for various pV molecules, upfield shifting was correlated to a decrease in electron density upon the metal center.[23] The observed upfield trend is consistent with hydrogen bonding to the metal centered complex, in the second coordination sphere.

The linewidth of each ^{51}V NMR signal is a function of both the spin-lattice (1/T1) and transverse (1/T2) relaxation rates.[24] In these host-guest solutions, two vanadium species compete in solution, free and complexed bpV. Upon host extraction, in $CDCl_3$ at room temperature, a single broad ^{51}V NMR resonance is observed. This peak, considered to be in the fast exchange domain, has a chemical shift that is the average of the shifts

characterizing each species involved in the exchange. The transverse relaxation, thus the linewidth, of this peak is affected by this chemical exchange.[24]

The broadening, however, is more complicated than this simple exchange broadening model, due to the quadrupolar vanadium (7/2) nuclei. The quadrupolar contribution to the relaxation rate, is dependent upon the electrical field gradient at the nucleus and its molecular correlation time in solution.[24] Any interaction at the metal site, even in the second coordination sphere, is likely to affect both of these parameters, and therefore, alter the relaxation time and linewidth.

A broadening effect is clearly noted for all bU's (Table 3.2.2), again with the exception of bU(cyclohexyl). Also notable are the considerably larger peak widths at half height obtained with both piperazine based hosts, bU(piper-COOEt) and bU(piper-Cl). Titration experiments with these receptors also showed anomalous behavior, (see Section 3.2.2.3), with significant drifting of the urea NH proton NMR frequencies after the addition of one equivalent of guest. The flexibility and large size of these two hosts could allow for the binding of two bpV molecules to a single host. This may provide a rationale for both of these experimental results.

3.2.2.2 ^{1}H NMR Spectroscopic Effects of Complexation

^{1}H NMR spectroscopy demonstrated several effects, reproducible with each receptor-bpV pair. Most pronounced were the downfield complexation induced shifts (CIS) in both NH signals, NH-Phenyl (c or r) and NH-CH_2 (d or s) (Table 3.2.3). These observations suggest that both NH's are involved in hydrogen bonding to form a single complex.[21]

Table 3.2.3 ^{1}H NMR CIS Values (1:1 solutions)

Host[a]	CIS (ppm) (N**H**-Ph, N**H**-CH_2)	J[b](Hz), δ[c] (Hz) (Me_4-Phen-**H**)	$CDCl_3$:DMSOd^6
bU(phenyl)	1.14, 2.00	9.64, 49.24	3:1
bU(Cl)	0.85, 1.81	9.40, 74.17	3:1
bU(OMe)	1.04, 0.91	9.40, 21.18	3:1
tU(Cl)	0.88, 1.00	9.37, 50.45	3:1
bU(piper-Cl)	0.95, 1.13	9.64, 29.09	10:1
bU(piper-COOEt)	1.19, 1.50	9.64, 39.11	10:1
tU(phenyl)	1.25, 1.26	9.40, 49.55	10:1
tU(OMe)	1.12, 1.13	9.40, 41.26	10:1
bU(COOEt)	1.47, 2.40	9.67, 89.32	10:1
tU(COOEt)	1.01, 1.08	9.64, 74.17	10:1

a 1:1 solutions of bpV guest : bU cyclohexyl and bU benzyl hosts could not be prepared in 3:1 $CDCl_3$:DMSO-d^6.

b J represents the measure coupling constant between the 2 Me_4-phen protons, (n and o)

c δ= (va - vb), calculated for the AB quartet [25]

These shifts compare well with literature studies of analogous amide and urea based hosts involved in intermolecular hydrogen bonding interactions with various anionic guests.[5,6,10,21,26-28]

The bU hosts (Figure 3.2.3-I) are based upon the para xylene backbone, with a single aromatic hydrogen (a) located between the two urea arms. This proton, indecipherable before addition of guest, shifted downfield by $\Delta\delta$ = 0.5-0.7 ppm and became clearly identifiable in the complicated aromatic region of each spectra. The two inner (e) and two outer (f) protons of each para substituted phenyl ring, at the end of each urea arm, shifted upfield on average, $\Delta\delta$ = -0.7 and -0.4 ppm, respectively. The protons located closer to

the urea group would be expected to show the larger shift upon substrate binding at the urea sites. Upfield shifts of this magnitude have been noted previously with π-stacking host-guest complexes.[29,30] Complexation did not produce inequivalence between, for example, both aromatic (e) protons upon a single urea arm. Complexation induced inequivalence, while noted for other π–stacking hosts with chemically equivalent aromatic porotons, appears to require very slow exchange of the complexed and free host.[31] Protons upon substituents of the aromatic bU and tU arms, ie. X= OMe, COOEt, showed very little changes ($\Delta\delta$= 0.1 ppm) upon complex formation.

The tU receptors, based upon the triethylamino backbone, showed very weak shifts ($\Delta\delta$= 0.1 ppm) in the two sets of methylene protons (p, q). The NH and aromatic protons of the three urea arms, for these tU hosts, showed complexation induced shifts that were very similar to those of the bU hosts (Table 3.2.3).

The guest, introduced as its tetraethylammonium salt, also showed proton shifts assignable to complexation. Most notably, the two protons, (n, o) on the distant phenyl ring of the tetramethylphenanthroline ligand, appear as a distinct AB doublet[25] pattern (figure 3.2.4 -II).

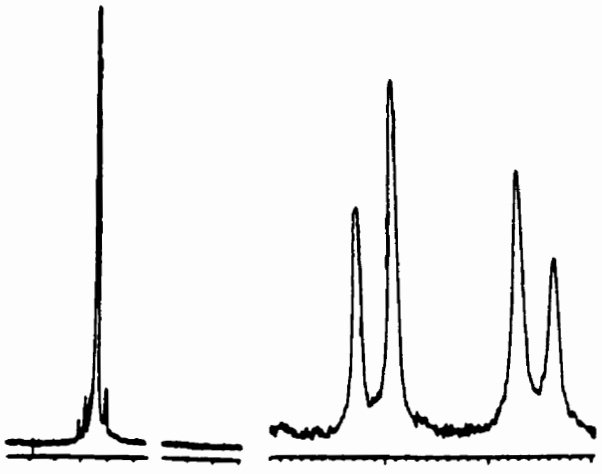

Figure 3.2.4 Splitting of the Phenanthroline Guest Protons (n, o) without (I) and with (II) Complexation

In the uncomplexed bpV guest, these two chemically inequivalent protons form an indecipherable superimposed multiplet (Figure 3.2.4-I). Host-guest complexation simplified the NMR spectrum and produced a distinct AB pattern, allowing calculations of its defining, J_{AB} and $\delta = \nu_A - \nu_B$, values.[25] The strength of this splitting (J, δ) was dependent upon both the host and solvent (Table 3.2.3). The strongest splitting (δ, Hz) occurred upon complexation with bU(COOEt). Coupling constants for each doublet, (J, Hz), remain nearly constant. The chemical shifts of the other two aromatic protons of the bpV guest, the protons cis (h) and trans (J) to the oxo group, shift downfield, on average, $\Delta\delta$ = 0.2 and 0.3 ppm, respectively. These two singlets, of the Me_4-phen ligand, were assigned to cis and trans positions, relative to the bpV oxo ligand, under the assumption that the trans effect of the electron withdrawing oxo ligand (V=O) would lead to the evidenced downfield shift at the trans position (J, 9.59 ppm), relative to the cis position (c, 8.41 ppm). This assignment was reinforced by comparison to the ^{1}H NMR data for the bpV(acet-pic)[32] and bpV(3-OH-pic)[33] complexes. Neither of these bpV species have a hydrogen atom situated trans to the oxo bond (V=O), and consequently all reported ^{1}H signals lie below 8.40 ppm. All other ^{1}H NMR peak assignments were made with respect to the NOESY interactions between adjacent protons of the Me_4-phen ligand.

The four methyl groups, cis (l), distal cis (m), trans (j), distal trans (k), show shifting, with average $\Delta\delta$ values of: -0.1, -0.1, -0.3 and -0.4 ppm, respectively. These changes are consistent with a stronger interaction between the trans segment of the vanadium coordinated tetramethylphenanthroline ligand and the polyurea hosts, than the cis. This correlates well with the NOE data, discussed below (Section 3.2.2.6).

The tetraethylammonium counterion also showed appreciable upfield shifts in the presence of host. Tetraalkylammonium cations have been studied for potential adduct formation with large macrocyclic cavities, such as calixarene anions[34] and macrocyclic polyethers.[35]

However, in this case it is believed that these shifts are the result of dissociation from the bpV anion. Urea receptors complex chlorine anions,[3,28] therefore a titration study of Et_4N•Cl with bU(phenyl) was conducted. This study showed similar upfield shifts of the Et_4N^+ protons ($\Delta\delta$= –0.39, –0.21) with increasing host concentration (Table 3.2.4). The changes to the Et_4N^+ spectra are more pronounced in the case of the bpV anion, ($\Delta\delta$= –0.82, –0.55), inferring a stronger electrostatic attraction between the Et_4N•bpV ion pair, versus Et_4N•Cl, in the absence of host.

Table 3.2.4 Et_4N^+ ^1H NMR Chemical Shifts

Complex	δ (ppm) $^+N(C\underline{H}_2CH_3)_4$	δ (ppm) $^+N(CH_2C\underline{H}_3)_4$
Et_4N•bpV(Me_4-phen)	3.57	1.43
Et_4N•Cl	3.32	1.23
Et_4N•Cl•bU(phenyl)	2.93	1.02
Et_4N•bpV(Me_4-phen)•bU(phenyl)	2.75	0.88

3.2.2.3 Binding Constants (K): Titration, Dilution Experiments

NMR titration experiments, with various nuclei, have proven useful in the detection of second sphere coordination, determination of complex stoichiometries as well as in the calculation of binding constants.[2,19] A titration experiment consists of incremental increases in the host:guest ratio, while maintaining the nature of the surrounding medium constant. Changes in the resonance frequency, peak shape or T1 values of one component of the host:guest system are generally followed as a function of the ratio of host:guest concentrations. For the bpV•polyurea complexes, both changes in their ^1H and ^{51}V NMR chemical shifts (δ, ppm) were noted as a result of titration. However, the broadness of the ^{51}V NMR peaks, as well as significant drifting of the ^{51}V chemical shift frequences precluded the use of this data in the determination of binding constants. Therefore, solely ^1H NMR data was employed to calculate binding constants (Table 3.2.5).

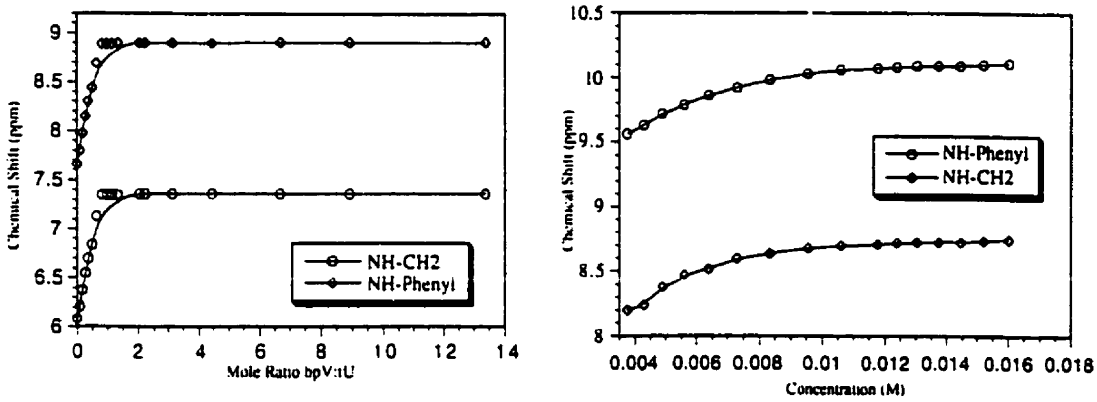

Figure 3.2.5 Example of I) ^{1}H NMR titration plots and II) ^{1}H NMR Dilution Plots

Plots were prepared of mole ratio (guest:host) vs. ^{1}H NMR signal (Figure 3.2.5-I). In many cases, several plots were made resulting from concomitant shifts in several host and guest protons. From these plots the stoichiometry of complex formation was observed. Binding constants were calculated according to the equation, $K=\alpha/[(1-\alpha)([Go]-\alpha[Ho])]$,[1,36] where $\alpha=(\delta-\delta_o)/(\delta max-\delta_o)$, δ_o is the initial chemical shift (host only), δ is the chemical shift at each titration point, and δmax is the chemical shift when the receptor is completely bound. K values were obtained at each point of the titration, for each proton of interest. Using these values, as well as the initial concentrations of host [Ho] and guest [Go] species at each titration point, a value for the concentration of complex (C) present in solution was calculated,

$C=(1/2)\{(Kd[Go][Ho])-(((Kd)[Ho][Go])^2-4((Kd)[Ho][Go]))^{1/2}\}$, where $Kd= 1/K$.[37]

It has been suggested that association constants should be measured only when the value of 'p', the binding probability, lies between 0.2 and 0.8.[37,38] The 'p' value was calculated according to p=C/[Xo], where Xo represents the initial concentration of the less concentrated component, either host or guest. The average K value, for a specific host or

guest proton, was calculated from all titration points with 'p' values between 0.2 and 0.8. In several cases multiple proton shifts ($\Delta\delta$) were measured simultaneously and for each proton, α, p and individual K values were obtained at every titration point. The average of all K's (between p=0.2 and 0.8) became the 'whole molecule' association constant. Each titration experiment was repeated at least three times and the final reported K values represent the averages from all three experiments. Errors, in all cases, were estimated as the standard deviations.

All shifting of the bU (xylene based) and tU (triethylamine based) hosts leveled off after one equivalent of bpV guest had been added. Receptors based upon the piperazine backbone, bU(piper-Cl) and bU(piper-COOEt), showed a gradual upfield drift (+ 0.1 ppm/eqvt. guest). It is likely that several species of more complex stoichiometries exist in these solutions. This is analogous to the situation noted with the bG•mpV(nta) systems, in which large flexible hosts produced indecipherable complex stoichiometries.

Table 3.2.5 Host-bpV Binding Constants

Host	**Solvent $CDCl_3$:DMSOd^6**	**K (M^{-1}) +/- (294 K)**	**Δ G° (kJ/mol)**
tU(phenyl)	10:1	498 +/- 89	15.2
tU(OMe)	10:1	333 +/- 129	14.2
tU(COOEt)	10:1	588 +/- 202	15.6
bU(COOEt)	10:1	478 +/- 133	15.1
	1:0	2684 +/- 749	19.3
bU(piper-Cl)	10:1	331 +/- 128	14.1
bU(piper-COOEt)	10:1	379 +/- 131	14.5
bU(phenyl)	3:1	268 +/- 64	13.7

While widely used to give a quantitative evaluation of outer sphere complexation strength, binding constants (K) are solvent dependent and recent literature documents a high degree of variation dependent upon experimental protocol and data treatment.[38,39] In these experiments, the K values and standard deviations calculated for all 10:1 solutions were found to lie within an order of magnitude, making relative comparisons tentative at best.

With reference to Table 3.2.5, it appears that the introduction of a third urea hydrogen bonding arm in the tU hosts does not appreciably increase binding strength, versus bU hosts. Several studies have shown the tendency of electron withdrawing substituents, positioned para to a phenyl amide bond, to increase binding strengths.[21,40,41] Studies of carboxylate binding to very similar bU hosts in DMSO have shown that introduction of NO_2, upon the aromatic ring at the para position, increased binding by a factor of forty versus an identical host substituted with the donor group, $N(Me)_2$.[21] This effect was attributed to polarization of the amide NH bond, producing a more acidic hydrogen bond donor.[42] The studies reported here with the bpV guests show that amongst a series of tU hosts, the K values decrease in the order, tU(COOEt)>tU(phenyl)>tU(OMe), however these changes are not considered statistically significant.

In all titration experiments the bpV complex was introduced as its hydrated salt, therefore the concentration of water gradually increased throughout each titration. Water is a competitive inhibitor of binding. Aqueous saturation of organic solvents decreases binding and significantly impedes complexation.[15] Control titration experiments showed no effects of water concentration upon the ^1H NMR resonance frequencies of pure bpV guest or pure poly urea hosts, in chloroform. As well, the ^1H NMR chemical shifts of the pure bpV and polyurea hosts were not dependent upon concentration. However, once complexed, dilution of a 1:1 host guest complex produced shifts for both NH peaks of the host (Figure 3.2.5 -II). This dilution method[1] was employed to determine stability constants in pure

chloroform. Each dilution experiment required a series of ^1H NMR spectra, each spectrum was taken with a decreased concentration of the prepared 1:1 host:guest solution. Association constants were calculated at each titration point for each urea proton, using the equation, $K= \alpha / (1-\alpha)^2[c]$, where c=concentration (host or guest), $\alpha=(\delta-\delta_0)/(\delta max-\delta_0)$, δ_0 is the initial chemical shift (host only), δ is the chemical shift at each titration point, and δmax is the chemical shift when the receptor is completely bound.[1,36] Values of 'p' were calculated (as described above) at each step of the dilution experiment, for both urea protons. Average K values were obtained from the dilution points with 'p' values between 0.2 and 0.8. Each experiment was repeated at least three times and the final reported K values represent averages amongst all three experiments. Errors, in all cases, were estimated as the standard deviations.

Notably, for a dilution experiment, the chemical shifts of the uncomplexed host in $CDCl_3$ must be known. Therefore only hosts showing some chloroform solubility at room temperature could be studied in this manner. A dilution titration binding constant was calculated for the bU(COOEt) host. A comparison of the two binding constants obtained by titration (478 M^{-1}) and dilution (2674 M^{-1}), show the strong ion solvating ability of DMSO. In the case of bU(COOEt), binding was decreased by greater than a factor of five in the presence of DMSO (1:10, DMSO-d^6:$CDCl_3$). This effect has been noted in published studies with amide[15] and guanidinium[43] based receptors. Also of interest is the binding constant for bU(phenyl), (268 M^{-1}) obtained in 3:1 solution. This value is of similar magnitude to those for bU's in 10:1 solutions, which suggests that the solvation effects of DMSO are saturable in nature. Dilution experiments with both bU(piper) based hosts, which also displayed weak chloroform solubility, failed due to the insufficient dependence of the host:guest complex chemical shifts upon concentration.

As discussed, ^{51}V NMR titration experiments were also used to study these host-guest interactions. These experiments provide less information than ^{1}H NMR, and introduce greater errors due to broadening of the peaks.

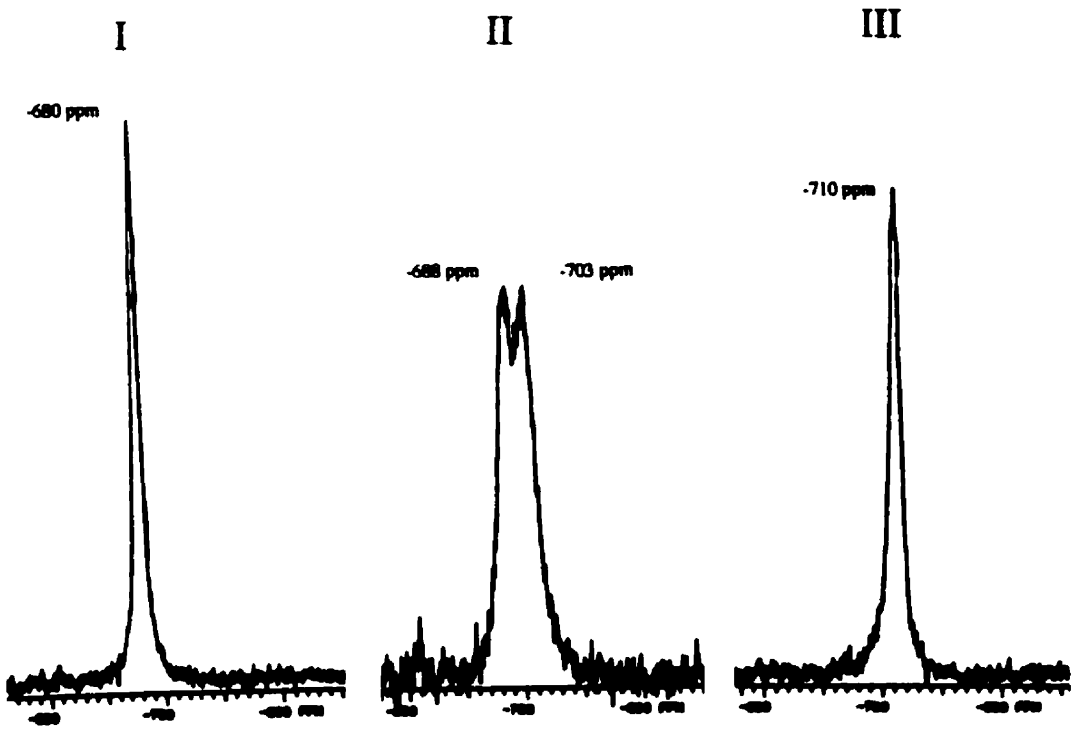

Figure 3.2.6 ^{51}V NMR Titration of bpV(Me_4-phen) with bU(phenyl) in 5:1 $CDCl_3$:DMSOd^6 at host:guest ratios of I) 0:1, II) 0.75:1 and III) 4:1

Titration of bpV with tU(phenyl) produced an upfield shift in the ^{51}V NMR resonance, from -680 ppm (Figure 3.2.6-I) to -710 ppm at a host:guest ratio of 4:1, (Figure 3.2.6-III). At a host:guest ratio of 0.75:1, two unresolved peaks at -688 and -703 ppm, were observed (Figure 3.2.6-II). Other hosts showed similar upfield shifts with increasing host:guest

ratios, and all solutions displayed a single resonance beyond their titration equivalence points. However, the ^{51}V NMR peaks shifted after formation of the 1:1 complex, at the rate of approximately 1ppm/eqvt.. ^{51}V NMR chemical shifts are sensitive to ionic strength and minor solvent changes. As discussed above, the upfield shifts in the ^{51}V NMR spectra correlate with a decrease in electron density at the metal center, as expected upon complexation to an acidic host in solution.[23]

The evaluation of binding constants, over a range of temperatures, was attempted in order to separate the entropic and enthalpic contributions to binding. These studies, using both the titration and dilution methods, were not reproducible. This is perhaps not surprising due to the well documented variability in pV reactivity[44,45] as well as the complicated experimental conditions (mixed solvents, host and guest species, interacting cation, and water saturation). Indeed, non linearity of van't Hoff plots, the relationship between Rln K and 1/T, has been attributed to solvent-solute interaction effects upon the stability of host-guest complexes.[46]

3.2.2.4 Variable Temperature ^{1}H NMR

Variable temperature ^{1}H NMR has been frequently used in attempts to 'freeze out' the adduct and view the complexed and uncomplexed ^{1}H NMR frequencies of both the host and guest species simultaneously.[47,48] In the event of fast exchange, free and complexed host and guest species exchange too rapidly, on the ^{1}H NMR time scale, for simultaneous detection of the free (f) and complexed (c) species. This results in a weighted averaged peak frequency, dependent upon the ratio (R) of complexed:free species, V ave = R Vc +1/R Vf. Cooling slows this rate of exchange, sometimes allowing both the bound and unbound species to be detected. A 1:1 solution of bpV and bU(COOEt) was prepared in

$CDCl_3$ and studied over the following temperature cycle: 20, 0 -10, -20, -30, -40, -50, -30, -10, 0, 20 °C. Control solutions of the pure bU and bpV were also subjected to a similar cycle.

Changes in the bU•bpV complex spectra included a new broad resonance at approximately 5.00 ppm, as well as very small baseline inflections at 1.30, 3.29, 7.75 and 10.2 ppm. The new peak appeared at -10°C and shifted downfield with decreasing temperature (0.15ppm/10°C). The chemical shift of water shifted downfield, from 2.10 ppm at 20°C to 2.60 ppm at -50°C. The broad peak at approximately 5.00 ppm also appeared in the bpV control study, while none of the small baseline peaks were reproduced in either control sample. The initial and final spectra taken at 20°C were identical and showed little decomposition. The large new peak is hypothesized to be due to water in the outer sphere of the bpV complex, due to its highly temperature dependent chemical shift and presence in the bpV control sample. The small high field inflections (1.3 and 3.3 ppm) may be the result of Et_4N^+ interacting with the anionic bpV complex.

3.2.2.5 Variable Temperature ^{51}V NMR

The Et_4N•bpV(Me_4-phen)•bU(COOEt) system was also studied by variable temperature ^{51}V NMR spectroscopy. The rapid relaxation rate of ^{51}V quadrupolar (I=7/2) nuclei, versus ^1H NMR, improves the likelyhood of viewing rapidly exchanging species simultaneously.

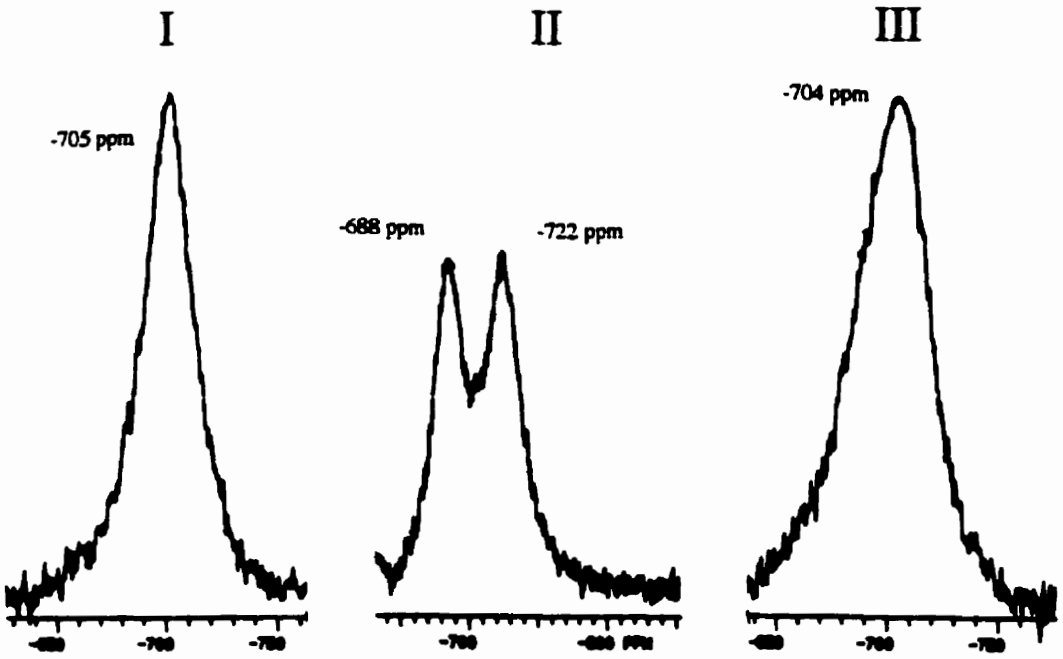

Figure 3.2.7 ^{51}V NMR Spectra of bpV:bU (0.75:1) in 5:1 $CDCl_3$:DMSO at I)40°C and II)-10°C III)40°C

At 40°C, the spectrum of bU:bpV (2:1) in 5:1 $CDCl_3$:DMSO, showed a single broad, peak at -705 ppm (figure 3.2.7-I). Decreasing the temperature to -10°C gave two poorly resolved resonances, at -688 and -722 ppm (Figure 3.2.7-II). The two resonances merged, to a single peak at -704 ppm, upon return to 30°C (Figure 3.2.7-III). Lower temperature ^{51}V NMR studies (-10 to -40°C), with various host-guest and $CDCl_3$:DMSO ratios, failed to improve the resolution of these two peaks.

At room temperature in pure $CDCl_3$ solutions, only a single vanadium peak was ever noted in spectra taken with host:guest ratios in the range from 0.1 to 2.0. Attempts to detect the two ^{51}V NMR frequencies, in pure chloroform, by lowering the temperature to -50°C were unsuccessful. This effect is due to DMSO solvation, which significantly slows the exchange rate for host-guest association, as noted in similar phosphate-host interactions.[27]

3.2.2.6 NOESY Spectroscopy

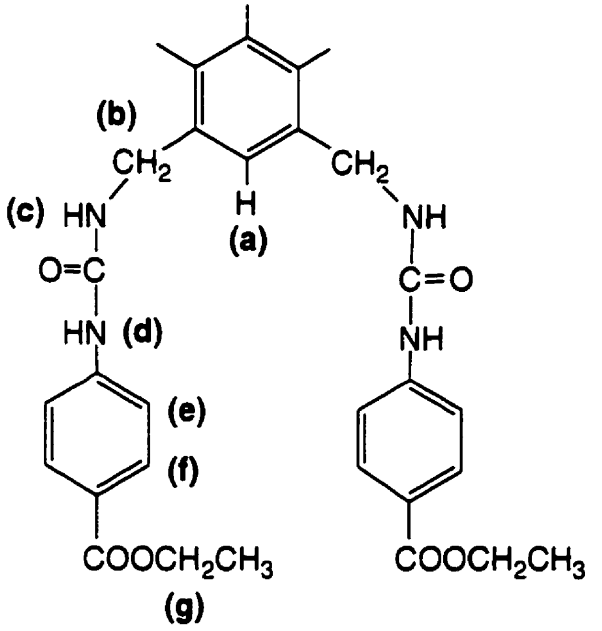

bU(COOEt)

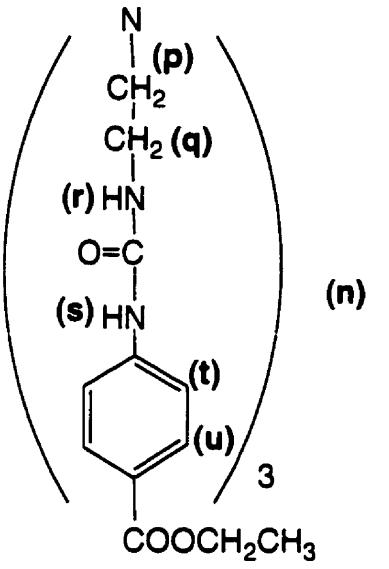

tU(COOEt)

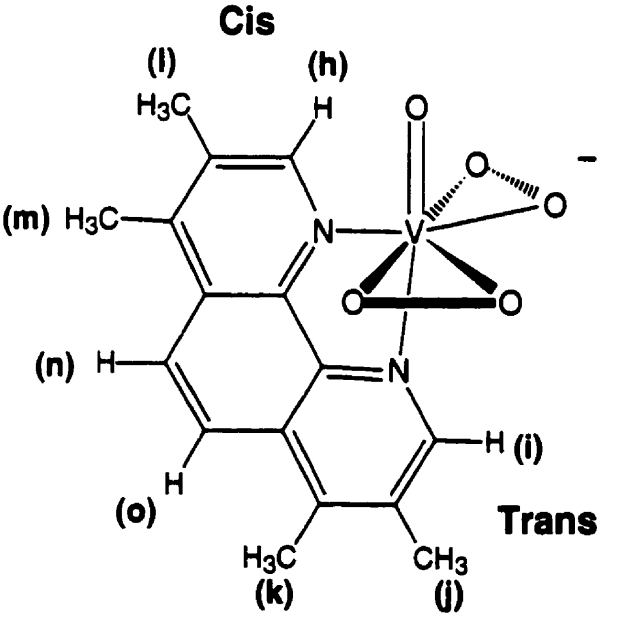

bpV(Me$_4$-phen)

Figure 3.2.8 Labelled Structures of Representative NOESY host-guest complexes

3.2.2.6.1 pV(Me_4-phen):bU(COOEt) NOESY Spectroscopy

A complete NOESY spectrum was obtained for a 1:1 solution of bpV(Me_4-phen):bU(COOEt) (Figure 3.2.8) in pure $CDCl_3$. Intramolecular NOE measurements permitted the assignment of each tetramethyl phenanthroline frequency, enabling full characterization of a complicated spectrum (See also Section 3.2.2.2). With each resonance now correctly assigned, intermolecular NOE's were easily interpreted. Notable interactions (see Figure 3.2.10 for a schematic representation) were found between the neutral host and anionic guest species.

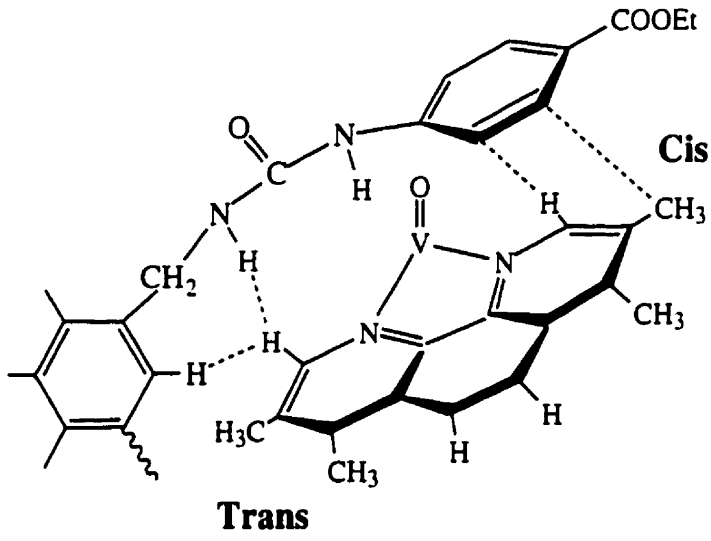

Figure 3.2.9 Postulated bpV(Me_4-phen):bU(COOEt) Structure as per NOESY Interactions; ----- represents NOE interactions

The aromatic proton (a) at 8.00 ppm, located between the two arms of the bU receptor, is in contact with the proton (h) at 8.41 ppm, the phenanthroline proton located cis to the oxo group. As well, this phenanthroline proton (h) interacts with the N**H**-CH_2 protons (c) at 8.87 ppm. In contrast, the phenanthroline proton (i) at 9.59 ppm trans to the oxo ligand, shows NOE interactions with the aromatic protons (e) and (f), at 7.23 and 7.47 ppm respectively, upon the two urea arms of the host. These NOE interactions appear to position the bpV molecule with the cis portion of the phenanthroline ring directed towards

the interior of the bU host. Consequently, the trans portion of the phenanthroline ligand is surrounded by the ends of the arms of the bU host. This hypothesized interaction is consistent with well documented π–stacking noted in many aromatic host-guest systems.[30,31,49,50] The inability to detect any binding by bU(cyclohexyl) supports this statement.

The trans methyl group (j) at 2.49 ppm, also shows weak interactions with the aromatic protons of the two urea arms (e) and (f), whereas the distal trans methyl group (k) at 2.88 ppm, does not. The two cis methyl groups (l) and (m), at 2.12 and 2.37 ppm respectively, do not interact with the bU host. This correlates well with the complex induced shifting, observed in the ^{1}H NMR studies, for each methyl resonance (Section 3.2.2.2). However, while the two protons on the distal aromatic ring of bpV(Me_4-phen) (n) and (o) 7.87 and 8.04 ppm respectively, showed large changes in their ^{1}H NMR spectra upon complexation, (Section 3.2.2.2), only proton (n) shows weak NOE interactions with an aromatic proton (f) and the $COOCH_2$ protons (g), at 4.27 ppm, of the bU arms.

As noted in the ^{1}H NMR titration studies, (Table 3.2.4) the tetraethylammonium counterion is not a simple spectator to complexation. Medium strength NOE interactions are evident between the Et_4N protons and those of the water molecules (1.72 ppm), as well as with one aromatic proton (e), and the ph-C**H$_2$**NH (c) protons, of the two urea arms. The tetraethylammonium cation might be expected to remain in close contact with the anionic host-bpV complex due to extensive charge pairing in solvents of weak polarity, such as $CDCl_3$.

3.2.2.6.2 tU(COOEt)•bpV(Me$_4$-phen)NOESY Spectroscopy

A second NOESY spectrum, representative of tU-bpV host guest interactions, was obtained for a 1:1 solution of tU(COOEt):bpV(Me$_4$-phen) (Figure 3.2.8) in pure $CDCl_3$. Intermolecular interactions were found between the neutral host and anionic guest species. Most notably, the aromatic protons of the tU host, (t) and (u) at 7.52 and 7.17 ppm respectively, were in contact with the phenanthroline proton (i), as well as with the methyl protons (j), both of which reside trans to the oxo bpV ligand. The urea protons adjacent to the aromatic rings, (s) at 9.40 ppm, were in contact with the cis phenanthroline proton (h). No intermolecular interactions were noted for the ethyl groups of the tU host (p, q), at 3.39 and 2.67 ppm respectively, nor for their adjacent urea protons (r) at 7.49 ppm. This is consistent with the weak ^{1}H NMR shifting for the ethyl protons and suggests that the large CIS values (Table 3.2.3) observed for the alkyl urea protons (r) result from interaction with the oxygen rich bpV domains. Once again, NOE interactions are observed between the Et_4N^+ protons and the water molecules (1.80 ppm), as well as with protons of both the host and guest molecules. The portion of the tetramethylphenanthroline ancillary ligand located cis to the vanadium oxo ligand is envisoned to be inserted into the tU cavity, with the trans portion protruding to interact with the aromatic rings of the urea arms. However, this is a very flexible host and it could accomodate many different structural conformations.

3.3 Conclusions

Second sphere coordination of a bpV(Me$_4$-phen) guest with neutral hosts capable of π–stacking and hydrogen bonding interactions, has been demonstrated using ^{1}H and ^{51}V NMR. Structural features of complexation, investigated by ^{1}H and NOESY NMR spectroscopy, demonstrate the presence of the tetramethylphenanthroline ancillary ligand in the center of the host. The urea functionalities are likely involved in hydrogen bonding to the oxo and peroxo pV ligands. Binding constants have been calculated for various hosts,

in several different solvent systems. The effects of DMSO and water solvation have been explored. DMSO appears to inhibit binding and slow the rate of exchange between complexed and free bpV guest. The strongest spectral effects upon complexation were induced by the bU(COOEt) host, however, these spectroscopic effects did not correlate to the largest binding constant; the largest K calculated was for tU(COOEt). Additional hydrogen bonding sites, introduced in the tU hosts, did not significantly increase binding constants. All binding constants were of the same order of magnitude and similar trends in the spectroscopic changes were observed for all hosts. These observations suggest similar modes of coordination.

The second sphere coordination of anions is a rapidly developing field, with one of its main goals being to emulate biological binding and transport mechanisms for biochemically relevant species, such as phosphate, phosphate esters and polycarboxylates eg. citrate.[51] Peroxovanadium complexes are biologically active due to their oxidizing nature and perhaps their ability to structurally mimic phosphate esters. Biochemically, these second sphere coordinating systems are potential analogs for the manner by which pV species obtain access to the intracellular domain.[52,53] As well, second sphere complexation may have the potential to fine tune the activity and selectivity of pV complexes, in their role as widely used organic oxidants.

3.4 Experimental

3.4.1 General

3.4.1.1 Chemicals

All pV compounds were prepared as described or as per the references given in chapter 2. Distilled water was used in all preparations. $CDCl_3$, DMSO-d^6 and D_2O were obtained from various suppliers. Anhydrous DMSO was purchased from Laboratoire MAT, Beauport, Quebec. All other solvents were ACS reagent grade, from various suppliers.

3.4.1.2 Spectroscopy

Refer to Chapter 2, Section 2.5.1.2 for general ^{51}V and ^{1}H spectrocopic parameters. Variable temperature NMR was performed upon both the Varian XL-300 (^{51}V VT-NMR) as well as the JOEL 270MHz (^{1}H-VT-NMR) spectrometer. NOESY experiments were performed upon a Unity 500 spectrometer. Infra red spectra were obtained as KBr pellets using either an ANALECT or IFS-48 FT-IR spectrometer. A typical experiment consisted of 64 scans. UV-Vis spectroscopy was obtained with a HP8453 UV-Vis spectrophotometer, operating with a tungsten/deuterium lamp.

3.4.2 Extraction Experiments

A 0.009 M solution of Et_4N•bpV(Me_4-phen) (5mg/600uL) in $CDCl_3$, was prepared. To the clear bright orange solution, 2 equivalents of solid polyurea host were added. The solution was stirred for 2 minutes and then placed in an NMR tube. ^{1}H and ^{51}V NMR spectra of this solution were then obtained, at room temperature, within ten minutes of sample preparation. The extraction ratio (ER) was calculated by the relative integration ratios of the two NH urea resonances (c,d or r,s) to the two phenanthroline singlets upon the bpV guest (h,j).

3.4.3 Titration Experiments

3.4.3.1 ^{1}H NMR Titration Experiments: General Procedure

Solution A: 1mL of a 0.001-0.01 M solution of host was prepared in either DMSO-d^6, CD_3OD, $CDCl_3$ or mixtures thereof. Solution B: 2-3mL of a 0.05-0.10 M solution of pV was prepared in the same deuterated solvent as in solution A. All volumes were measured using micropipettes. The ^{1}H NMR spectrum of solution A (600uL) was obtained. Additional spectra were obtained following the addition of known amounts (10-3000uL) of solution B to solution A. The titration experiments covered the receptor/pV mole ratio ranging from 0 to > 5.0. All titrations were completed within 240 minutes, to minimize decomposition of the bpV complex which was monitored by the appearance of peaks due to free tetramethylphenanthroline in the ^{1}H NMR spectra. Binding constants were calculated according to the methodology of Kelly et al.,[1] as fully described in the results section.

3.4.3.2 ^{51}V NMR Titration: General Procedure

Solution A: 1mL of a 0.005-0.01 M solution of pV was made in mixtures of D_2O/H_2O, CD_3OD/CH_3OD, $CDCl_3/CHCl_3$, DMSO-d^6/DMSO. **Solution B**: 2mL of a 0.01-0.02 M solution of host was made in the same solvent mixture as A. The ^{51}V NMR spectrum of solution A was taken. Aliquots of solution B (10-2000uL) were added to solution A and the spectra of the resulting solutions were obtained. A range of host/guest mole from 0-5 was covered in each titration, resulting in 12-15 spectra. Plots were prepared of host/guest mole ratio vs. ^{51}V NMR signal.

3.4.3.3 UV-Vis Titration Experiments

UV-Vis titration experiments were performed according to the same procedures as described for the NMR experiments. Solution A: 25.0 mL of a 2.0 mM solution of a guest was prepared in anhydrous DMSO or DMF, using a volummetric flask. Solution B:

5.0 mL of a 0.2 M solution of host was made in the same solvent as solution A, using a 5.0 mL volummetric flask. Solid guest was then added to the host solution, to give a 2.0 mM solution. A spectrum of solution A was then taken. The consecutive addition of volumes from 10 to 1500uL of solution B, allowed between 6 and 10 spectra to be obtained with host:guest ratios in the range of 1:25 to 5:1. Plots were prepared of absorbance maxima (nm) versus host:guest mole ratio.

3.4.4 ^{1}H NMR Dilution Experiments

Stock solution, 2.0 mL, 0.01-0.02 M in host and in guest, was prepared in pure $CDCl_3$ and an initial NMR spectrum was recorded. Progressively more dilute solutions were made by removing 100-200 uL aliquots of the original stock solution and diluting it with an equivalent amount of pure $CDCl_3$. All volumes were measured using micropipettes. Ten to fifteen spectra were obtained, with concentrations ranging from 0.01 to 0.003M. Graphs were then plotted of both urea proton chemical shifts versus concentration of host/guest. Binding constants were calculated using the methods of Kelly et al.,[1] as described in the results section.

3.4.5 NOESY Spectroscopy

A pure $CDCl_3$ solution of each 1:1 host-guest complex was prepared by dissolving the solid components (0.2mM) in 700uL $CDCl_3$. The 2D-NOESY spectra were obtained upon an Unity-500 Spectrometer. Parameters are as follows: spectral window: 8000Hz, number of points: 32768, number of increments: 32, mixing time: 0.8 s, total acquisition time: 3 hours. The data was processed with a Gaussian function and zerofilled in an evolution domain. NOESY Experiments were performed by Dr. F. Sauriol, McGill University,1998.

3.5 References

(1) Kelly, R.; Kim, M. *J. Am. Chem. Soc.* **1994**, *116*, 7072-7080.

(2) Dietrich, B.; Fyles, D. Helv. Chim Acta, 1979, 62, 2763-2785

(3) Sherry, A. D.; Zarzycki, R.; Geraldes, C. F. G. C. *Magn. Reson. Chem.* **1994**, *32*, 361.

(4) Mayzel, O. *J. Chem. Soc., Chem. Commun.* **1995**, 1183-1184.

(5) Hamann, B.; Branda, N.; Rebek, J. J. *Tet. Lett.* **1993**, *34*, 6837-6840.

(6) Mo, H.; Pochapsky, T.C. *Prog. NMR Spect.* **1997**, *30*, 1-38.

(7) Nishizawa, S.; Bühlmann, P.; Iwao, M.; Umezawa, Y. *Tet. Lett.* **1995**, *36*, 6483-6486.

(8) Claude, S.; Lehn, J. M.; Schmidt, F.; Vigneron, J. P. *J. Chem. Soc., Chem. Commun.* **1991**, 1183-4.

(9) Czarnik, A. *Acc. Chem. Res.* **1994**, *27*, 302-308.

(10) Bonal, C.; Morel, J. P.; Morel-Desrosiers, N. *J. Chem. Soc. Faraday Trans.* **1996**, *92*, 4957-4963.

(11) Godinez, L.; Lin, J.; Munoz, M.; Coleman, A.; Kaifer, A. *Electroanalysis* **1996**, *8*, 1072-1074.

(12) Lee, H.; Yang, X.; McBreen, J. *J. Electrochem. Soc.* **1996**, *143*, 3825-3829.

(13) Diaz-Moreno, S.; Munoz-Paez, A.; Martinez, J.; Pappaardo, R.; Marcos, S. *J. Am. Chem. Soc.* **1996**, *118*, 12654-12664.

(14) Bisson, A.; Lynch, V.; Monahan, M. K.; Anslyn, E. V. *Angew. Chem. Int. Ed. Engl.* **1997**, *36*, 2340-2342.

(15) Fan, E.; Van Arman, S.; Hamilton, A. D. *J. Am. Chem. Soc.* **1993**, 115, 369-370.

(16) Batinic-Haberle, I.; Crumbliss, A. *Inorganic Chemistry* **1995**, *34*, 929-932.

(17) Kneeland, D. M.; Ariga, K.; Lynch, V. M.; Huang, C.-Y.; Anslyn, E. V. *J. Am. Chem. Soc.* **1993**, *115*, 10042-10055.

(18) Ando, I.; Daisuke, I.; Kikujiro, U.; Kirondo, K. *Inorg. Chem.* **1994**, *33*, 5010-5014.

(19) Oost, T.; Filippazzi, A.; Kalesse, M. *Liebigs Ann.* **1997**, 1005-1011.

(20) *Ultraviolet and Visible Spectroscopy: Chemical Applications*; 3rd Ed.; Rao, C. N., Ed., Butterworth & Co. Ltd.: London, **1975**, 164-166.

(21) Jeong, K. S.; Park, J.; Cho, Y. *Tet. Lett.* **1996**, *37*, 2795-2798.

(22) Schmidtchen, F. *Pure Appl. Chem.* **1989**, *61*, 1535-1546.

(23) Howarth, O. *Prog. NMR Spectrosc.* **1990**, *22*, 453-485.

(24) Modern NMR Techniques and Their Applications in Chemistry; Popov, A. Hallenga, K., Ed: Marcel Dekker, Inc.: New York, 1990; Vol.11, pp 485-521.

(25) Leydon, D.E.; Cox, R. H. In Chemical Analysis; P.J. Elving and J. D. Winefordner, Ed.; John Wiley and Sons: New York, 1977; Vol. 48; pp. 100-117.

(26) Vicent, C.; Fan, E.; Hamilton, A. *Tet. Lett.* **1992**, *33*, 4269-4272.

(27) Raposo, C.; Almaraz, M.; Martin, M.; Weinrich, V.; Mussón, M.; Alcázar, V. *Chem. Lett.* **1995**, 759-760.

(28) Bühlmann, P.; Nishizawa, S.; Xiao, K.; Umezawa, Y. *Tetrahedron* **1997**, *53*, 1647-1654.

(29) Colquhoun, H.; Stoddart, J. F.; Williams, D.; Wolstenholme, J. B.; Zarzycki, R. *Angew. Chem. Int. Ed. Engl.* **1981**, *20*, 1051-3.

(30) Bencini, A.; Bianchi, A.; Fusi, V.; Giorgi, C.; Paoletti, P.; Valtancoli, B. *Tetrahedron Letters* **1997**, *38*, 5327-5330.

(31) Wallimann, P.; Mattei, S.; Seiler, P.; Diederich, F. *Helv. Chim. Acta.* **1997**, 80, 2368-2389.

(32) Shaver, A.; Hall, D. A.; Ng, J. B.; Lebuis, Am.-M.; Hynes, R. C.; Posner, B. I. *Inorg. Chim. Acta* **1995**, 229, 253-260

(33) Shaver, A.; Ng, J.B.; Hall, D. A.; Soo Lum, B.; Posner, B.I. *Inorg. Chem.* **1993**, 32, 3109-3113.

(34) Fraternali, F.; Wipff, G. *Journal of Inclusion Phenomena and Molecular Recognition in Chemistry* **1997**, *28*, 63-78.

(35) Kyba, E.; Helgeson, R.; Madan, K.; Gokel, G.; Tarnowski, T.; Moore, S.; Cram, D. *J. A. Chem. Soc.* **1977**, *99*, 2564-2571.

(36) Horman, I.; Dreux, B. *Anal. Chem.* **1983**, *55*, 1219-1221.

(37) Connors, K. C. *Binding Constants*, New York: Wiley, **1987**, 24-28.

(38) Deranleau, D. A. *J. Am. Chem. Soc.* **1969**, 91, 4044-4048.

(39) Person, W. B. *J. Am. Chem. Soc.* **1965**, 87, 167.

(40) Jagessar, R.; Burns, D. *Chem. Comm.* **1997**, 1685-1686.

(41) Valiyaveettil, S.; Engbersen J.; Verboom, W.; Reinhoudt, D. *Angew. Chem. Int. Ed. Engl.* **1993**, *32*, 900-901.

(42) Wilcox, C. S.; Kim, E.; Romano, D.; Kuo, L. H.; Burt, A. L.; Curran, D. P. *Tetrahedron* **1995**, *51*, 621-634.

(43) Schiessl, P.; Schmidtchen, F. *The Journal of Organic Chemistry* **1994**, *59*, 509-511.

(44) Crans, D.; Mahroof-Tahir, M.; Keramidas, A. *Mol. Cell. Biochem.* **1995**, *153*, 17-24.

(45) Hall, D. Ph.D. Thesis, McGill University, 1996.

(46) Hayashi, T.; Miyahara, T.; Koide, N.; Kato, Y.; Masuda, H.; Ogoshi, H. *J. Am. Chem. Soc.* **1997**, *119*, 7281-7290.

(47) Dodziuk, H.; Sitkowski, T.; Stefaniak, L.; Sybilska, D.; Jurczak, J.; Chmurski, K. *Polish J. Chem.* **1997**, 71, 757-766.

(48) Valdes, C.; Toledo, L. M.; Spitz, U.; Rebek, J. *Chem. Eur. J.* **1996**, 2, 989-991.

(49) Bernardo, A.; Stoddart, J. F.; Kaifer, A. *J. Am. Chem. Soc.* **1992**, 114, 10624-10631.

(50) Cudic, P. *J. Chem. Soc., Chem. Commun.* **1995**, 1073-1074.

(51) Metzger, A.; Lynch, V.; Anslyn, E. V. *Angew. Chem.* **1997**, *109*, 911-914.

(52) Palet, C.; Muñoz, M.; Valiente, M.; Cynkowski, T.; Daunert, S.; Bachas, L. *Anal. Chim. Acta* **1997**, *343*, 287-294.

(53) Araki, K. *Pro. Indian. Acad. Sci.* **1996**, *108*, 539-554.

Chapter 4 The Stability of bpV and mpV Complexes in DMEM

4.1 Introduction

The increasing use of pV complexes in biological research requires knowledge of the stability of these complexes under experimental conditions. A study of the interaction of pV complexes with common components of biological buffers, including HEPES, 4-(2-hydroxyethyl)-1-piperazineethanesulfonic acid, TRIS, tris(hydroxymethyl)aminomethane, PIPES, 1,4-piperazinebis(ethanesulfonic acid), MOPS, 4-morpholinepropanesulfonic acid, and triethanolamine resulted in the definition of MOPS as the buffer of choice.[1] It has also been shown that DDT, (1,1,1-trichloro-2,2-bis[4-chlorophenyl]ethane), a common constituent of PTPase assay buffers, reacts with pV species to produce vanadate.[2] Recently, the stabilities of a single mpV, two vanadium(V) and a vanadium(IV) derivative in DMEM, a multi component biological medium, were assessed.[3] This medium contains over fifty constituents ranging from amino acids to inorganic salts. It has been noted that many of these components interact with vanadium(5^+). Examples include valine, leucine, alanine, arginine, lysine, tryptophan, histidine, serine[4] and glycine[5] As well, solid pV complexes have been isolated with DMEM constituents as ancillary ligands, such as phosphate, $[NH_4)_5[V_2O_2(O_2)_4PO_4]\cdot H_2O$[6], imidazole $N_2C_3H_5[VO(O_2)_2(N_2C_3H_4)]\cdot H_2O$[7], glycine, $NH_4[VO(O_2)_2GlyH]\cdot H_2O$[8], and cystine, $[K_2[V_2O_2(O_2)_3(cysH)_2]H_2O]$.[9]

This work aims to assess, using ^{51}V NMR, the stability of three mpV complexes, mpV(nta), mpV(2,6-pdc) and mpV(pic), and three bpV complexes, bpV(phen), bpV(bipy), and bpV(pic), maintained at 37°C in DMEM medium.

4.2 Results/Discussion

In studying the aqueous decomposition mechanisms for reactive V(V) species, there is precedent for oxidation reactions[10,11], photoreduction to its 4^+ or 3^+ oxidation states,[10,12] as well as radical[13] and decomplexation reactions i.e. hydrolysis.[1] The decomposition rates for pV complexes in DMEM could therefore be a complicated superposition of competing processes. For this reason, interpretation will center upon descriptive and qualitative comparisons between the three bpV and three mpV complexes.

The solution state decomposition of pV complexes has been shown to have a strong dependence upon concentration.[7] Therefore, the decomposition of the six compounds (Figure 2.1-IIa,b) at six concentrations, ranging from 0.5 to 5.0 mM, were monitored. ^{51}V NMR chemical shifts are sensitive to concentration and temperature. Consequently, all decomposition is discussed with reference to the spectra obtained with 1.0 mM solutions at 37°C.

To identify possible hydrolysis products, a 5mM solution of pervanadate[14] was prepared in DMEM. The ^{51}V NMR spectrum of this solution exhibited peaks due to the bpV(aquo) complex $[VO(O_2)_2(H_2O)_x]$, -741ppm, the mpV(aquo) - $[VO(O_2)(H_2O)_x]$ complex, -620ppm, V_4 - $[H_xV_4O_{12}]^{-(4-x)}$, -574ppm, and V_2 - $[H_xV_2O_7]^{-(4-x)}$, -552 ppm. In the cases where the presence of initial complex was unclear at time zero, ie. bpV(ox), spectra were taken with large excesses of the appropriate ancillary ligand. For solutions of bpV(ox) this resulted in a new weak bpV resonance at -750 ppm, assigned to the parent bpV(ox). The major peak at -720 ppm was assumed to be a bpV species free of the ox ligand. The peaks due to bpV(pic) were detected and assigned in an analogous manner.

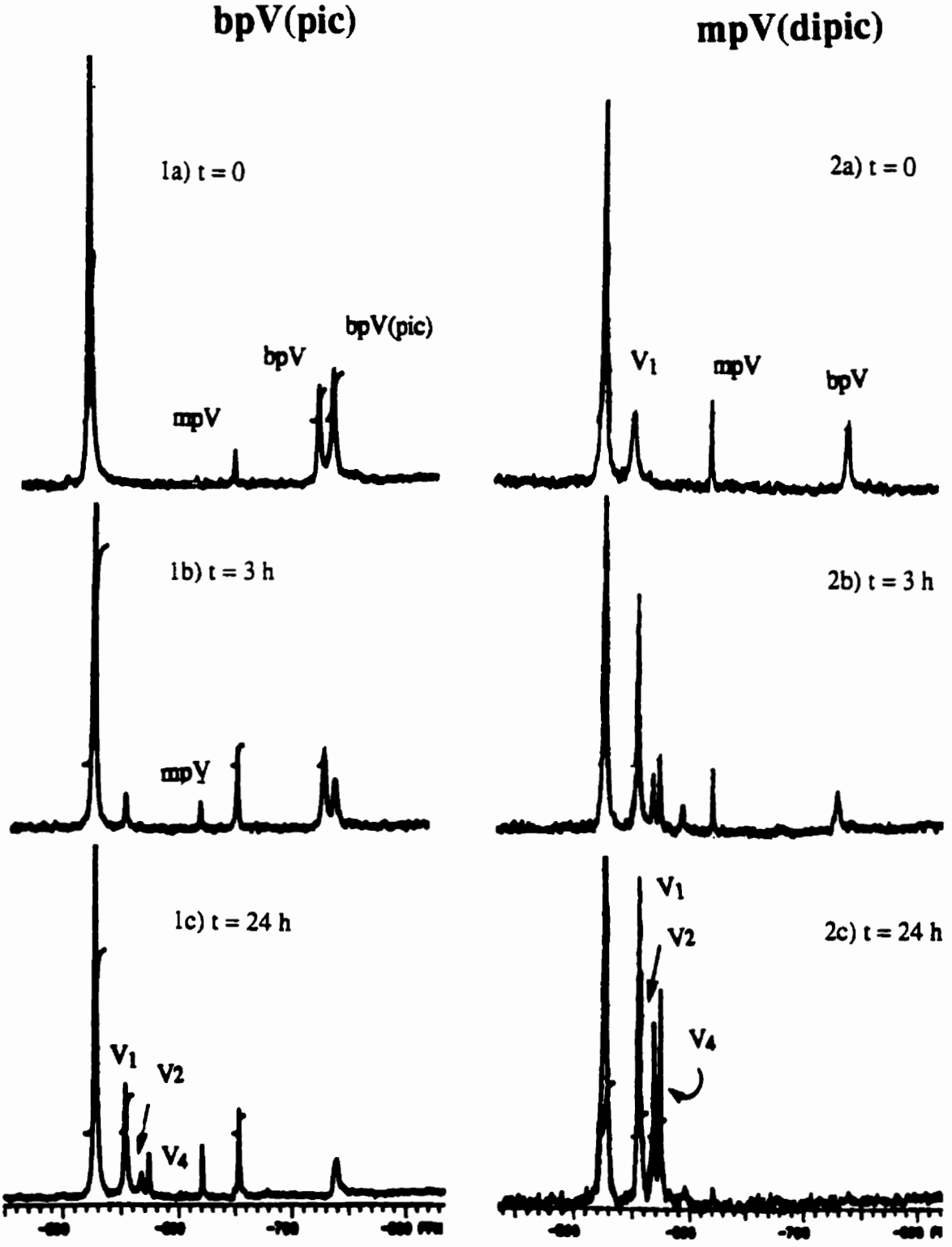

Figure 4.1 ^{51}V NMR spectra of panel 1) 2.0 mM bpV(pic) and panel 2) 2.0 mM mpV(2,6-pdc) in DMEM at time 0, 3 and 24 hours

4.2.1 Bisperoxovanadium Complexes (bpV(ox), bpV(pic), bpV(phen))

Figure 4.1, panel 1, shows the ^{51}V NMR spectra of 2.0 mM bpV(pic) at three different times. At time zero (panel 1a), bpV(pic), -739 ppm, is present as well as decomposition products at -730 ppm, a bpV species, and -657 ppm. After 3 hours incubation at 37°C, (panel 1b) the bpV(pic) peak was diminished, while the bpV species at -730 ppm had increased in magnitude. The relative intensity of the peak at -657 ppm has increased, while a new peak at -622 ppm appeared. After 24 hours (panel 1c), only a very small amount of the bpV species remained, with most of the complex having been converted to mpV and vanadate (V_1, V_2, V_4) species. A comparative summary of the ^{51}V NMR results, for all three bpV complexes in DMEM, follows.

In DMEM solution, at 37°C, the relative stability of these complexes is bpV(phen)>bpV(pic)>bpV(ox). At all concentrations studied, bpV(phen), –744 ppm, had not decomposed at time zero. The complex decomposed linearly over time, producing a species at -656 ppm, which was assigned to an mpV complex. This is the initial and main decomposition product of bpV(phen). First order rate constants (k, min^{-1}) were calculated at 0.5, 1, 2, 3, 4 and 5mM concentrations, and a linear relationship between rate (min^{-1}) and concentration (mM) was observed. Extrapolation to lower concentrations, such as 100uM, suggests a calculated half life for bpV(phen) in DMEM, of approximately six hours (See appendix A.6 for stability study plots).

By comparison, both bpV(pic) and bpV(ox) showed a high degree of initial decomposition, at all concentrations. At time zero in each of the 0.5, 1, 2 and 3 mM concentrations, over 50% of the bpV(pic) had decomposed to an aquo bpV species, resonating near -730 ppm (Figure 4.1, panel 1a). Within 24 hours, solutions of bpV(pic) in DMEM, kept at 37°C, completely converted to the aforementioned bpV aquo species, as well as two mpV decomposition products, at -653 and -621 ppm (Figure 4.1, panel 1c).

bpV(ox) behaved very differently from either bpV(phen) or bpV(pic). No peaks corresponding to the intact bpV(ox) species were noted at any concentration. Dissolution of bpV(ox) appears to completely hydrolyze this complex to a bpV species, whose peak resonates near -720 ppm. The new bpV species is remarkably stable with the 0.5mM solution decomposing over a period of 48 hours. Two phases in the decomposition were apparent: a notable time delay prior to decomposition; followed by an exponential decay to mpV species resonating near -656 and -621 ppm. The final products of all three bpV decomposition reactions were vanadate species, in varying ratios, at or near -573, (V_4) -565, (V_2) and -547 ppm (V_1).

In pure water the relative stability of these complexes is bpV(phen)>bpV(pic)>bpV(ox). All the complexes decomposed via initial formation of a bpV(aquo) complex, −705 ppm, resulting from hydrolysis of the ancillary ligand. In DMEM, at 37°C, the relative stability of these complexes is the same, however their decomposition pathways are different. At relevant biological concentrations, ranging from 0.1 to 100uM, bpV(pic) and bpV(ox) are predicted to be completely hydrolyzed at time zero. Conversely, bpV(phen) is expected to retain its initial structure, with a decomposition half life of approximately 6 hours. The studies with bpV(ox) are interesting due to the considerable stability of the bpV decomposition product. The stability of this species suggests that a component of DMEM may be involved as a ligand replacing the ox ligand. This long lived intermediate bpV complex could explain the high toxicity of bpV(ox).[15] It is also important to note that all bpV decomposition pathways involved biologically active mpV species.

Previous research (Chapters 2,3) has shown that the physical characteristics of pV complexes are dependent upon counterion. Therefore, the DMEM stability of guanidine•bpV(phen) salt, $[C(NH_2)_3][VO(O_2)_2(phen)]$, was assessed. Its decomposition products were the same as K•bpV(phen) but the guanidinium salt was twice as stable at 4

and 5mM. At lower concentrations (2 and 1 mM) there were insignificant differences. The counterion may, at high concentrations, be acting to delay decomposition by associating with the bpV complex. At lower bpV concentrations, the constituents of DMEM likely overwhelm any stabilizing counterion effects and induce decomposition.

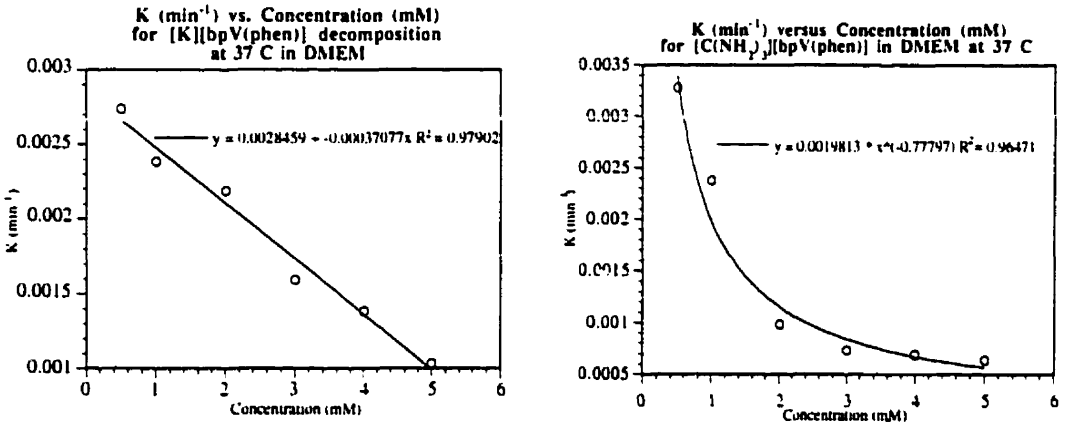

Figure 4.2 Decomposition Rate (K, min^{-1}) vs. Concentration (mM) for bpV(phen) as its potassium a) and guanidinium b) salts, in DMEM at 37°C

4.2.2 Monoperoxovanadium Complexes (mpV(nta), mpV(2,6-pdc), mpV(pic))

Figure 4.1, panel 2, shows the ^{51}V NMR spectra for 2.0 mM mpV(2,6-pdc) at three different times. At time zero (panel 2a), bpV, -744ppm, mpV, -622ppm, and vanadate (V_1), -554 ppm, species are evident. In contrast to the bpV(pic) spectra (panel 1a), no peak is found for the intact mpV(2,6-pdc) complex. Following incubation at 37 °C for 3 hours, (panel 2b), the mpV and vanadate species have increased at the expense of the bpV complex. After 24 hours (panel 2c) all of the pV complexes have converted to the V_1, V_2 and V_4 vanadate oligomers. The results for all three mpV complexes can be summarized as follows.

In DMEM solution, at 37°C, the relative stability of these complexes is mpV(nta)>>>mpV(2,6-pdc)≈mpV(pic). At all six concentrations mpV(pic) and mpV(2,6-

pdc) were completely hydrolyzed at time zero. mpV(pic) decomposition products appeared at -556, -574, -622, -656 and -744 ppm, while mpV(2,6-pdc) showed decomposition products at -554, -622 and -744 ppm. (Figure 4.1, panel 2a) The peak at -622 ppm, assigned to the mpV(aquo) complex, was also a common decomposition product of all the bpV complexes. mpV(pic) and mpV(2,6-pdc), rapidly equilibrated in DMEM to form mpV and bpV species. Table 4.1 reflects the time zero ratios, obtained by summation of ^{51}V NMR integrations.for all peaks assigned to bpV, mpV and vanadate (V_1, V_2 and V_4) species, in 1.0 mM mpV solutions.

Table 4.1 Relative Ratios of the Time Zero Decomposition Products for mpV Complexes, 1.0mM in DMEM

Initial mpV Complex	bpV	mpV	Vanadate
mpV(2,6-pdc)	60	30	1
mpV(pic)	50	40	1
mpV(nta)	0	65	1

The major vanadium species at time zero in a DMEM solution of mpV(2,6-pdc) or mpV(pic), was a bpV complex. In contrast, mpV(nta), while hydrolyzed by approximately 40% upon initial dissolution in DMEM, does not form detectable concentrations of any bpV species. (Table 4.1) Decomposition products of mpV(nta) at t=0 appear at -554 and -622 ppm. A series of decomposition studies for mpV(nta) in DMEM have been published by Etcheverry et al.,[3] and the behavior noted here is comparable.

In water and DMEM the relative stability of these complexes is mpV(nta)>>>mpV(2,6-pdc)≈mpV(pic). Nta, 2,6-pdc and pic are tetradentate, tridentate and bidentate ligands, respectively. The chelate effect of the ancillary ligand seems to predominate in determining their relative stability. Notably, both mpV(pic) and mpV(2,6-pdc) have a bpV species as

their major decomposition product (Table 4.1). This is interesting in view of the nearly two fold greater biological activity observed for bpV species over mpV species.[16] Both mpV(pic) and mpV(2,6-pdc), at biologically relevant concentrations, will be completely hydrolyzed upon dissolution. In comparison, mpV(nta) will remain partially intact. This high stability, attributed to the tetradentate nta ligand, may play a role in its increased toxicity.[15]

4.3 Conclusions

Peroxovanadium complexes, although more stable than aqueous peroxovanadates formed in situ (pervanadate), still decompose significantly. This decomposition is particularly relevant because it occurs under commonly applied conditions in biological experiments, for example in DMEM medium which contains variety of amino acids, vitamins, hormones and oligelements. In contrast, the same compounds were very stable in saline; bpV(pic) and bpV(phen) having $t_{1/2}$'s of 8.5 and 10 days in saline, respectively.[17] DMEM medium significantly accelerates decomposition ($t_{1/2} < 8$ hours). These studies indicate that the relatively small difference, in *in vitro* culture studies, between the mpV and bpV subgroups[15] are due to the commonality of their decomposition products. For instance, results show that mpV complexes yield bpV species and vice versa, when maintained at 37°C in DMEM.

bpV(phen) has been identified as the pV of choice for further biochemical studies. Stability studies with bpV(phen) are easily monitored and highly reproducible. Within an estimated time frame of 0-6 hours, biochemical effects can be confidently attributed to bpV(phen).

4.4 Experimental

4.4.1 General

Abbreviations are as follows: phen – 1,10-phenanthroline; 2,6-pdc – 2,6-pyridinedicarboxylato; pic – pyridine-2-carboxylato; ox – oxalato; nta – nitrilotriacetato; bpV(phen) – $K[VO(O_2)_2(C_8H_{10}N_2)]\cdot 3H_2O$; bpV(ox) – $K_3[VO(O_2)_2(C_2O_4)]\cdot 2H_2O$; bpV(pic) – $K_2[VO(O_2)_2(C_7H_4O_2N)]\cdot 2H_20$; mpV(nta) – $Na_2[VO(O_2)(C_6H_6NO_6)]\cdot 5H_2O$; mpV(2,6-pdc) – $K[VO(O_2)(C_7H_3O_4N)(H_2O)]\cdot 2H_2O$; mpV(pic) – $[VO(O_2)(C_7H_4O_2N)(H_2O)_2]$; V(2,6-pdc) – $NH_4[V(O)_2(C_7H_3O_4N)]$.

All ^{51}V NMR spectra were obtained with a Varian XL-300 NMR spectrometer operating at 78.891 MHz. ^{51}V NMR chemical shifts were measured in parts per million using $VOCl_3$ as an external standard at 0.00 ppm. Measurements of pH were taken with an Orion 5202A pH meter using an NMR combination electrode (Aldrich).

4.4.2 Chemicals

All six pV compounds were prepared as previously described in the literature.[18,19,20] Distilled water was used in all preparations. All chemicals were purchased from Aldrich Canada, and used without further purification. Bovine Liver Catalase was purchased from Sigma Chemical Co. DMEM and RMPI, with added fetal bovine serum, streptomycine, and penicillin, were obtained from GIBCO BRL.

4.4.3 Procedure

Detailed experimental is given for the stability study with bpV(phen), however analagous procedures were used for each pV complex.

3.0, 4.0 and 5.0 mM Concentrations

Stock solutions (3.0, 4.0, 5.0 mM) were made in DMEM/D_2O (4:1). The pH of this solution was measured and adjusted, if required, with 0.1 M NaOH or 0.1 M HCl to obtain a pH value in the range from 7.3-7.5. One mL of this solution was then placed in a 5mm NMR tube. A sealed melting point capillary, containing 0.50 mM internal reference solution, V(2,6pdc)[1] was inserted into each tube. ^{51}V NMR spectra were taken at room temperature, within 10 minutes of sample preparation (t=0). Samples were then incubated at 37°C +/- 2°C, shielded from light. ^{51}V NMR spectra were taken at approximately t= 1, 2, 3, 4, 8, 12, 20, and 24 hours. All samples were monitored until complete decomposition to vanadate species had occurred. Each spectrum consisted of 5000 scans, at 37°C +/- 2°C probe temperature, using a 6.9 second pulse width with no relaxation delay and a 90° pulse angle. All studies were repeated a minimum of two times.

1.0, 2.0 mM Concentrations

Experimental protocols for the 1.0 and 2.0 mM concentrations are identical with the following exceptions: the internal reference capillary tubes contained a solution of 0.25mM V(2,6-pdc), spectra were taken at time intervals of approximately 1, 2, 3, 5, 7, 10, 20 and 24 hours and each spectrum consisted of 10 000 scans.

0.5 mM Concentrations

Solutions of 0.5 mM bpV(phen) were prepared in DMEM/D_2O (4:1). 5 mL was placed in a 10mm NMR tube along with a reference capillary tube containing a solution of 0.25mM V(2,6-pdc). Spectra were taken at time intervals of 1, 2, 3, 5, 7, 10, 20, and 24 hours.

Each spectrum consisted of 12000 scans, operating with a 10 mm broad band NMR probe at 37°C+/-2°C, using a 14.2 second pulse width and an 80° pulse angle.

DMEM-Pervanadate Solution (5 mM)

A stock solution (250mM)was prepared by dissolving of V_2O_5 (1.65g) in NaOH (10mL, 0.1M). This solution was stirred at room temperature for 2 days, until its initial yellow color had completely dissipated. 100µL of this stock solution was added to 500µL of 250mM H_2O_2 solution. 400µL of D_2O was then added to the bright yellow solution. This solution was stirred for 5 minutes, followed by the addition of 100µg of solid catalase. Dilution of the pervanadate solution to 5mL with DMEM produced the final 5 mM DMEM-pervanadate sample. A sealed melting point capillary, containing 0.5mM internal reference solution, V(2,6pdc), was inserted into this tube. The time zero ^{51}V NMR spectrum was taken at room temperature, within 10 minutes of sample preparation. A second spectrum was obtained after one hour at 37°C.

4.4.4 Data Analysis

Fresh aqueous solutions of each complex at 5.0, 4.0, 3.0, 2.0, 1.0 and 0.5 mM concentrations were prepared as above but in H_2O/D_2O (4:1), and their spectra were measured within ten minutes. The relative integration of the peak due to the complex to that of the internal reference was assigned the value equal to no decomposition (ie. bpV(phen)=100%).

The percentage of the initial complex that remained was calculated for each spectrum obtained in the presence of DMEM. Rate constants for the first order decomposition of the initial complex were obtained for bpV(phen) while in the case of bpV(pic), bpV(ox), mpV(2,6-pdc) and mpV(pic), the rate of loss of the decomposition products, bpV and mpV, were followed to facilitate comparisons. Linear decomposition rate constants were

determined for six concentrations of bpV(phen). A plot of decomposition rate constants (k min^{-1}) vs. concentration (mM) demonstrated a linear relationship. This equation was then used to calculate approximate half lives for bpV(phen) at concentrations such as 100uM, which are not detectable by ^{51}V NMR.

References

(1) Hall, D. Ph.D. Thesis, McGill University, 1996.

(2) Huyer, G.; Liu, S.; Kelly, J.; Moffat, J.; Payette, P.; Kennedy, B.; Tsaprailis, G.; Gresser, M.; Ramachandran, C. *J. Biol. Chem.* **1997**, *272*, 843-851.

(3) Etcheverry, S.; Crans, D.; Keramidas, A.; Cortizo, A. *Arch. Biochem. Biophys.* **1997**, *338*, 7-14.

(4) Tracey, A. S.; Jaswal, J. S. *Inorg. Chem.* **1993**, *32*, 4235-4243.

(5) Crans, D. C.; Shin, P. K. *J. Am. Chem. Soc.* **1994**, *116*, 1305-1315.

(6) Schwendt, P.; Tyrselová, J.; Pavelcik, F. *Inorg. chem.* **1995**, *34*, 1964-1966.

(7) Shisheva, A.; Shechter, Y. *Biochemistry* **1992**, *31*, 8059-8063.

(8) Bhattacharjee, M.; Chaudhuri, M. K.; Islam, N. S.; Paul, P. C. *Inorg. Chim. Acta* **1990**, *169*, 97-100.

(9) Chaudhuri, M. K.; Paul, P. C. *Ind. J. Chem.* **1992**, *31A*, 466-468.

(10) Butler, A.; Clague, M. J.; Meister, G. E. *Chem. Rev.* **1994**, *94*, 625-638.

(11) Zhang, Y.; Holm, R. H. *Inorg. Chem.* **1990**, *29*, 911-917.

(12) Bonchio, M.; Conte, V.; Di Furia, F.; Modena, G.; Moro, S.; Carofiglio, T.; Magno, F.; Pastore, P. *Inorg. Chem.* **1993**, *32*, 5797-5799.

(13) Bonchio, M.; Conte, V.; Di Furio, F.; Modena, G.; Moro, S.; Edwards, J. O. *Inorg. Chem.* **1994**, *33*, 1631-1637.

(14) Kadota, S., Fantus, I. G., Deragon, G., Guyda, H. J., Hersh, B., Posner, B. I. *Biochem. Biophys. Res. Comm.* **1987**, 259-266.

(15) Maysinger, D.; Yaccato, K.; Shaver, A. Manuscript in Preparation, 1998.

(16) Shaver, A.; Ng, J. B.; Hall, D. A.; Posner, B. I. *Mol. and Cell. Biochem.* **1995**, *153*, 5-15.

(17) Posner, B. I.; Faure, R.; Burgess, J. W.; Bevan, A. P.; Lachance, D.; Zhang-Sun, G.; Fantus, I. G.; Ng, J. B.; Hall, D. A.; Soo Lum, B.; Shaver, A. *J. Biol. Chem.* **1994**, *269*, 4596-4604.

(18) Mimoun, H.; Saussine, L.; Daire, E.; Postel, M.; Fischer, J.; Weiss, R. *J. Am. Chem. Soc.* **1983**, *105*, 3101-3110.

(19) Galeffi, B.; Tracey, A. S. *Inorg. Chem.* **1989**, *28*, 1726-1734.

(20) Hartkamp, H. *Angew. Chem.* **1959**, *71*, 553.

A.1. Crystallographic Tables & Figures for bG(piper)•bpV(pic)

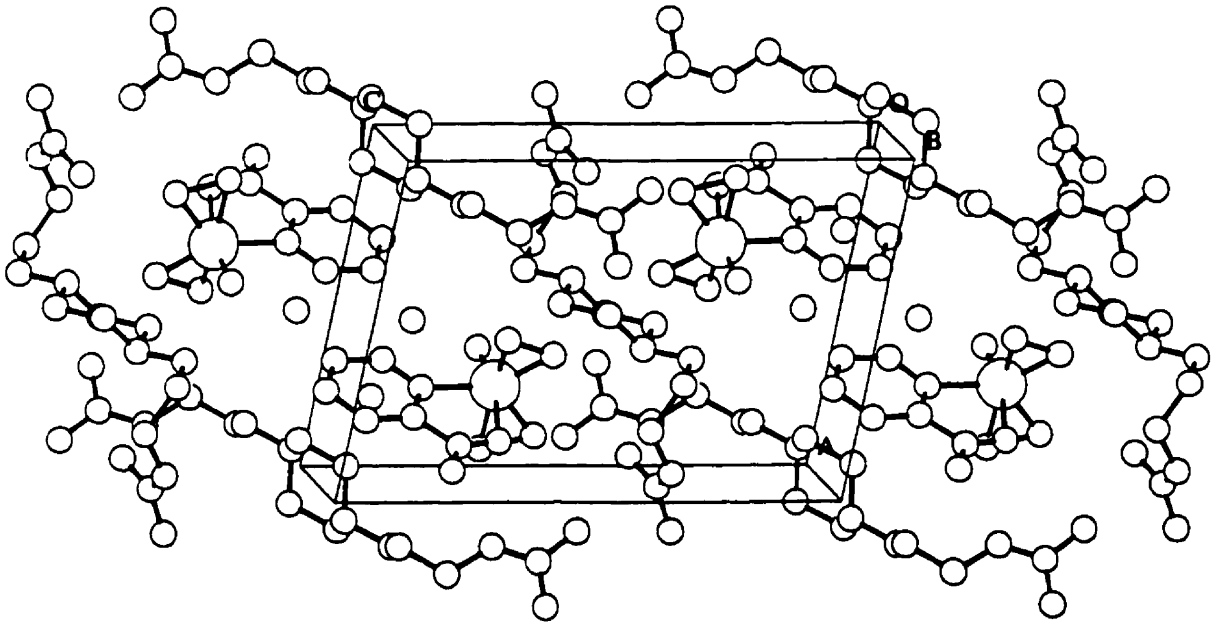

Figure A.1.1 Packing diagram for bG(piper)•bpV(pic)

Table A.1.1 Crystallographic parameters for.bG(piper)•bpV(pic).

	bG(piper)•bpV(pic)
	$C_{18}H_{38}N_9O_9V$
fw	575.51
Crystal System	Triclinic
Space Group	P -1
Temperature (°C)	20 ± 2
l (Å)	0.70930
a (Å)	9.207(8)
b (Å)	10.858(4)
c (Å)	13.586(3)
a (°)	84.73(4)
b (°)	77.08(4)
g (°)	82.74(5)
r calc (g cm^{-3})	1.459
V ($Å^3$)	1310.3(13)
F(000)	608
No. measured	10356
No. observed ref.	3514
No. independ. ref.	5177
Rint	0.076
Z	2
$R1^a$ (final), $R1^a$ (all data)	0.0628, 0.1031
$wR2^b$ (final), $wR2^b$ (all data)	0.1340, 0.1479
S	1.029
Secondary Extinction	0.0047(14)
μ (mm^{-1})	0.426 (MoKa)
Scan Type	w/2q

$^a R1 = \sum \| Fo | - | Fc \| / \sum | Fo |$

$^b wR2 = \{ [\sum w (| Fo | - | Fc |)^2 / \sum w | Fo |^2] \}^{1/2}$

$GoF = [\sum [w(Fo^2-Fc^2)^2] / (\text{No. of refIns - No. of params.})]^{1/2}$

Table A.1.2 Bond lengths and angles for bG(piper)•bpV(pic)

V(1)-O(1)	1.601(3)	V(1)-O(5)	1.880(3)
V(1)-O(3)	1.889(3)	V(1)-O(4)	1.893(3)
V(1)-O(2)	1.930(3)	V(1)-N(1)	2.132(3)
V(1)-O(6)	2.332(3)	O(2)-O(3)	1.470(3)
O(4)-O(5)	1.460(4)	O(6)-C(7)	1.247(5)
O(7)-C(7)	1.238(5)	N(1)-C(6)	1.333(5)
N(1)-C(2)	1.343(4)	C(2)-C(3)	1.377(6)
C(2)-H(2)	0.9300	C(3)-C(4)	1.362(6)
C(3)-H(3)	0.9300	C(4)-C(5)	1.390(6)
C(4)-H(4)	0.9300	C(5)-C(6)	1.375(5)
C(5)-H(5)	0.9300	C(6)-C(7)	1.521(5)
N(2)-C(12)	1.463(5)	N(2)-C(8)	1.466(4)
N(2)-C(13)	1.472(4)	N(3)-C(11)	1.330(4)
N(3)-C(10)	1.458(5)	N(3)-H(33)	0.92(4)
N(4)-C(11)	1.315(5)	N(4)-H(44A)	0.99(5)
N(4)-H(44B)	0.78(4)	N(5)-C(11)	1.330(5)
N(5)-H(55A)	0.83(4)	N(5)-H(55B)	0.73(5)
C(8)-C(9)	1.517(5)	C(8)-H(8A)	0.9700
C(8)-H(8B)	0.9700	C(9)-C(10)	1.519(5)
C(9)-H(9A)	0.9700	C(9)-H(9B)	0.9700
C(10)-H(10A)	0.9700	C(10)-H(10B)	0.9700
C(12)-C(13)#1	1.515(5)	C(12)-H(12A)	0.9700
C(12)-H(12B)	0.9700	C(13)-C(12)#1	1.515(5)
C(13)-H(13A)	0.9700	C(13)-H(13B)	0.9700
N(6)-C(18)	1.460(5)	N(6)-C(19)	1.464(5)
N(6)-C(14)	1.477(5)	N(7)-C(17)	1.324(5)
N(7)-C(16)	1.457(5)	N(7)-H(77)	0.92(4)
N(8)-C(17)	1.330(6)	N(8)-H(88A)	0.87(5)
N(8)-H(88B)	0.77(4)	N(9)-C(17)	1.318(5)
N(9)-H(99A)	0.73(4)	N(9)-H(99B)	0.88(5)
C(14)-C(15)	1.513(6)	C(14)-H(14A)	0.9700
C(14)-H(14B)	0.9700	C(15)-C(16)	1.511(6)
C(15)-H(15A)	0.9700	C(15)-H(15B)	0.9700
C(16)-H(16A)	0.9700	C(16)-H(16B)	0.9700
C(18)-C(19)#2	1.508(6)	C(18)-H(18A)	0.9700
C(18)-H(18B)	0.9700	C(19)-C(18)#2	1.508(6)
C(19)-H(19A)	0.9700	C(19)-H(19B)	0.9700
O(8)-HO8A	1.03(4)	O(8)-HO8B	1.13(5)
O(8)-HO8C	1.13(5)		

O(1)-V(1)-O(5)	103.29(13)	O(1)-V(1)-O(3)	103.98(14)
O(5)-V(1)-O(3)	91.87(13)	O(1)-V(1)-O(4)	101.77(14)
O(5)-V(1)-O(4)	45.52(13)	O(3)-V(1)-O(4)	134.40(13)
O(1)-V(1)-O(2)	98.81(13)	O(5)-V(1)-O(2)	135.67(12)
O(3)-V(1)-O(2)	45.26(11)	O(4)-V(1)-O(2)	157.95(12)
O(1)-V(1)-N(1)	92.81(13)	O(5)-V(1)-N(1)	128.44(13)
O(3)-V(1)-N(1)	131.42(12)	O(4)-V(1)-N(1)	83.52(12)
O(2)-V(1)-N(1)	87.67(12)	O(1)-V(1)-O(6)	165.76(12)
O(5)-V(1)-O(6)	87.68(11)	O(3)-V(1)-O(6)	84.44(11)
O(4)-V(1)-O(6)	79.31(12)	O(2)-V(1)-O(6)	78.80(11)
N(1)-V(1)-O(6)	73.12(10)	O(3)-O(2)-V(1)	65.9(2)
O(2)-O(3)-V(1)	68.83(14)	O(5)-O(4)-V(1)	66.8(2)

O(4)-O(5)-V(1)	67.7(2)	C(7)-O(6)-V(1)	115.3(2)
C(6)-N(1)-C(2)	118.8(3)	C(6)-N(1)-V(1)	118.9(2)
C(2)-N(1)-V(1)	122.2(3)	N(1)-C(2)-C(3)	122.4(4)
N(1)-C(2)-H(2)	118.8	C(3)-C(2)-H(2)	118.8
C(4)-C(3)-C(2)	119.0(4)	C(4)-C(3)-H(3)	120.5
C(2)-C(3)-H(3)	120.5	C(3)-C(4)-C(5)	118.8(4)
C(3)-C(4)-H(4)	120.6	C(5)-C(4)-H(4)	120.6
C(6)-C(5)-C(4)	119.5(4)	C(6)-C(5)-H(5)	120.3
C(4)-C(5)-H(5)	120.3	N(1)-C(6)-C(5)	121.5(4)
N(1)-C(6)-C(7)	116.3(3)	C(5)-C(6)-C(7)	122.2(4)
O(7)-C(7)-O(6)	127.4(4)	O(7)-C(7)-C(6)	116.4(4)
O(6)-C(7)-C(6)	116.2(3)	C(12)-N(2)-C(8)	111.7(3)
C(12)-N(2)-C(13)	108.0(3)	C(8)-N(2)-C(13)	108.8(3)
C(11)-N(3)-C(10)	121.9(3)	C(11)-N(3)-H(33)	114(2)
C(10)-N(3)-H(33)	120(2)	C(11)-N(4)-H(44A)	124(2)
C(11)-N(4)-H(44B)	117(3)	H(44A)-N(4)-H(44B)	118(4)
C(11)-N(5)-H(55A)	115(2)	C(11)-N(5)-H(55B)	121(4)
H(55A)-N(5)-H(55B)	122(5)	N(2)-C(8)-C(9)	113.3(3)
N(2)-C(8)-H(8A)	108.9(2)	C(9)-C(8)-H(8A)	108.9
N(2)-C(8)-H(8B)	108.9(2)	C(9)-C(8)-H(8B)	108.9
H(8A)-C(8)-H(8B)	107.7	C(8)-C(9)-C(10)	113.1(3)
C(8)-C(9)-H(9A)	109.0(2)	C(10)-C(9)-H(9A)	109.0
C(8)-C(9)-H(9B)	109.0(2)	C(10)-C(9)-H(9B)	109.0
H(9A)-C(9)-H(9B)	107.8	N(3)-C(10)-C(9)	110.8(3)
N(3)-C(10)-H(10A)	109.5(2)	C(9)-C(10)-H(10A)	109.5
N(3)-C(10)-H(10B)	109.5(2)	C(9)-C(10)-H(10B)	109.5
H(10A)-C(10)-H(10B)	108.1	N(4)-C(11)-N(5)	120.7(4)
N(4)-C(11)-N(3)	120.0(4)	N(5)-C(11)-N(3)	119.3(4)
N(2)-C(12)-C(13)#1	110.9(3)	N(2)-C(12)-H(12A)	109.5
C(13)#1-C(12)-H(12A)	109.5	N(2)-C(12)-H(12B)	109.5
C(13)#1-C(12)-H(12B)	109.5	H(12A)-C(12)-H(12B)	108.0
N(2)-C(13)-C(12)#1	111.0(3)	N(2)-C(13)-H(13A)	109.4
C(12)#1-C(13)-H(13A)	109.4	N(2)-C(13)-H(13B)	109.4
C(12)#1-C(13)-H(13B)	109.4	H(13A)-C(13)-H(13B)	108.0
C(18)-N(6)-C(19)	108.6(3)	C(18)-N(6)-C(14)	112.2(3)
C(19)-N(6)-C(14)	109.6(3)	C(17)-N(7)-C(16)	125.2(4)
C(17)-N(7)-H(77)	120(3)	C(16)-N(7)-H(77)	111(3)
C(17)-N(8)-H(88A)	111(3)	C(17)-N(8)-H(88B)	120(3)
H(88A)-N(8)-H(88B)	120(5)	C(17)-N(9)-H(99A)	114(3)
C(17)-N(9)-H(99B)	124(3)	H(99A)-N(9)-H(99B)	120(5)
N(6)-C(14)-C(15)	113.8(3)	N(6)-C(14)-H(14A)	108.8
C(15)-C(14)-H(14A)	108.8	N(6)-C(14)-H(14B)	108.8
C(15)-C(14)-H(14B)	108.8	H(14A)-C(14)-H(14B)	107.7
C(16)-C(15)-C(14)	115.5(3)	C(16)-C(15)-H(15A)	108.4
C(14)-C(15)-H(15A)	108.4	C(16)-C(15)-H(15B)	108.4
C(14)-C(15)-H(15B)	108.4	H(15A)-C(15)-H(15B)	107.5
N(7)-C(16)-C(15)	115.1(3)	N(7)-C(16)-H(16A)	108.5
C(15)-C(16)-H(16A)	108.5	N(7)-C(16)-H(16B)	108.5
C(15)-C(16)-H(16B)	108.5	H(16A)-C(16)-H(16B)	107.5
N(9)-C(17)-N(7)	120.8(4)	N(9)-C(17)-N(8)	119.7(4)
N(7)-C(17)-N(8)	119.5(4)	N(6)-C(18)-C(19)#2	110.8(3)
N(6)-C(18)-H(18A)	109.5	C(19)#2-C(18)-H(18A)	109.5
N(6)-C(18)-H(18B)	109.5	C(19)#2-C(18)-H(18B)	109.5
H(18A)-C(18)-H(18B)	108.1	N(6)-C(19)-C(18)#2	111.2(3)

N(6)-C(19)-H(19A)	109.4	C(18)#2-C(19)-H(19A)	109.4
N(6)-C(19)-H(19B)	109.4	C(18)#2-C(19)-H(19B)	109.4
H(19A)-C(19)-H(19B)	108.0	HO8A-O(8)-HO8B	88(4)
HO8A-O(8)-HO8C	155(4)	HO8B-O(8)-HO8C	111(5)

Symmetry transformations used to generate equivalent atoms:
#1 -x+2,-y+1,-z+2 #2 -x+1,-y+1,-z+1

Table A.1.3 Atomic coordinates and equivalent isotropic displacement parameters for bG(piper)•bpV(pic)

Atom	x	y	z	U~eq~
V(1)	0.67473(7)	0.82057(6)	0.71961(5)	2.63(2)
O(1)	0.5751(3)	0.7083(2)	0.7605(2)	3.72(6)
O(2)	0.8706(3)	0.7312(2)	0.7161(2)	3.33(6)
O(3)	0.8298(3)	0.7522(3)	0.6169(2)	4.13(7)
O(4)	0.5264(3)	0.9588(2)	0.7241(2)	4.12(7)
O(5)	0.5757(3)	0.9100(3)	0.6241(2)	4.44(7)
O(6)	0.8219(3)	0.9842(2)	0.7023(2)	3.45(6)
O(7)	0.8936(4)	1.1165(3)	0.7934(2)	7.04(11)
N(1)	0.6750(3)	0.8670(3)	0.8687(2)	2.73(7)
C(2)	0.5980(4)	0.8083(4)	0.9516(3)	3.86(10)
C(3)	0.5958(5)	0.8395(4)	1.0479(3)	4.71(11)
C(4)	0.6751(6)	0.9327(4)	1.0599(3)	5.52(13)
C(5)	0.7553(5)	0.9935(4)	0.9742(3)	4.84(11)
C(6)	0.7512(4)	0.9594(3)	0.8800(3)	3.15(8)
C(7)	0.8300(4)	1.0261(3)	0.7831(3)	3.61(9)
N(2)	1.0967(3)	0.5877(3)	0.9399(2)	2.74(7)
N(3)	1.1480(3)	0.8246(3)	0.6584(2)	2.97(7)
N(4)	1.3110(4)	0.9277(3)	0.5357(3)	3.47(8)
N(5)	1.1000(5)	0.8662(4)	0.4994(3)	4.29(9)
C(8)	1.1658(4)	0.6454(3)	0.8415(3)	3.01(8)
C(9)	1.1507(4)	0.7863(3)	0.8386(3)	3.38(9)
C(10)	1.2251(4)	0.8455(4)	0.7372(3)	3.36(9)
C(11)	1.1860(4)	0.8750(3)	0.5646(3)	2.84(8)
C(12)	0.9332(4)	0.6123(3)	0.9607(3)	3.39(9)
C(13)	1.1364(4)	0.4520(3)	0.9392(3)	3.40(9)
N(6)	0.4074(4)	0.4269(3)	0.5777(2)	3.58(8)
N(7)	0.0506(4)	0.3059(3)	0.6755(3)	4.25(9)
N(8)	-0.1361(5)	0.4666(4)	0.7115(4)	5.69(12)
N(9)	0.0839(5)	0.5016(4)	0.6005(3)	4.62(10)
C(14)	0.3849(5)	0.3410(4)	0.6693(3)	4.57(11)
C(15)	0.3213(5)	0.2234(4)	0.6558(3)	4.68(11)
C(16)	0.1823(5)	0.2421(3)	0.6122(3)	3.93(10)
C(17)	0.0005(5)	0.4247(4)	0.6623(3)	3.85(9)
C(18)	0.5124(5)	0.3703(4)	0.4924(3)	4.21(10)
C(19)	0.4653(5)	0.5387(4)	0.5991(3)	4.57(11)
O(8)	0.2398(5)	0.6762(4)	0.0829(3)	7.91(12)
O(9)	0.5179(6)	0.4772(6)	0.8818(6)	18.7(3)
H(2)	0.5443	0.7442	0.9436	4.6
H(3)	0.5410	0.7975	1.1040	5.6
H(4)	0.6756	0.9554	1.1242	6.6
H(5)	0.8113	1.0567	0.9806	5.8

H(33)	1.053(4)	0.801(4)	0.675(3)	4.1(11)
H(44A)	1.386(5)	0.928(4)	0.578(3)	5.8(14)
H(44B)	1.329(5)	0.958(4)	0.481(3)	4.8(14)
H(55A)	1.016(4)	0.845(3)	0.525(3)	2.3(10)
H(55B)	1.118(5)	0.894(4)	0.447(4)	5(2)
H(8A)	1.1197	0.6205	0.7900	3.6
H(8B)	1.2714	0.6145	0.8252	3.6
H(9A)	1.1952	0.8113	0.8910	4.1
H(9B)	1.0452	0.8173	0.8536	4.1
H(10A)	1.2235	0.9342	0.7424	4.0
H(10B)	1.3290	0.8102	0.7193	4.0
H(12A)	0.8958	0.5828	0.9068	4.1
H(12B)	0.9043	0.7012	0.9626	4.1
H(13A)	1.2445	0.4334	0.9265	4.1
H(13B)	1.1015	0.4207	0.8850	4.1
H(77)	-0.013(5)	0.250(4)	0.709(3)	5.5(14)
H(88A)	-0.147(5)	0.547(5)	0.713(3)	5.5(14)
H(88B)	-0.178(5)	0.427(4)	0.756(3)	4.2(14)
H(99A)	0.045(4)	0.564(4)	0.594(3)	3.0(13)
H(99B)	0.182(6)	0.489(4)	0.583(4)	6(2)
H(14A)	0.3175	0.3841	0.7241	5.5
H(14B)	0.4803	0.3186	0.6890	5.5
H(15A)	0.3983	0.1720	0.6120	5.6
H(15B)	0.2982	0.1777	0.7212	5.6
H(16A)	0.2046	0.2893	0.5475	4.7
H(16B)	0.1583	0.1613	0.5996	4.7
H(18A)	0.4741	0.2972	0.4762	5.1
H(18B)	0.6079	0.3442	0.5110	5.1
H(19A)	0.5601	0.5156	0.6195	5.5
H(19B)	0.3954	0.5782	0.6547	5.5
HO8A	0.327(5)	0.612(4)	0.052(3)	5.2(14)
HO8B	0.175(7)	0.647(6)	0.029(5)	3.5(14)
HO8C	0.189(8)	0.769(5)	0.113(5)	3.5(14)

U~eq~ = (1/3)sum~i~sum~j~U~ij~a^*^~i~a^*^~j~a~i~.a~j~

Table A.1.4 Anisotropic parameters for bG(piper)•bpV(pic)

Atom	U11	U22	U33	U23	U13	U12
V(1)	2.69(3)	2.81(4)	2.40(3)	0.50(2)	-0.63(2)	-0.74(3)
O(1)	3.8(2)	3.7(2)	4.0(2)	0.54(12)	-1.06(12)	-1.57(12)
O(2)	2.89(14)	3.4(2)	3.56(14)	0.15(11)	-0.53(11)	-0.34(11)
O(3)	4.4(2)	5.4(2)	2.60(14)	-0.94(13)	-0.21(12)	-1.13(14)
O(4)	3.7(2)	4.0(2)	4.4(2)	0.99(13)	-1.06(13)	-0.13(13)
O(5)	4.5(2)	5.5(2)	3.6(2)	2.05(13)	-2.01(13)	-1.70(14)
O(6)	4.0(2)	3.5(2)	2.65(14)	0.57(11)	-0.34(12)	-0.84(12)
O(7)	10.2(3)	5.9(2)	6.0(2)	0.6(2)	-1.7(2)	-5.4(2)
N(1)	2.9(2)	2.7(2)	2.3(2)	0.36(12)	-0.34(13)	-0.23(13)
C(2)	3.8(2)	3.7(2)	3.3(2)	0.6(2)	0.3(2)	-0.2(2)
C(3)	5.8(3)	4.9(3)	2.5(2)	0.7(2)	0.1(2)	0.3(2)
C(4)	8.0(4)	5.4(3)	2.9(2)	-0.8(2)	-1.1(2)	0.6(3)
C(5)	6.9(3)	4.1(3)	3.6(2)	-0.9(2)	-1.1(2)	-0.6(2)

C(6)	4.0(2)	2.4(2)	2.9(2)	-0.2(2)	-0.7(2)	0.0(2)
C(7)	4.0(2)	2.9(2)	4.0(2)	0.2(2)	-0.8(2)	-0.8(2)
N(2)	2.9(2)	2.7(2)	2.1(2)	0.60(12)	0.02(12)	-0.11(13)
N(3)	2.7(2)	3.6(2)	2.6(2)	0.69(13)	-0.40(13)	-0.89(14)
N(4)	3.8(2)	3.7(2)	2.5(2)	1.3(2)	-0.1(2)	-0.9(2)
N(5)	3.7(2)	6.0(3)	3.0(2)	1.2(2)	-0.7(2)	-0.9(2)
C(8)	3.4(2)	3.1(2)	2.1(2)	0.5(2)	-0.1(2)	-0.4(2)
C(9)	4.4(2)	3.1(2)	2.6(2)	0.2(2)	-0.5(2)	-0.8(2)
C(10)	3.7(2)	3.4(2)	3.1(2)	0.6(2)	-0.9(2)	-0.9(2)
C(11)	3.1(2)	2.0(2)	3.2(2)	0.2(2)	-0.4(2)	0.2(2)
C(12)	3.2(2)	3.1(2)	3.3(2)	0.9(2)	0.0(2)	0.0(2)
C(13)	3.1(2)	2.9(2)	3.4(2)	0.4(2)	0.4(2)	0.3(2)
N(6)	4.2(2)	3.1(2)	2.9(2)	-0.54(14)	0.47(14)	-0.5(2)
N(7)	4.6(2)	2.5(2)	5.2(2)	0.4(2)	-0.3(2)	-0.6(2)
N(8)	5.5(3)	3.6(2)	7.1(3)	0.4(2)	0.1(2)	-0.4(2)
N(9)	4.8(3)	3.1(2)	5.6(3)	0.8(2)	-0.8(2)	-0.3(2)
C(14)	5.0(3)	4.8(3)	4.0(2)	0.3(2)	-1.2(2)	-1.2(2)
C(15)	5.3(3)	3.9(2)	4.4(3)	0.9(2)	-0.7(2)	-0.4(2)
C(16)	5.0(3)	2.4(2)	4.3(2)	-0.7(2)	-0.7(2)	0.0(2)
C(17)	4.4(2)	3.1(2)	4.1(2)	-0.4(2)	-0.8(2)	-0.4(2)
C(18)	4.6(2)	3.0(2)	4.6(2)	-1.1(2)	0.2(2)	-0.3(2)
C(19)	5.5(3)	4.2(3)	3.7(2)	-1.8(2)	0.6(2)	-1.3(2)
O(8)	10.3(3)	6.5(3)	7.8(3)	-0.1(2)	-3.8(3)	-1.4(2)
O(9)	10.2(4)	16.1(6)	29.0(9)	10.6(6)	-5.6(5)	-4.1(4)

The anisotropic displacement factor exponent takes the form:
-2 pi^2 [h^2 a*^2 U11 + ... + 2 h k a* b* U12]

A.2. Crystallographic Tables & Figures for pA(putrescine)•bpV(bipy)

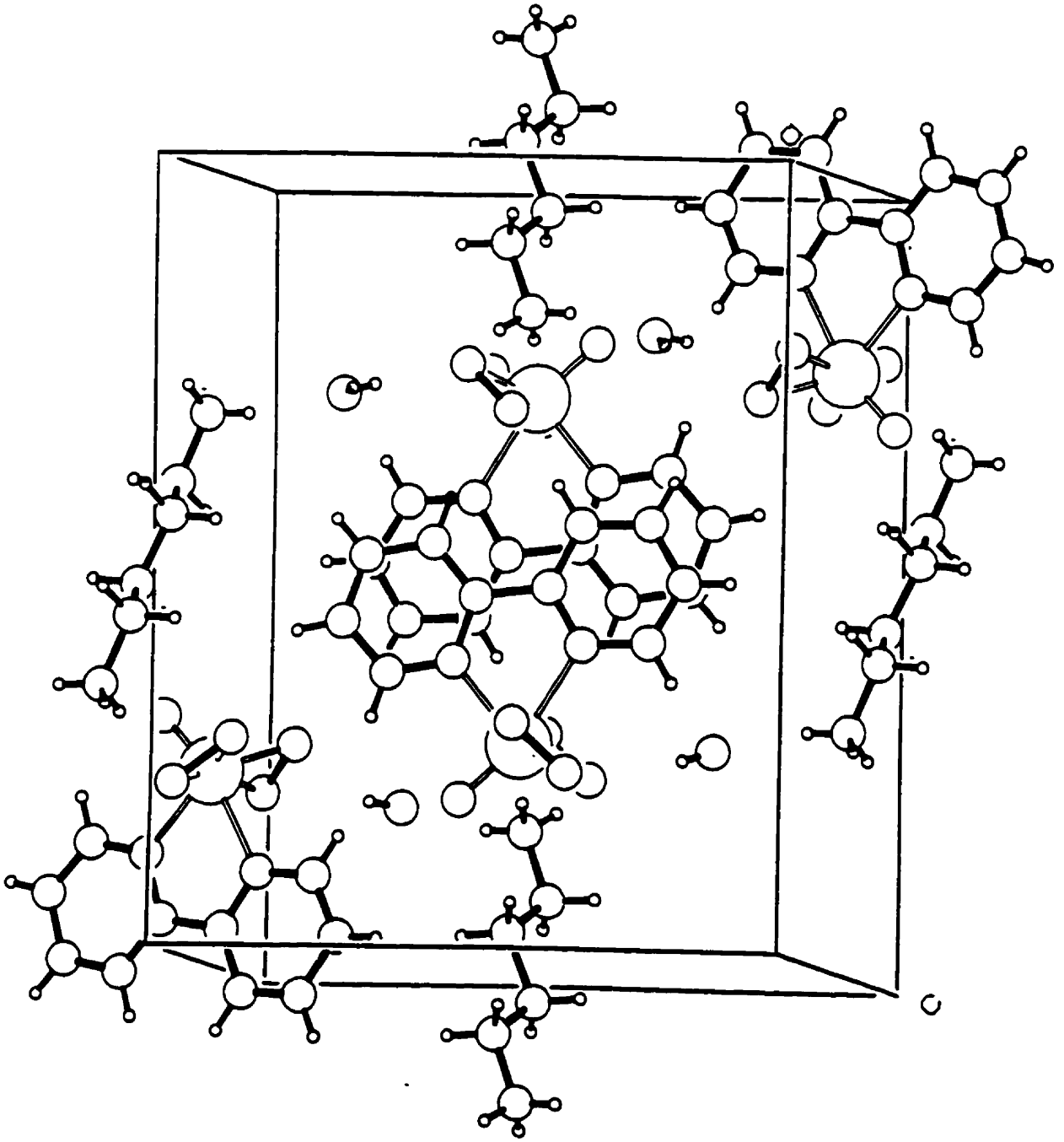

Figure A.2.1 Packing diagram for pA(putrescine)•bpV(bipy)

Table A.2.1 Crystallographic parameters for pA(putrescine)•bpV(bipy)

	pA(putrescine)•bpV(bipy)
	$C_{12}H_4N_3O_6V$
fw	350.23
Crystal System	Monoclinic
Space Group	P 2(1) / n
Temperature (°C)	20 ± 2
l (Å)	0.70930
a (Å)	7.155(2)
b (Å)	13.407(2)
c (Å)	15.589(3)
a (°)	90
b (°)	96.74 (2)
g (°)	90
r calc (g cm^{-3})	1.566
V ($Å^3$)	1485.0(6)
No. variables	220
No. measured	11359
No. observed ref.	2050
No. unique ref.	2928
Rint	0.078
Z	3
R1[a]	0.0481
wR2[b]	0.0884
S	1.046
Secondary Extinction	
μ (mm^{-1})	1.47 (MoKa)
Scan Type	w/2q

[a] $R1 = \Sigma \| Fo | - | Fc \| / \Sigma | Fo |$ [b] $wR2 = \{ |\Sigma w (| Fo | - | Fc |)^2 / \Sigma w | Fo |^2 \}^{1/2}$

$w = 1/[\backslash s^2(Fo^2) + (0.0334P)^2 + 0.9982P]$ $P = (Fo^2 + 2Fc^2)/3$

$S = [\Sigma w(|Fo| - |Fc|)^2 / (n-v)]^{1/2}$

Table A.2.2 Bond lengths and angles for pA(putrescine)•bpV(bipy)

V(1)-O(1)	1.616(3)	V(1)-O(2)	1.848(2)
V(1)-O(5)	2.047(2)	V(1)-O(3)	2.127(3)
V(1)-O(3)#1	2.127(3)	V(1)-N(1)	2.192(3)
N(1)-C(3)	1.484(3)	N(1)-C(1)#1	1.501(7)
N(1)-C(1)	1.501(6)	O(2)-O(2)#1	1.427(5)
C(1)-C(2)	1.497(7)	C(1)-H(1A)	0.97
C(1)-H(1B)	0.97	C(2)-O(4)#1	1.215(11)
C(2)-O(4)	1.215(10)	C(2)-O(3)	1.276(5)
O(3)-C(2)#1	1.276(5)	O(4)-C(2)#1	1.215(10)
C(3)-C(4)	1.501(4)	C(3)-H(3A)	0.97
C(3)-H(3B)	0.97	C(4)-O(6)	1.226(4)
C(4)-O(5)	1.289(3)	C(5)-N(2)	1.315(4)
C(5)-N(4)	1.323(4)	C(5)-N(3)	1.325(4)
N(2)-HN2A	0.86	N(2)-HN2B	0.86
N(3)-HN3A	0.86	N(3)-HN3B	0.86
N(4)-C(6)	1.462(4)	N(4)-HN4	0.86
C(6)-C(7)	1.547(6)	C(6)-H(6A)	0.97
C(6)-H(6B)	0.97	C(7)-C(7)#3	1.525(10)
C(7)-H(7A)	0.97	C(7)-H(7B)	0.97
C(61)-C(71)	1.575(10)	C(61)-H(61A)	0.970(10)
C(61)-H(61B)	0.970(11)	C(71)-C(71)#3	1.52(2)
C(71)-H(71B)	0.97	C(71)-H(71B)	0.97

O(1)-V(1)-O(2)	105.22(13)	O(1)-V(1)-O(2)#1	105.22(13)
O(2)#1-V(1)-O(2)	45.42(14)	O(1)-V(1)-O(5)	93.93(7)
O(2)#1-V(1)-O(5)	125.22(9)	O(2)-V(1)-O(5)	80.28(9)
O(1)-V(1)-O(5)#1	93.93(7)	O(2)#1-V(1)-O(5)#1	80.28(9)
O(2)-V(1)-O(5)#1	125.22(9)	O(5)-V(1)-O(5)#1	149.84(12)
O(1)-V(1)-O(3)	167.20(13)	O(2)#1-V(1)-O(3)	86.56(11)
O(2)-V(1)-O(3)	86.55(11)	O(5)-V(1)-O(3)	82.96(7)
O(5)#1-V(1)-O(3)	82.96(7)	O(1)-V(1)-O(3)#1	167.20(13)
O(2)#1-V(1)-O(3)#1	86.56(11)	O(2)-V(1)-O(3)#1	86.55(11)
O(5)-V(1)-O(3)#1	82.96(7)	O(5)#1-V(1)-O(3)#1	82.96(7)
O(1)-V(1)-N(1)	89.40(14)	O(2)#1-V(1)-N(1)	152.50(9)
O(2)-V(1)-N(1)	152.50(9)	O(5)-V(1)-N(1)	75.51(6)
O(5)#1-V(1)-N(1)	75.51(6)	O(3)-V(1)-N(1)	77.81(11)
O(3)#1-V(1)-N(1)	77.81(11)	C(3)#1-N(1)-C(3)	113.5(3)
C(3)#1-N(1)-C(1)#1	106.5(14)	C(3)-N(1)-C(1)#1	115.4(14)
C(3)#1-N(1)-C(1)	115.4(14)	C(3)-N(1)-C(1)	106.5(14)
C(3)#1-N(1)-V(1)	105.5(2)	C(3)-N(1)-V(1)	105.5(2)
C(1)#1-N(1)-V(1)	110.2(2)	C(1)-N(1)-V(1)	110.2(2)
O(2)#1-O(2)-V(1)	67.29(7)	C(2)-C(1)-N(1)	114.6(6)
C(2)-C(1)-H(1A)	108.6	N(1)-C(1)-H(1A)	108.6
C(2)-C(1)-H(1B)	108.6	N(1)-C(1)-H(1B)	108.6
H(1A)-C(1)-H(1B)	107.6	O(4)-C(2)-O(3)	124.7(5)
O(4)-C(2)-C(1)	115.8(7)	O(3)-C(2)-C(1)	116.6(4)
C(2)-O(3)-V(1)	119.9(3)	N(1)-C(3)-C(4)	108.3(2)
N(1)-C(3)-H(3A)	110.0	C(4)-C(3)-H(3A)	110.0
N(1)-C(3)-H(3B)	110.0	C(4)-C(3)-H(3B)	110.0
H(3A)-C(3)-H(3B)	108.4	O(6)-C(4)-O(5)	123.5(3)
O(6)-C(4)-C(3)	121.0(3)	O(5)-C(4)-C(3)	115.5(2)
C(4)-O(5)-V(1)	118.7(2)	N(2)-C(5)-N(4)	121.4(3)
N(2)-C(5)-N(3)	120.6(3)	N(4)-C(5)-N(3)	118.0(3)
C(5)-N(2)-HN2A	120.0	C(5)-N(2)-HN2B	120.0
HN2A-N(2)-HN2B	120.0	C(5)-N(3)-HN3A	120.0

C(5)-N(3)-HN3B	120.0	HN3A-N(3)-HN3B	120.0
C(5)-N(4)-C(61)	126.0(3)	C(5)-N(4)-C(6)	126.0(3)
C(5)-N(4)-HN4	117.0	C(6)-N(4)-HN4	117.0
N(4)-C(6)-C(7)	108.8(3)	N(4)-C(6)-H(6A)	109.9
C(7)-C(6)-H(6A)	109.9	N(4)-C(6)-H(6B)	109.9
C(7)-C(6)-H(6B)	109.9	H(6A)-C(6)-H(6B)	108.3
C(7)#3-C(7)-C(6)	111.9(6)	C(7)#3-C(7)-H(7A)	109.2
C(6)-C(7)-H(7A)	109.2	C(7)#3-C(7)-H(7B)	109.2
C(6)-C(7)-H(7B)	109.2	H(7A)-C(7)-H(7B)	107.9
N(4)-C(61)-C(71)	108.2(4)	N(4)-C(61)-H(61A)	110.1
C(71)-C(61)-H(61A)	110.1	N(4)-C(61)-H(61B)	110.1
C(71)-C(61)-H(61B)	110.1	H(61A)-C(61)-H(61B)	108.4
C(71)#3-C(71)-C(61)	109.4(9)	C(71)#3-C(71)-H(71B)	109.8
C(61)-C(71)-H(71B)	109.8	C(71)#3-C(71)-H(71B)	109.8
C(61)-C(71)-H(71B)	109.8	H(71B)-C(71)-H(71B)	108.2

Symmetry transformations used to generate equivalent atoms:
#1 x,-y+3/2,z #2 x,y,z #3 -x,-y+1,-z+1

Table A.2.3 Anisotropic paramters for pA(putrescine)•bpV(bipy)

Atom	U11	U22	U33	U23	U13	U12
V	2.70(3)	2.80(3)	2.02(3)	0.06(3)	0.14(2)	-0.15(3)
O(1)	4.73(14)	4.03(14)	2.41(12)	0.56(11)	0.58(10)	0.38(12)
O(2)	2.76(12)	3.69(14)	3.71(13)	-0.45(11)	0.37(10)	-0.47(10)
O(3)	4.10(14)	3.67(14)	3.26(13)	-0.58(11)	0.61(11)	0.43(11)
O(4)	5.1(2)	5.3(2)	4.4(2)	-0.83(13)	-0.37(13)	-1.88(14)
O(5)	2.72(13)	6.1(2)	4.1(2)	1.15(13)	0.02(11)	-0.38(12)
N(1)	2.49(14)	2.8(2)	2.6(2)	0.20(12)	0.29(11)	-0.33(11)
N(2)	2.58(13)	2.9(2)	2.21(13)	0.12(12)	0.22(11)	0.13(11)
C(1)	3.7(2)	2.9(2)	4.1(2)	0.1(2)	0.6(2)	-0.5(2)
C(2)	4.3(2)	3.1(2)	5.2(2)	1.4(2)	0.7(2)	-0.1(2)
C(3)	3.9(2)	5.1(3)	3.9(2)	2.3(2)	-0.2(2)	-0.4(2)
C(4)	4.1(2)	4.2(2)	2.5(2)	0.5(2)	-0.1(2)	-0.4(2)
C(5)	1.9(2)	3.5(2)	2.2(2)	0.13(13)	0.09(12)	-0.59(13)
C(6)	1.8(2)	3.2(2)	2.6(2)	0.05(14)	0.40(12)	-0.15(13)
C(7)	3.9(2)	4.1(2)	2.6(2)	-0.2(2)	0.3(2)	0.0(2)
C(8)	4.9(2)	3.7(2)	3.9(2)	-1.0(2)	0.4(2)	0.3(2)
C(9)	4.9(2)	3.4(2)	4.6(2)	-0.2(2)	0.6(2)	1.1(2)
C(10)	4.5(2)	3.3(2)	2.8(2)	0.6(2)	0.4(2)	0.7(2)
N(3)	3.1(2)	3.5(2)	2.6(2)	-0.1(2)	0.17(13)	0.1(2)
C(11)	3.8(2)	4.6(2)	2.4(2)	0.4(2)	0.4(2)	-0.3(2)
C(12)	3.0(2)	3.2(2)	2.8(2)	-0.21(14)	0.41(14)	-0.10(14)
O(6)	4.4(2)	3.5(2)	7.5(2)	0.90(14)	0.3(2)	-0.4(2)

The anisotropic displacement factor exponent takes the form:
$-2\pi^2 [h^2 a^{*2} U11 + ... + 2 h k a^* b^* U12]$

Table A.2.4 Atomic coordinates and equivalent isotropic displacement parameters for pA(putrescine)•bpV(bipy)

Atom	X	Y	Z	U~eq~
V	0.27580(7)	0.04391(4)	0.23244(3)	2.52(2)
O(1)	0.3174(3)	-0.0417(2)	0.30464(13)	3.71(6)
O(2)	0.0087(3)	0.0332(2)	0.20606(14)	3.39(5)
O(3)	0.0677(3)	0.1149(2)	0.26539(14)	3.67(6)
O(4)	0.4371(4)	0.1474(2)	0.2742(2)	5.00(7)
O(5)	0.5283(3)	0.0806(2)	0.2172(2)	4.34(7)
N(1)	0.2276(3)	0.1313(2)	0.1036(2)	2.62(6)
N(2)	0.2954(3)	-0.0597(2)	0.1287(2)	2.56(6)
C(1)	0.1893(5)	0.2284(2)	0.0971(2)	3.54(8)
C(2)	0.1439(5)	0.2753(3)	0.0187(2)	4.19(9)
C(3)	0.1394(5)	0.2203(3)	-0.0558(2)	4.34(10)
C(4)	0.1806(5)	0.1195(3)	-0.0503(2)	3.63(8)
C(5)	0.2237(4)	0.0771(2)	0.0310(2)	2.54(7)
C(6)	0.2686(4)	-0.0298(2)	0.0449(2)	2.54(7)
C(7)	0.2832(5)	-0.0965(3)	-0.0220(2)	3.52(8)
C(8)	0.3269(5)	-0.1943(3)	-0.0035(2)	4.19(9)
C(9)	0.3525(5)	-0.2251(3)	0.0814(2)	4.30(9)
C(10)	0.3353(5)	-0.1558(2)	0.1452(2)	3.54(8)
N(3)	0.7257(4)	0.4606(3)	0.1826(2)	3.08(6)
C(11)	0.7013(5)	0.5021(3)	0.0942(2)	3.60(8)
C(12)	0.5132(4)	0.4761(2)	0.0448(2)	3.00(8)
O(6)	0.7722(5)	0.2541(2)	0.2127(2)	5.16(8)
H(1)	0.1932(5)	0.2660(2)	0.1474(2)	4.2
H(2)	0.1168(5)	0.3432(3)	0.0163(2)	5.0
H(3)	0.1090(5)	0.2504(3)	-0.1094(2)	5.2
H(4)	0.1795(5)	0.0809(3)	-0.0999(2)	4.4
H(7)	0.2634(5)	-0.0750(3)	-0.0791(2)	4.2
H(8)	0.3393(5)	-0.2394(3)	-0.0478(2)	5.0
H(9)	0.3808(5)	-0.2913(3)	0.0953(2)	5.2
H(10)	0.3521(5)	-0.1768(2)	0.2025(2)	4.2
H(3A)	0.832(6)	0.489(3)	0.211(3)	6.2(13)
H(3B)	0.736(5)	0.397(3)	0.184(2)	4.3(12)
H(3C)	0.629(6)	0.473(3)	0.213(3)	6.6(14)
H(11A)	0.8008(5)	0.4770(3)	0.0628(2)	4.3
H(11B)	0.7134(5)	0.5741(3)	0.0975(2)	4.3
H(12A)	0.4134(4)	0.4983(2)	0.0773(2)	3.6
H(12B)	0.5034(4)	0.4042(2)	0.0388(2)	3.6
H(6A)	0.675(6)	0.223(3)	0.216(3)	6(2)

(U~eq~ = (1/3)sum~i~sum~j~U~ij~a^*^~i~a^*^~j~a~i~.a~j~.)

A.3. Crystallographic Tables & Figures for mG(diamino)•mpV(2,6-pdc)

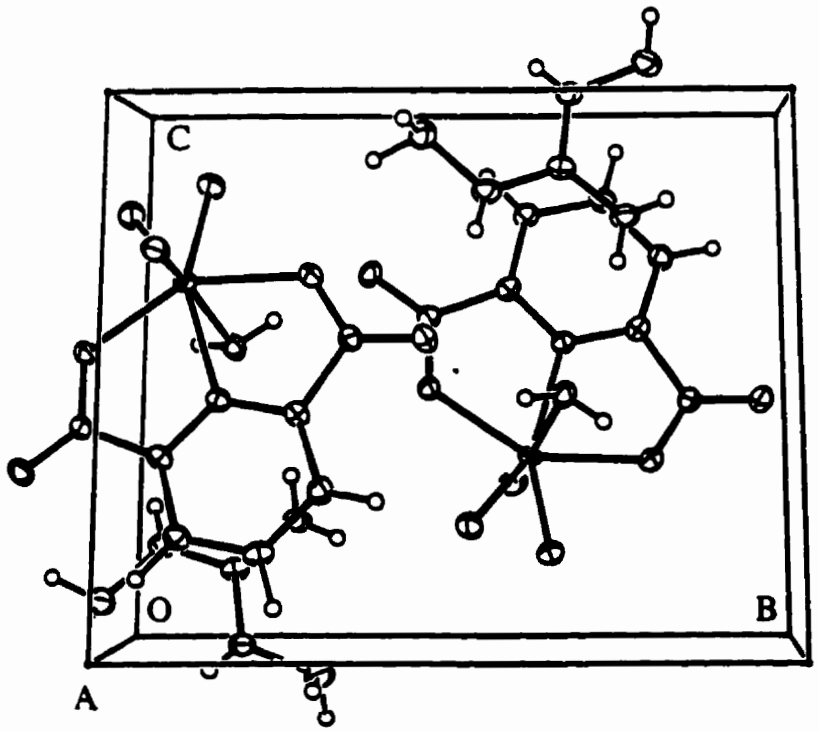

Figure A.3.1 Packing diagram for mG(diamino)•mpV(2,6-pdc)

Table A.3.1 Crystallographic parameters for.mG(diamino)•mpV(2,6-pdc)

	mG(diamino)•mpV(2,6-pdc)
	$C_8H_{13}N_6O_8V$
fw	372.17
Crystal System	Monoclinic
Space Group	P21
Temperature (°C)	-53 ± 2
l (Å)	1.54056
a (Å)	6.761(2)
b (Å)	11.045(5)
c (Å)	9.570(2)
a (°)	90
b (°)	110.14(2)
g (°)	90
r calc (g cm^{-3})	1.842
V ($Å^3$)	670.9(4)
F(000)	380
No. measured	4987
No. observed ref.	2520
No. indep. ref.	2534
Rint	0.085
Z	2
$R1^a$, $R1^a$ (all data)	0.0400, 0.0401
$wR2^b$, $wR2^b$ (all data)	0.1118, 0.1119
S	1.131
Secondary Extinction	0.066(3)
μ (mm^{-1})	6.766 (CuKa)
Scan Type	w/2q

$^aR1 = \sum \| Fo | - | Fc \| / \sum | Fo |$

$^bwR2 = \{ [\sum w (| Fo | - | Fc |)^2 / \sum w | Fo |^2] \}^{1/2}$

$GoF = [\sum [w(Fo^2-Fc^2)^2] / (\text{No. of refIns.} - \text{No. of params.})]^{1/2}$

Table A.3.2 Bond lengths and angles for mG(diamino)•mpV(2,6-pdc)

V(1)-O(1)	1.596(3)	V(1)-O(3)	1.866(3)
V(1)-O(2)	1.868(3)	V(1)-O(7)	2.053(3)
V(1)-O(5)	2.054(3)	V(1)-N(1)	2.092(3)
V(1)-O(4)	2.317(3)	O(2)-O(3)	1.422(5)
O(4)-H(4A)	0.81(2)	O(4)-H(4B)	0.82(2)
O(5)-C(7)	1.288(4)	O(6)-C(7)	1.230(4)
O(7)-C(8)	1.289(4)	O(8)-C(8)	1.229(4)
N(1)-C(6)	1.321(4)	N(1)-C(2)	1.330(5)
C(2)-C(3)	1.373(5)	C(2)-C(8)	1.495(5)
C(3)-C(4)	1.398(5)	C(3)-H(3)	0.9400
C(4)-C(5)	1.381(6)	C(4)-H(4)	0.9400
C(5)-C(6)	1.386(5)	C(5)-H(5)	0.9400
C(6)-C(7)	1.496(5)	C(1)-N(2)	1.314(5)
C(1)-N(5)	1.327(5)	C(1)-N(3)	1.331(5)
N(2)-H(22A)	0.77(7)	N(2)-H(22B)	0.80(5)
N(3)-N(4)	1.409(5)	N(3)-H(33)	0.79(5)
N(4)-H(44A)	1.06(9)	N(4)-H(44B)	0.92(8)
N(5)-N(6)	1.401(5)	N(5)-H(55)	0.69(5)
N(6)-H(66A)	0.84(5)	N(6)-H(66B)	0.86(6)

O(1)-V(1)-O(3)	103.68(14)	O(1)-V(1)-O(2)	105.0(2)
O(3)-V(1)-O(2)	44.76(14)	O(1)-V(1)-O(7)	94.63(13)
O(3)-V(1)-O(7)	81.15(12)	O(2)-V(1)-O(7)	125.12(12)
O(1)-V(1)-O(5)	94.93(12)	O(3)-V(1)-O(5)	125.52(12)
O(2)-V(1)-O(5)	81.15(12)	O(7)-V(1)-O(5)	148.16(10)
O(1)-V(1)-N(1)	92.92(12)	O(3)-V(1)-N(1)	151.26(13)
O(2)-V(1)-N(1)	151.33(13)	O(7)-V(1)-N(1)	74.17(11)
O(5)-V(1)-N(1)	75.07(11)	O(1)-V(1)-O(4)	169.86(12)
O(3)-V(1)-O(4)	85.30(12)	O(2)-V(1)-O(4)	84.66(13)
O(7)-V(1)-O(4)	81.96(10)	O(5)-V(1)-O(4)	83.35(10)
N(1)-V(1)-O(4)	76.98(10)	O(3)-O(2)-V(1)	67.6(2)
O(2)-O(3)-V(1)	67.7(2)	V(1)-O(4)-H(4A)	107(4)
V(1)-O(4)-H(4B)	103(4)	H(4A)-O(4)-H(4B)	112(5)
C(7)-O(5)-V(1)	119.3(2)	C(8)-O(7)-V(1)	120.9(2)
C(6)-N(1)-C(2)	122.1(3)	C(6)-N(1)-V(1)	118.2(2)
C(2)-N(1)-V(1)	119.6(2)	N(1)-C(2)-C(3)	120.9(3)
N(1)-C(2)-C(8)	111.0(3)	C(3)-C(2)-C(8)	128.0(3)
C(2)-C(3)-C(4)	117.8(3)	C(2)-C(3)-H(3)	121.1
C(4)-C(3)-H(3)	121.1	C(5)-C(4)-C(3)	120.4(3)
C(5)-C(4)-H(4)	119.8	C(3)-C(4)-H(4)	119.8
C(4)-C(5)-C(6)	118.0(3)	C(4)-C(5)-H(5)	121.0
C(6)-C(5)-H(5)	121.0	N(1)-C(6)-C(5)	120.7(3)
N(1)-C(6)-C(7)	112.0(3)	C(5)-C(6)-C(7)	127.3(3)
O(6)-C(7)-O(5)	124.7(3)	O(6)-C(7)-C(6)	120.8(3)
O(5)-C(7)-C(6)	114.4(3)	O(8)-C(8)-O(7)	124.3(3)
O(8)-C(8)-C(2)	121.6(3)	O(7)-C(8)-C(2)	114.1(3)
N(2)-C(1)-N(5)	121.0(4)	N(2)-C(1)-N(3)	121.0(3)
N(5)-C(1)-N(3)	118.0(3)	C(1)-N(2)-H2B)	119(3)
H(22A)-N(2)-H(22B)	126(5)	C(1)-N(3)-N(4)	117.6(3)
C(1)-N(3)-H(33)	126(4)	N(4)-N(3)-H(33)	115(4)
N(3)-N(4)-H(44A)	103(5)	N(3)-N(4)-H(44B)	112(5)
H(44A)-N(4)-H(44B)	91(7)	C(1)-N(5)-N(6)	119.8(4)
C(1)-N(5)-H(55)	118(4)	N(6)-N(5)-H(55)	121(4)
N(5)-N(6)-H(66A)	102(4)	N(5)-N(6)-H(66B)	106(4)

Table A.3.3 Atomic coordinates and equivalent isotropic displacement parameters for mG(diamino)•mpV(2,6-pdc)

Atom	X	Y	Z	U~eq~
V(1)	0.23697(8)	0.60764(5)	0.33927(5)	2.53(2)
O(1)	-0.0090(4)	0.5781(2)	0.2848(3)	3.70(7)
O(2)	0.3402(6)	0.5175(3)	0.2142(3)	4.46(7)
O(3)	0.2877(5)	0.6381(3)	0.1627(3)	4.18(8)
O(4)	0.5859(4)	0.6624(2)	0.4566(3)	2.73(5)
O(5)	0.3264(4)	0.4546(2)	0.4675(3)	2.76(5)
O(6)	0.3467(4)	0.3641(2)	0.6804(3)	3.15(6)
O(7)	0.1966(4)	0.7920(2)	0.3301(3)	2.83(5)
O(8)	0.1549(4)	0.9611(2)	0.4438(3)	2.94(5)
N(1)	0.2455(4)	0.6597(3)	0.5514(3)	2.15(5)
C(2)	0.2111(5)	0.7748(3)	0.5771(4)	2.33(6)
C(3)	0.2043(5)	0.8105(3)	0.7128(4)	2.76(7)
C(4)	0.2366(5)	0.7223(4)	0.8230(4)	2.99(8)
C(5)	0.2743(5)	0.6035(4)	0.7948(4)	2.54(6)
C(6)	0.2781(5)	0.5752(3)	0.6547(4)	2.31(7)
C(7)	0.3189(5)	0.4541(3)	0.6002(4)	2.34(6)
C(8)	0.1844(5)	0.8513(3)	0.4430(4)	2.30(7)
C(1)	0.2366(5)	0.1613(4)	0.1317(4)	2.56(7)
N(2)	0.2641(5)	0.2545(4)	0.2217(4)	3.11(7)
N(3)	0.2067(6)	0.0506(3)	0.1757(4)	3.27(7)
N(4)	0.1767(7)	-0.0445(3)	0.0724(4)	4.21(8)
N(5)	0.2415(5)	0.1744(3)	-0.0049(4)	3.09(7)
N(6)	0.2539(7)	0.2905(4)	-0.0602(4)	4.02(8)
H(4A)	0.658(7)	0.605(4)	0.451(5)	4.4(13)
H(4B)	0.601(9)	0.720(4)	0.407(6)	5(2)
H(3)	0.1788	0.8917	0.7309	3.3
H(4)	0.2327	0.7439	0.9170	3.6
H(5)	0.2966	0.5436	0.8684	3.0
H(22A)	0.283(9)	0.316(7)	0.190(7)	5(2)
H(22B)	0.262(6)	0.243(4)	0.304(6)	1.6(9)
H(33)	0.176(7)	0.035(5)	0.246(5)	3.2(12)
H(44A)	0.017(14)	-0.068(9)	0.050(8)	9(2)
H(44B)	0.221(11)	-0.118(7)	0.118(8)	7(2)
H(55)	0.214(6)	0.125(5)	-0.052(4)	1.6(10)
H(66A)	0.364(8)	0.285(5)	-0.081(5)	3.8(13)
H(66B)	0.146(9)	0.297(5)	-0.140(7)	4.3(13)

(U~eq~ = (1/3)sum~i~sum~j~U~ij~a^*^~i~a^*^~j~a~i~.a~j~.)

Table A.3.4 Anisotropic parameters for mG(diamino)•mpV(2,6-pdc)

Atom	U11	U22	U33	U23	U13	U12
V(1)	3.71(3)	2.28(3)	1.69(3)	0.02(2)	1.06(2)	-0.42(2)
O(1)	4.18(14)	3.8(2)	2.57(12)	0.49(10)	0.41(10)	-1.22(11)
O(2)	8.1(2)	3.16(14)	3.07(14)	-0.27(12)	3.2(2)	-0.42(14)
O(3)	7.3(2)	3.3(2)	2.51(14)	0.31(10)	2.38(13)	-0.35(12)
O(4)	3.43(12)	2.35(12)	2.82(12)	0.26(10)	1.61(10)	0.17(10)
O(5)	4.48(13)	2.00(11)	2.26(11)	0.19(9)	1.74(10)	0.01(10)

O(6)	4.8(2)	2.52(13)	2.97(13)	0.61(10)	2.36(11)	0.49(11)
O(7)	3.66(12)	2.56(13)	2.43(12)	0.43(9)	1.26(9)	0.00(10)
O(8)	3.24(12)	2.56(13)	3.19(13)	0.49(10)	1.33(10)	0.14(9)
N(1)	2.25(12)	2.37(13)	2.05(14)	0.20(11)	1.01(10)	-0.10(10)
C(2)	2.07(13)	2.4(2)	2.7(2)	0.34(13)	1.07(12)	0.20(12)
C(3)	3.0(2)	2.6(2)	3.0(2)	-0.17(13)	1.43(13)	0.29(13)
C(4)	3.4(2)	3.7(2)	2.5(2)	-0.3(2)	1.71(14)	0.15(14)
C(5)	2.66(13)	2.8(2)	2.45(14)	0.2(2)	1.32(11)	0.0(2)
C(6)	2.10(14)	2.6(2)	2.5(2)	0.46(11)	1.12(12)	0.08(10)
C(7)	2.8(2)	2.4(2)	2.2(2)	0.13(13)	1.36(12)	-0.31(12)
C(8)	2.13(14)	2.3(2)	2.6(2)	0.16(13)	0.85(12)	-0.06(11)
C(1)	2.10(13)	3.5(2)	2.2(2)	0.17(14)	0.93(11)	-0.05(12)
N(2)	3.6(2)	3.7(2)	2.1(2)	-0.28(13)	1.18(12)	-0.31(13)
N(3)	4.2(2)	3.8(2)	2.34(14)	-0.07(13)	1.77(13)	-0.59(13)
N(4)	6.1(2)	3.5(2)	3.2(2)	-0.2(2)	1.8(2)	-0.9(2)
N(5)	4.2(2)	3.0(2)	2.0(2)	-0.08(13)	0.94(13)	-0.66(13)
N(6)	5.3(2)	3.8(2)	2.7(2)	0.52(14)	1.1(2)	-0.9(2)

The anisotropic displacement factor exponent takes the form:

```
-2 pi^2 [ h^2 a*^2 U11 + ... + 2 h k a* b* U12 ]
```

A.4. Crystallographic Tables & Figures for bg$(CH_2)_4$•mpV(nta)

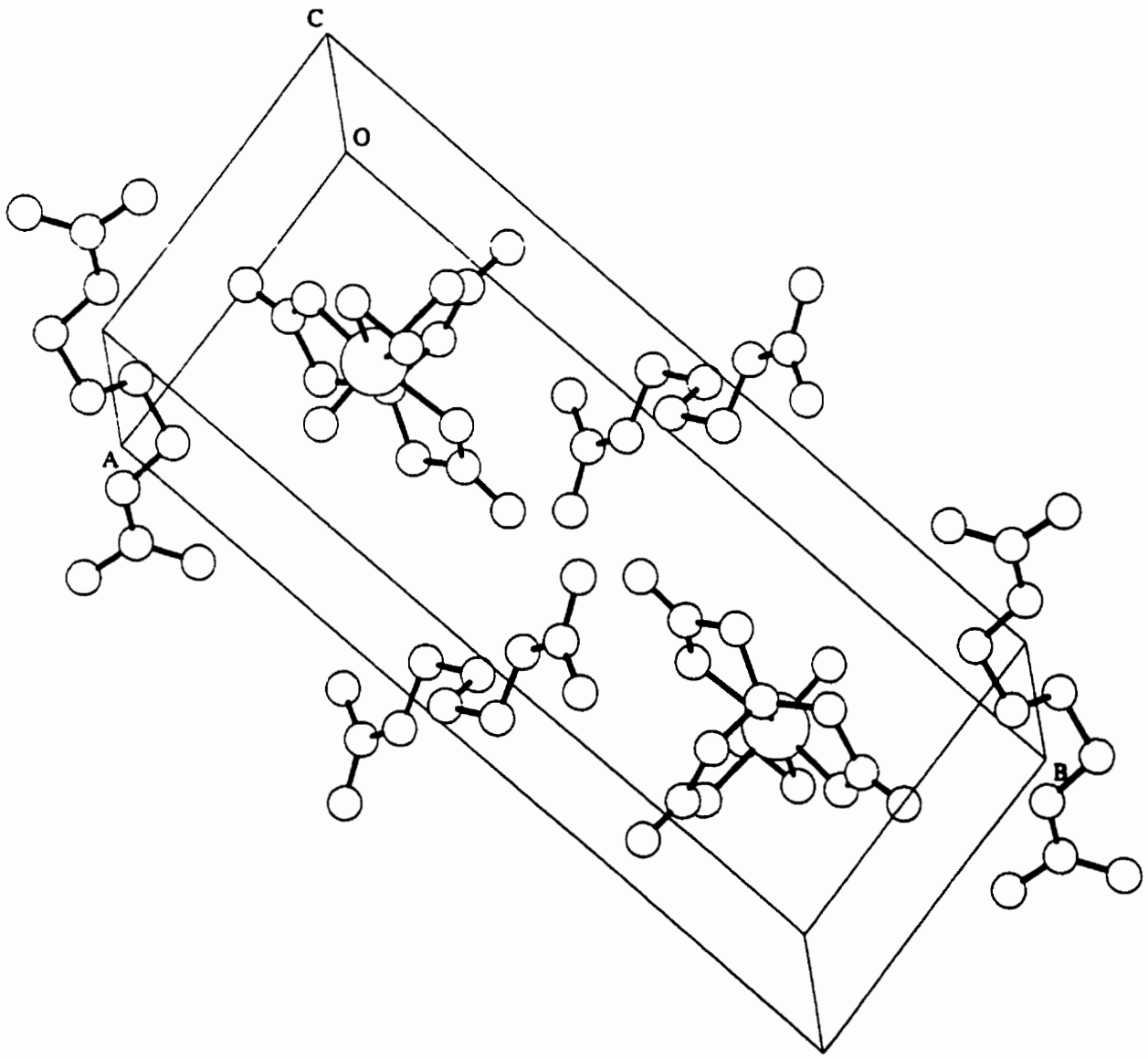

Figure A.4.1 Packing diagram for bg$(CH_2)_4$•mpV(nta)

Table A.4.1 Crystallographic parameters for.bg$(CH_2)_4$•mpV(nta)

	bg$(CH_2)_4$•mpV(nta)
	$C_{12}H_{24}N_7O_9V$
fw	461.32
Crystal System	Monoclinic
Space Group	P 2(1) / m
Temperature (°C)	21 ± 2
l (Å)	0.71073
a (Å)	7.325(3)
b (Å)	18.704(8)
c (Å)	7.390(3)
a (°)	90
b (°)	110.47(3)
g (°)	90
r calc (g cm^{-3})	1.615
V ($Å^3$)	948.5(7)
No. variables	480
No. measured	7352
No. observed ref.	1501
No. unique ref.	1922
Rint	0.074
Z	2
$R1^a$ (final), $R1^a$ (all data)	0.0457, 0.0659
$wR2^b$ (final), $wR2^b$ (all data)	0.1026, 0.1119
S	1.044
Secondary Extinction	0.004(2)
μ (mm^{-1})	0.587 (MoKa)
Scan Type	w/2q

$aR1 = \sum || Fo | - | Fc || / \sum | Fo |$

$bwR2 = \{ | \sum w (| Fo | - | Fc |)^2 / \sum w | Fo |^2 \}^{1/2}$

$w = 1/[\backslash s^2(Fo^2) + (0.0495P)^2 + 0.8857P]$

$P = (Fo^2 + 2Fc^2)/3$

$S = [\sum w(|Fo| - |Fc|)^2 / (n-v)]^{1/2}$

$GoF = [\sum [w(Fo^2 - Fc^2)^2] / (\text{No. of refIns - No. of params.})]^{1/2}$

Table A.4.2 Bond lengths and angles for bg$(CH_2)_4$•mpV(nta)

V(1)-O(1)	1.616(3)	V(1)-O(2)	1.848(2)
V(1)-O(5)	2.047(2)	V(1)-O(3)	2.127(3)
V(1)-O(3)#1	2.127(3)	V(1)-N(1)	2.192(3)
N(1)-C(3)	1.484(3)	N(1)-C(1)#1	1.501(7)
N(1)-C(1)	1.501(6)	O(2)-O(2)#1	1.427(5)
C(1)-C(2)	1.497(7)	C(1)-H(1A)	0.97
C(1)-H(1B)	0.97	C(2)-O(4)#1	1.215(11)
C(2)-O(4)	1.215(10)	C(2)-O(3)	1.276(5)
O(3)-C(2)#1	1.276(5)	O(4)-C(2)#1	1.215(10)
C(3)-C(4)	1.501(4)	C(3)-H(3A)	0.97
C(3)-H(3B)	0.97	C(4)-O(6)	1.226(4)
C(4)-O(5)	1.289(3)	C(5)-N(2)	1.315(4)
C(5)-N(4)	1.323(4)	C(5)-N(3)	1.325(4)
N(2)-HN2A	0.86	N(2)-HN2B	0.86
N(3)-HN3A	0.86	N(3)-HN3B	0.86
N(4)-C(6)	1.462(4)	N(4)-HN4	0.86
C(6)-C(7)	1.547(6)	C(6)-H(6A)	0.97
C(6)-H(6B)	0.97	C(7)-C(7)#3	1.525(10)
C(7)-H(7A)	0.97	C(7)-H(7B)	0.97
C(61)-C(71)	1.575(10)	C(61)-H(61A)	0.970(10)
C(61)-H(61B)	0.970(11)	C(71)-C(71)#3	1.52(2)
C(71)-H(71B)	0.97	C(71)-H(71B)	0.97

O(1)-V(1)-O(2)	105.22(13)	O(1)-V(1)-O(2)#1	105.22(13)
O(2)#1-V(1)-O(2)	45.42(14)	O(1)-V(1)-O(5)	93.93(7)
O(2)#1-V(1)-O(5)	125.22(9)	O(2)-V(1)-O(5)	80.28(9)
O(1)-V(1)-O(5)#1	93.93(7)	O(2)#1-V(1)-O(5)#1	80.28(9)
O(2)-V(1)-O(5)#1	125.22(9)	O(5)-V(1)-O(5)#1	149.84(12)
O(1)-V(1)-O(3)	167.20(13)	O(2)#1-V(1)-O(3)	86.56(11)
O(2)-V(1)-O(3)	86.55(11)	O(5)-V(1)-O(3)	82.96(7)
O(5)#1-V(1)-O(3)	82.96(7)	O(1)-V(1)-O(3)#1	167.20(13)
O(2)#1-V(1)-O(3)#1	86.56(11)	O(2)-V(1)-O(3)#1	86.55(11)
O(5)-V(1)-O(3)#1	82.96(7)	O(5)#1-V(1)-O(3)#1	82.96(7)
O(1)-V(1)-N(1)	89.40(14)	O(2)#1-V(1)-N(1)	152.50(9)
O(2)-V(1)-N(1)	152.50(9)	O(5)-V(1)-N(1)	75.51(6)
O(5)#1-V(1)-N(1)	75.51(6)	O(3)-V(1)-N(1)	77.81(11)
O(3)#1-V(1)-N(1)	77.81(11)	C(3)#1-N(1)-C(3)	113.5(3)
C(3)#1-N(1)-C(1)#1	106.5(14)	C(3)-N(1)-C(1)#1	115.4(14)
C(3)#1-N(1)-C(1)	115.4(14)	C(3)-N(1)-C(1)	106.5(14)
C(3)#1-N(1)-V(1)	105.5(2)	C(3)-N(1)-V(1)	105.5(2)
C(1)#1-N(1)-V(1)	110.2(2)	C(1)-N(1)-V(1)	110.2(2)
O(2)#1-O(2)-V(1)	67.29(7)	C(2)-C(1)-N(1)	114.6(6)
C(2)-C(1)-H(1A)	108.6	N(1)-C(1)-H(1A)	108.6
C(2)-C(1)-H(1B)	108.6	N(1)-C(1)-H(1B)	108.6
H(1A)-C(1)-H(1B)	107.6	O(4)-C(2)-O(3)	124.7(5)
O(4)-C(2)-C(1)	115.8(7)	O(3)-C(2)-C(1)	116.6(4)
C(2)-O(3)-V(1)	119.9(3)	N(1)-C(3)-C(4)	108.3(2)
N(1)-C(3)-H(3A)	110.0	C(4)-C(3)-H(3A)	110.0
N(1)-C(3)-H(3B)	110.0	C(4)-C(3)-H(3B)	110.0
H(3A)-C(3)-H(3B)	108.4	O(6)-C(4)-O(5)	123.5(3)

O(6)-C(4)-C(3)	121.0(3)	O(5)-C(4)-C(3)	115.5(2)
C(4)-O(5)-V(1)	118.7(2)	N(2)-C(5)-N(4)	121.4(3)
N(2)-C(5)-N(3)	120.6(3)	N(4)-C(5)-N(3)	118.0(3)
C(5)-N(2)-HN2A	120.0	C(5)-N(2)-HN2B	120.0
HN2A-N(2)-HN2B	120.0	C(5)-N(3)-HN3A	120.0
C(5)-N(3)-HN3B	120.0	HN3A-N(3)-HN3B	120.0
C(5)-N(4)-C(61)	126.0(3)	C(5)-N(4)-C(6)	126.0(3)
C(5)-N(4)-HN4	117.0	C(6)-N(4)-HN4	117.0
N(4)-C(6)-C(7)	108.8(3)	N(4)-C(6)-H(6A)	109.9
C(7)-C(6)-H(6A)	109.9	N(4)-C(6)-H(6B)	109.9
C(7)-C(6)-H(6B)	109.9	H(6A)-C(6)-H(6B)	108.3
C(7)#3-C(7)-C(6)	111.9(6)	C(7)#3-C(7)-H(7A)	109.2
C(6)-C(7)-H(7A)	109.2	C(7)#3-C(7)-H(7B)	109.2
C(6)-C(7)-H(7B)	109.2	H(7A)-C(7)-H(7B)	107.9
N(4)-C(61)-C(71)	108.2(4)	N(4)-C(61)-H(61A)	110.1
C(71)-C(61)-H(61A)	110.1	N(4)-C(61)-H(61B)	110.1
C(71)-C(61)-H(61B)	110.1	H(61A)-C(61)-H(61B)	108.4
C(71)#3-C(71)-C(61)	109.4(9)	C(71)#3-C(71)-H(71B)	109.8
C(61)-C(71)-H(71B)	109.8	C(71)#3-C(71)-H(71B)	109.8
C(61)-C(71)-H(71B)	109.8	H(71B)-C(71)-H(71B)	108.2

Symmetry transformations used to generate equivalent atoms:
#1 x,-y+3/2,z #2 x,y,z #3 -x,-y+1,-z+1

Table A.4.3 Atomic coordinates and equivalent isotropic displacement parameters for bg(CH_2)4•mpV(nta)

Atom	X	Y	Z	U~eq~
V(1)	0.42748(10)	0.7500	0.05394(9)	2.29(2)
N(1)	0.4632(4)	0.7500	0.3611(4)	1.78(6)
O(1)	0.1938(4)	0.7500	-0.0004(4)	3.65(7)
O(2)	0.4685(3)	0.71185(12)	-0.1593(3)	4.02(6)
C(1)	0.6748(7)	0.743(2)	0.4828(7)	2.6(4)
C(2)	0.8119(6)	0.7500	0.3738(6)	3.88(11)
O(3)	0.7359(4)	0.7500	0.1898(4)	3.32(7)
O(4)	0.9816(6)	0.736(2)	0.4645(7)	8.2(9)
C(3)	0.3666(4)	0.68366(14)	0.3916(4)	2.56(6)
C(4)	0.4153(4)	0.6245(2)	0.2789(4)	2.83(6)
O(5)	0.4569(3)	0.64435(11)	0.1308(3)	3.28(5)
O(6)	0.4147(4)	0.56186(11)	0.3278(3)	4.54(6)
C(5)	0.1995(5)	0.4117(2)	0.1228(4)	3.16(7)
N(2)	0.1098(4)	0.3537(2)	0.0349(4)	4.27(7)
N(3)	0.3549(4)	0.4363(2)	0.0904(4)	4.32(7)
N(4)	0.1344(4)	0.4484(2)	0.2409(4)	4.53(8)
C(6)	-0.0381(5)	0.4314(2)	0.2889(5)	4.28(9)
C(7)	-0.0809(7)	0.4947(4)	0.4025(7)	4.49(14)
C(61)	-0.0381(5)	0.4314(2)	0.2889(5)	4.28(9)
C(71)	-0.003(2)	0.4593(5)	0.4993(14)	4.0(2)
H(1A)	0.7068(7)	0.779(2)	0.5826(7)	3.1
H(1B)	0.6952(7)	0.697(2)	0.5464(7)	3.1
H(3A)	0.2266(4)	0.69058(14)	0.3480(4)	3.1
H(3B)	0.4122(4)	0.67163(14)	0.5279(4)	3.1

HN2A	0.0067(4)	0.3390(2)	0.0536(4)	5.1
HN2B	0.1544(4)	0.3306(2)	-0.0413(4)	5.1
HN3A	0.3980(4)	0.4143(2)	0.0113(4)	5.2
HN3B	0.4127(4)	0.4742(2)	0.1485(4)	5.2
HN4	0.1996(4)	0.4857(2)	0.2943(4)	5.4
H(6A)	-0.0154(5)	0.3883(2)	0.3665(5)	5.1
H(6B)	-0.1488(5)	0.4232(2)	0.1715(5)	5.1
H(7A)	-0.0954(7)	0.5381(4)	0.3268(7)	5.4
H(7B)	-0.2029(7)	0.4861(4)	0.4228(7)	5.4
H(61A)	-0.060(2)	0.3801(5)	0.2825(14)	5.1
H(61B)	-0.152(2)	0.4542(5)	0.1976(14)	5.1
H(71B)	-0.108(2)	0.4430(5)	0.5415(14)	4.8
H(71B)	0.119(2)	0.4405(5)	0.5879(14)	4.8

U~eq~ = (1/3)sum~i~sum~j~U~ij~a^*^~i~a^*^~j~a~i~.a~j~.

Table A.4.4 Anisotropic parameters for bg$(CH_2)_4$•mpV(nta)

Atom	U11	U22	U33	U23	U13	U12
V(1)	2.86(4)	2.84(4)	1.35(3)	0.0	0.95(3)	0.0
N(1)	2.4(2)	1.9(2)	1.46(14)	0.0	1.13(13)	0.0
O(1)	3.0(2)	4.7(2)	2.8(2)	0.0	0.47(13)	0.0
O(2)	5.8(2)	4.82(13)	2.07(11)	-0.80(9)	2.11(10)	-0.07(11)
C(1)	3.2(2)	2.5(12)	1.6(2)	0.5(5)	0.3(2)	-0.4(4)
C(2)	2.8(2)	6.0(3)	3.0(2)	0.0	1.2(2)	0.0
O(3)	3.1(2)	4.9(2)	2.3(2)	0.0	1.33(12)	0.0
O(4)	3.0(2)	17(3)	4.4(2)	2.8(8)	1.1(2)	2.5(8)
C(3)	3.6(2)	2.3(2)	2.35(14)	0.08(11)	1.66(12)	-0.37(12)
C(4)	3.5(2)	2.5(2)	2.8(2)	-0.43(12)	1.39(13)	-0.60(12)
O(5)	5.21(13)	2.71(11)	2.60(10)	-0.50(9)	2.21(10)	-0.06(10)
O(6)	7.5(2)	2.11(12)	5.0(2)	-0.32(10)	3.41(13)	-0.77(11)
C(5)	4.0(2)	3.1(2)	2.8(2)	-0.26(13)	1.74(13)	0.05(13)
N(2)	4.3(2)	4.2(2)	5.0(2)	-2.31(14)	2.60(14)	-0.87(13)
N(3)	5.7(2)	3.2(2)	5.7(2)	-1.87(13)	4.1(2)	-1.14(13)
N(4)	5.5(2)	4.3(2)	5.4(2)	-2.56(14)	3.9(2)	-1.72(14)
C(6)	4.5(2)	4.8(2)	4.5(2)	-1.7(2)	2.8(2)	-1.3(2)
C(7)	3.1(3)	7.5(4)	3.3(3)	-0.6(3)	1.7(2)	1.1(3)
C(61)	4.5(2)	4.8(2)	4.5(2)	-1.7(2)	2.8(2)	-1.3(2)

The anisotropic displacement factor exponent takes the form:
-2 pi^2 [h^2 a*^2 U11 + ... + 2 h k a* b* U12]

A.5. ^{1}H NMR Titration Plots for [Et_4N]bpV(Me_4-phen) with bU and tU host species.

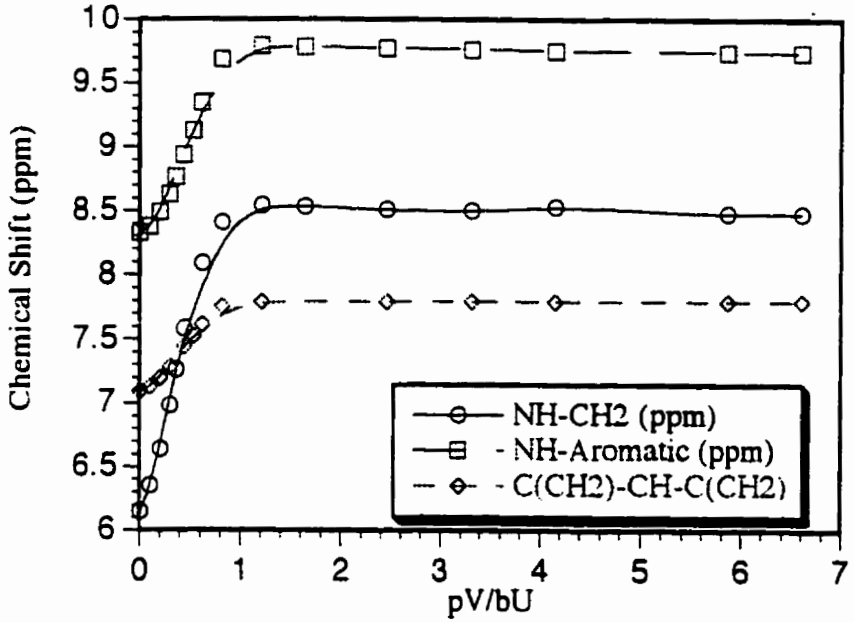

Graph A.5.1 Graph of pV/bU vs. Chemical Shift (ppm) for ^{1}H NMR titration of bU(COOEt) with [Et_4N]bpV(Me_4-phen)

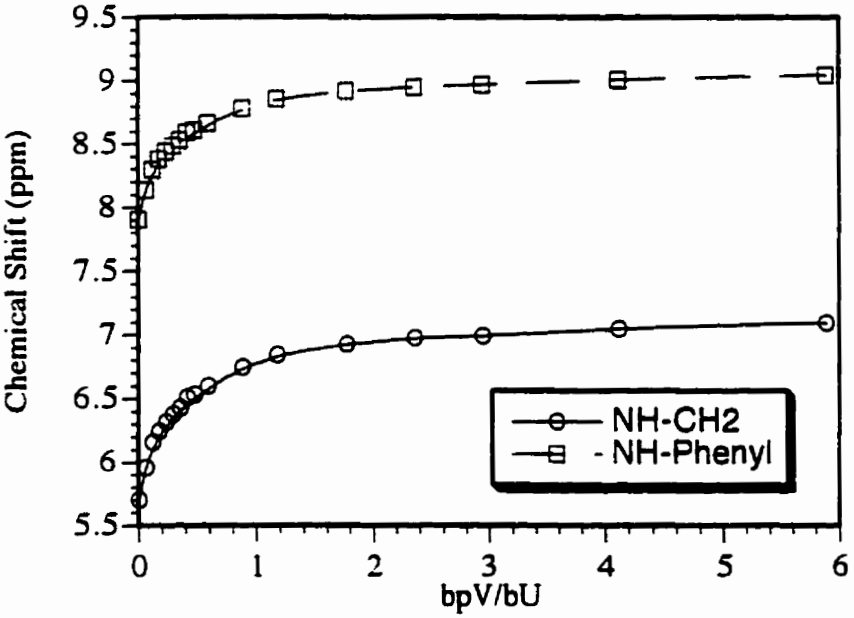

Graph A.5.2 Graph of pV/bU vs. Chemical Shift (ppm) for ^{1}H NMR titration of bU(piper-Cl) with [Et_4N]bpV(Me_4-phen)

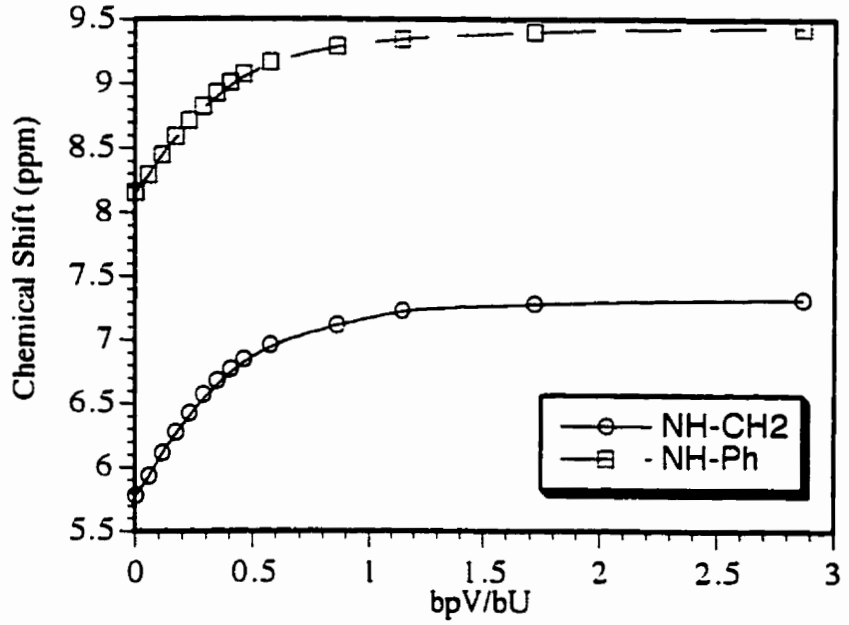

Graph A.5.3 Graph of pV/bU vs. Chemical Shift (ppm) for ^{1}H NMR titration of bU(piper-COOEt) with [Et_4N]bpV(Me_4-phen)

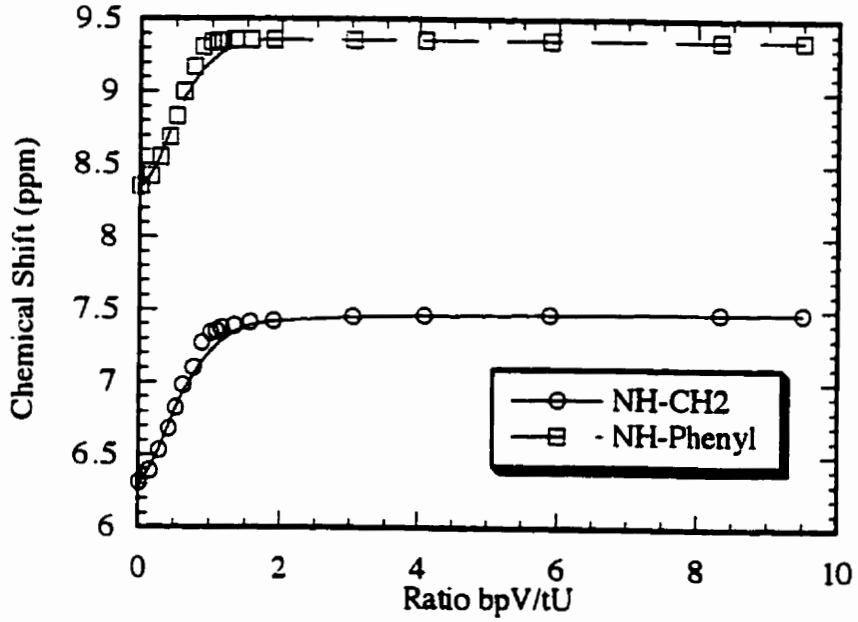

Graph A.5.4 Graph of pV/bU vs. Chemical Shift (ppm) for ^{1}H NMR titration of tU(COOEt) with [Et_4N]bpV(Me_4-phen)

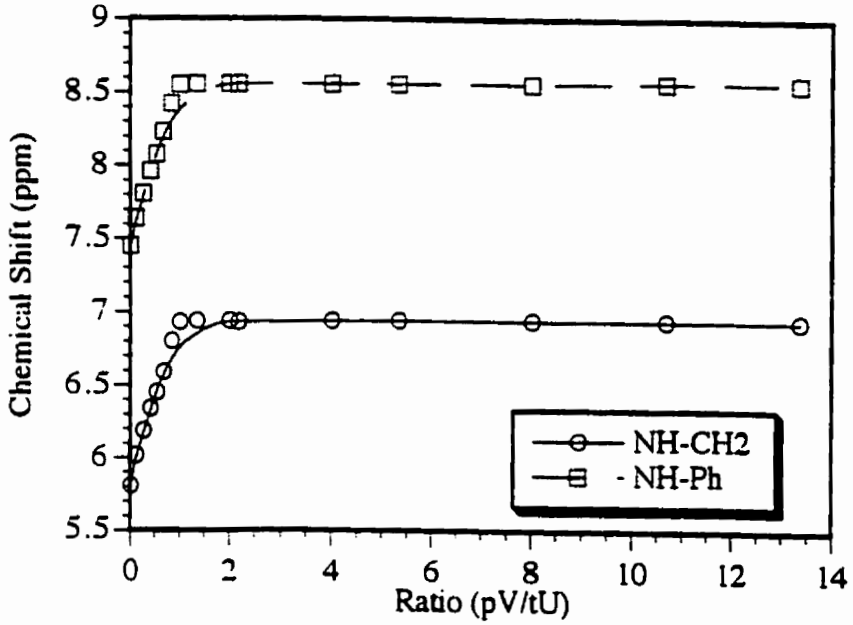

Graph A.5.5 Graph of pV/bU vs. Chemical Shift (ppm) for ^{1}H NMR titration of tU(OMe) with [Et_4N]bpV(Me_4-phen)

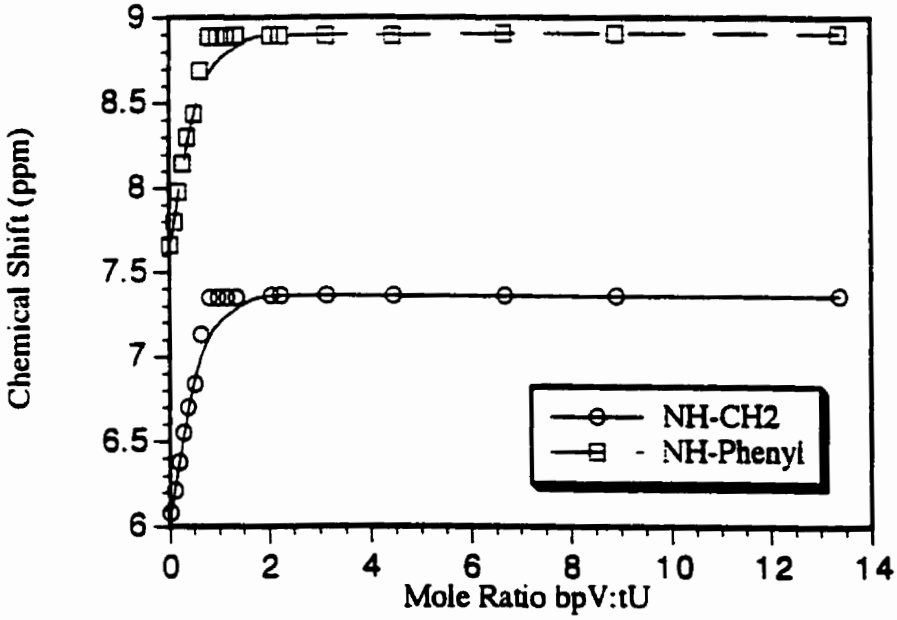

Graph A.5.6 Graph of pV/bU vs. Chemical Shift (ppm) for ^{1}H NMR titration of tU(phenyl) with [Et_4N]bpV(Me_4-phen)

A.6. Stability Studies: ln(Co/C) vs. Time Plots for $[C(NH_2)_3][bpV(phen)]$ and K[bpV(phen)] Decomposition in DMEM at 37°C

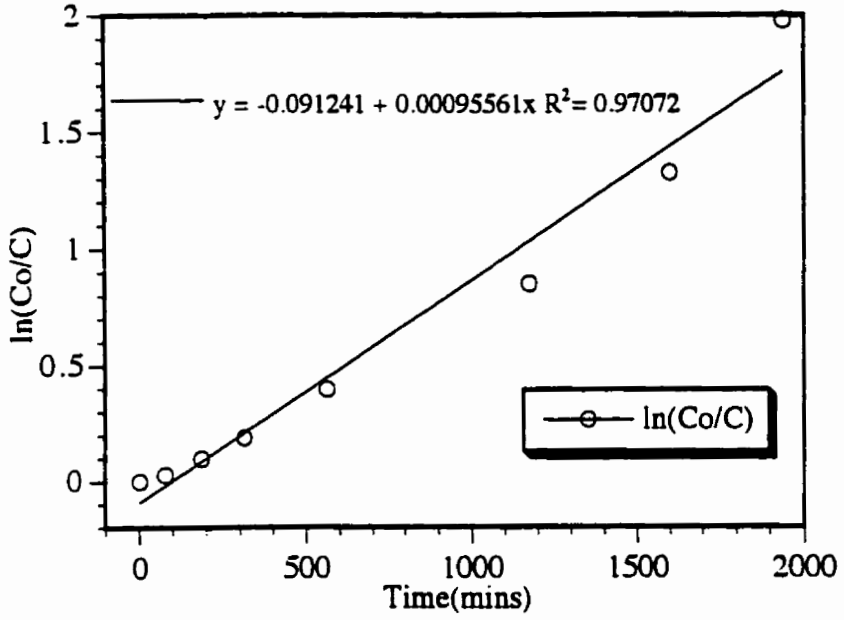

Graph A.6.1 ln (Co/C) vs. Time (mins) for 5.0 mM K[bpV(phen)] in DMEM at 37°C

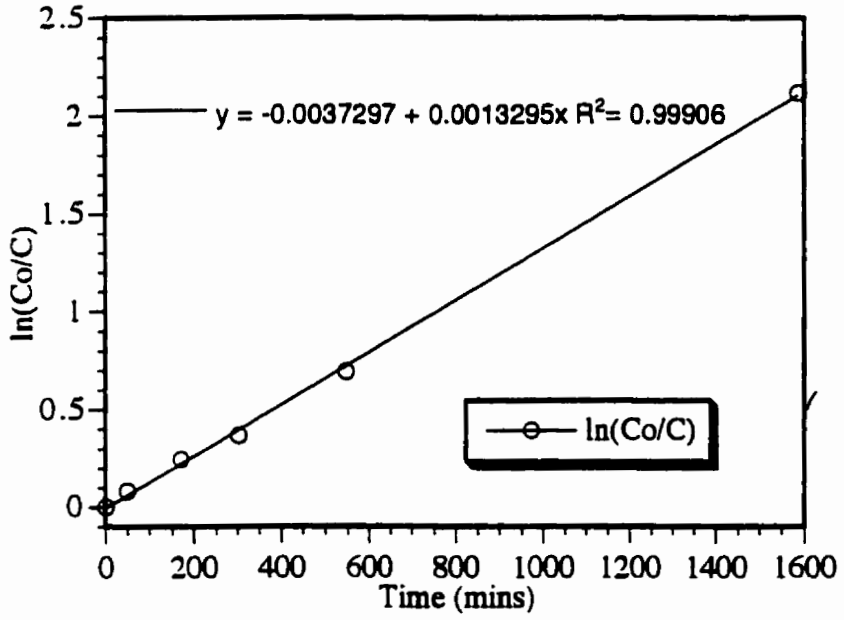

Graph A.6.2 ln (Co/C) vs. Time (mins) for 4.0 mM K[bpV(phen)] in DMEM at 37°C

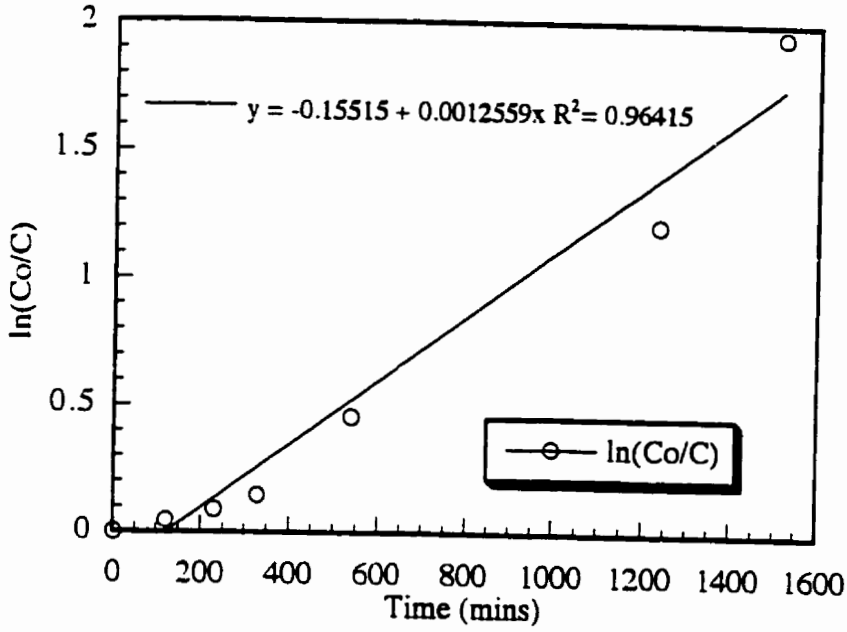

Graph A.6.3 ln (Co/C) vs. Time (mins) for 3.0 mM K[bpV(phen)] in DMEM at 37°C

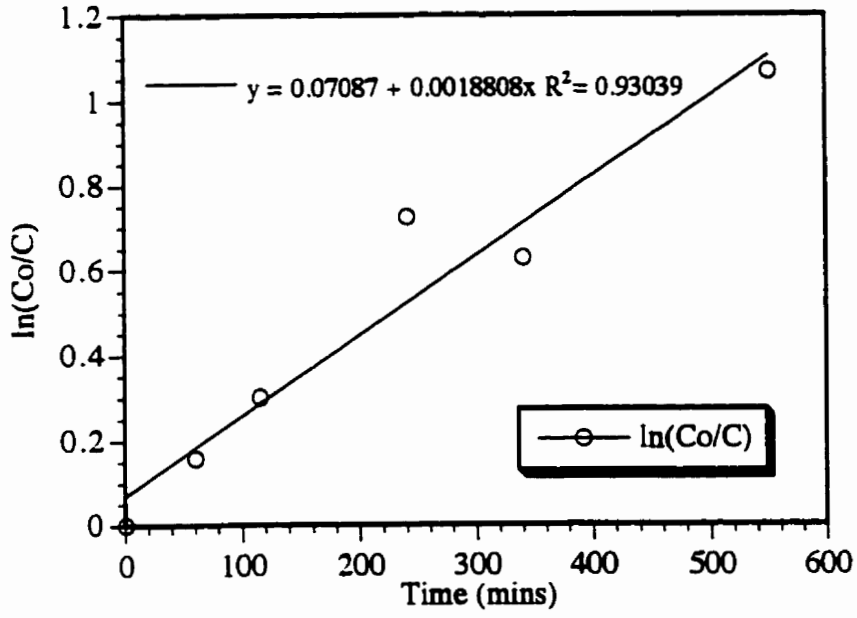

Graph A.6.4 ln (Co/C) vs. Time (mins) for 2.0 mM K[bpV(phen)] in DMEM at 37°C

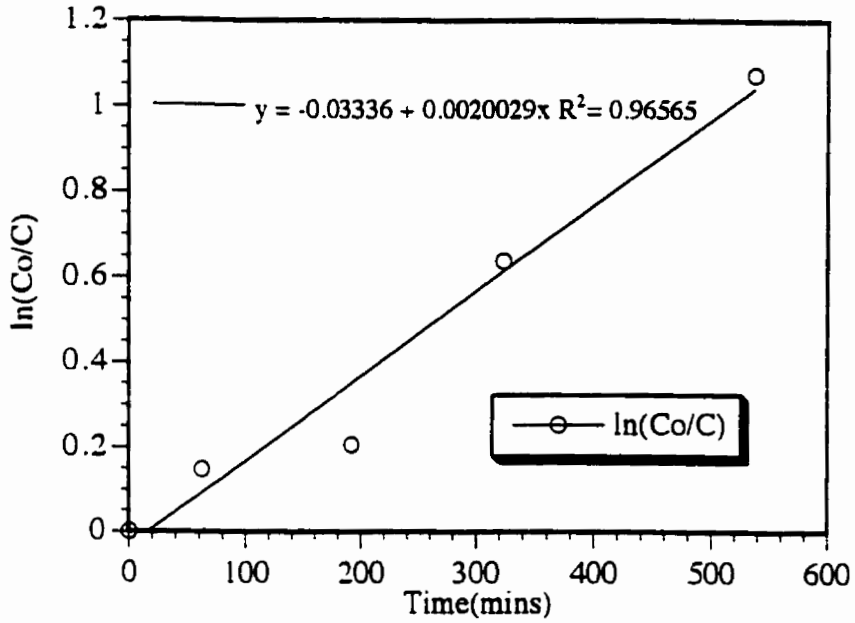

Graph A.6.5 ln (Co/C) vs. Time (mins) for 1.0 mM K[bpV(phen)] in DMEM at 37°C

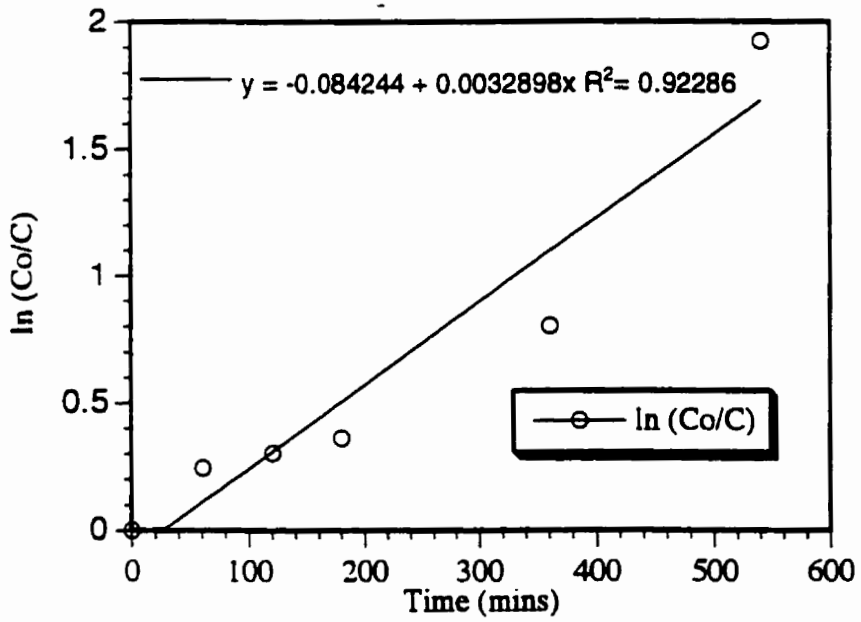

Graph A.6.6 ln (Co/C) vs. Time (mins) for 0.5 mM K[bpV(phen)] in DMEM at 37°C

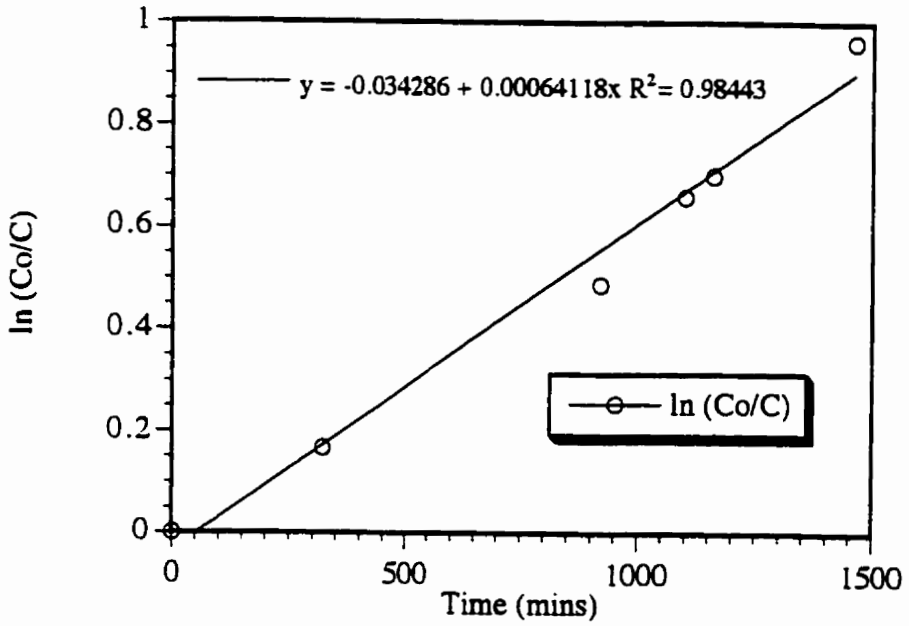

Graph A.6.7 ln (Co/C) vs. Time (mins) for 5.0 mM $[C(NH_2)_3][bpV(phen)]$ in DMEM at 37°C

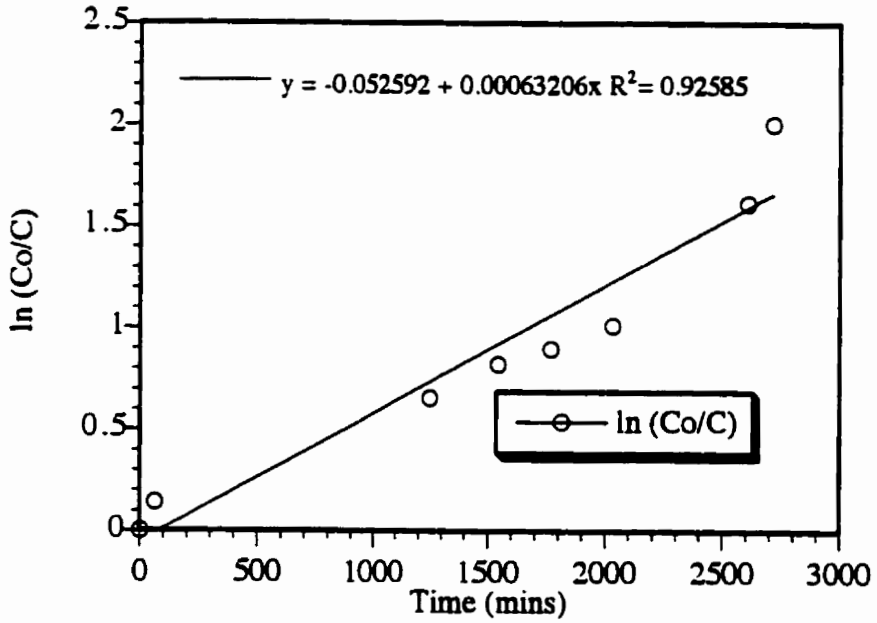

Graph A.6.8 ln (Co/C) vs. Time (mins) for 4.0 mM $[C(NH_2)_3][bpV(phen)]$ in DMEM at 37°C

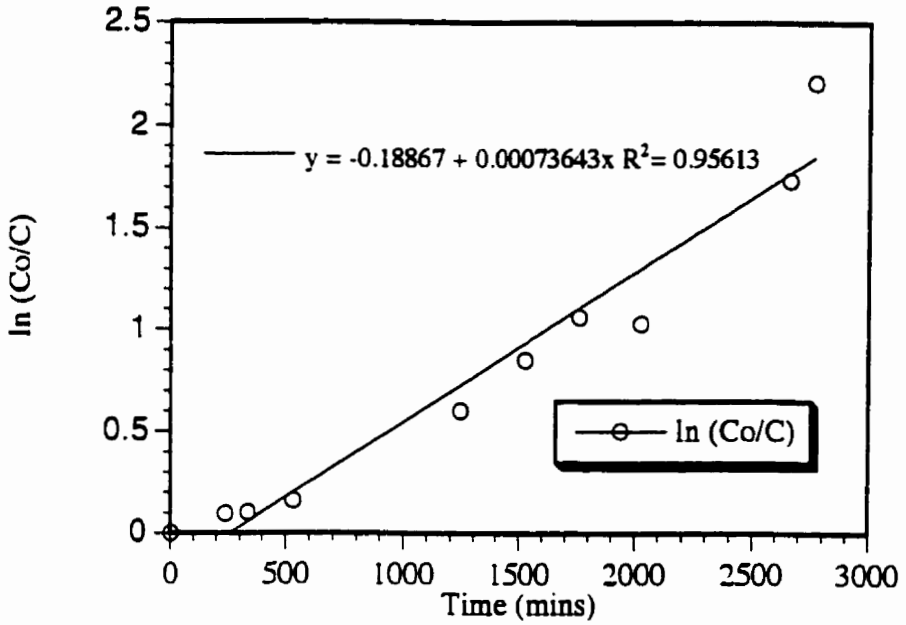

Graph A.6.9 ln (Co/C) vs. Time (mins) for 3.0 mM $[C(NH_2)_3][bpV(phen)]$ in DMEM at 37°C

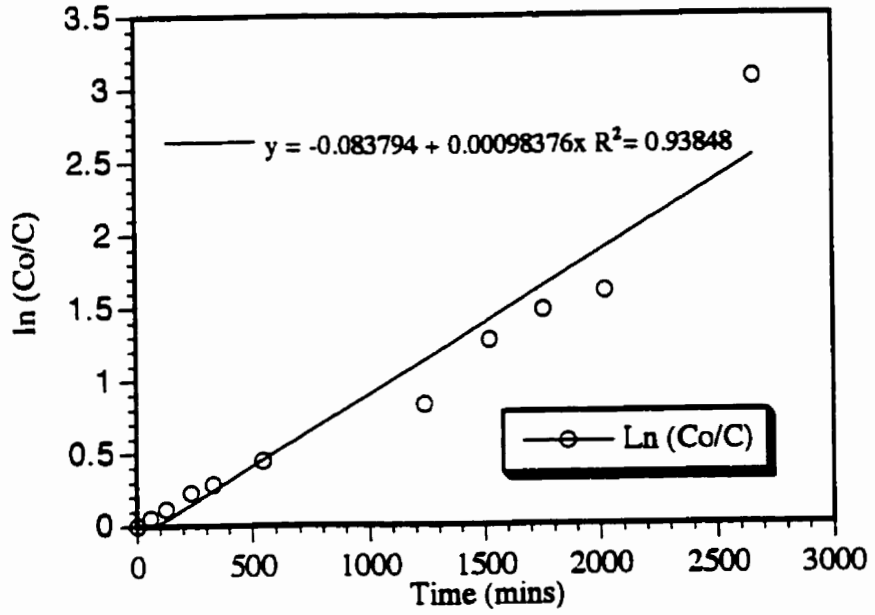

Graph A.6.10 ln (Co/C) vs. Time (mins) for 2.0 mM $[C(NH_2)_3][bpV(phen)]$ in DMEM at 37°C

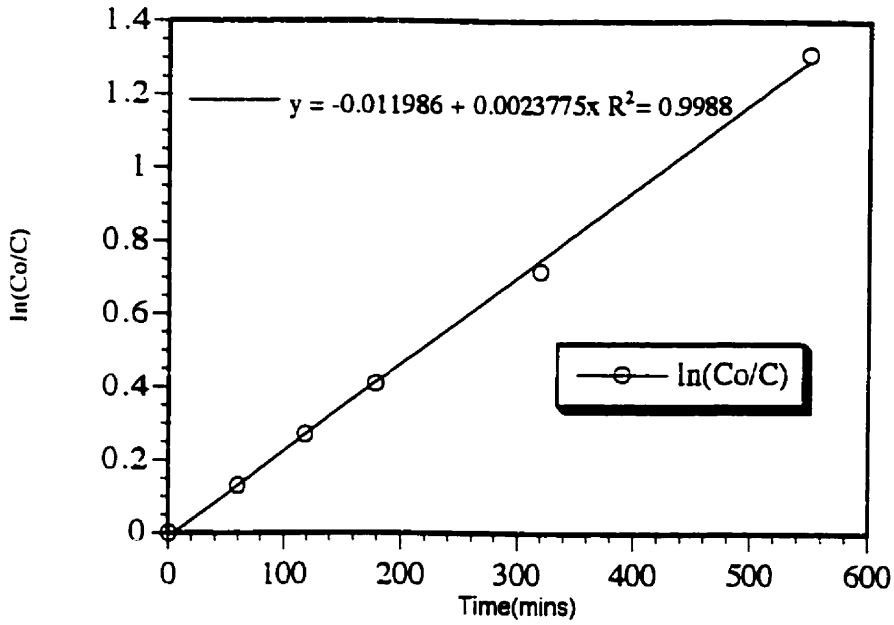

Graph A.6.11 ln (Co/C) vs. Time (mins) for 1.0 mM $[C(NH_2)_3][bpV(phen)]$ in DMEM at 37°C

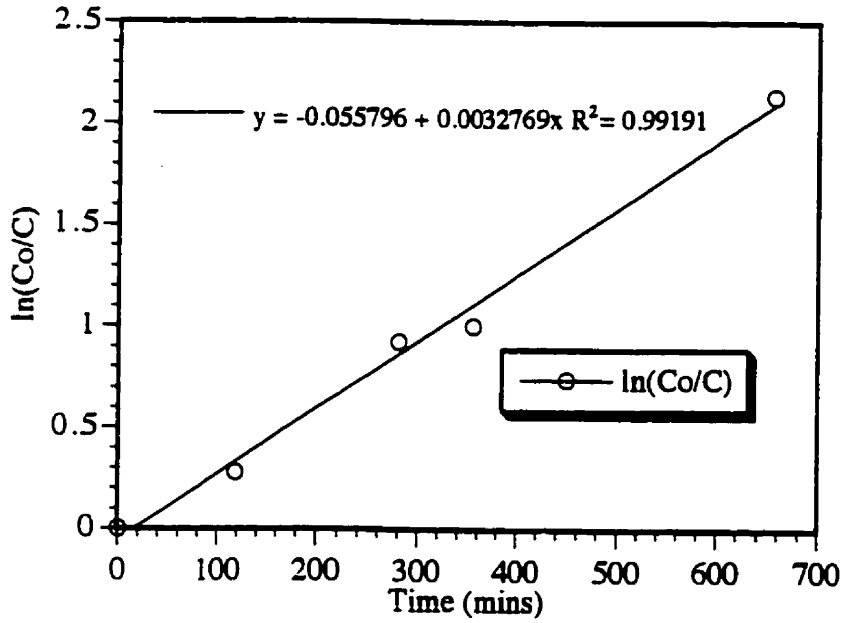

Graph A.6.12 ln (Co/C) vs. Time (mins) for 0.5 mM $[C(NH_2)_3][bpV(phen)]$ in DMEM at 37°C